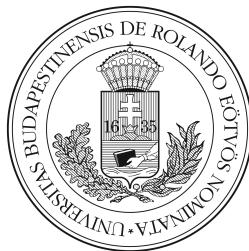


EÖTVÖS LORÁND UNIVERSITY
FACULTY OF INFORMATICS
INSTITUTE OF CARTOGRAPHY AND GEOINFORMATICS

KERKOVITS KRISZTIÁN ANDRÁS, PhD

Map projections

Lecture notes for students in **Cartography** and
Geoinformatics MSc programme



Budapest, 2023

Proof-read by: GERCSÁK GÁBOR, PhD

This material has been published using the funds awarded through the grant application for textbooks and lecture notes of ELTE IK in 2023.

This document was typeset in the program $\text{\LaTeX} 2\epsilon$.

This publication may be freely used and distributed for non-profit educational, informational, and research purposes, provided that the original author and any modifications are clearly indicated. Any other use, in particular use for financial gain, requires the prior written permission of the author.

Contents

Preface	8
1st Theory of map projections	10
I Parametrization of the sphere and the ellipsoid	11
I.1 Units of measurement	11
I.2 Surfaces of revolution	12
I.3 The sphere	13
I.4 The ellipsoid of revolution	15
II Introduction to spherical geometry	19
II.1 Non-Euclidean geometries	19
II.2 Notable parts of the sphere	20
II.3 The spherical triangle	22
III Navigation in spherical geometry	24
III.1 Spherical trigonometry	24
III.2 Orthodromic navigation.	27
III.3 Loxodromic navigation	28
IV Curvature and arc length on the ellipsoid	33
IV.1 Meridional radius of curvature	33
IV.2 Prime-vertical radius	36
IV.3 Latitude, longitude, and height in space	37
IV.4 Area of the ellipsoidal quadrangle	39
V Geodetic problems	41
V.1 Geodetic problems on the plane	41
V.2 Geodetic problems on the sphere	42
V.3 Metacoordinates	43
V.4 Geodetic problems on the ellipsoid	47

VI The basics of map projections	51
VI.1 The Theorema Egregium	51
VI.2 What is a map projection?.	52
VI.3 Surfaces approximating the Earth's figure	53
VI.4 Geodetic datums	54
VI.5 The radius of the Earth	57
VI.6 Classification of projections.	58
VII Distortions in terms of partial derivatives	61
VII.1 The linear scale.	61
VII.2 Intersection angle between graticule lines	64
VII.3 The areal scale	65
VIII Tissot's theory of map distortion	67
VIII.1 Map projections as local affine transforms.	67
VIII.2 The ellipse of distortion	69
VIII.3 Calculation of extremal linear scales	71
VIII.4 Maximum angular deviation	72
IX Map distortions in practice	74
IX.1 Visualizing distortions.	74
IX.2 Distortions not predicted by Tissot's theory	75
IX.3 Auxiliary spheres.	78
2nd Conical map projections	81
X Perspective azimuthals	82
X.1 Azimuthals in general	82
X.2 Vertical perspective projection	83
X.3 Gnomonic projection	85
X.4 Orthographic projection.	86
X.5 Stereographic projection	87
XI Non-perspective azimuthals	91
XI.1 Azimuthal equidistant.	91
XI.2 LAMBERT azimuthal equal-area	93
XI.3 GINZBURG's scheme.	95
XI.4 Ellipsoidal azimuthals.	96

XII Perspective & equal-area cylindricals	100
XII.1 General formulæ	100
XII.2 Central cylindrical projection	101
XII.3 Quasi-perspective cylindricals	102
XII.4 Equal-area cylindricals	105
XIII Other cylindrical projections	108
XIII.1 Equidistant cylindricals	108
XIII.2 MERCATOR projection	110
XIII.3 Rarely occurring cylindricals	113
XIV Cylindricals for the ellipsoid of revolution	115
XIV.1 Cylindricals in normal aspect	115
XIV.2 CASSINI–SOLDNER projection	116
XIV.3 The Pseudo Mercator	116
XIV.4 GAUSS–KRÜGER projection	117
XIV.5 The systems of NATO	121
XIV.6 ROSENMUND and HOTINE projections	122
XV Aphylactic conic projections	125
XV.1 Conic projections	125
XV.2 Perspective conics	126
XV.3 Conic projection with equidistant parallels	128
XV.4 Equidistant conic	129
XVI Equal-area & conformal conic mappings	134
XVI.1 ALBERS equal-area conic	134
XVI.2 LAMBERT conformal conic	138
XVI.3 Ellipsoidal conic projections	143
XVII Applied theory of map projections	145
XVII.1 Can distortion be useful?	145
XVII.2 The focus of map projections	146
XVII.3 Map projections and GIS	148
XVII.4 Georeferencing	150
XVIII Transformations between reference systems	153
XVIII.1 Transform via the reference frame	153
XVIII.2 Transform with control points	155
XVIII.3 The method of least squares	156

3rd Non-conical map projections	162
XIX Theory of non-conical projections	163
XIX.1 The shape of the graticule	163
XIX.2 Seven aspects of a non-conical projection	164
XIX.3 Map distortions	168
XIX.4 Application of non-conical projections	169
XX Earlier pseudocylindrical maps	171
XX.1 Distortions of pseudocylindricals	171
XX.2 Globular projections	172
XX.3 Extended globular projections	176
XX.4 Sinusoidal projection	176
XXI Aphylactic pseudocylindrical projections	179
XXI.1 Loximuthal projection	179
XXI.2 Blended projections	180
XXI.3 Polyhedric projection	185
XXII Auxiliary angles in equal-area mappings	187
XXII.1 ECKERT's equal-area mappings	187
XXII.2 MOLLWEIDE projection	192
XXIII Renumbering the graticule	195
XXIII.1 The method 'Umbeziffern'	195
XXIII.2 KAVRAYSKIY VII projection	197
XXIII.3 The WAGNER transform	199
XXIII.4 Composite projections	202
XXIV Modern pseudocylindrical maps	205
XXIV.1 The BARANYI projections	205
XXIV.2 Projections given by tables	209
XXV Pseudoconic & pseudoazimuthal mappings	213
XXV.1 Map projections with circular parallels	213
XXV.2 Pseudoconic projections	214
XXV.3 Pseudoazimuthal projections	218
XXVI Polyconic projections	221
XXVI.1 Properties of polyconic projections	221
XXVI.2 American polyconic	222
XXVI.3 Rectangular polyconic	225

XXVI.4 Equal-area polyconic	227
XXVII Pseudopolyconic projections	229
XXVII.1 LAGRANGE projection	229
XXVII.2 Maps with circular graticule	232
XXVII.3 Further pseudopolyconics.	237
XXVII.4 Polyazimuthal projections.	237
XXVIII Modified azimuthal projections	240
XXVIII.1 AITOFF & HAMMER projections	240
XXVIII.2 WINKEL III projection	242
XXVIII.3 WAGNER's modified azimuthals	244
XXVIII.4 Retroazimuthal mappings	246
XXVIII.5 Projections of RAISZ	246
XXVIII.6 Star projections	247
XXIX Exotic map projections	249
XXIX.1 Conformal projections	249
XXIX.2 Polyhedral projections	253
XXIX.3 Projection analysis	255
XXX Selecting a map projection	259
XXX.1 Traditional methods	259
XXX.2 The local distortion value	261
XXX.3 The global distortion value	262
XXX.4 Final thoughts	265
Appendices	267
A Basic mathematical relations	268
B Rare formulæ in spherical trigonometry	272
C BORKOWSKI's formula for the latitude	276
D Vertical datums.	280
E Alternative derivation of Tissot's theory	285
F Old projection systems in Hungary	290
G Projection systems in Europe	295
H Inverse formulæ of oblique projections	300
J Pseudocylindricals with straight meridians.	305
K Approximate formulæ of BARANYI's maps.	310
L Modified polyconic projection	316
M Index.	319

Preface

This work contains the translation of the Hungarian language lecture notes used in the course of mathematical cartography in Eötvös Loránd University.

The lessons of this curriculum do not follow a thematic logic, but gradually build up the concepts from the simple to the more complex. This is why there are many references back to much earlier material in relating calculations. The blue links in the text are clickable and facilitate navigation within the work.

The lessons are grouped into three parts: Lessons of the first part define general concepts and derive basic formulæ of map projection theory. In the second part, the reader will learn about the characteristics, history and classification of conical projections followed by some technical notes about their application in GIS and geodesy. In the third part, the focus is on non-conical projections. After a systematic description of each projection, you will find a guide about recognizing projections and approximate calculations of mappings with the smallest distortion possible.

Although I have endeavoured to cover topics that are related in each lesson, to fit the topics into 90-minute long lectures, some loosely related material may have been included in a single lesson. Colour formulæ can be found throughout the note. This is intended to aid understanding during complex transformations. If you see expressions with the same colour on both sides of an equals sign, they have the same value. Often, before or after simplifying fractions or equations, expressions of the same colour appear on both sides to highlight the transformation. It is therefore not recommended printing the notes in greyscale.

In the description of the course material, I have tried to use language that is understandable to students of cartography, and have therefore avoided using formal mathematical terminology wherever possible. However, understanding some topics (such as conformal projections) requires deep mathematical knowledge, which is understandably not part of a master's degree in cartography. In such cases, I have endeavoured to highlight, as far as possible, the complexity of the mathematical problems involved so that the projections that arise and can be applied in practice are not presented as a fairy tale; at the same time, the tone of the text is more informative than scientific. Therefore, I do not give the usual standard definitions used in mathematical literature for new concepts, but try to convey their visual

Preface

meaning. At the same time, where this is possible, I also include a few mathematical points of interest in the form of footnotes.

I hope that this adventure of discovery will be enjoyable for both the students of the courses and for the interested readers!

First module

Theory of map projections

Lesson one

Parametrization of the sphere and the ellipsoid

1.1 Units of measurement

When interpreting coordinate systems, it is very important to know what units of measurement they use. Although the usage of the metric system seems obvious today, it is not so evident on foreign or old maps.

Angles are usually given in degrees on maps, but minutes and seconds are also common: $1^\circ = 60' = 3600''$. On French maps, we can find the decimal gradian, the right angle used to be divided into 100^g instead of 90° . The gradian is divided into centesimal minutes and centesimal seconds: $1^g = 100^c = 10000^{cc}$. On old French maps, therefore, proceed with caution!

Formulae are often simpler if you calculate in radians, which is the ratio between the length of the arc subtending the angle and the radius of the circle: $180^\circ = \pi$ radians. We denote radians by omitting the unit of measurement. In this note, the notation $\widehat{\alpha}$ (arc) indicates that the angle α must be substituted into the formula in radians. For example, the arc length s of radius R subtending the angle ϑ *in radians*, can be calculated using the formula $s = R\widehat{\vartheta}$.

Theoretically, the unit of measurement called mil on military maps of the Soviet era would be a thousandth of a radian, but in the Eastern Bloc countries, for simplification, the turn is divided into 6000 mils instead of ~ 6283 . The mil is denoted by placing a dash between the places of tens and hundreds: the right angle expressed in mils is therefore 15-00.

Common coordinate systems usually use metres for distances.* The old definition of a metre is a ten-millionth of a terrestrial half meridian, i.e. 1 km is approximately the length of the meridian arc subtending the angle of 1^c (centesimal minute). There may be other units of measurement besides the metre:

* Since the Germans happened to have an old standard 15 μm longer than the others, the metre on maps of former German colonies (e.g. Namibia) may still differ from the real metre, and this must be adjusted in the GIS if necessary!

I. Parametrization of the sphere and the ellipsoid

- 1 US mile ≈ 1609 m
- 1 nautical mile ≈ 1852 m (the length of the meridian arc subtending the angle $1'$ at the centre of the Earth)
- 1 US foot ≈ 30.48 cm (used for altitude on air navigation maps)
- 1 Viennese klafter ≈ 1.896 m (used on old Hungarian surveying and military maps)
- 1 Viennese mile = 4000 klafters ≈ 7586 m

Using the examples of the metre and the nautical mile, it can be seen that distances on the Earth can be described by the angle they subtend, since the radius of the Earth ($R \approx 6371$ km) is known. As a rule of thumb, the $1^\circ \approx 111$ km estimate can be used, but it is important to note that this only gives a good value along meridians!

I.2 Surfaces of revolution

If an arbitrary smooth plane curve is rotated about an *axis of rotation* lying in the same plane, the surface that the curve generates is called a *surface of revolution*. The green generatrices on Fig. I.1 congruent with the original plane curve are called *meridians*, and the blue circles in the planes perpendicular to the axis of rotation are called *parallels*. Parallels and meridians are always perpendicular to each other.

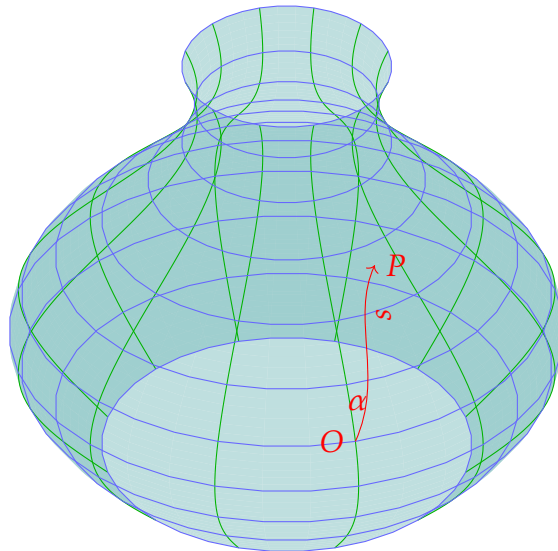


Figure I.1: Polar coordinates on a surface of revolution

The figure also shows one possible coordinate system, the polar coordinate system of the surface of revolution, similar to the polar coordinate

I. Parametrization of the sphere and the ellipsoid

system of planes. The *radial distance* s between the origin O and the point P is measured along the shortest possible path on the surface. This shortest path is called the *geodesic*. All meridians on a surface of revolution are also geodesics, but parallels are usually not geodesics. The equivalent of the polar angle here is the *azimuth* α , which is always measured clockwise from the meridian passing through the origin.*

The other possible reference system is the *parametric frame*, which can be defined by an arbitrary function $f(u, v) \mapsto (x, y, z)$, with the constraint that the Cartesian coordinates (x, y, z) returned by the function must fall on a point of our surface for all (u, v) in the domain. In this case, the original pair (u, v) is called the *parametric coordinate* of the surface, and the function $f(u, v)$ is called the *parametric representation* of the surface. We call *coordinate curves* those curves on the surface along which either parameter u or v is constant.

1.3 The sphere

A locus of points equidistant from a point is called a *sphere*. The points of a sphere of radius R centred at the origin always satisfy the following equation:

$$x^2 + y^2 + z^2 - R^2 = 0$$

The sphere can have multiple parametric representations. One possible parametrization is where the parameters u, v are the *latitude* φ and *longitude* λ . The former is defined as the angle between the vector pointing to the point and the plane subtended by axes x, y , the latter angle is measured between axis x and the vector pointing to the point orthogonally projected onto the plane x, y . This parametric representation can be formulated as shown in Fig. I.2:

$$\begin{aligned}x &= R \cos \varphi \cos \lambda \\y &= R \cos \varphi \sin \lambda \\z &= R \sin \varphi\end{aligned}$$

It can be seen that the coordinate curves φ are parallels of the sphere, their radius is $R \cos \varphi$, while the coordinate curves λ are meridians of the

* In very rare cases, it may be possible to connect two points on the surface of revolution by several geodesics with different azimuths. An example is two points on the opposite sides of a sphere. In such cases, the azimuth of the point is not unique, but the inverse relation is always unique: a certain azimuth and distance still represent a single point on the surface.

I. Parametrization of the sphere and the ellipsoid

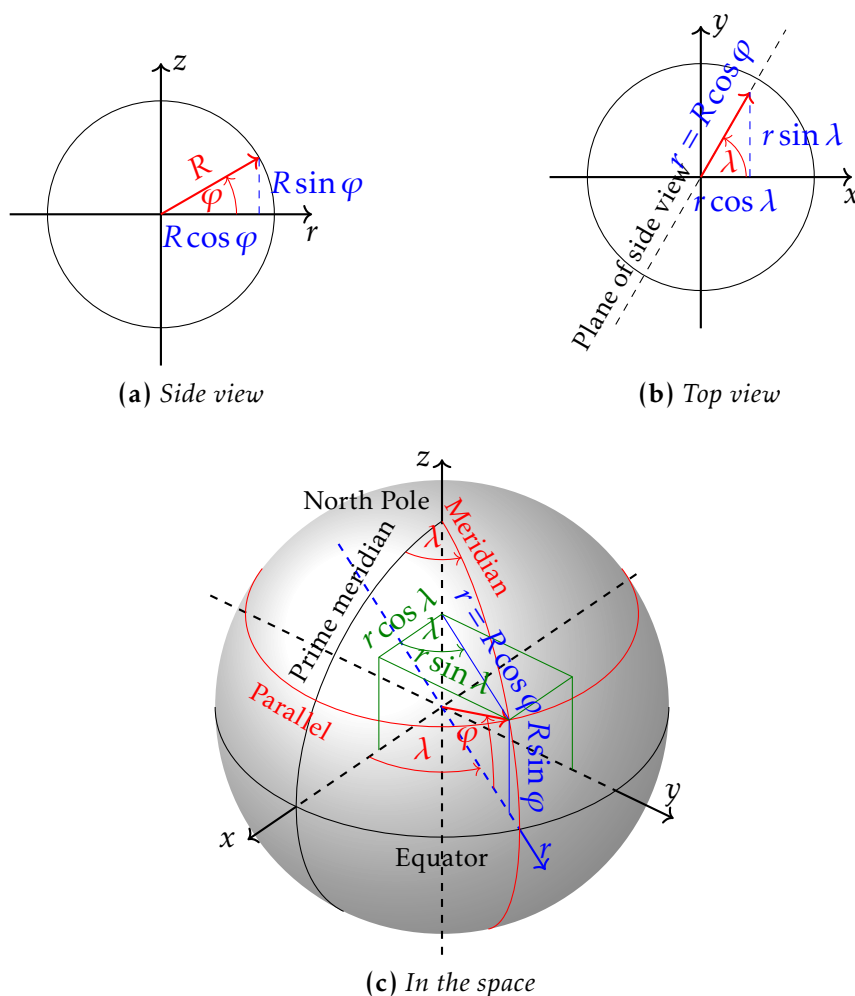


Figure I.2: Geographical coordinates of the sphere

sphere, their radius is R . If we want to get geographic coordinates from Cartesian ones, we can also read from the figure that:

$$\sin \varphi = \frac{z}{R} = \frac{z}{\sqrt{x^2 + y^2 + z^2}}$$

$$\tan \lambda = \frac{y}{x}$$

In the case of the Earth, axis z is placed in the direction of the axis of rotation, so the latitude is measured from the plane perpendicular to it. The coordinate curve of latitude 0° is called the *Equator*. However, the measurement of longitudes is not straightforward because axis x can be

I. Parametrization of the sphere and the ellipsoid

rotated in the direction of any *Prime meridian*. In practice, the most common Prime meridian is the meridian through the Greenwich Observatory,^{*} but other Prime meridians are also used: for example, until recently, the French often indicated longitudes starting from Paris,[†] and on old maps we frequently find longitudes measured from Ferro.[‡] For national surveying purposes, most countries have also designated their own Prime meridians. In Hungary, it passes through Gellérthegy at the end of the Citadel near the Statue of Liberty.

I.4 The ellipsoid of revolution

An *ellipsoid of revolution* is obtained by rotating an ellipse around one of its axes. The ellipsoid can be characterized by two data, the *major semi-axis* a and the *minor semi-axis* b . The points constituting the ellipsoid with axis of rotation z centred at the origin can be described by the following equation:

$$\frac{x^2}{a^2} + \frac{y^2}{a^2} + \frac{z^2}{b^2} - 1 = 0$$

The shape of the rotation ellipsoid can also be characterized by the *flattening* f , the *first eccentricity* e and the *second eccentricity* e' :

$$f = \frac{a - b}{a}$$
$$e = \sqrt{\frac{a^2 - b^2}{a^2}}$$
$$e' = \sqrt{\frac{a^2 - b^2}{b^2}}$$

The flattening is usually given by its reciprocal ($f \approx 1/300$), while the first eccentricity is often found squared in the literature. However, sometimes

^{*} In fact, the International Prime meridian is located 102 m east of the observatory to correct for the vertical deflection.

[†] Moreover, it is in gradians, so pay special attention.

[‡] This Prime meridian was defined as being 20° west of Paris in the Atlantic Ocean.

I. Parametrization of the sphere and the ellipsoid

the eccentricity is not given at all, in which case we have to calculate it from the flattening:

$$e = \sqrt{\frac{a+b}{a} \frac{a-b}{a}} = \sqrt{\frac{2a-(a-b)}{a} f} = \sqrt{(2-f)f} = \sqrt{2f-f^2}$$

By transforming the formula for the first eccentricity, we can obtain a very important relation:

$$\begin{aligned} e^2 &= \frac{a^2 - b^2}{a^2} \\ e^2 - 1 &= -\frac{b^2}{a^2} \\ a^2(1 - e^2) &= b^2 \\ b &= a\sqrt{1 - e^2} \end{aligned}$$

We will use this expression often! For example, we can get the flattening from the first eccentricity:

$$f = \frac{a - a\sqrt{1 - e^2}}{a} = 1 - \sqrt{1 - e^2}$$

Or the relation between the first and second eccentricities:

$$e' = \sqrt{\frac{a^2 - b^2}{a^2(1 - e^2)}} = \frac{e}{\sqrt{1 - e^2}}$$

On the ellipsoid, we define the longitude Λ in the same way as before on the sphere. However, we can define three different latitudes (Fig. I.3):

- The *geocentric latitude* Ψ is the angle between the vector from the centre of the ellipsoid to the point and the plane of the Equator.
- The *geodesic or geographic latitude* Φ is the angle between the normal (local vertical) of the surface and the plane of the Equator.
- The *parametric latitude* Θ is the latitude that would be measured on the sphere of radius a if the ellipsoid were stretched by a factor of a/b in the direction of axis z .

In cartographic practice, we most commonly use the geodesic latitude. This is because it was easy to measure using astronomical methods: latitude is equal to the angle between the tangent plane of the ellipsoid (local horizontal) and the direction of the Earth's axis of rotation (North Star).

I. Parametrization of the sphere and the ellipsoid

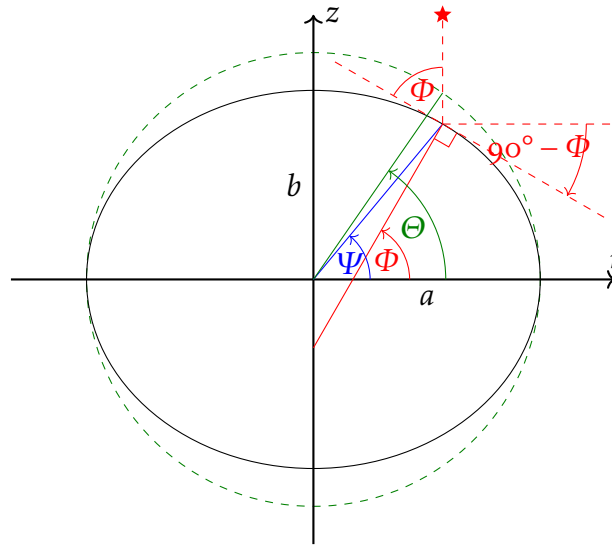


Figure I.3: Latitudes on an ellipsoid

To convert between the three definitions of latitude, let us first formulate the equation of the ellipse shown in the figure:

$$\frac{r^2}{a^2} + \frac{z^2}{b^2} - 1 = 0$$

Expressing z :

$$z = b\sqrt{1 - \frac{r^2}{a^2}} = \frac{b}{a}\sqrt{a^2 - r^2}$$

The derivative is the slope of the tangent line of the ellipse:

$$\frac{dz}{dr} = \frac{-br}{a\sqrt{a^2 - r^2}}$$

In the figure, it can be seen that the slope angle of the tangent line of the ellipse marked by the red dashed line supplements the latitude just to the right angle. Knowing that the derivative is the signed slope of

I. Parametrization of the sphere and the ellipsoid

the tangent line, and taking into account that the derivative is negative: $dz/dr = -\tan(90^\circ - \Phi) = -\cot \Phi$. That is:

$$\begin{aligned} \frac{-br}{a\sqrt{a^2 - r^2}} &= -\frac{\cos \Phi}{\sin \Phi} \\ \frac{b^2 r^2}{a^4 - a^2 r^2} &= \frac{\cos^2 \Phi}{\sin^2 \Phi} \\ b^2 r^2 \sin^2 \Phi &= a^4 \cos^2 \Phi - a^2 r^2 \cos^2 \Phi \\ r^2 (a^2 \cos^2 \Phi + b^2 \sin^2 \Phi) &= a^4 \cos^2 \Phi \\ r &= \frac{a^2 \cos \Phi}{\sqrt{a^2 \cos^2 \Phi + b^2 \sin^2 \Phi}} \end{aligned}$$

This gives the radius of the parallel at latitude Φ . Substitute the result into the equation of the ellipse to get z :

$$\begin{aligned} z &= \frac{b}{a} \sqrt{a^2 - r^2} = \frac{b}{a} \sqrt{a^2 - \frac{a^4 \cos^2 \Phi}{a^2 \cos^2 \Phi + b^2 \sin^2 \Phi}} \\ &= \sqrt{\frac{b^2 a^2 \cos^2 \Phi + b^2 b^2 \sin^2 \Phi - a^2 b^2 \cos^2 \Phi}{a^2 \cos^2 \Phi + b^2 \sin^2 \Phi}} = \frac{b^2 \sin \Phi}{\sqrt{a^2 \cos^2 \Phi + b^2 \sin^2 \Phi}} \end{aligned}$$

The figure shows that $\tan \Psi = z/r$, so

$$\tan \Psi = \frac{b^2 \sin \Phi}{a^2 \cos \Phi} = \frac{b^2}{a^2} \tan \Phi$$

However, Θ is by definition the image of Ψ after stretching by a factor of a/b :

$$\tan \Theta = \frac{a}{b} \tan \Psi$$

Substituting the two equations into each other:

$$\tan \Theta = \frac{b}{a} \tan \Phi$$

Thus, from any latitude, the other two can be calculated, and the relation $\Psi \leq \Theta \leq \Phi$ can be demonstrated in the Northern Hemisphere.

Lesson two

Introduction to spherical geometry

II.1 Non-Euclidean geometries

The Euclidean geometry taught in secondary school covers the geometric relationships on a flat plane well, but in practice, we see differences. For example, the first surveyors found that the sum of the interior angles of triangles measured in the field was slightly greater than 180° . This is due to the curvature of the Earth.

The geometries of curved spaces are called *non-Euclidean geometries*. There are three main types:

- *Hyperbolic geometry*: the interior angles of triangles add up to less than 180° , a line can have several non-intersecting lines drawn through a point outside it in the same plane. Such is the case in BOLYAI geometry.*
- *Parabolic geometry*: the interior angles of triangles add up to 180° , a single parallel line can be drawn for a line through a point outside it. An example is the Euclidean geometry.
- *Elliptic geometry*: the interior angles of triangles add up to greater than 180° , any two lines lying in a plane intersect each other. This includes the spherical geometry we are discussing.

In spherical geometry, the role of the plane is replaced by the sphere. Points are defined in the usual way. We look for the equivalent of the straight line that still represents the shortest distance between any two points: this is the geodesic. Spherical geodesics are circles whose centre is at the centre of the sphere and whose radius is equal to the radius of the sphere.† The spherical straight line is also called the *great circle*.

Loci of points equidistant from a point on a sphere are also circles, but they are called *small circles*, distinct from spherical lines. In fact, spherical

* Such geometries play an important role in EINSTEIN'S theory of general relativity.

† Some of the statements can be demonstrated at home: take a roughly spherical orange with a thick peel and stick pins or toothpicks into it. The rubber band stretches along the geodesics of the orange.

lines can be considered as special spherical circles with a maximum possible radius. Angles are measured in the usual way between the tangents, while the angle subtended by the vectors from the centre of the sphere to the two points is used to characterize the distance. Coordinates are interpreted here in the geographic coordinate system.

II.2 Notable parts of the sphere

A shape bounded by two concentric small circles and two great circles perpendicular to them is a *geographical quadrangle*. Contrary to its name, it is not a spherical polygon, because only two of its bounding sides are spherical straight sections, the other two are arcs of spherical circles.

The surface area of the quadrangle can be calculated as follows: divide its area into thin bands with concentric (latitude) circles. Then the surface of each band can be approximated by a rectangle whose area is the product of the base and the height (Fig. II.1). It is known that the radius of a parallel is $r = R \cos \varphi$ (Sec. I.3). The length of the arc forming the base is the product of the radius r and the subtended angle (in radians!). However, the subtended angle is the difference in longitude $\lambda_2 - \lambda_1$, so the length of the base is $R \cos \varphi (\widehat{\lambda}_2 - \widehat{\lambda}_1)$. The height of the tiny rectangle is a tiny arc of circle whose length is the product of the change in latitude in radians and the radius of the sphere ($R \widehat{\Delta \varphi}$). Thus, the area of the small rectangle is given by $R^2 (\widehat{\lambda}_2 - \widehat{\lambda}_1) \cos \varphi \widehat{\Delta \varphi}$. Refining the partitioning, the summation of the infinitesimal rectangles becomes an integration between the bounding latitudes φ_1 and φ_2 :

$$A = \int_{\varphi_1}^{\varphi_2} R^2 (\widehat{\lambda}_2 - \widehat{\lambda}_1) \cos \varphi \, d\varphi = R^2 (\widehat{\lambda}_2 - \widehat{\lambda}_1) (\sin \varphi_2 - \sin \varphi_1)$$

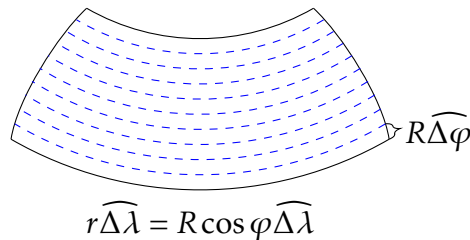


Figure II.1: Dividing the area of a quadrangle into small rectangles

The surface bounded by a spherical small circle is the spherical cap, and the surface between two concentric spherical circles is the spherical

II. Introduction to spherical geometry

zone (Fig. II.2). The surface area of a spherical zone can be calculated simply from the previous formula by substituting $\pm 180^\circ$ for the bounding longitudes:

$$A_{\odot} = R^2[\pi - (-\pi)](\sin \varphi_2 - \sin \varphi_1) = 2R^2\pi(\sin \varphi_2 - \sin \varphi_1)$$

In the formula above, substituting the latitudes of the North and South Poles ($\pm 90^\circ$) for the bounding latitudes gives the surface area of the entire sphere:

$$A_{\circ} = 2\pi R^2[1 - (-1)] = 4R^2\pi$$

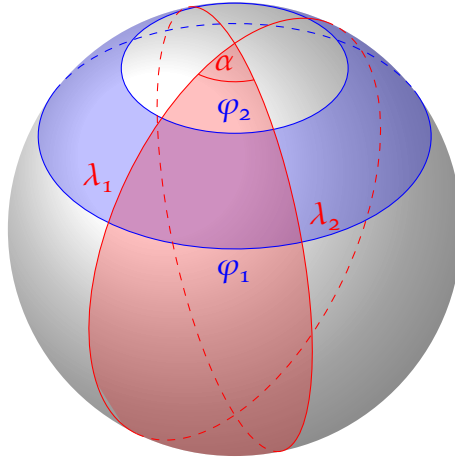


Figure II.2: Zone (blue), lune (red), and quadrangle (purple)

As mentioned earlier, in spherical geometry, any two spherical lines (great circles) intersect each other. In addition, it is observed that two spherical lines have not only one, but two points of intersection, which are *antipodal points* of each other. It is thus possible to construct a spherical polygon bounded by only two spherical sections and two vertices. This shape is called a *spherical lune* (Fig. II.2). The surface area of the lune is in direct proportion to the angle $\widehat{\alpha}$ at the vertex, which is now measured in radians for simplicity. If the angle of the lune is a turn (2π), then it covers the entire surface of the sphere ($4R^2\pi$). From this, we obtain the surface of the lune using proportions:

$$A_0 = 2R^2\widehat{\alpha}$$

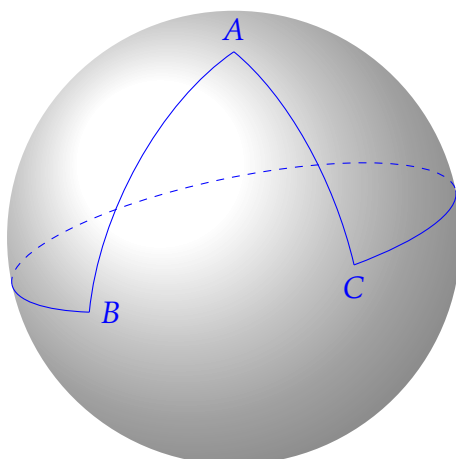


Figure II.3: Concave spherical triangle

II.3 The spherical triangle

The equivalent of a planar triangle on a sphere is called a *spherical triangle*, bounded by three spherical sections. It is possible to construct a spherical triangle that has a concave angle (Fig. II.3); however, we usually do not consider these, and the statements are given for convex spherical triangles.

The area of the triangle is obtained from the formula for the area of the lune. Let us cover the sphere with two antipodal lunes of angle α starting from vertex A . The combined surface area of the two lunes is $4R^2\widehat{\alpha}$. Repeat it for vertices B and C and two of each corresponding lunes of angles β and γ ! Now the combined surface area of the lunes is $4R^2(\widehat{\alpha} + \widehat{\beta} + \widehat{\gamma})$. The six lunes completely cover the surface of the sphere ($4R^2\pi$), but we have managed to cover the triangle in question and its antipodal three times (Fig. II.4). This means that the area of the spherical triangle was covered four times unnecessarily. So if we subtract the surface of the sphere from that of the six spherical lunes ($4R^2(\widehat{\alpha} + \widehat{\beta} + \widehat{\gamma} - \pi)$), we have four times the area of the triangle. From this, it follows that:

$$A_{\Delta} = R^2(\widehat{\alpha} + \widehat{\beta} + \widehat{\gamma} - \pi)$$

From the formula above, we can draw two very important conclusions:

- The *spherical excess* obtained by subtracting 180° from the sum of the interior angles of the triangle is in direct proportion to the surface area of the spherical triangle. So the larger the triangle, the more its properties differ from those of Euclidean geometry.
- The sum of the interior angles of a triangle is always greater than 180° , otherwise the surface would be negative. However, the sum

II. Introduction to spherical geometry

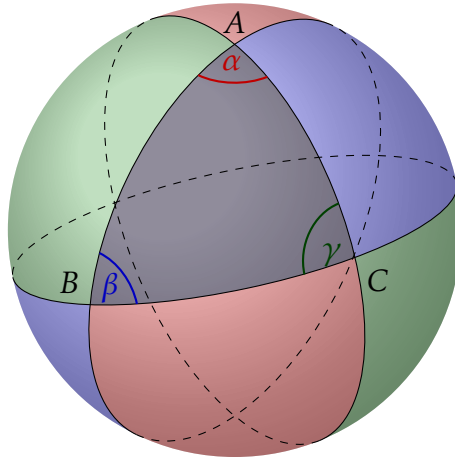


Figure II.4: Calculating the area of a convex spherical triangle using two each of red, blue, and green lunes

of the interior angles of a convex triangle is certainly less than 540° , otherwise at least one of the angles would have to be concave.

Lesson three

Navigation in spherical geometry

III.1 Spherical trigonometry

When examining spherical triangles, we can see that many properties known from Euclidean geometry still hold. For example, the sum of two sides is greater than the third, a larger side corresponds to a larger opposite angle, or three data uniquely define a triangle. In fact, three angles are now sufficient to define a triangle, since the sum of the interior angles is not a fixed value. It can be seen, therefore, that the rules of sines and cosines used to calculate unknown data of planar triangles have counterparts in spherical geometry.

For simplicity, we assume in this section that the sphere has unit radius so that the sides and their subtended angles (in radians) are equal. Furthermore, the Cartesian coordinate system is rotated so that axis z coincides with one vertex of the triangle, while another vertex of the triangle lies on the plane subtended by axes x and z . Then the Cartesian coordinates of the vertices can be simply described using formulæ between the polar and Cartesian coordinates (Fig. III.1. on the next page).

Let us consider case (a) and formulate the volume of the parallelepiped generated by the vectors $\vec{A}, \vec{B}, \vec{C}$ starting from the origin. This is the triple product (determinant) of the three vectors:

$$\begin{vmatrix} 0 & 0 & 1 \\ \sin c & 0 & \cos c \\ \sin b \cos \alpha & \sin b \sin \alpha & \cos b \end{vmatrix} = \sin c \sin b \sin \alpha$$

Case (b) shows the same triangle, but with the coordinate axes rotated. Calculate the volume of the parallelepiped again. This time, it is useful to expand the determinant along the second line:

$$\begin{vmatrix} \sin c \cos \beta & \sin c \sin \beta & \cos \beta \\ 0 & 0 & 1 \\ \sin a & 0 & \cos a \end{vmatrix} = \sin a \sin c \sin \beta$$

III. Navigation in spherical geometry

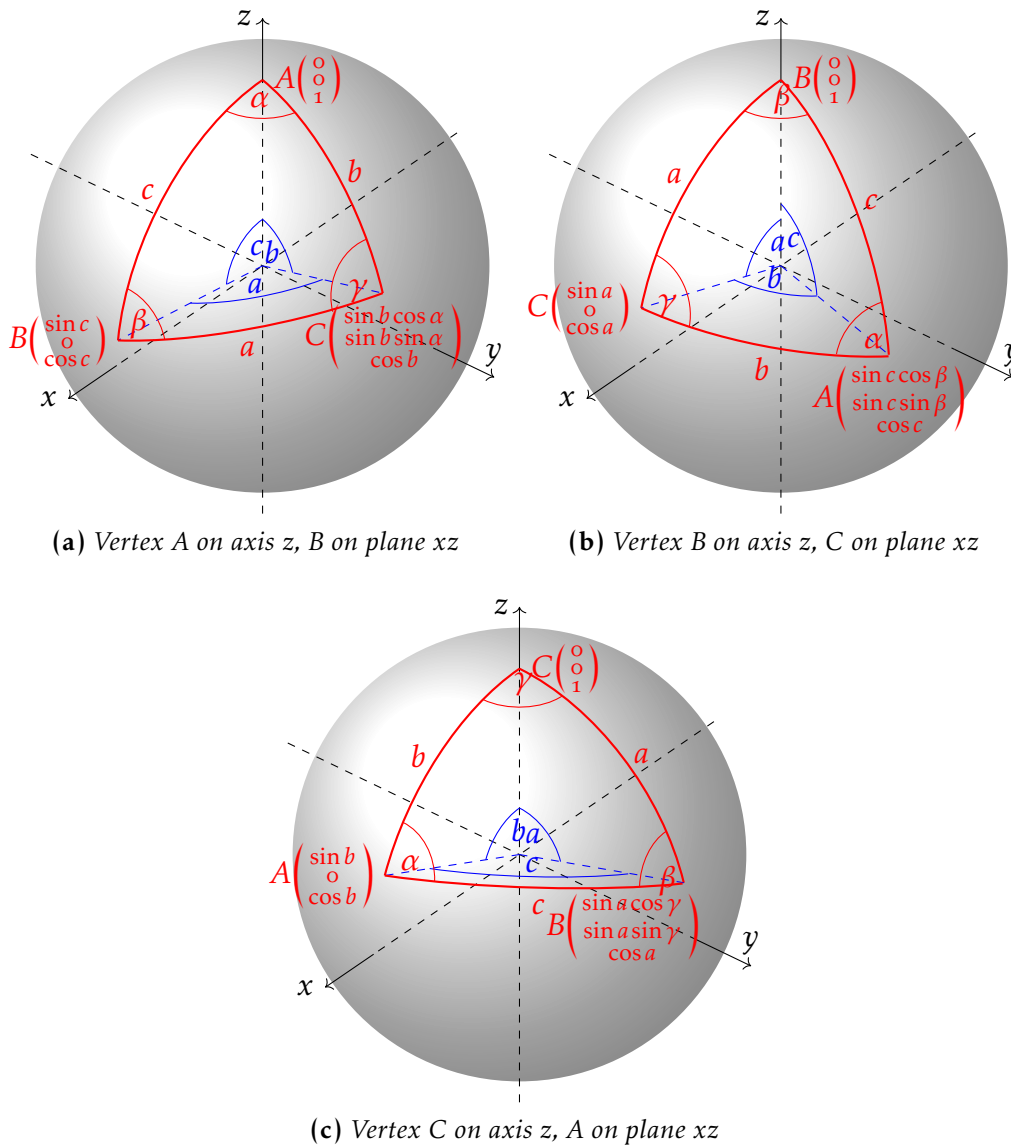


Figure III.1: Cartesian coordinates of vertices in a spherical triangle

III. Navigation in spherical geometry

The volume of the parallelepiped cannot depend on the rotation of the coordinate system. This means that the two previous expressions must be equal to each other:

$$\sin c \sin b \sin \alpha = \sin a \sin c \sin \beta$$

Simplifying by $\sin c$ and rearranging, we get this:

$$\frac{\sin a}{\sin \alpha} = \frac{\sin b}{\sin \beta}$$

The above relation is very similar to the sine rule of Euclidean geometry, so we call it the *spherical rule of sines* and will use it regularly in the following.

Let us also examine the rotation in figure (c). This time, let us form the scalar product of the vectors \vec{A} and \vec{B} . The scalar product can be calculated by multiplying the lengths of the vectors and the cosine of the angle c between them. This is quite simple, since the lengths of \vec{A} and \vec{B} pointing to the surface of a unit sphere are exactly one. However, it is also possible to calculate the scalar product by the pairwise multiplication of the coordinates, and then we should obtain the same result:

$$1 \times 1 \times \cos c = \sin b \times \sin a \cos \gamma + 0 \times \sin a \sin \gamma + \cos b \times \cos a$$

Converted to an easy-to-remember form:

$$\cos c = \cos a \cos b + \sin a \sin b \cos \gamma$$

The equation obtained above is of fundamental importance in cartography. It is called the *spherical rule of cosines*, and it establishes a relationship between three sides and one angle of a triangle, similarly to rule of cosines used in secondary schools.

Since a spherical triangle can be defined by three angles, a formula is missing that allows to determine the length of at least one side based on the three angles. This has no analogy in Euclidean geometry. The missing formula is called the *second spherical rule of cosines*, the proof of which is given in App. B:

$$\cos \gamma = -\cos \alpha \cos \beta + \sin \alpha \sin \beta \cos c$$

The three relations can now be used to compute the unknown data for any spherical triangle, but sometimes several steps are required. For this reason, the *cotangent four-part formula* is useful in rare cases:^{*}

$$\cot a \sin b = \cos b \cos \gamma + \sin \gamma \cot \alpha$$

For all four formulæ, it makes sense to say that it does not matter which vertex of the triangle is denoted by A , B , and C , as long as the corresponding notations a, b, c, α, β , and γ are used consistently.

^{*} For example, it is easier to use it to find the intersection of great circles.

III.2 Orthodromic navigation

An example of the importance of spherical trigonometry is the navigation task of finding the direction and the length of a path between two points of known coordinates. The formulæ derived here are still used in marine navigation and aviation today. Two types of navigation have developed throughout history, orthodromic and loxodromic.

In solving navigation problems, terrestrial geodesics are called *orthodromes*. Its clear advantage is that its formulæ are guaranteed to show the shortest route to your destination. To develop the formulæ for the orthodrome, we will use a spherical triangle with one vertex at the pole and the other two vertices at the origin and destination.

We want to go from point A to point B in Fig. III.2. The angle appearing at the northern vertex of the blue triangle is the difference in longitude $\lambda_B - \lambda_A$. We also know two sides of the triangle, since they supplement the latitude to 90° . Then we can write the rule of cosines for the third side to be calculated, which subtends angle s/R° (converted to degrees) corresponding to the arc length s in question. Note that $\cos(90^\circ - \delta) = \sin \delta$ and $\sin(90^\circ - \delta) = \cos \delta$!

$$\cos \frac{s^\circ}{R} = \sin \varphi_A \sin \varphi_B + \cos \varphi_A \cos \varphi_B \cos(\lambda_B - \lambda_A)$$

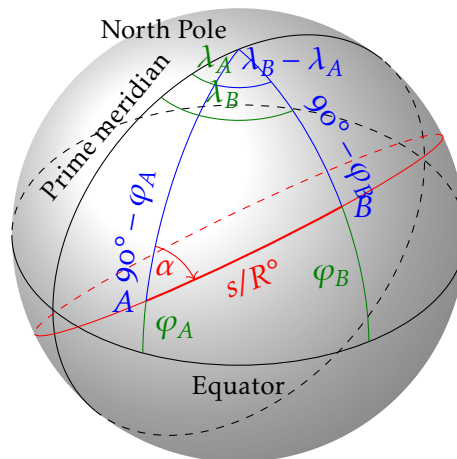


Figure III.2: Calculation of the great-circle distance

In the previous formula, the degree sign next to s/R warns that the angle in degrees must be converted back to radians, and only then multiplied by the radius of the Earth to get the distance s .

III. Navigation in spherical geometry

There are two ways of calculating the direction of the orthodrome, i.e. the *azimuth* defined in Sec. I.2. It is simpler to formulate using the rule of sines:

$$\frac{\sin(s/R)^\circ}{\sin(\lambda_B - \lambda_A)} = \frac{\cos \varphi_B}{\sin \alpha}$$

$$\sin \alpha = \frac{\sin(\lambda_B - \lambda_A) \cos \varphi_B}{\sin(s/R)^\circ}$$

But the rule of cosines is also useful:

$$\sin \varphi_B = \sin \varphi_A \cos \frac{s^\circ}{R} + \cos \varphi_A \sin \frac{s^\circ}{R} \cos \alpha$$

$$\cos \alpha = \frac{\sin \varphi_B - \sin \varphi_A \cos(s/R)^\circ}{\cos \varphi_A \sin(s/R)^\circ}$$

For practical calculations, both formulæ are needed, because neither the sine nor the cosine characterizes the azimuth uniquely: $\sin \alpha = \sin(180^\circ - \alpha)$ and $\cos \alpha = \cos(360^\circ - \alpha)$. Thus, in both cases we have two solutions: for the sine rule, α and $180^\circ - \alpha$; for cosine rule, α and $360^\circ - \alpha$. One of the two roots is false, so we have to consider which solution to accept. Note that negative azimuths are not used, so if the result of the arc sine is negative, either 360° must be added to the value or it must be subtracted from 180° . The correct decision can be made by drawing, or by using both formulæ to calculate the two solutions for the azimuth, because in this case there is usually only one common root.

In addition, the sine varies only slightly for nearly right angles for large differences in the angle, while the same can be said for the cosine for nearly straight angles. Thus, for east-west paths, the rule of cosines, while for north-south paths, the rule of sines provides more numerical stability.

III.3 Loxodromic navigation

Spirals with constant azimuth on a surface of revolution are called *rhumb lines*. Such curves connecting two points are usually longer than the geodesic.* These lines are called *loxodromes* on Earth. It can be seen that the meridians on a surface of revolution are not only orthodromes, but also loxodromes corresponding to azimuth 0° . Although parallels are typically not orthodromes, they are loxodromes of azimuth 90° . The Equator is an exception because it is both an orthodrome and a loxodrome.

* Except on the cylinder, where geodesics and rhumb lines always coincide.

III. Navigation in spherical geometry

The navigational importance of the loxodrome is that our heading may maintain a constant bearing to the compass, which is easily achieved. Counter-intuitively, to do this, you have to keep turning the vehicle (Fig. III.3).^{*} It is typically barely longer than the orthodrome, and in the pre-GPS era, the changing azimuth of the orthodrome would have been difficult to follow, so it used to be popular among sailors. Today's air navigation has moved to more economical, orthodromic navigation.[†]

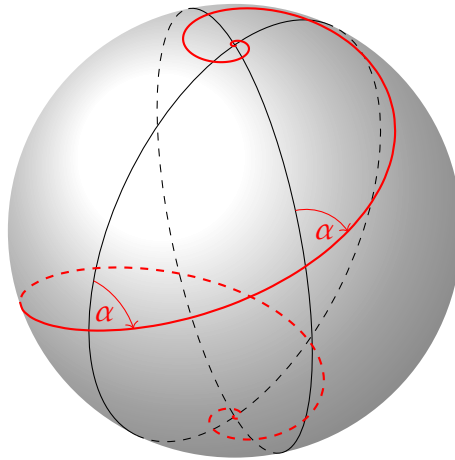


Figure III.3: *The path of a rhumb line*

Plot an infinitesimal section of length Δs along the loxodrome of azimuth α . The arc lengths along the parallel and meridian (small arcs of circles) can be calculated from the radii of the corresponding parallel and meridian and from the subtended angles. Fig. III.4 clearly shows that:

$$\tan \alpha = \frac{R \cos \varphi \widehat{\Delta \lambda}}{R \widehat{\Delta \varphi}}$$

$$\frac{\widehat{\Delta \varphi} \tan \alpha}{\cos \varphi} = \widehat{\Delta \lambda}$$

^{*} Loxodromes are usually spiral curves. Before reaching the pole, they wind around it infinitely many times in sharper turns, yet their length is still finite.

[†] This is only partly true: points are calculated along the orthodrome, but traffic between two calculated points still follows the loxodrome. This technique was used to a limited extent before GPS.

III. Navigation in spherical geometry

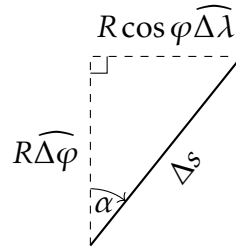


Figure III.4: An infinitesimal section of a loxodrome

Integrate both sides between the starting point A and the end point B , knowing that α is constant:

$$\int_{\varphi_A}^{\varphi_B} \frac{\tan \alpha}{\cos \varphi} d\varphi = \int_{\lambda_A}^{\lambda_B} d\lambda$$

$$\tan \alpha \left[\ln \tan \left(45^\circ + \frac{\varphi_B}{2} \right) - \ln \tan \left(45^\circ + \frac{\varphi_A}{2} \right) \right] = \widehat{\lambda}_B - \widehat{\lambda}_A$$

$$\tan \alpha = \frac{\widehat{\lambda}_B - \widehat{\lambda}_A}{\ln \tan(45^\circ + \varphi_B/2) - \ln \tan(45^\circ + \varphi_A/2)}$$

So we have found the azimuth of the loxodrome between points A and B . However, it is important to note that this time we have two solutions: $\tan \alpha = \tan(180^\circ + \alpha)$. Whether we need to add 180° is a matter of common sense. The arc tangent function of the calculator can also give a negative value, in which case we need to add 180 or 360 degrees (again, using common sense to decide which).

It is important to note that the difference of longitudes in the numerator is always calculated strictly in radians! The difference in longitudes must always be within the range $\pm 180^\circ$ ($\pm \pi$)! Larger longitude differences for paths crossing meridian 180° must be constrained within the range by adding or subtracting 360° (2π)!

In the previous calculation, the antiderivative of $1/\cos \varphi$ was substituted without derivation, so check this by differentiating!

$$\left[\ln \tan \left(45^\circ + \frac{\varphi}{2} \right) \right]' = \frac{1}{2 \tan \left(45^\circ + \frac{\varphi}{2} \right) \cos^2 \left(45^\circ + \frac{\varphi}{2} \right)}$$

$$= \frac{1}{2 \sin \left(45^\circ + \frac{\varphi}{2} \right) \cos \left(45^\circ + \frac{\varphi}{2} \right)} = \frac{1}{\sin(90^\circ + \varphi)} = \frac{1}{\cos \varphi}$$

III. Navigation in spherical geometry

Note that some textbooks do not write the antiderivative of $1/\cos \varphi$ as $\ln \tan(45^\circ + \varphi)$, but as a seemingly very different expression, but a simple transformation yields it:

$$\begin{aligned} \ln \tan\left(45^\circ + \frac{\varphi}{2}\right) &= \ln \sqrt{\frac{2 \sin^2\left(45^\circ + \frac{\varphi}{2}\right)}{2 \cos^2\left(45^\circ + \frac{\varphi}{2}\right)}} \\ &= \frac{1}{2} \ln \frac{\sin^2\left(45^\circ + \frac{\varphi}{2}\right) + \cos^2\left(45^\circ + \frac{\varphi}{2}\right) + \sin^2\left(45^\circ + \frac{\varphi}{2}\right) - \cos^2\left(45^\circ + \frac{\varphi}{2}\right)}{\cos^2\left(45^\circ + \frac{\varphi}{2}\right) + \sin^2\left(45^\circ + \frac{\varphi}{2}\right) + \cos^2\left(45^\circ + \frac{\varphi}{2}\right) - \sin^2\left(45^\circ + \frac{\varphi}{2}\right)} \\ &= \frac{1}{2} \ln \frac{1 - \cos(90^\circ + \varphi)}{1 + \cos(90^\circ + \varphi)} = \frac{1}{2} \ln \frac{1 + \sin \varphi}{1 - \sin \varphi} = \operatorname{artanh} \sin \varphi \end{aligned}$$

So, the formula can be written in this form:

$$\tan \alpha = \frac{\widehat{\lambda}_B - \widehat{\lambda}_A}{\operatorname{artanh} \sin \varphi_B - \operatorname{artanh} \sin \varphi_A}$$

We still do not know how far we have to travel. To calculate the distance, let us formulate the cosine of α from the figure:

$$\begin{aligned} \cos \alpha &= \frac{R \widehat{\Delta \varphi}}{\Delta s} \\ \Delta s &= \frac{R \widehat{\Delta \varphi}}{\cos \alpha} \end{aligned}$$

Let us integrate both sides again, α is still constant, and the constant of integration on the left side can be omitted, because s is zero at the starting point:

$$\begin{aligned} \int ds &= \int_{\varphi_A}^{\varphi_B} \frac{R}{\cos \alpha} d\varphi \\ s &= R \frac{\widehat{\varphi}_B - \widehat{\varphi}_A}{\cos \alpha} \end{aligned}$$

If the distance is negative, check that we have not swapped the starting and ending points during the process, or forgotten the signs of the hemispheres and have constrained the difference in longitudes $\widehat{\lambda}_B - \widehat{\lambda}_A$ within the range $\pm\pi$ by adding or subtracting 2π . If neither, then we have chosen the wrong one of the two solutions for the azimuth. Then add 180° to α and invert the sign of s .

III. Navigation in spherical geometry

For formulæ of both the loxodrome and the orthodrome, it is very important to use the correct signs. Our formulæ give the correct result if we substitute north latitude and east longitude with positive signs and south latitude and west longitude with negative signs. Failure to do so for paths crossing the Equator or the Prime meridian will lead to a serious error! Among formulæ discussed so far, this remark is also true for the area of the geographical quadrangle.

Lesson four

Curvature and arc length on the ellipsoid

IV.1 Meridional radius of curvature

The spherical geometry discussed so far was based on a surface of constant curvature. This cannot be said for the ellipsoid of revolution, whose curvature varies from place to place. The internal scale relations of such surfaces are discussed by the discipline of *differential geometry*. Let us first define some necessary concepts.

The *osculating circle* of a smooth plane curve at a given point is the circle tangent to the curve at the point in question, its tangent coincides with that of the curve (so its centre is on the normal of the curve) and its second derivative is equal to that of the curve at the point. The latter causes the tangents of the curve and the osculating circle to be close to each other near the point (Fig. IV.1), so if one draws perpendiculars to the curve close to the point, their intersection will tend to the centre of the osculating circle. The *radius of curvature* of the curve at a point is the radius of the osculating circle at that point.

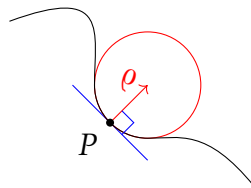


Figure IV.1: The radius of curvature ρ of a plane curve at point P

The curve obtained as the intersection of a surface and an arbitrary plane is called the *section* of the surface. All sections of an ellipsoid of revolution are ellipses. The *normal section* of a surface at a point is the section whose plane contains the point and the normal (local vertical) of the surface. All other sections containing the point are called *oblique sections*. The *radius*

IV. Curvature and arc length on the ellipsoid

of curvature of a surface for a given point and direction is the radius of curvature of the normal section that passes through that point and its plane contains that direction. We will consider normal sections containing and perpendicular to meridians.*

The *meridional radius of curvature*, denoted by $M(\Phi)$, is the radius of curvature on the ellipsoid in the direction of meridians (Fig. IV.2) Consider a point at latitude Φ on the meridian and plot perpendiculars at latitudes $\Phi_1 = \Phi - \Delta\Phi/2$ and $\Phi_2 = \Phi + \Delta\Phi/2$, as $\Delta\Phi \rightarrow 0$! To calculate the angle subtended by the arc of the osculating circle between latitudes Φ_1 and Φ_2 , consider the triangle of blue legs in part (b). Its upper right angle is Φ_1 and its upper left angle is $180^\circ - \Phi_2$. The sum of the interior angles is 180° , so the third angle must be $\Phi_2 - \Phi_1 = \Delta\Phi$. Multiplying this by radius $M(\Phi)$ gives the small arc length of the osculating circle between the two points: $M(\Phi)\widehat{\Delta\Phi}$.

The limit of the secant passing through latitudes Φ_1 and Φ_2 is the tangent and is therefore perpendicular to the normal at latitude Φ . The other arm of the upper angle in the right triangle at part (c) is perpendicular to the plane of the Equator, so this angle is equal to Φ . From this, the chord length between the two outer points is $-\Delta r/\sin \Phi$, where the horizontal leg Δr is the tiny change in the radius of the parallel with respect to the difference in latitude $\Delta\Phi$ (the negative sign in the formula makes the chord length positive: Δr is negative in the Northern Hemisphere, while $\sin \Phi$ is negative in the Southern Hemisphere). If $\Delta\Phi \rightarrow 0$, the distance between these two points along the osculating circle and the chord is the same:

$$\lim_{\Delta\Phi \rightarrow 0} M(\Phi)\widehat{\Delta\Phi} = \lim_{\Delta\Phi \rightarrow 0} \frac{-\Delta r}{\sin \Phi}$$

Recall that we have already calculated the radius r of the parallel in Sec. I.4!

$$\begin{aligned} r &= \frac{a^2 \cos \Phi}{\sqrt{a^2 \cos^2 \Phi + b^2 \sin^2 \Phi}} = \frac{a \cos \Phi}{\sqrt{\cos^2 \Phi + \frac{b^2}{a^2} \sin^2 \Phi}} \\ &= \frac{a \cos \Phi}{\sqrt{1 - \sin^2 \Phi + \frac{b^2}{a^2} \sin^2 \Phi}} = \frac{a \cos \Phi}{\sqrt{1 - e^2 \sin^2 \Phi}} \end{aligned}$$

* The reason why it is sufficient to consider the curvature of these two directions is deeply rooted in the foundations of differential geometry: the German mathematician GAUSS showed that if we know the extremal values of the curvatures at a given point on a surface, we can calculate the curvature of the smooth elementary surface in any direction. He also proved that the minimum and maximum curvatures always occur in directions perpendicular to each other, and that on surfaces of revolution the direction of one of the extrema is always in the plane of the meridian.

IV. Curvature and arc length on the ellipsoid

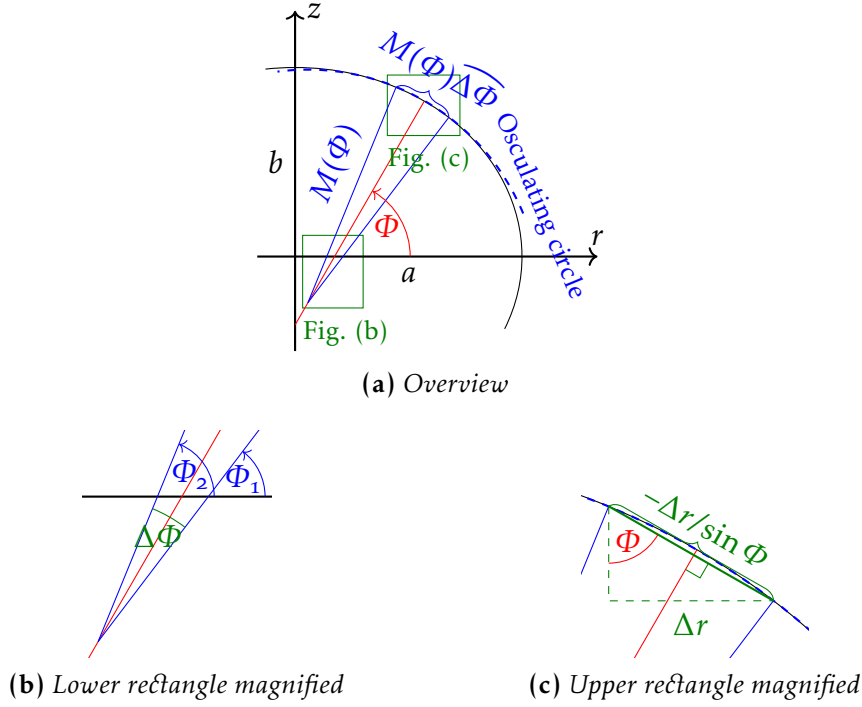


Figure IV.2: Calculating the meridional radius of curvature

From the first equation, $M(\Phi)$ can be expressed, using that the limit of $\Delta r/\Delta\Phi$ is the derivative:

$$\begin{aligned}
 M(\Phi) &= \lim_{\Delta\Phi \rightarrow 0} \frac{-\Delta r}{\Delta\Phi \sin \Phi} = \frac{-1}{\sin \Phi} \frac{dr}{d\Phi} \\
 &= \frac{-1}{\sin \Phi} \frac{-a \sin \Phi \sqrt{1 - e^2 \sin^2 \Phi} - a \cos \Phi \frac{-2e^2 \sin \Phi \cos \Phi}{2\sqrt{1 - e^2 \sin^2 \Phi}}}{1 - e^2 \sin^2 \Phi} \\
 &= a \frac{1 - e^2 \sin^2 \Phi - e^2 \cos^2 \Phi}{(1 - e^2 \sin^2 \Phi)^{3/2}} = \frac{a(1 - e^2)}{(1 - e^2 \sin^2 \Phi)^{3/2}}
 \end{aligned}$$

Now also calculate the arc length of the meridian between latitudes Φ_1 and Φ_2 ! To do this, we split the arc of the ellipse into tiny segments approximated by arcs of circles. In the previous derivation, we obtained $\Delta s = M(\Phi)\Delta\Phi$ for the small arc length (Fig. IV.3). Refining partitions, the summation becomes an integration:

$$s = \int_{\Phi_1}^{\Phi_2} M(\Phi) d\Phi = \int_{\Phi_1}^{\Phi_2} \frac{a(1 - e^2)}{(1 - e^2 \sin^2 \Phi)^{3/2}} d\Phi$$

IV. Curvature and arc length on the ellipsoid

The antiderivative of the integrand above cannot be formulated using standard mathematical functions because it is an *elliptic integral**. It can be solved by numerical approximation or by using tables. Modern GIS typically uses FOURIER series for approximation.

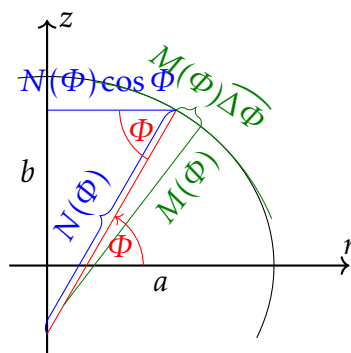


Figure IV.3: Radii of curvature on the ellipsoid of revolution

IV.2 Prime-vertical radius

The radius of curvature of the normal section perpendicular to the meridian is the *transverse* or *prime-vertical radius of curvature*, denoted by $N(\Phi)$. Before calculating it, perform a thought experiment on an arbitrary surface of revolution. Select two points symmetrically on a normal section perpendicular to the meridian of the point in question. From each of these two points, drop a perpendicular line onto the surface. Then, due to symmetry, the intersection of the two lines must lie on the axis of rotation. Now approach the two points simultaneously and symmetrically towards the point in question. The normals at the two points will then be closer and closer to the plane of the normal section, while their intersection will remain on the axis of revolution. It follows that centre of osculating circle is also on the axis of revolution. In this case, it can be seen from the figure that the radius

* Elliptic integrals are called as such, because they were first discovered when the circumference of an ellipse was computed. Since then, they have been found to occur in countless fields of science. They can be used to derive the formula for many conformal projections elegantly. See Sec. XXIX.1.

IV. Curvature and arc length on the ellipsoid

r of the parallel is $r = N(\Phi) \cos \Phi$.^{*} From the previous formula for r :

$$N(\Phi) = \frac{a}{\sqrt{1 - e^2 \sin^2 \Phi}}$$

The arc length along parallels of radius r on an ellipsoid of revolution between longitudes Λ_1 and Λ_2 can be formulated as the product of the radius and the subtended angle:

$$s = N(\Phi) \cos \Phi (\widehat{\Lambda_2} - \widehat{\Lambda_1})$$

IV.3 Latitude, longitude, and height in space

Satellite navigation measures the distance between the satellite and the instrument based on the time the signal is received. The known distance from each satellite represents a sphere. We are at the common intersection point of them. The coordinates of the intersection point can be calculated in an x, y, z Cartesian coordinate system. How do we get geographic coordinates from this?

Less exciting, but equally useful, is the question of obtaining the Cartesian coordinates of a point from its geographic coordinates. This may be needed if we want to treat points referenced to differently sized and positioned ellipsoids in a uniform coordinate system. It is easy to see that the two problems are the inverse of each other.

Dealing first with the second problem, let us plot the ellipsoidal meridian on which we are located on the plane r, z . Here, the horizontal coordinate r on the surface of the ellipsoid will coincide exactly with the radius of the parallel, and z will coincide with the axis z of the spatial system. We are at latitude Φ and height h above the ellipsoid. Assuming a small height, we measure the height in a straight line perpendicular to the ellipsoid. Then we can read from Fig. IV.4:

$$\begin{aligned} r &= r_0 + h \cos \Phi \\ z &= z_0 + h \sin \Phi \end{aligned}$$

^{*} Here we have in fact proven a special case of MEUSNIER'S theorem, well known in differential geometry. This theorem is not only true for a surface of revolution, and the ratio between the radii of curvature of any normal section and oblique section tangent to each other at the point in question is found to be the cosine of the angle between the planes of the sections.

IV. Curvature and arc length on the ellipsoid

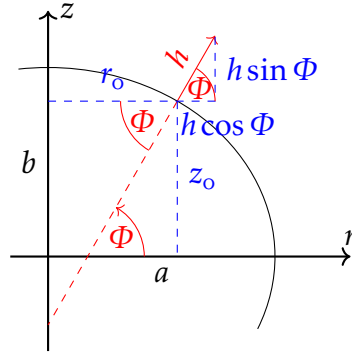


Figure IV.4: Coordinates of a point at height h above ellipsoid

The radius r_0 of the parallel is already known ($N(\Phi)\cos\Phi$), and the formula z_0 has already been calculated in Sec. I.4, which we now rearrange:

$$\begin{aligned} z_0 &= \frac{b^2 \sin \Phi}{\sqrt{a^2 \cos^2 \Phi + b^2 \sin^2 \Phi}} = \frac{a^2(1-e^2) \sin \Phi}{\sqrt{a^2 \cos^2 \Phi + b^2 \sin^2 \Phi}} \\ &= \frac{a(1-e^2) \sin \Phi}{\sqrt{1-e^2 \sin^2 \Phi}} = (1-e^2)N(\Phi) \sin \Phi \end{aligned}$$

We know from the definition of longitude (Sec. I.3) that $x = r \cos \Lambda$ and $y = r \sin \Lambda$. Knowing this, we can use the previous relation to calculate:

$$\begin{aligned} x &= [N(\Phi) + h] \cos \Phi \cos \Lambda \\ y &= [N(\Phi) + h] \cos \Phi \sin \Lambda \\ z &= [(1-e^2)N(\Phi) + h] \sin \Phi \end{aligned}$$

Now we know where a point of a given geographic coordinate is located in the Cartesian coordinate system. For the other problem (i.e. GPS navigation), we need to invert this. Dividing the second equation by the first one gives us:

$$\tan \Lambda = \frac{y}{x}$$

So we already know the longitude. The squared sum of the first and second equations:

$$\begin{aligned} x^2 + y^2 &= [N(\Phi) + h]^2 \cos^2 \Phi \\ h &= \frac{\sqrt{x^2 + y^2}}{\cos \Phi} - N(\Phi) \end{aligned}$$

IV. Curvature and arc length on the ellipsoid

Substitute this into the formula z :

$$z = \left[\frac{\sqrt{x^2 + y^2}}{\cos \Phi} - e^2 N(\Phi) \right] \sin \Phi$$

Transforming the formula above, we get a quartic equation of $\tan \Phi$. The quartic equation can be solved, for example, by FERRARI'S method, the derivation for which is given in App. C. Then, knowing Φ , h can be obtained from the formula before the previous one. It is important to note that h is not measured above the sea level, but is the height above ellipsoid, which is corrected by the value of geoid undulation by our GPS device.

The derivation of closed conversion formulæ is credited to BORKOWSKI. Although closed formulæ are more commonly used in modern satellite navigation, for ease of computation, BOWRING'S formula is also given, which gives an approximation to Φ that can be refined to an arbitrary precision. The recursive formula:

$$\tan \Phi'' = \frac{z + (e')^2 b \sin^3 \Theta'}{\sqrt{x^2 + y^2} - e^2 a \cos^3 \Theta'}$$

Where the parametric latitude $\tan \Theta = b/a \tan \Phi$ converted from the corrected Φ (Sec. I.4) is substituted back into the formula above to get a further corrected Φ . The proposed initial value of Θ is derived from the condition $h \approx 0$:

$$\tan \Theta \approx \frac{az}{b\sqrt{x^2 + y^2}}$$

In general, even one iteration gives surprisingly good accuracy.

IV.4 Area of the ellipsoidal quadrangle

Another possible use of radii of curvature is to calculate the surface area of the ellipsoidal geographical quadrangle. Recall that on a sphere, this could be calculated by partitioning the sphere into small rectangles as illustrated in Fig. II.1. The only difference is that now the length of the base parallel is $N(\Phi) \cos \Phi (\widehat{\Lambda_2} - \widehat{\Lambda_1})$, while the length of the tiny meridian arc on the

IV. Curvature and arc length on the ellipsoid

ellipsoid is $M(\Phi)\widehat{\Delta\Phi}$. The summation of the small rectangles is also an integration:

$$\begin{aligned} A &= \int_{\Phi_1}^{\Phi_2} M(\Phi)N(\Phi) \cos \Phi (\widehat{\Lambda}_2 - \widehat{\Lambda}_1) d\Phi \\ &= a^2(1-e^2)(\widehat{\Lambda}_2 - \widehat{\Lambda}_1) \int_{\Phi_1}^{\Phi_2} \frac{\cos \Phi}{(1-e^2 \sin^2 \Phi)^2} d\Phi \end{aligned}$$

The antiderivative of the integrand:

$$\begin{aligned} &\int \frac{\cos \Phi}{(1-e^2 \sin^2 \Phi)^2} d\Phi \\ &= \int \frac{\cos \Phi + e^2 \sin^2 \Phi \cos \Phi}{2(1-e^2 \sin^2 \Phi)^2} + \frac{\cos \Phi(1-e^2 \sin^2 \Phi)}{2(1-e^2 \sin^2 \Phi)^2} d\Phi \\ &= \int \frac{\cos \Phi + e^2 \sin^2 \Phi \cos \Phi}{2(1-e^2 \sin^2 \Phi)^2} + \frac{e \cos \Phi}{2e(1-e^2 \sin^2 \Phi)} d\Phi \\ &= \frac{\sin \Phi}{2(1-e^2 \sin^2 \Phi)} + \frac{1}{2e} \operatorname{artanh}(e \sin \Phi) + c \end{aligned}$$

The last step can be checked by deriving back. Knowing that the area hyperbolic tangent can be written as $1/2 \ln[(1+x)/(1-x)]$, we can substitute it back into the equation, obtaining the formula for the surface of the quadrangle:

$$\begin{aligned} A &= a^2(1-e^2)(\widehat{\Lambda}_2 - \widehat{\Lambda}_1) \left[\frac{\sin \Phi_2}{2(1-e^2 \sin^2 \Phi_2)} \right. \\ &\quad \left. + \frac{1}{4e} \ln \frac{1+e \sin \Phi_2}{1-e \sin \Phi_2} - \frac{\sin \Phi_1}{2(1-e^2 \sin^2 \Phi_1)} - \frac{1}{4e} \ln \frac{1+e \sin \Phi_1}{1-e \sin \Phi_1} \right] \end{aligned}$$

Substituting $\pm 180^\circ$ for the longitudes and $\pm 90^\circ$ for the latitudes gives the surface of the entire ellipsoid:

$$A_{\circ} = 4a^2 \pi (1-e^2) \left[\frac{1}{2(1-e^2)} + \frac{1}{4e} \ln \frac{1+e}{1-e} \right] = 2a^2 \pi \left(1 + \frac{1-e^2}{2e} \ln \frac{1+e}{1-e} \right)$$

Lesson five

Geodetic problems

V.1 Geodetic problems on the plane

Geodetic instruments are mainly used to measure distance and angle (direction), while we need the coordinates of the measured point. It is therefore very common to determine the coordinates of an unknown point in terms of the azimuth and distance measured from a point. This is called the *first* or *direct geodetic problem*. For the orientation of instruments and for the determination of the North direction, we reverse this, and we calculate distance and azimuth from coordinates. This is the *second* or *inverse geodetic problem*.

Our measurements are most often made at such small distances that we can neglect the curvature of the Earth and use the formulæ of ordinary Euclidean plane geometry. Let us look at Fig. V.1. The formulæ for the direct geodetic problem are easy to read (for distance s and azimuth α):

$$x_B = x_A + s \sin \alpha$$

$$y_B = y_A + s \cos \alpha$$

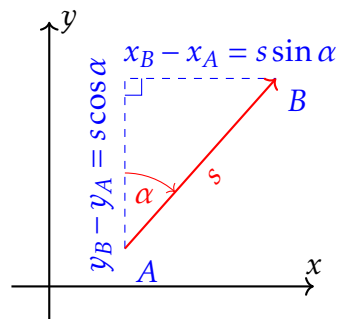


Figure V.1: Geodetic problems on the plane

The formulæ of the inverse problem are derived from the Pythagorean theorem:

$$s = \sqrt{(x_B - x_A)^2 + (y_B - y_A)^2}$$

$$\tan \alpha = \frac{x_B - x_A}{y_B - y_A}$$

We have two solutions for the azimuth, because the period of the tangent is 180° . So we may need to add 180° (or 360°) to the result. The function \arctan_2 was invented for the discussion between the two solutions. The exact syntax is different in every programming language, usually a comma or semicolon is written in place of the fraction bar: $\text{atan}_2(\Delta x, \Delta y)$ instead of $\text{atan}(\Delta x/\Delta y)$, but in Excel, for example, the order of the denominator and numerator is reversed. Always check the manual of the programming language! Beware that this can also give a negative result, in which case 360° must be added. It is not always correct to use \arctan_2 instead of \arctan ! This is specifically for calculating azimuth, but it can also be used for formulæ involving the tangent of longitude.

V.2 Geodetic problems on the sphere

To calculate the spherical geodetic problems, return to Fig. III.2. For the first problem, φ_A, λ_A, s and α are known, the question is the position of point B . Apply the spherical rule of cosines for the unknown φ_B .

$$\sin \varphi_B = \sin \varphi_A \cos \frac{s^\circ}{R} + \cos \varphi_A \sin \frac{s^\circ}{R} \cos \alpha$$

The degree sign warns that in the formula, s/R is always in radians, if the calculator is set to degrees, it must be converted from radians to degrees! Now we can apply the spherical rule of sines for the unknown difference in longitude.

$$\frac{\cos \varphi_B}{\sin \alpha} = \frac{\sin(s/R)^\circ}{\sin(\lambda_B - \lambda_A)}$$

$$\lambda_B = \lambda_A + \arcsin \frac{\sin \alpha \sin(s/R)^\circ}{\cos \varphi_B}$$

Note that the two-valued arc sine is not a problem here, because longitude differences greater than $\pm 90^\circ$ are extremely rare in geodetic practice.

The second problem, the calculation of distance and azimuth on a sphere, has already been covered in Sec. III.2, so it will not be discussed again.

With regard to the calculation on computers, let me add the suggestion that azimuth can be obtained from the cotangent four-part formula. This expression is suitable to apply the function arctan2 so that the two-valued formulæ can be resolved:

$$\begin{aligned} \tan \varphi_B \cos \varphi_A &= \sin \varphi_A \cos(\lambda_B - \lambda_A) + \sin(\lambda_B - \lambda_A) \cot \alpha \\ \frac{\tan \varphi_B \cos \varphi_A - \sin \varphi_A \cos(\lambda_B - \lambda_A)}{\cot \alpha} &= \sin(\lambda_B - \lambda_A) \\ \tan \alpha &= \frac{\sin(\lambda_B - \lambda_A)}{\tan \varphi_B \cos \varphi_A - \sin \varphi_A \cos(\lambda_B - \lambda_A)} \end{aligned}$$

V.3 Metacoordinates

A special application of the spherical problems of geodesy is the *graticule rotation*, which means that not the Earth's axis of rotation but an arbitrarily chosen other axis is considered to be the axis of revolution (Fig. V.2). The poles so designated are called *metapoles*, and the corresponding coordinates are called the *metacoordinates*. Its two parameters (*metalatitude* and *metalongitude*) are distinguished from the geographic coordinates by a prime. The positioning of the rotated system is given by the geographic coordinates of the *metapole*. The prime metameridian is defined as always passing through the North Pole.*

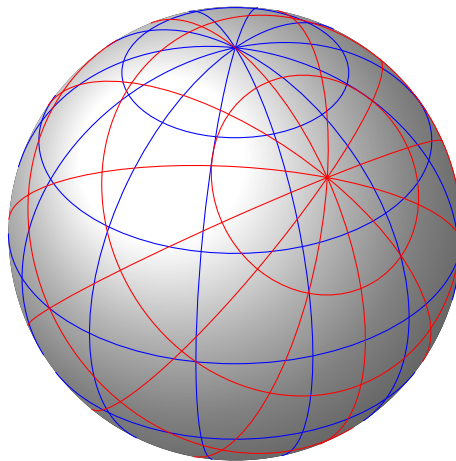


Figure V.2: Rotating the graticule

* It only makes sense to use a different placement in non-conical projections. See Sec. XIX.2.

dividing them by each other and then substituting $\sin \varphi'$:

$$\begin{aligned}
 \tan \lambda' &= \frac{-\frac{\sin(\lambda-\lambda_0)\cos\varphi}{\cos\varphi'}}{\frac{\sin\varphi - \sin\varphi' \sin\varphi_0}{\cos\varphi' \cos\varphi_0}} \\
 &= \frac{-\sin(\lambda-\lambda_0)\cos\varphi\cos\varphi_0}{\sin\varphi - [\sin\varphi\sin\varphi_0 + \cos\varphi\cos\varphi_0\cos(\lambda-\lambda_0)]\sin\varphi_0} \\
 &= \frac{-\sin(\lambda-\lambda_0)\cos\varphi\cos\varphi_0}{\sin\varphi - \sin\varphi(1-\cos^2\varphi_0) - \cos\varphi\cos\varphi_0\cos(\lambda-\lambda_0)\sin\varphi_0} \\
 &= \frac{-\sin(\lambda-\lambda_0)\cos\varphi\cos\varphi_0}{\sin\varphi - \sin\varphi + \sin\varphi\cos^2\varphi_0 - \cos\varphi\cos(\lambda-\lambda_0)\cos\varphi_0\sin\varphi_0} \\
 &= \frac{-\sin(\lambda-\lambda_0)}{\tan\varphi\cos\varphi_0 - \cos(\lambda-\lambda_0)\sin\varphi_0}
 \end{aligned}$$

The resulting formula is suitable for using the function $\arctan 2$ so that λ' can be uniquely determined.

The formulæ for the inverse calculation (this is essentially the first geodetic problem) can be derived in the same way:

$$\begin{aligned}
 \sin\varphi &= \sin\varphi' \sin\varphi_0 + \cos\varphi' \cos\varphi_0 \cos\lambda' \\
 \tan(\lambda-\lambda_0) &= \frac{-\sin\lambda'}{\tan\varphi' \cos\varphi_0 - \cos\lambda' \sin\varphi_0}
 \end{aligned}$$

Sometimes it may also be useful to add additional relations. Rearranging the rule of sines for λ' :

$$\sin\lambda' \cos\varphi' = -\sin(\lambda-\lambda_0)\cos\varphi$$

Furthermore, from the previous relations:

$$\begin{aligned}
 \cos\lambda' \cos\varphi' &= \frac{\sin\lambda' \cos\varphi'}{\tan\lambda'} = \frac{-\sin(\lambda-\lambda_0)\cos\varphi}{\frac{-\sin(\lambda-\lambda_0)}{\tan\varphi\cos\varphi_0 - \cos(\lambda-\lambda_0)\sin\varphi_0}} \\
 &= \cos\varphi [\tan\varphi\cos\varphi_0 - \sin\varphi_0\cos(\lambda-\lambda_0)] \\
 &= \sin\varphi\cos\varphi_0 - \cos\varphi\sin\varphi_0\cos(\lambda-\lambda_0)
 \end{aligned}$$

In transverse aspect ($\varphi_0 = 0$), the formulæ are greatly simplified since $\sin\varphi_0 = 0$ and $\cos\varphi_0 = 1$:

$$\begin{aligned}
 \sin\varphi' &= \cos\varphi\cos(\lambda-\lambda_0) \\
 \sin\lambda' &= \frac{\sin(\lambda-\lambda_0)\cos\varphi}{\cos\varphi'} = \frac{\sin(\lambda-\lambda_0)\cos\varphi}{\sqrt{1-\cos^2\varphi\cos^2(\lambda-\lambda_0)}} \\
 \cos\lambda' &= -\frac{\sin\varphi}{\cos\varphi'} = -\frac{\sin\varphi}{\sqrt{1-\cos^2\varphi\cos^2(\lambda-\lambda_0)}}
 \end{aligned}$$

The sign of trigonometric functions of λ' has just been reversed because otherwise the resulting maps would be oriented south-up, not north-up.

The other possibility is when the intersection of the metaequator and the prime metameridian is known. Look at Fig. V.4. The reader may notice that only two data of the spherical triangle have changed compared to the previous one: instead of $90^\circ - \varphi_0$, the corresponding side is φ_c , so $\cos \varphi_c$ should be written instead of $\sin \varphi_0$ and vice versa $\sin \varphi_c$ should be written instead of $\cos \varphi_0$. The other difference is that the angle at the pole is $180^\circ + \lambda_c - \lambda$ instead of $\lambda_0 - \lambda$. Because of the latter, we substitute $-\cos(\lambda - \lambda_c)$ for $\cos(\lambda - \lambda_0)$ and $\sin(\lambda - \lambda_c)$ for $-\sin(\lambda - \lambda_0)$ (of course, the formulæ will be the same if derived again as before):

$$\begin{aligned}\sin \varphi' &= \sin \varphi \cos \varphi_c - \cos \varphi \sin \varphi_c \cos(\lambda - \lambda_c) \\ \tan \lambda' &= \frac{\sin(\lambda - \lambda_c)}{\tan \varphi \sin \varphi_c + \cos(\lambda - \lambda_c) \cos \varphi_c} \\ \sin \varphi &= \sin \varphi' \cos \varphi_c + \cos \varphi' \sin \varphi_c \cos \lambda' \\ \tan(\lambda - \lambda_c) &= \frac{\sin \lambda'}{\tan \varphi' \sin \varphi_c - \cos \lambda' \cos \varphi_c}\end{aligned}$$

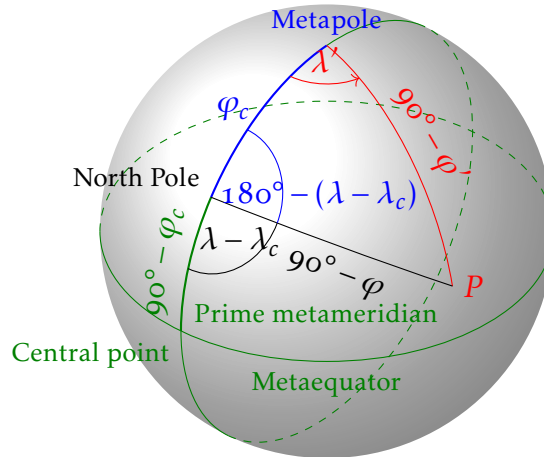


Figure V.4: The intersection of the metaequator and the prime metameridian is known

The purpose of the graticule rotation is to move the mapped area on the sphere into the areas of favourable distortion. For example, as shown in Fig. IX.2, a stereographic projection is the best possible conformal projection for circles centred on the pole. If our area is roughly circular but is not near the pole, we simply rotate the graticule so that the metapole falls in the centre of the area we want to display. In the projections rotated so, we simply substitute metacoordinates for latitudes and longitudes.

V.4 Geodetic problems on the ellipsoid

Imagine a point-like trolley on a surface of revolution and push it with a unit initial speed. The trolley is only affected by the gravity of surface, friction is neglected. Gravity is perpendicular everywhere to the surface of revolution considered as an equipotential surface, and therefore also to the path of the trolley. Thus, gravity does not do any work on the trolley, its speed remains constant. Since it is not subject to lateral forces, its trajectory can be considered to be straight within the surface, i.e. the trolley follows a geodesic on the surface of revolution.

Let the current azimuth of the trajectory of the trolley be α , then the component of its velocity in the direction of parallels is $\sin \alpha$. This is also the peripheral velocity of the trolley with respect to the axis of rotation of the surface. The direction of the gravity force (the normal of the surface) intersects the axis of rotation due to symmetry, so it has no torque with respect to the axis of rotation. Due to the conservation of angular momentum, the peripheral velocity of the trolley travelling along the geodesic multiplied by the radius r of the parallel (i.e. the distance from the axis of rotation) must be constant (*CLAIRAUT's relation*):*

$$r \sin \alpha = \text{const.}$$

At first glance, we did not learn much about the geodesics on the ellipsoid of revolution, although this information alone should be enough to determine the path. Let us start with the direct geodetic problem! From Fig. V.5, we can see that:

$$\begin{aligned} \cos \alpha &= \frac{M(\Phi) \widehat{\Delta\Phi}}{\Delta s} \\ \sin \alpha &= \frac{N(\Phi) \cos \Phi \widehat{\Delta\Lambda}}{\Delta s} \end{aligned}$$

Rearrange, knowing that the ratio between infinitesimally small distances tends to the derivative:

$$\begin{aligned} \frac{d\Phi}{ds} &= \frac{\cos \alpha}{M(\Phi)} \\ \frac{d\Lambda}{ds} &= \frac{\sin \alpha}{N(\Phi) \cos \Phi} \end{aligned}$$

* In fact, we are back in the depths of differential geometry. A rigorous proof of the relation obtained here requires calculus of variations and the solution of complicated differential equations.

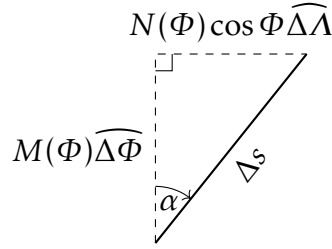


Figure V.5: An infinitesimal section of an ellipsoidal geodesic

We will also need the following derivative:

$$\begin{aligned}
 \frac{dr}{ds} &= \frac{dN(\Phi) \cos \Phi}{d\Phi} \frac{d\Phi}{ds} = \left[\frac{dN(\Phi)}{d\Phi} \cos \Phi + N(\Phi) \frac{d \cos \Phi}{d\Phi} \right] \frac{\cos \alpha}{M(\Phi)} \\
 &= \left[\frac{ae^2 \sin \Phi \cos \Phi}{(1 - e^2 \sin^2 \Phi)^{3/2}} \cos \Phi - N(\Phi) \sin \Phi \right] \frac{\cos \alpha}{M(\Phi)} \\
 &= M(\Phi) \frac{e^2 \sin \Phi \cos^2 \Phi}{1 - e^2} \frac{\cos \alpha}{M(\Phi)} - N(\Phi) \sin \Phi \frac{\cos \alpha}{M(\Phi)} \\
 &= \frac{e^2 \cos^2 \Phi \sin \Phi \cos \alpha}{1 - e^2} - \frac{a(1 - e^2 \sin^2 \Phi)^{3/2} \sin \Phi \cos \alpha}{a(1 - e^2) \sqrt{1 - e^2 \sin^2 \Phi}} \\
 &= \frac{e^2 (1 - \sin^2 \Phi) \sin \Phi \cos \alpha - (1 - e^2 \sin^2 \Phi) \sin \Phi \cos \alpha}{1 - e^2} \\
 &= \frac{e^2 - e^2 \sin^2 \Phi - 1 + e^2 \sin^2 \Phi}{1 - e^2} \sin \Phi \cos \alpha = -\sin \Phi \cos \alpha
 \end{aligned}$$

Next, let us also derive CLAIRAUT's relation!

$$\begin{aligned}
 \frac{dr}{ds} \sin \alpha + r \cos \alpha \frac{d\alpha}{ds} &= 0 \\
 N(\Phi) \cos \Phi \cos \alpha \frac{d\alpha}{ds} &= \sin \Phi \cos \alpha \sin \alpha \\
 \frac{d\alpha}{ds} &= \frac{\tan \Phi \sin \alpha}{N(\Phi)}
 \end{aligned}$$

A function f differentiable any times in the neighbourhood of the point $x = a$ can be approximated with arbitrary precision by its *TAYLOR series*, i.e:

$$f(x) = f(a) + \frac{x-a}{1!} f'(a) + \frac{(x-a)^2}{2!} f''(a) + \frac{(x-a)^3}{3!} f'''(a) + \dots$$

Of course, exact equality would only exist if all the infinitely many members were added together, but the series converges quickly, so the

small summands at the end of the series can be ignored.* Now let us see why this was necessary! let us formulate Φ_B and Λ_B as a function of the distance s from the point Φ_A, Λ_A . Let Φ and Λ be decomposed into TAYLOR series around $s = 0$!

$$\begin{aligned}\Phi_B &= \Phi_A + \frac{s}{1!} \left. \frac{d\Phi}{ds} \right|_{s=0} + \frac{s^2}{2!} \left. \frac{d^2\Phi}{ds^2} \right|_{s=0} + \frac{s^3}{3!} \left. \frac{d^3\Phi}{ds^3} \right|_{s=0} + \dots \\ \Lambda_B &= \Lambda_A + \frac{s}{1!} \left. \frac{d\Lambda}{ds} \right|_{s=0} + \frac{s^2}{2!} \left. \frac{d^2\Lambda}{ds^2} \right|_{s=0} + \frac{s^3}{3!} \left. \frac{d^3\Lambda}{ds^3} \right|_{s=0} + \dots\end{aligned}$$

The first derivatives are known, while the higher order derivatives follow naturally from further derivations of the first derivatives. If we look at the formulæ of the derivatives of Φ and Λ , we see that they also depend on s through α , but this is not a problem, since we have calculated the derivative of α , so we can substitute it while using the chain rule.

This method is due to LEGENDRE. Although its derivation is insightful and relatively simple to understand, it is not very applicable in practice. The reason is that it converges very slowly, the sixth derivative is needed for geodetic accuracy, and these higher order derivatives are extremely difficult to compute. In addition to this, the high-degree terms in s makes the solution of the inverse problem even more difficult: Then s is the unknown, and there is a solver formula only for equations containing the fourth power of s .

Geodesists typically use GAUSS's method, which decomposes the function into a TAYLOR series around the bisector between the two points, resulting in much faster convergence (it is sufficient to consider the second derivative). The disadvantage of this method is that the coordinates of the bisector are not known, and one can get better results by iteration after a first guess.

All the previously discussed methods assumed that s is relatively short (< 1000 km). For longer distances, exact solutions are needed. A popular solution is BESSEL's one, which reduces the problem to the simple spherical geodetic problems and then corrects for the difference between the sphere and the ellipsoid by elliptic integrals. BESSEL's formulæ were adapted for computer execution by KARNEY. Modern open-source GIS almost invariably uses his formulæ, and their results are considered highly reliable, in contrast to VINCENTY's formulæ in slightly older packages. The latter converge only at distances shorter than 10 000 km.

The calculation of long geodesics also provides an opportunity to illustrate them. Fig. V.6 shows that, unlike the sphere, ellipsoidal geodesics do

* The method works with all smooth functions, and can be used to efficiently approximate complicated functions. The pocket calculator, for example, uses TAYLOR series to calculate trigonometric functions.

not return to themselves but move a bit back. The only exceptions are the circular Equator and the elliptical bimeridians.

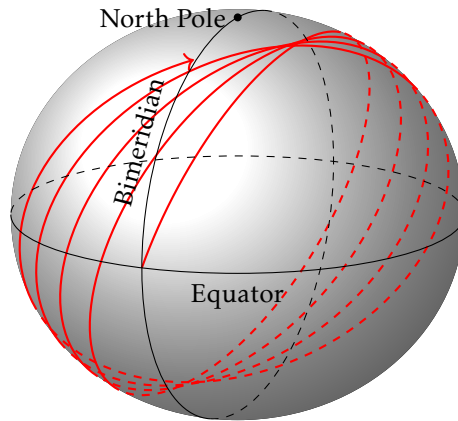


Figure V.6: Paths of geodesics on an ellipsoid ($f = 1/10$)

The results are used in satellite remote sensing. The orbit of a satellite is a geodesic (remember the trolley). Some satellites orbit in a heliosynchronous orbit, i.e. they always pass over areas at the same local time to provide the same light conditions. As the Earth orbits the Sun, the orbital plane of the satellite must be constantly varied to maintain a constant angle with the Sun (i.e. the satellite's orbital plane rotates 90° in three months, see Fig. V.7). On a spherical Earth, this would be impossible because spherical geodesics are flat curves and satellites would not change their orbital plane. On the ellipsoid, however, only the meridians and the Equator are plane curves, the orbital planes of the other geodesics precess. If the orbit subtends just a tiny angle ($\sim 1^\circ$) with the meridians, it is possible to achieve a tiny precession of the geodesic that changes the orbital plane of the satellite just as much as we need. Without the not-so-friendly calculations above, there would be no LANDSAT, SPOT and many other similar successful projects.

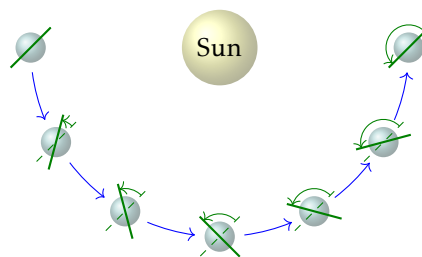


Figure V.7: Precession of a heliosynchronous orbit

Lesson six

The basics of map projections

VI.1 The Theorema Egregium

Take a round pizza slice and grab it by the edge! The tip of the pizza slice towards you will immediately bend and the toppings will run off! A common solution is to slightly lift the two corners of the pizza slice and bend them into a curve. This will keep the pizza slice almost horizontal. How is this possible, and how can you start a lecture on map projections with such an example?

To examine the phenomenon, we introduce the concept of *Gaussian curvature*. The *curvature* of a curve is the signed reciprocal of its radius of curvature introduced in Sec. IV.1 (the sign depends on whether the turn is to the right or left). The curvature of a smooth surface is the curvature of its normal section (Sec. IV.1), which depends on position and direction. The *Gaussian curvature* of a surface at a given point is the product of the minimal and maximal curvatures at that point.

Some examples: the curvature of a plane is zero in all directions, so is also the Gaussian curvature. The cone has no curvature in the direction of the generating lines and positive curvature in all other directions. Consequently, the Gaussian curvature is zero (since the minimal curvature can be multiplied by anything). The Gaussian curvature of saddle-shaped potato crisps is negative since the extremal curvatures have opposite signs (opposite directions). The curvature of the sphere at all points and in all directions is $1/R$, so its Gaussian curvature is constant (positive) $1/R^2$. The radii of curvature of an ellipsoid of revolution with major semi-axis a and first eccentricity e are (Sec. IV.1–IV.2):

$$N(\Phi) = \frac{a}{\sqrt{1 - e^2 \sin^2 \Phi}}$$
$$M(\Phi) = \frac{a(1 - e^2)}{(1 - e^2 \sin^2 \Phi)^{3/2}}$$

The Gaussian curvature of the ellipsoid of revolution varies with latitude: $1/N(\Phi)M(\Phi)$.

VI. The basics of map projections

GAUSS's famous theorem, the *Theorema Egregium* (remarkable theorem), states: *a distortion-free mapping (preserving distances, angles, and areas) can be established between parts of two smooth surfaces if and only if their Gaussian curvature is the same for each point.* In other words, there are strict conditions for distortion-free mappings (note that twisting a flat slice of pizza is a distortion-free mapping):

- Both the cone and the plane have zero Gaussian curvature, so a distortion-free mapping between them is possible. The flat pizza slice can be bent into a cone.
- The Gaussian curvature of the sphere is constant positive. There is no distortion-free projection between sphere and plane. If you bend the pizza slice in one direction, you cannot simultaneously twist it in the direction perpendicular to it. It is not possible to cover even a part of a sphere with a slice of pizza without wrinkling or tearing.
- The Gaussian curvature of the rotation ellipsoid, although also positive, is only constant along the parallels. It is not possible to map the entire ellipsoid of revolution onto the sphere without distortion, but it is possible to map the infinitesimally small neighbourhood of a selected latitude (see Sec. IX.3).
- Potato crisps are fried into surfaces with negative Gaussian curvatures (saddles) because they give great stability: they cannot be bent into other shapes without distortion.

The proof of *Theorema Egregium* is extremely complicated, it uses second-order partial derivatives and tensor algebra.

VI.2 What is a map projection?

The relation $f : \mathbb{R}^2 \supset \rightarrow \mathbb{R}^2$ between some parametrizations of two smooth surfaces is called a *map projection*. The domain is called the *reference frame*, the codomain is the mapped plane. The rule of association, also called the *formulae of the projection*, is usually given in the form of $x = f_1(\varphi, \lambda)$, $y = f_2(\varphi, \lambda)$.

We can make the following practical assumptions for map projections, but counterexamples can be found for all of them:

- The reference frame should be a surface of revolution describable in closed form so that we have simple formulae. However, the shape of certain small celestial bodies cannot be approximated by a surface of revolution, so Russian cartographers have developed projections for them with a triaxial ellipsoid as the reference frame.

- The face), since we want a flat map. In contrast, Google Earth uses a map projection between the ellipsoid of revolution and a sphere.
- We do not want the same point of the reference frame to appear in multiple places on the map, i.e. the mapping should be single-valued. However, we can find maps that show the poles as lines and maps that show the meridian $\pm 180^\circ$ twice.
- We do not want the map to have breaks and discontinuities, i.e. the map projection should be a multiple times differentiable function. This is impossible to satisfy everywhere based on the results of topology; in every projection, we find a point or line, along which continuity is not satisfied.
- We do not want the map to bend under itself, i.e. the mapping should be injective. Especially among perspective projections, we will see many counterexamples, where the problematic parts are simply not drawn at all.

The reference frame of the projection will typically be a sphere of radius R parametrized by the latitude φ and longitude λ (Sec. I.3). The other common reference frame, the ellipsoid of revolution, is characterized by the major semi-axis a and the first eccentricity e . Parallels Φ are still circles of radius $N(\Phi)\cos\Phi$ (Sec. IV.2). However, the meridians Λ are semi-ellipses with radius of curvature $M(\Phi)$ (Sec. IV.1).

VI.3 Surfaces approximating the Earth's figure

What shape of the Earth should we consider for our calculations? We have seen that planar computations are quite simple, the derivation of the spherical formulæ are also easy to follow, but the formulæ for the ellipsoid of revolution are quite complicated. Imagine then how difficult an irregular surface like a geoid is to handle. Obviously, although the Earth is a geoid, we only take this into account when measuring height, simplifying for horizontal calculations. Four cases are distinguished according to the longest extent of the area:

- We map a small area (extent < 4 km): the curvature of the Earth causes negligible error, we can consider the Earth as plane and apply the simple formulæ.
- When measuring longer distances (< 13 km), the curvature of the Earth is assumed to be constant, and an osculating sphere is chosen that fits the surface well.
- For even larger areas, it is necessary to calculate on the ellipsoid of revolution.

- If our area is very large (> 3500 km) and we are not aiming for geodetic accuracy, but simply draw a small-scale map, the deviation between ellipsoid and sphere (~ 20 km) is below the accuracy of the small-scale map. In this case, we can also use a sphere, but its radius, the *mean Earth radius*, may be significantly different from the radius of the osculating sphere described earlier!

VI.4 Geodetic datums

From the above requirements, it is clear that the shape of the Earth (geoid) is approximated by an ellipsoid of revolution even if the highest accuracy is required. This approximation is not unique for two reasons. On the one hand, different measurements at different locations give different data for the Earth's major semi-axis and its flattening. On the other hand, it is not certain that the centre of a well-fitting ellipsoid of revolution will lie exactly at the geoid's centre of mass, and its axis of revolution may even differ from the Earth's true axis of rotation. Together, the dimensions and the placement of the ellipsoid of revolution are called the *geodetic datum*. There can be a difference of up to ~ 100 m between the same geographic coordinates interpreted on different datums, so it is always important to check which datum your data uses!

Older ellipsoids of revolution (e.g. the ZÁCH–ORIANI of 1810) had a major semi-axis and flattening smaller than those used today (Tab. VI.1). This is because the first measurements were limited to Europe, and the shape of the geoid corresponds to these dimensions here. Later ellipsoids (e.g. the BESSEL of 1841) were based on measurements taken in several places averaged out and are therefore close to the shape of the Earth as we know it today. Current ellipsoids (e.g. WGS84) are based on satellite measurements.

Table VI.1: Sizes of a few terrestrial ellipsoids

Name	Year	a (m)	b (m)	$1/f$
ZÁCH–ORIANI	1810	6 376 130	6 355 561.839	310
BESSEL	1841	6 377 397.155	6 356 078.963	299.152 815
CLARKE	1880	6 378 249.145	6 356 514.870	293.465
HAYFORD	1924	6 378 388	6 356 911.946	297
KRASOVSKIY	1940	6 378 245	6 356 863.019	298.3
IUGG67	1967	6 378 160	6 356 774.516	298.247 167
WGS84	1984	6 378 137	6 356 752.314	298.257 224

For satellite surveys, the Earth's centre of mass and axis of rotation are measured easily, so the ellipsoid is positioned so that its centre and axis of rotation coincide with that of the Earth. The resulting datum is called a *global datum*, and it fits the geoid everywhere quite well (Fig. VI.1). An example is WGS84, which is based on the WGS84 ellipsoid of the same name.

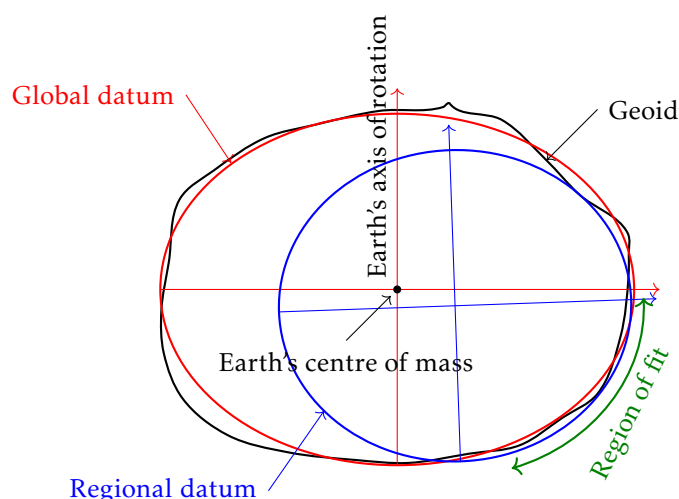


Figure VI.1: The relationship between the geoid and the datums

For ground surveys, we can only rely on data from local measurements, so we fit the ellipsoid locally to our area (*regional datum*)*. The centre of the ellipsoid placed such is offset (~ 100 m) from the Earth's centre of mass, and its axis of revolution deviates ($\sim 1''$) from the Earth's axis of rotation, but it fits the geoid well in our region. Importantly, the parameters of the ellipsoid (major semi-axis, flattening) are not changed in the process, it will be an ellipsoid based on a previous international measurement. In Hungary, we use the datum HD72, which is based on the major semi-axis and flattening of the ellipsoid IUGG67.†

* This does not actually mean that the difference in height (*geoid undulation*) between the ellipsoid and the geoid is minimal, but that the deviation between the local vertical direction of the geoid measured by astronomical methods and the normal of the ellipsoid (*vertical deflection*) is as small as possible at the *LAPLACE points* used for the fit. This also minimizes the discrepancy between geodetic latitudes measured with respect to the stars and those calculated on the ellipsoid (see also App. D).

† The realization of regional datums relies on marked points, the latitude and longitude of which are recorded on a sheet of paper, so the regional datum can slowly depart from its original position as the tectonic plates move. Its typical rate is about one metre every 25 years.

VI. The basics of map projections

For the conversion between the different datums, we can take into account 7 parameters: the translations Δx , Δy , and Δz in the three directions of space, the rotations σ_x , σ_y , and σ_z around the three axes and a rescaling s .^{*} Since the angles σ are small, we use the approximations $\sin \sigma \approx \widehat{\sigma}$, $\cos \sigma \approx 1$, and $\sigma_i \sigma_j \approx 0$ to obtain the rotational matrix in a simpler form. Then, rescaling involves multiplication by a scalar, while translation involves the addition of the corresponding vector:

$$\begin{pmatrix} x' \\ y' \\ z' \end{pmatrix} = \begin{pmatrix} \Delta x \\ \Delta y \\ \Delta z \end{pmatrix} + (1 + s) \begin{pmatrix} 1 & \widehat{\sigma}_z & -\widehat{\sigma}_y \\ -\widehat{\sigma}_z & 1 & \widehat{\sigma}_x \\ \widehat{\sigma}_y & -\widehat{\sigma}_x & 1 \end{pmatrix} \begin{pmatrix} x \\ y \\ z \end{pmatrix}$$

The upper transformation is called *HELMERT transform* (rarely *BURŠA–WOLF transform*). It can be seen that the transformation requires Cartesian coordinates rather than geographic ones. The formulæ for the conversion are given Sec. IV.3. The accuracy of the transformation is typically around metres. It is important to note that some GIS packages use the opposite sign convention for the direction of rotations, so if the conversion does not work in a program with the parameters given in the literature, always try to flip the signs of rotations!

Sometimes, for simplicity, only the translation is considered, in which case the error is typically around five metres. This is called a *MOLODENSKIY transform*, which has only three parameters. Although a form of the MOLODENSKIY transform can provide a direct relationship between the geographic coordinates of two datums (*abridged transform*), for simplicity, we will use Cartesian coordinates:

$$\begin{pmatrix} x' \\ y' \\ z' \end{pmatrix} = \begin{pmatrix} \Delta x \\ \Delta y \\ \Delta z \end{pmatrix} + \begin{pmatrix} x \\ y \\ z \end{pmatrix}$$

Alternatively, for greater accuracy, a *grid shift* transform is usually provided by GIS, which effectively adds or subtracts different values from the geographic coordinates from place to place by interpolating data from a raster file. This results in an accuracy of decimetres, but is computationally expensive, as it is slow to extract the locally valid offsets from the raster.

^{*} Due to the adjustment for measurement errors during triangulation, the scale relations of regional and global datums are inconsistent, and this is taken into account in the transform, but the measurement accuracy of the angles is more reliable, so we take care to preserve them. This is why we have chosen a similarity transformation.

VI.5 The radius of the Earth

We are now dealing with the sphere as a reference frame. There are several ways to derive the radius of the Earth, now assumed to be spherical, from the data of the ellipsoid of revolution. In this section, the values given are the radii of the spheres approximating the ellipsoid WGS84, i.e. $a = 6\,378\,137$ m, $f = 1/298.257\,223\,563$. The *volumetric radius*, which represents a sphere having the same volume as the ellipsoid of revolution, is the most commonly used radius in small-scale mapping. Its value is less than one metre greater than 6371 km. To calculate it, formulate the volume of the sphere and that of the ellipsoid:

$$\frac{4R^3\pi}{3} = \frac{4a^2b\pi}{3}$$

$$R = \sqrt[3]{a^2b} = a\sqrt[3]{1-e^2}$$

The surface of the sphere corresponding to the *authalic radius* is the same as that of the ellipsoid. Its value is 6371.007 km. When calculating, recall that the surface of the sphere was obtained in Sec. II.2, while the surface of the ellipsoid of revolution was obtained in Sec. IV.4:

$$4R^2\pi = 2a^2\pi\left(1 + \frac{1-e^2}{2e} \ln \frac{1+e}{1-e}\right)$$

$$R = \sqrt{\frac{a^2}{2}\left(1 + \frac{1-e^2}{2e} \ln \frac{1+e}{1-e}\right)}$$

Likewise, the length of the meridians remains unchanged if a sphere of *rectifying radius* is chosen. This is 6367.449 km, its calculation:

$$2R\pi = 2 \int_{-90^\circ}^{90^\circ} M(\Phi) d\Phi$$

For local mapping, we use the radius of the *osculating sphere* or the *Gaussian radius of curvature*, which varies from place to place. Its value is the geometric mean of the radii of curvature taken at the point:

$$R = \sqrt{M(\Phi)N(\Phi)}$$

It is easy to see that according to the Theorema Egregium, a projection between the ellipsoid and the osculating sphere can be distortion-free in the infinitesimal neighbourhood of latitude Φ , as here they have the same Gaussian curvature.

VI.6 Classification of projections

Projections can be classified in several ways. Most often, we classify them according to *the shape of the graticule*. We then call *conical* projections those mappings in which:

- the mapped parallels are concentric circles, arcs of circles, or parallel straight lines;
- the mapped meridians are concurrent or parallel straight lines;
- parallels and meridians are everywhere perpendicular to each other;
- the meridians are spaced along the parallels evenly (in proportion to their longitude).

If only one condition is not fulfilled, then we speak of a *non-conical* projection.

Based on the images of the parallel circles, both conical and non-conical projections are grouped further (Fig. VI.2):

- If the images of the parallels are complete circles, an *azimuthal* or a *pseudoazimuthal* projection is obtained.
- If they are mapped only to arcs of circles, we speak of a *(pseudo)conic* projection.
- If the mapped parallels are parallel lines, we have a *(pseudo)cylindrical* map.
- Some non-conical projections do not fit either of these groups. These are the *miscellaneous* projections.

Projections are also grouped according to their *geometric construction*: a projection is *perspective* if it can be generated by a central perspective projection (using light rays from a centre placed on the common axis of revolution of a developable surface and the reference frame), all other projections are *non-perspective*. All perspective projections are also conical ones.

The projections must have some distortion due to the Theorema Egregium. The distortions are characterized by *local distortions*. These are the ratios of the corresponding mapped and original quantities as the quantity on the reference frame approaches zero. Let l denote the *linear scale*, p the *areal scale* and i the *angular distortion*. Let Δs , ΔS , and μ denote distances, areas, and angles, respectively, on the reference frame; and $\Delta s'$, $\Delta S'$, and μ' denote their corresponding mapped images. The distortions are defined as follows:

$$l = \lim_{\Delta s \rightarrow 0} \frac{\Delta s'}{\Delta s}$$

$$p = \lim_{\Delta S \rightarrow 0} \frac{\Delta S'}{\Delta S}$$

VI. The basics of map projections

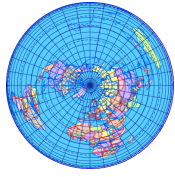
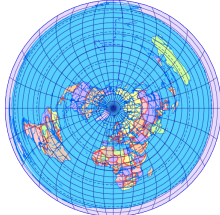
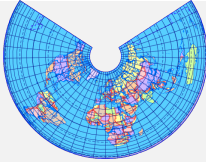
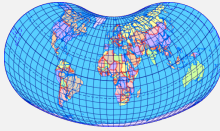
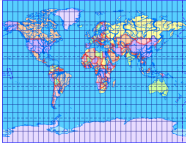


Parallels	Conical	Non-conical
Circles	 Azimuthal	 Pseudoazimuthal
Arcs	 Conic	 Pseudoconic
Straight	 Cylindrical	 Pseudocylindrical
Other	—	 Miscellaneous

Figure VI.2: Classification according to the shape of the graticule

$$i = \frac{\tan \mu'}{\tan \mu}$$

So a projection is distortion-free where all three distortions are one. On this basis, we can also group projections according to *distortion characteristics*: if at each point $p = 1$, then the projection is *equal-area* or *equivalent*. If $i = 1$ for the whole map then our mapping is *conformal*. If at all points and in all directions $l = 1$ then we have miscalculated something. This would imply the absence of distortion, which is ruled out by the Theorema Egregium. There are projections that have *equidistant* points, lines, and even infinitely many lines (all meridians or all parallels) can be equidistant, but even then they cannot be true-scale in all directions at the same time. So our third possible category is *aphylactic* (neither equivalent nor conformal).

On the projections of all three categories, there may be points or lines, along which there is absolutely no distortion. This is called a *true-scale* or

VI. The basics of map projections

Standard line of the projection and if it is a parallel, we may also use the term *standard parallel*.

We can also classify projections according to their *aspect*: this grouping is first defined on a sphere using the metageographic coordinate system. We conceptualize this as rotating the graticule so that an arbitrarily chosen point, the *metapole*, behaves like the original pole. The exact definition and formulæ are given in Sec. V.3. Subsequently, the projection will be plotted in terms of the metageographic coordinates rather than the geographic coordinates.

If the metapole coincides with one of the poles, the aspect is *normal*. If the metapole is on the Equator, it is *transverse*. Otherwise, it is *oblique*. For an ellipsoid of revolution, we generalize this definition by considering the aspect of the spherical projection obtained from the ellipsoidal formulæ by substituting $e = 0$. Projections not of normal aspect are classified according to the image of the metagraticule (i.e. the network of mapped metaparallels and metameridians) instead of the original graticule.

It is important to keep in mind that the rotation of the graticule preserves the distortion characteristics of the projection (e.g. conformality and equivalency), but special properties of the graticule (e.g. equidistant meridians, intersection angle between graticule lines) will apply to the metagraticule, the original graticule will lose these properties. This does not affect the classification according to the shape of the graticule; if the properties of conical projections are satisfied for the metagraticule and the projection is called a conical projection even if the mapped graticule would lead us to conclude the opposite.

Lesson seven

Distortions in terms of partial derivatives

VII.1 The linear scale

Consider an infinitesimal section Δs on the reference frame considered as a plane due to small dimensions! The infinitesimal geographical quadrangle enclosing the section is approximately a rectangle. Assuming from the differentiability that the mapped slopes of the sides are essentially the same, as they are close to each other, so the quadrangle is mapped to a tiny parallelogram (Fig. VII.1).

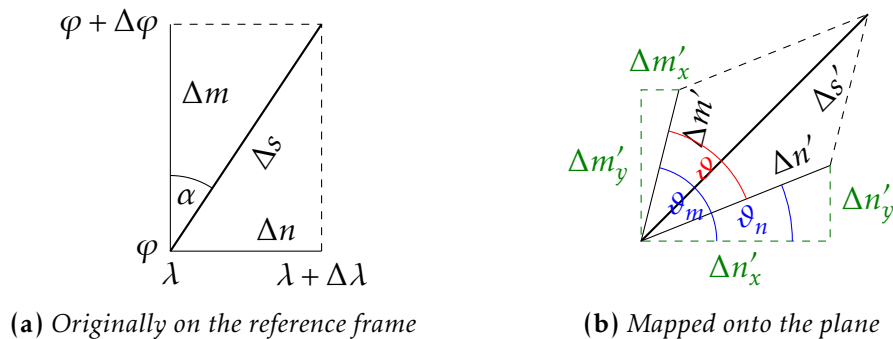


Figure VII.1: *Infinitesimal geographic quadrangle and its image*

Projections are described by the pair of functions $x(\varphi, \lambda), y(\varphi, \lambda)$. The definition of the partial derivative is $\partial_x f(x, y) = \lim_{\Delta x \rightarrow 0} [f(x + \Delta x, y) - f(x, y)] / \Delta x$. Rearranged: $f(x + \Delta x, y) - f(x, y) \approx \Delta x \times \partial_x f(x, y)$. Using this relation, we can approximate the length of the green sections:

$$\Delta m'_x \approx \frac{\partial x}{\partial \varphi} \widehat{\Delta \varphi}$$

$$\Delta m'_y \approx \frac{\partial y}{\partial \varphi} \widehat{\Delta \varphi}$$

VII. Distortions in terms of partial derivatives

$$\Delta n'_x \approx \frac{\partial x}{\partial \lambda} \widehat{\Delta \lambda}$$

$$\Delta n'_y \approx \frac{\partial y}{\partial \lambda} \widehat{\Delta \lambda}$$

From the PYTHAGOREAN theorem for $\Delta s'$, it follows that:

$$\begin{aligned} \Delta^2 s' &= (\Delta m'_x + \Delta n'_x)^2 + (\Delta m'_y + \Delta n'_y)^2 \\ &\approx \left(\frac{\partial x}{\partial \varphi} \widehat{\Delta \varphi} + \frac{\partial x}{\partial \lambda} \widehat{\Delta \lambda} \right)^2 + \left(\frac{\partial y}{\partial \varphi} \widehat{\Delta \varphi} + \frac{\partial y}{\partial \lambda} \widehat{\Delta \lambda} \right)^2 \\ &= \left[\left(\frac{\partial x}{\partial \varphi} \right)^2 + \left(\frac{\partial y}{\partial \varphi} \right)^2 \right] (\widehat{\Delta \varphi})^2 + 2 \left[\frac{\partial x}{\partial \varphi} \frac{\partial x}{\partial \lambda} + \frac{\partial y}{\partial \varphi} \frac{\partial y}{\partial \lambda} \right] \widehat{\Delta \varphi} \widehat{\Delta \lambda} + \left[\left(\frac{\partial x}{\partial \lambda} \right)^2 + \left(\frac{\partial y}{\partial \lambda} \right)^2 \right] (\widehat{\Delta \lambda})^2 \end{aligned}$$

The factors in square brackets* will be denoted by E, F, G respectively for brevity:

$$\Delta^2 s' = E(\widehat{\Delta \varphi})^2 + 2F\widehat{\Delta \varphi}\widehat{\Delta \lambda} + G(\widehat{\Delta \lambda})^2$$

The sides of the rectangle on the reference frame in the directions of parallels and meridians are Δn and Δm , respectively, so:

$$\Delta^2 s = \Delta^2 m + \Delta^2 n \approx \left(\frac{dm}{d\varphi} \right)^2 (\widehat{\Delta \varphi})^2 + \left(\frac{dn}{d\lambda} \right)^2 (\widehat{\Delta \lambda})^2$$

For the angle from the meridian to the section and the meridian (*azimuth* α):

$$\tan \alpha = \frac{\Delta n}{\Delta m} \approx \frac{\frac{dn}{d\lambda} \widehat{\Delta \lambda}}{\frac{dm}{d\varphi} \widehat{\Delta \varphi}}$$

$$\frac{\widehat{\Delta \lambda}}{\widehat{\Delta \varphi}} \approx \frac{dm}{d\varphi} \tan \alpha$$

The definition of the linear scale is:

$$l = \lim_{\Delta s \rightarrow 0} \frac{\Delta s'}{\Delta s}$$

* These quantities are called the *coefficients of the Gaussian first fundamental form*.

VII. Distortions in terms of partial derivatives

Now we can count the linear scale!

$$\begin{aligned}
 l^2 &= \frac{\Delta^2 s'}{\Delta^2 s} = \frac{E(\widehat{\Delta\varphi})^2 + 2F\widehat{\Delta\varphi}\widehat{\Delta\lambda} + G(\widehat{\Delta\lambda})^2}{\left(\frac{dm}{d\varphi}\right)^2(\widehat{\Delta\varphi})^2 + \left(\frac{dn}{d\lambda}\right)^2(\widehat{\Delta\lambda})^2} = \frac{E + 2F\frac{\widehat{\Delta\lambda}}{\widehat{\Delta\varphi}} + G\frac{(\widehat{\Delta\lambda})^2}{(\widehat{\Delta\varphi})^2}}{\left(\frac{dm}{d\varphi}\right)^2 + \left(\frac{dn}{d\lambda}\right)^2\frac{(\widehat{\Delta\lambda})^2}{(\widehat{\Delta\varphi})^2}} \\
 &= \frac{E + 2F\frac{\frac{dm}{d\varphi}}{\frac{dn}{d\lambda}}\tan\alpha + G\frac{\left(\frac{dm}{d\varphi}\right)^2}{\left(\frac{dn}{d\lambda}\right)^2}\tan^2\alpha}{\left(\frac{dm}{d\varphi}\right)^2 + \left(\frac{dn}{d\lambda}\right)^2\frac{\left(\frac{dm}{d\varphi}\right)^2}{\left(\frac{dn}{d\lambda}\right)^2}\tan^2\alpha} = \frac{E\frac{\cos^2\alpha}{\left(\frac{dm}{d\varphi}\right)^2} + 2F\frac{\tan\alpha\cos^2\alpha}{\frac{dm}{d\varphi}\frac{dn}{d\lambda}} + G\frac{\tan^2\alpha\cos^2\alpha}{\left(\frac{dn}{d\lambda}\right)^2}}{\cos^2\alpha + \tan^2\alpha\cos^2\alpha} \\
 &= E\frac{\cos^2\alpha}{\left(\frac{dm}{d\varphi}\right)^2} + 2F\frac{\sin\alpha\cos\alpha}{\frac{dm}{d\varphi}\frac{dn}{d\lambda}} + G\frac{\sin^2\alpha}{\left(\frac{dn}{d\lambda}\right)^2}
 \end{aligned}$$

We know that the small arc length on the reference frame is equal to the product of the radius and the subtended angle (in the following formulæ, the ones on the left are for a sphere, the ones on the right are for the ellipsoid of revolution):

$$\begin{aligned}
 \Delta m &= R\widehat{\Delta\varphi} & \Delta m &= M(\Phi)\widehat{\Delta\Phi} \\
 \frac{dm}{d\varphi} &= R & \frac{dm}{d\Phi} &= M(\Phi) \\
 \Delta n &= R\cos\varphi\widehat{\Delta\lambda} & \Delta n &= N(\Phi)\cos\Phi\widehat{\Delta\Lambda} \\
 \frac{dn}{d\lambda} &= R\cos\varphi & \frac{dn}{d\Lambda} &= N(\Phi)\cos\Phi
 \end{aligned}$$

That is, on the sphere, expanding also the notations E, F, G :

$$\begin{aligned}
 l^2 &= \left[\left(\frac{\partial x}{\partial \varphi} \right)^2 + \left(\frac{\partial y}{\partial \varphi} \right)^2 \right] \frac{\cos^2 \alpha}{R^2} \\
 &\quad + \left[\left(\frac{\partial x}{\partial \lambda} \right)^2 + \left(\frac{\partial y}{\partial \lambda} \right)^2 \right] \frac{\sin^2 \alpha}{R^2 \cos^2 \varphi} + 2 \left[\frac{\partial x}{\partial \varphi} \frac{\partial x}{\partial \lambda} + \frac{\partial y}{\partial \varphi} \frac{\partial y}{\partial \lambda} \right] \frac{\sin \alpha \cos \alpha}{R^2 \cos \varphi}
 \end{aligned}$$

And on the ellipsoid of revolution:

$$\begin{aligned}
 l^2 &= \left[\left(\frac{\partial x}{\partial \Phi} \right)^2 + \left(\frac{\partial y}{\partial \Phi} \right)^2 \right] \frac{\cos^2 \alpha}{M^2(\Phi)} \\
 &\quad + \left[\left(\frac{\partial x}{\partial \Lambda} \right)^2 + \left(\frac{\partial y}{\partial \Lambda} \right)^2 \right] \frac{\sin^2 \alpha}{N^2(\Phi) \cos^2 \Phi} + 2 \left[\frac{\partial x}{\partial \Phi} \frac{\partial x}{\partial \Lambda} + \frac{\partial y}{\partial \Phi} \frac{\partial y}{\partial \Lambda} \right] \frac{\sin \alpha \cos \alpha}{M(\Phi)N(\Phi)\cos\Phi}
 \end{aligned}$$

It can be seen that the linear scale depends (via the partial derivatives) on both the location and the direction α . Let us calculate the *linear scales along*

VII. Distortions in terms of partial derivatives

graticule lines! If $\alpha = 0^\circ$, we obtain the *linear scale along meridians* denoted by h and if $\alpha = 90^\circ$, we obtain the *linear scale along parallels* denoted by k :

$$\begin{aligned} h &= \frac{\sqrt{\left(\frac{\partial x}{\partial \varphi}\right)^2 + \left(\frac{\partial y}{\partial \varphi}\right)^2}}{R} & h &= \frac{\sqrt{\left(\frac{\partial x}{\partial \Phi}\right)^2 + \left(\frac{\partial y}{\partial \Phi}\right)^2}}{M(\Phi)} \\ k &= \frac{\sqrt{\left(\frac{\partial x}{\partial \lambda}\right)^2 + \left(\frac{\partial y}{\partial \lambda}\right)^2}}{R \cos \varphi} & k &= \frac{\sqrt{\left(\frac{\partial x}{\partial \Lambda}\right)^2 + \left(\frac{\partial y}{\partial \Lambda}\right)^2}}{N(\Phi) \cos \Phi} \end{aligned}$$

We can find equidistant projections in meridians with the condition $h = 1$, while we can find equidistant projections in parallels imposing $k = 1$.

VII.2 Intersection angle between graticule lines

Going back to Fig. VII.1, we can see that the angles ϑ_m and ϑ_n can be easily derived from the corresponding right triangles:

$$\begin{aligned} \sin \vartheta_m &= \frac{\Delta m'_y}{\Delta m'} = \frac{\frac{\partial y}{\partial \varphi} \widehat{\Delta \varphi}}{\Delta m'} \\ \cos \vartheta_m &= \frac{\Delta m'_x}{\Delta m'} = \frac{\frac{\partial x}{\partial \varphi} \widehat{\Delta \varphi}}{\Delta m'} \\ \sin \vartheta_n &= \frac{\Delta n'_y}{\Delta n'} = \frac{\frac{\partial y}{\partial \lambda} \widehat{\Delta \lambda}}{\Delta n'} \\ \cos \vartheta_n &= \frac{\Delta n'_x}{\Delta n'} = \frac{\frac{\partial x}{\partial \lambda} \widehat{\Delta \lambda}}{\Delta n'} \end{aligned}$$

Let ϑ denote the *intersection angle between parallels and meridians*. Then, using that according to the figure $\vartheta = \vartheta_m - \vartheta_n$:

$$\begin{aligned} \sin \vartheta &= \sin(\vartheta_m - \vartheta_n) = \sin \vartheta_m \cos \vartheta_n - \cos \vartheta_m \sin \vartheta_n \\ &= \left(\frac{\partial y}{\partial \varphi} \frac{\partial x}{\partial \lambda} - \frac{\partial x}{\partial \varphi} \frac{\partial y}{\partial \lambda} \right) \frac{\widehat{\Delta \varphi} \widehat{\Delta \lambda}}{\Delta m' \Delta n'} \\ \cos \vartheta &= \cos(\vartheta_m - \vartheta_n) = \cos \vartheta_m \cos \vartheta_n + \sin \vartheta_m \sin \vartheta_n \\ &= \left(\frac{\partial x}{\partial \varphi} \frac{\partial x}{\partial \lambda} + \frac{\partial y}{\partial \varphi} \frac{\partial y}{\partial \lambda} \right) \frac{\widehat{\Delta \varphi} \widehat{\Delta \lambda}}{\Delta m' \Delta n'} \end{aligned}$$

VII. Distortions in terms of partial derivatives

Just one small step and you have a useful formula:

$$\cot \vartheta = \frac{\cos \vartheta}{\sin \vartheta} = \frac{\frac{\partial x}{\partial \varphi} \frac{\partial x}{\partial \lambda} + \frac{\partial y}{\partial \varphi} \frac{\partial y}{\partial \lambda}}{\frac{\partial y}{\partial \varphi} \frac{\partial x}{\partial \lambda} - \frac{\partial x}{\partial \varphi} \frac{\partial y}{\partial \lambda}}$$

The interesting thing about this formula, which is also valid for the ellipsoid of revolution, is that its numerator is the last coefficient of the formula for the linear scale and its denominator will occur in the formula for the areal scale. It is important to note that at all points of rectangular projections, $\cot \vartheta = 0$, which helps to find such projections.

VII.3 The areal scale

Let us go back to Fig. VII.1. The surface area ΔS of the small geographical quadrangle (rectangle) is the product of the sides, while the area $\Delta S'$ of the tiny parallelogram is the product of its two sides and the sine of the angle ϑ between them:

$$\begin{aligned}\Delta S &= \Delta m \Delta n \\ \Delta S' &= \Delta m' \Delta n' \sin \vartheta\end{aligned}$$

Substituting the value of $\sin \vartheta$ into the formula above:

$$\Delta S' = \left(\frac{\partial y}{\partial \varphi} \frac{\partial x}{\partial \lambda} - \frac{\partial x}{\partial \varphi} \frac{\partial y}{\partial \lambda} \right) \widehat{\Delta \varphi} \widehat{\Delta \lambda}$$

The definition of the areal scale is:

$$p = \lim_{\Delta S \rightarrow 0} \frac{\Delta S'}{\Delta S}$$

Two useful formulæ can be obtained for this, depending on which form of $\Delta S'$ is substituted. On the one hand:

$$p = \lim_{\substack{\Delta m \rightarrow 0 \\ \Delta n \rightarrow 0}} \frac{\Delta m' \Delta n' \sin \vartheta}{\Delta m \Delta n} = hk \sin \vartheta$$

VII. Distortions in terms of partial derivatives

On the other hand:^{*}

$$p = \lim_{\substack{\Delta m \rightarrow 0 \\ \Delta n \rightarrow 0}} \frac{\left(\frac{\partial y}{\partial \varphi} \frac{\partial x}{\partial \lambda} - \frac{\partial x}{\partial \varphi} \frac{\partial y}{\partial \lambda} \right) \widehat{\Delta \varphi} \widehat{\Delta \lambda}}{\Delta m \Delta n} = \frac{\frac{\partial y}{\partial \varphi} \frac{\partial x}{\partial \lambda} - \frac{\partial x}{\partial \varphi} \frac{\partial y}{\partial \lambda}}{\frac{dm}{d\varphi} \frac{dn}{d\lambda}}$$

Substituting the spherical and ellipsoidal quantities:

$$p = \frac{\frac{\partial y}{\partial \varphi} \frac{\partial x}{\partial \lambda} - \frac{\partial x}{\partial \varphi} \frac{\partial y}{\partial \lambda}}{R^2 \cos \varphi} \qquad p = \frac{\frac{\partial y}{\partial \Phi} \frac{\partial x}{\partial \Lambda} - \frac{\partial x}{\partial \Phi} \frac{\partial y}{\partial \Lambda}}{M(\Phi)N(\Phi) \cos \Phi}$$

Since $p = 1$ in equal-area projections, we can find equivalent projections simply by solving the equation $hk \sin \vartheta = 1$. In rectangular projections, $\sin \vartheta = 1$, it suffices to write the even simpler equation $hk = 1$ for such projections.

^{*} The bracketed term in the numerator is the determinant of the *JACOBIAN matrix* of partial derivatives. This implies that the *JACOBIAN determinant* of the projection is closely related to the areal scale.

Lesson eight

TISSOT'S theory of map distortion

VIII.1 Map projections as local affine transforms

The modern theory of map projections is based on the works of the French geodesist Tissot, written in the late 19th century. The main results of these studies are called *Tissot's theorem*. Since these theorems were summarized by later authors, there are differences in the number of propositions, numbering and wording of the theorems, but these formulations are equivalent to the statements in the original French text.

Tissot's theorem is summarized in three propositions in this lecture note:

- I. *Any differentiable mapping between two smooth surfaces can be interpreted as an ensemble of affine transformations of infinitely many infinitesimal areas.* For this reason, the mapped image of an infinitesimal circle on the reference frame is an ellipse that can be constructed from the original circle using stretching and uniform scaling.
- II. *At any point on the reference frame of such a differentiable map projection, there is at least one pair of perpendicular directions whose images on the map are also perpendicular to each other.* These special directions are called the *principal directions*.
- III. *The directions of the minimal and maximal linear scales measured at a single point always coincide with the principal directions.* The direction of the maximum linear scale is called the *first principal direction* and the direction of the minimum linear scale is called the *second principal direction*.

First, prove proposition II: Take a section and another section perpendicular to it on the plane tangent to the reference frame, and examine their image on the map (Fig. VIII.1). Since the two right angles on the reference frame form a straight angle and the map projection is assumed to be differentiable (smooth), it is certain that the directions on the map also form a straight angle (otherwise the images of the straight lines would be broken and the map projection would not be differentiable). This shows that the image of the other section on the map either divides the straight

VIII. Tissot's theory of map distortion

angle into two right angles or into an acute and an obtuse angle. In the former case, we have already found two principal directions of projection, in the latter case, we need to think further.

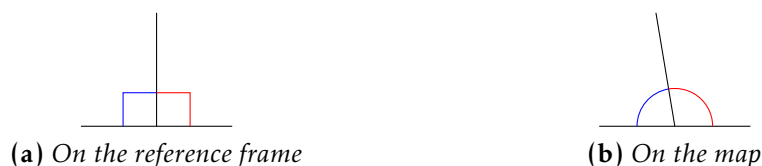


Figure VIII.1: *The image of two perpendicular directions*

Looking at the planar image, we see that the image of the red right angle became smaller, while that of the blue right angle became larger. Since the mapping is differentiable, we can apply BOLZANO'S theorem known in mathematical analysis to the images of right angles; that is, continuous functions on an interval $[a, b]$ take all possible values of the interval $[f(a), f(b)]$: If the image of one right angle is an obtuse angle and the image of the other one is an acute angle, there must surely be a right angle between these two right angles rotated by some angle whose image is a right angle. This completes the proof.

Next, we prove proposition I: Consider a rectangle of infinitesimal sides $\Delta\xi$ and $\Delta\eta$ on the reference frame (more precisely, on its tangent plane) such that its sides lie in the principal directions. Then the image of this rectangle on the map will be a rectangle since we have already seen that the principal directions are perpendicular to each other on the map. Let us superimpose the red rectangle of the reference frame and the corresponding mapped blue rectangle (Fig. VIII.2).

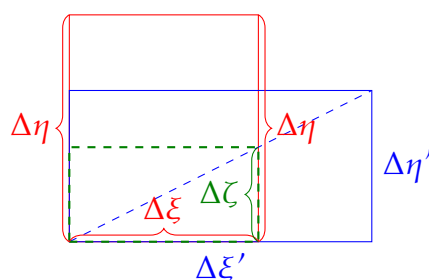


Figure VIII.2: *The infinitesimal rectangles superimposed*

The figure shows that the red rectangle can be transformed into the blue rectangle first by stretching in the vertical direction (green dashed rectangle) and then rescaling it to get the blue rectangle. If the factors of

VIII. Tissot's theory of map distortion

the stretching and the scaling are independent of the rectangle dimensions and depend only on the distortions of the map projection, then these two transformations perfectly describe the image of all points in the infinitely small neighbourhood of our point.

Let $a = \Delta\xi'/\Delta\xi$ denote the linear scale in one of the principal directions and $b = \Delta\eta'/\Delta\eta$ the linear scale in the other principal direction. The scale factor of between the red and green rectangles is then:

$$\frac{\Delta\zeta}{\Delta\eta} = \frac{\Delta\zeta}{\Delta\eta'} \frac{\Delta\eta'}{\Delta\eta} = \frac{\Delta\xi}{\Delta\xi'} \frac{\Delta\eta'}{\Delta\eta} = \frac{b}{a}$$

In the derivation above, we exploited the fact that the right triangles of legs $\Delta\xi, \Delta\zeta$ and $\Delta\xi', \Delta\eta'$ are similar, so the ratios of the corresponding legs are the same. From the result, we see that the scale factor is independent of the dimensions of the rectangle because we can express it from the linear scales.

Let us look at the scale factor between the green and blue rectangles:

$$\frac{\Delta\xi'}{\Delta\xi} = a$$

Since this is also independent of the dimensions of the rectangle, it is generally true that in the small neighbourhood of the point, the image of the original shapes can be obtained after stretching them by b/a and scaling by a , where a and b are the linear scales in the principal directions of the map projection. This completes the proof. A more lengthy, algebraic proof for those interested in of map projection theory can be found in App. E.

VIII.2 The ellipse of distortion

Before proving proposition III, we must consider the implications of the first two statements. If we find two principal directions at a point on the reference frame, let us denote the linear scales in these directions by a and b , with the notation chosen such that $a \geq b$. Let us call the direction of a the first principal direction and the direction of b the second principal direction. Consider a system of coordinates ξ, η on the tangent plane of the reference frame such that the axis ξ is in the first principal direction. Similarly, assume a coordinate system ξ', η' on the map in an analogous way.

Consider an infinitesimal circle on the reference frame assumed to be of unit radius (due to the small size and our constraint on the smooth surface, we can neglect the difference between the surface and its tangent plane).

Then, using proposition I, we obtain a shape on the mapped plane which is shrunk by a factor of b/a in the direction of the η axis and then enlarged by a factor of a . This is an ellipse of semi-axis a in the direction ξ' and semi-axis b in the direction η' . This ellipse is called an *ellipse of distortion* or *Tissor's indicatrix* (Fig. VIII.3).

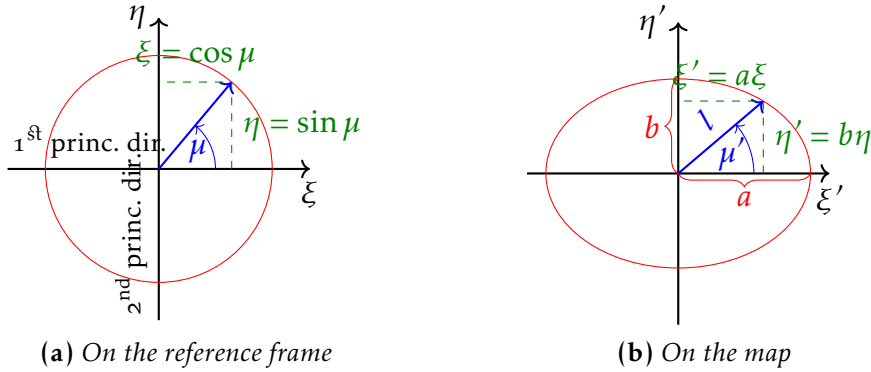


Figure VIII.3: Tissor's indicatrix

We know that the areal scale can be obtained as the ratio of a small mapped area divided by its corresponding area on the reference frame. Divide the area of the ellipse of distortion by the area of the original circle to obtain a third method for calculating the areal distortion:

$$p = \lim_{\Delta S \rightarrow 0} \frac{\Delta S'}{\Delta S} = \frac{ab\pi}{1^2\pi} = ab$$

That is, for equal-area projections $ab = 1$, the area of the ellipses of distortion is independent of location.

Let us examine the angular distortion of angles with one arm in the first principal direction:

$$i = \frac{\tan \mu'}{\tan \mu} = \frac{\frac{b\eta}{a\xi}}{\frac{\eta}{\xi}} = \frac{b}{a}$$

That is, in conformal projections, $a = b$. This means that in the case of conformality, the ellipses of distortion will be circles.

We can calculate the linear scale by taking the ratio of infinitesimal mapped distances to corresponding distances on the reference frame. The small radius subtending angle μ on the reference frame from the first principal direction is assumed to be unit. Its image is the small semi-diameter of the distortion ellipse, whose length can be calculated by multiplying the

coordinates on the tangent plane of the reference frame by a and b , taking into account the stretching by b/a and the scaling by a :

$$l = \frac{\sqrt{\xi'^2 + \eta'^2}}{1} = \sqrt{a^2 \xi^2 + b^2 \eta^2} = \sqrt{a^2 \cos^2 \mu + b^2 \sin^2 \mu}$$

Now we can prove proposition III. Earlier we stipulated that $a \geq b$ and since the linear scale is by definition positive, $a^2 \geq b^2$. Since $\cos^2 \mu + \sin^2 \mu = 1$, we have some weighted average of a^2 and b^2 under the square root. Its value is maximal if a^2 has weight 1 and b^2 has weight 0, and minimal if b^2 has weight 1 and a^2 has weight 0. It follows that $b \leq l \leq a$ and l has a maximum at $\mu = 0^\circ$ and a minimum at $\mu = 90^\circ$, which is also a principal direction of the map projection due to proposition II. Thus, the extrema are in the principal directions of the projection. This completes the proof. There is a problem if $a = l = b$ because in this case, there are extrema in all directions. However, in this case, the projection is conformal, any pair of perpendicular directions will be mapped to a pair of perpendicular directions. That is, in conformal projections, each direction is a principal direction. Tissot's theorem is thus fully proved.

Henceforth, a will be called *maximum* and b *minimum linear scale*. Another important result is that we have seen that in conformal projections, the linear scale is independent of the direction because $a = b = l$.

VIII.3 Calculation of extremal linear scales

In the following, we look for practical formulæ for a and b . Let v denote the angle on the reference frame formed by the parallel and the first principal direction! Then the meridian will form $v + 90^\circ$. The linear scale along the meridian and the parallel is obtained by the formula:

$$h = \sqrt{a^2 \cos^2(v + 90^\circ) + b^2 \sin^2(v + 90^\circ)}$$

$$k = \sqrt{a^2 \cos^2 v + b^2 \sin^2 v}$$

That is:*

$$h^2 + k^2 = a^2 \sin^2 v + b^2 \cos^2 v + a^2 \cos^2 v + b^2 \sin^2 v = a^2 + b^2$$

* The relation obtained here is generally valid: APOLLONIUS was the first to show that the sum of the squares of two *conjugate semi-diameters* of an ellipse (considering the ellipse as an affine image of a circle, the images of two perpendicular radii of the original circle) is constant.

VIII. Tissot's theory of map distortion

Any formula obtained for the areal scale should give the same value:

$$p = hk \sin \vartheta = ab$$

From the previous two equations:

$$\begin{aligned} (a+b)^2 &= a^2 + b^2 + 2ab = h^2 + k^2 + 2hk \sin \vartheta \\ (a-b)^2 &= a^2 + b^2 - 2ab = h^2 + k^2 - 2hk \sin \vartheta \end{aligned}$$

A simple transformation gives:

$$\begin{aligned} a &= \frac{a+b+a-b}{2} = \frac{\sqrt{(a+b)^2} + \sqrt{(a-b)^2}}{2} \\ b &= \frac{a+b-(a-b)}{2} = \frac{\sqrt{(a+b)^2} - \sqrt{(a-b)^2}}{2} \end{aligned}$$

That is, the final result:

$$\begin{aligned} a &= \frac{\sqrt{h^2 + k^2 + 2hk \sin \vartheta} + \sqrt{h^2 + k^2 - 2hk \sin \vartheta}}{2} \\ b &= \frac{\sqrt{h^2 + k^2 + 2hk \sin \vartheta} - \sqrt{h^2 + k^2 - 2hk \sin \vartheta}}{2} \end{aligned}$$

Let us make some observations! In projections with rectangular graticule (and hence in any conical projection), the graticule lines are principal directions, so h and k are also the extremal linear scales. In conformal projections, all directions, including the graticules, are principal directions, i.e. the graticule is always rectangular ($\vartheta = 90^\circ$). To prove the conformality if the graticule is rectangular, it is sufficient to check $h = k$, since h and k can be substituted for a and b .

VIII.4 Maximum angular deviation

Before we start, let us do some calculations with the angle μ and its image μ' subtended from the first principal direction. Consider the following fraction:

$$\begin{aligned} \frac{\sin(\mu - \mu')}{\sin(\mu + \mu')} &= \frac{\sin \mu \cos \mu' - \cos \mu \sin \mu'}{\sin \mu \cos \mu' + \cos \mu \sin \mu'} \\ &= \frac{\frac{\sin \mu \cos \mu'}{\cos \mu \sin \mu'} - 1}{\frac{\sin \mu \cos \mu'}{\cos \mu \sin \mu'} + 1} = \frac{\frac{\tan \mu}{\tan \mu'} - 1}{\frac{\tan \mu}{\tan \mu'} + 1} = \frac{\frac{a}{b} - 1}{\frac{a}{b} + 1} = \frac{a - b}{a + b} \end{aligned}$$

VIII. Tissot's theory of map distortion

We have just applied our previous knowledge that for such angles, $i = \tan \mu' / \tan \mu = b/a$. The equation above is multiplied by $\sin(\mu + \mu')$:

$$\begin{aligned}\sin(\mu - \mu') &= \frac{a-b}{a+b} \sin(\mu + \mu') \leq \frac{a-b}{a+b} \\ \mu - \mu' &\leq \arcsin \frac{a-b}{a+b}\end{aligned}$$

The relation above gives an upper bound on the maximal change in the direction an arm of angle can undergo during the projection. This necessarily leads to the conclusion that an angle will suffer the maximum possible angular deviation if both arms change by that amount. Then the *maximum angular deviation* is denoted by ω :

$$\omega = 2 \arcsin \frac{a-b}{a+b}$$

Considering that the arc sine never gives a value greater than 90° , ω is always less than or equal to 180° . The maximum angular deviation can sometimes be more illustrative than the angular distortion.

Lesson nine

Map distortions in practice

IX.1 Visualizing distortions

To choose the most appropriate projection for the purpose of our representation, we need to observe their distortions. We need to visualize the distortions in some way, typically by using the concepts of diagrams and isolines familiar from thematic cartography. The use of Tissot's indicatrices is obvious. The infinitely small ellipses of distortion must be enlarged using some convention in order to make them finite. The ellipses must be rotated so that the semi-axes are aligned with the corresponding principal directions of the projection. The distortions are read as follows (Fig. IX.1):

- The linear scale is directly proportional to the semi-diameter of the ellipse in the corresponding direction.
- The flattening of the ellipse illustrates the angular distortion. Circular indicatrices indicate conformal projections.
- The area of the ellipse represents the areal scale. Ellipses of the same area everywhere on the map suggest an equal-area projection.

Another option is the isoline of equal distortion (*isocol*). This can only show quantities that do not depend on direction, only on the location, so it is not possible to visualize linear scale in this way.* The areal scale, however, depends only on location, so the method can be applied to it. Sometimes p is replaced by its deviation from 1 on the maps. The angular distortion is only independent of the direction of the second arm if the first arm is in the first principal direction of the projection. Therefore, the maximum angular variation ω is often plotted on the map instead.

CHEBYSHEV's theorem is helpful in finding the projection suitable to the area to be plotted: *if one of the isocols of a conformal projection coincides with the boundary of the area to be plotted, then it has the lowest possible distortion among conformal projections.*† An example of CHEBYSHEV's theorem is that

* Except for conformal projections, as we have seen earlier that the linear scale in these projections is independent of direction.

† To put it more precisely, the difference between the logarithms of the minimal and maximal linear scales in the area shown is minimal.

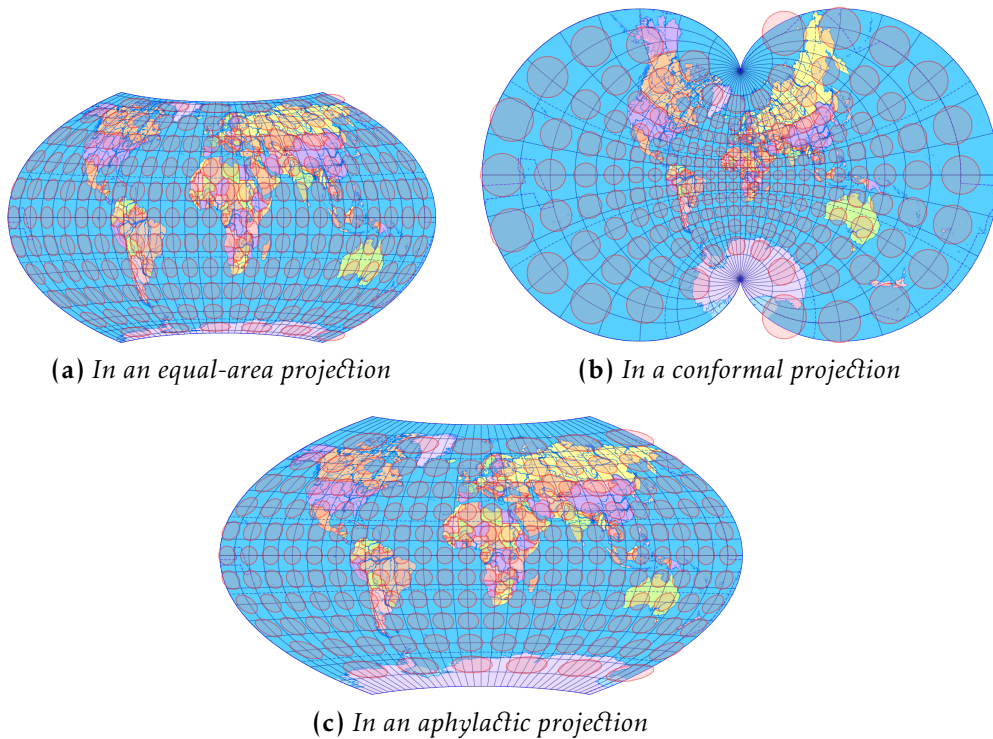


Figure IX.1: *Ellipses of distortion*

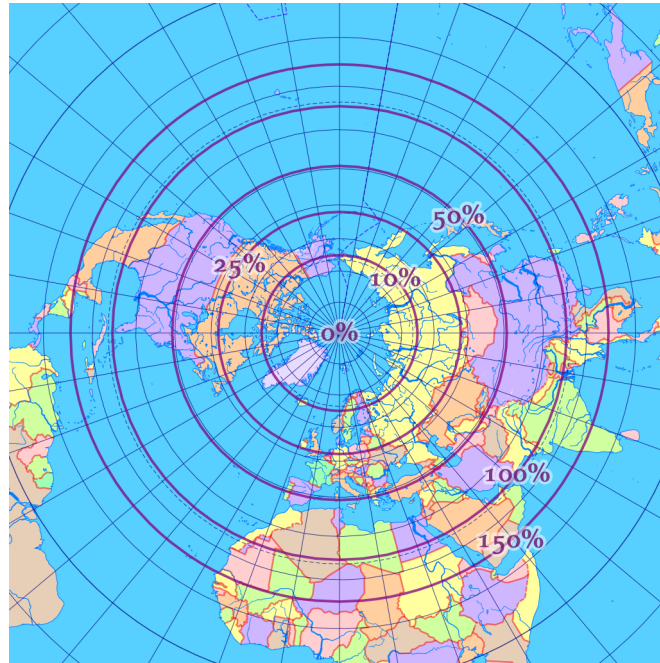
the stereographic projection has isocols as circles (Fig. IX.2), so it is the projection of the most favourable distortion for circular areas.

For non-conformal projections, the theorem does not hold, and a counter-example is easy to find: the projections of LAMBERT and WIECHEL are both equal-area and their isocols are circles (Fig. IX.2). Yet the WIECHEL projection has a much more unfavourable distortion, so the latter is certainly not the best equal-area projection for representing circular areas. Nevertheless, recent research suggests that the isocols of the best projections also follow the boundary of the area being plotted, so in such cases, we also tend to choose projections whose isocols are preferably parallel to the boundary of our area.

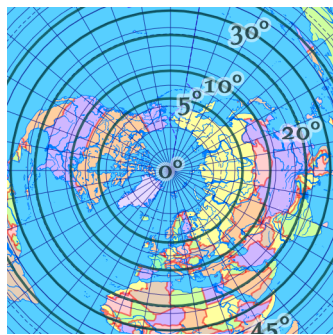
IX.2 Distortions not predicted by Tissot's theory

Our choice of map projection can also be affected by distortions that are not predicted by Tissot's theorem. For example, maps are typically oriented to the North. However, the projected graticule does not necessarily satisfy this at all points: the discrepancy between the vertical direction and true north is called *meridian convergence*. This is not a distortion in the classical

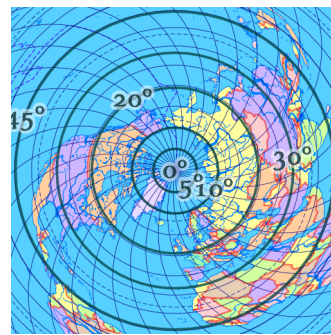
IX. Map distortions in practice



(a) In the stereographic projection ($p - 1$)



(b) In LAMBERT azimuthal (ω)



(c) In WIECHEL projection (ω)

Figure IX.2: Isocols

sense, because it only rotates parts of the map. The meridian convergence γ is calculated from the slope (derivative) of the tangent of the mapped meridian, where λ is constant:

$$\tan \gamma = \frac{dx}{dy} = \lim_{\Delta\varphi \rightarrow 0} \frac{x(\varphi + \Delta\varphi, \lambda) - x(\varphi, \lambda)}{y(\varphi + \Delta\varphi, \lambda) - y(\varphi, \lambda)} = \frac{\partial x}{\partial \varphi} \bigg/ \frac{\partial y}{\partial \varphi}$$

There is no meridian convergence in cylindrical projections, and no meridian convergence is expected for other projections in the centre of the map. This is usually achieved by adjusting the *central meridian** appropriately. This can be thought of as substituting $\lambda - \lambda_m$ for λ in the formulæ, where λ_m is the central meridian. Since in most projections, there is no meridian convergence at the central meridian ($\lambda = 0^\circ$), λ_m is usually the longitude running through the centre of our area.

It rather counts as a distortion, yet Tissot's theory does not predict that mapped geodetic lines are not necessarily straight lines. The deviation from this is expressed by the *flexion* f , which is the number of radians the geodetic line turns for a unit distance on the line:

$$f = \frac{d\alpha}{ds}$$

A projection that maps geodesics to straight lines can be constructed in case of a spherical surface, but not for an ellipsoid of revolution.

Conformal projections are locally similarity transformations according to Tissot's theory. Yet no one would think that, for example, MERCATOR'S projection (Fig. XIII.3) would show Greenland as similar to the original shape. The reason for the shape distortion seen here is that the linear scales change rapidly from place to place; whereas in the same projection, the shape of Africa looks less distorted because the linear scale changes slowly here. The resulting degree of shape distortion is indicated by the *skewness* s , which measures how the length distortion multiplies for a unit distance:

$$s = \frac{1}{l} \frac{dl}{ds}$$

Flexion and skewness were recently defined by two astrophysicists, GOLDBERG and GOTT, to study the distortion of planetary maps. The formulæ for practical calculations were derived by KERKOVITS.

* The Prime meridian is not the same as the central meridian! The Prime meridian is the 0° meridian from which λ is measured; while the central meridian is the longitude of typically round number that becomes the axis of symmetry of the mapped graticule. The longitude $\pm 180^\circ$ from the central meridian, in which most projections have discontinuities, is called the *antimeridian*.

IX.3 Auxiliary spheres

Sometimes, it is easier to derive a map projection for the ellipsoid as a *double mapping*: in the first step, we map the ellipsoid onto an *auxiliary sphere*, then a spherical projection is applied between the sphere and the plane. These spheres are not distortion-free, so it is important to use a sphere that has the same distortion characteristic as the desired projection: e.g. the authalic (equal-area) sphere should be chosen for an equal-area double mapping.

For all auxiliary spheres, we expect parallels and meridians get mapped onto parallels and meridians, respectively. We further expect that mapped parallels are evenly divided by meridians:

$$\begin{aligned}\varphi &= f(\Phi) \\ \lambda &= c\Lambda\end{aligned}$$

Calculate the linear scales of auxiliary spheres.

$$\begin{aligned}h &= \lim_{\Delta m \rightarrow 0} \frac{\Delta m'}{\Delta m} = \lim_{\Delta \Phi \rightarrow 0} \frac{R \widehat{\Delta \varphi}}{M(\Phi) \widehat{\Delta \Phi}} = \frac{R}{M(\Phi)} \frac{d\varphi}{d\Phi} \\ k &= \lim_{\Delta n \rightarrow 0} \frac{\Delta n'}{\Delta n} = \lim_{\Delta \Lambda \rightarrow 0} \frac{R \cos \varphi \widehat{\Delta \lambda}}{N(\Phi) \cos \Phi \widehat{\Delta \Lambda}} = \frac{R \cos \varphi}{N(\Phi) \cos \Phi}\end{aligned}$$

Note that all auxiliary spheres are rectangular ($\vartheta = 90^\circ$), so h and k are also the a and b maximal and minimal linear scales. The simplest auxiliary sphere is the spherical model of Google Earth:

$$\begin{aligned}\varphi &= \Phi \\ \lambda &= \Lambda\end{aligned}$$

It can be seen that the projection meets all our expectations. The radius of this sphere is the *equatorial radius* of the Earth (6378.137 km). The mapping is *aphylactic*, i.e. $h \neq k$ and $hk \neq 1$.

The *authalic sphere* is equal-area. We know that $hk = 1$.

$$\begin{aligned}\frac{R}{M(\Phi)} \frac{d\varphi}{d\Phi} \frac{R \cos \varphi}{N(\Phi) \cos \Phi} &= 1 \\ \cos \varphi d\varphi &= \frac{M(\Phi)N(\Phi) \cos \Phi}{R^2 c} d\Phi \\ \int \cos \varphi d\varphi &= \frac{a^2(1-e^2)}{R^2 c} \int \frac{\cos \Phi}{(1-e^2 \sin^2 \Phi)^2} d\Phi \\ \sin \varphi &= \frac{a^2(1-e^2)}{R^2 c} \left[\frac{\sin \Phi}{2(1-e^2 \sin^2 \Phi)} + \frac{1}{4e} \ln \frac{1+e \sin \Phi}{1-e \sin \Phi} \right] + \kappa\end{aligned}$$

IX. Map distortions in practice

Recall that we have already obtained the complicated integral on the right-hand side in Sec. IV.4, and we could substitute it. κ is a constant of integration, it can take any value. We usually choose $c = 1$ and $\kappa = 0$. Note that it makes sense to use this projection with the authalic radius (Sec. VI.5) only!

Let us also develop the *rectifying sphere*, which is equidistant in meridians ($h = 1$).

$$\begin{aligned}\frac{R}{M(\Phi)} \frac{d\varphi}{d\Phi} &= 1 \\ d\varphi &= \frac{M(\Phi)}{R} d\Phi \\ \varphi &= \frac{1}{R} \int M(\Phi) d\Phi + \kappa\end{aligned}$$

We usually use this projection with $c = 1$, $\kappa = 0$, but now we should substitute the rectifying radius for R .

Now only the calculation of the *conformal sphere* ($h = k$) is left:

$$\begin{aligned}\frac{R}{M(\Phi)} \frac{d\varphi}{d\Phi} &= \frac{Rc \cos \varphi}{N(\Phi) \cos \Phi} \\ \frac{1}{\cos \varphi} d\varphi &= \frac{cM(\Phi)}{N(\Phi) \cos \Phi} d\Phi \\ \int \frac{1}{\cos \varphi} d\varphi &= c \int \frac{1 - e^2}{\cos \Phi (1 - e^2 \sin^2 \Phi)} d\Phi\end{aligned}$$

The left-hand side integral is already known since Sec. III.3. The one on the right-hand side needs to be transformed:

$$\begin{aligned}\int \frac{1 - e^2}{\cos \Phi (1 - e^2 \sin^2 \Phi)} d\Phi &= \int \frac{1 - e^2 \sin^2 \Phi - e^2 \cos^2 \Phi}{\cos \Phi (1 - e^2 \sin^2 \Phi)} d\Phi \\ &= \int \frac{1}{\cos \Phi} - \frac{e^2 \cos \Phi}{1 - e^2 \sin^2 \Phi} d\Phi = \ln \tan\left(45^\circ + \frac{\Phi}{2}\right) - e \operatorname{artanh}(e \sin \Phi) + \ln \kappa\end{aligned}$$

The last step can be checked again by deriving back, this time the constant of integration is written as $\ln \kappa$. Substituted back into the previous equation:

$$\ln \tan\left(45^\circ + \frac{\varphi}{2}\right) = c \ln \tan\left(45^\circ + \frac{\Phi}{2}\right) - \frac{ce}{2} \ln \frac{1 + e \sin \Phi}{1 - e \sin \Phi} + \ln \kappa$$

$$\tan\left(45^\circ + \frac{\varphi}{2}\right) = \kappa \tan^c\left(45^\circ + \frac{\Phi}{2}\right) \left(\frac{1 - e \sin \Phi}{1 + e \sin \Phi}\right)^{ce/2}$$

$$\varphi = 2 \arctan \left[\kappa \tan^c\left(45^\circ + \frac{\Phi}{2}\right) \left(\frac{1 - e \sin \Phi}{1 + e \sin \Phi}\right)^{ce/2} \right] - 90^\circ$$

Φ cannot be expressed from the equation, but can be obtained using fixed-point iteration:

$$\Phi'' = 2 \operatorname{arctg}^c \sqrt{\frac{\operatorname{tg}\left(45^\circ + \frac{\varphi}{2}\right)}{\kappa \left(\frac{1 - e \sin \Phi'}{1 + e \sin \Phi'}\right)^{ce/2}}} - 90^\circ$$

First we use the approximation $\Phi \approx \varphi$, then we use the formula above to obtain further and further improved values. Usually four or five approximations are enough, the procedure converges rapidly. Remember that the formula $\lambda = c\Lambda$ still applies! The radius of the sphere does not affect conformality. At small scales, we can give it any value, and we usually choose $\kappa = 1$, $c = 1$.

At large scales, we choose the *Gaussian conformal sphere*, which declares an arbitrarily chosen parallel Φ_s as distortion-free, and minimizes distortions in the vicinity of the parallel (i.e. the first two derivatives of the logarithm of the linear scale are zero at this latitude). Skipping derivation, the chosen radius is the radius of the osculating sphere, the calculation of c and the spherical latitude φ_s of the standard parallel is:

$$\tan \varphi_s = \frac{\tan \Phi_s}{\sqrt{1 + (e')^2 \cos^2 \Phi_s}}$$

$$R = \sqrt{M(\Phi_s)N(\Phi_s)}$$

$$c = \frac{\sin \Phi_s}{\sin \varphi_s}$$

Then, by substituting Φ_s and φ_s back into the mapping formulæ, we also obtain the missing optimal value for κ . Sometimes, the spherical latitude of the standard parallel is given for this projection, but the constants can be calculated from the above formulæ in this case as well. This projection has a very low distortion: for Hungary, the deviation of the linear scale from one is less than 1 : 4 000 000, the correction in azimuth due to the difference between ellipsoidal and spherical geodesics can be ignored even for distances up to 50 km ($< 0.008''$).

Second module

Conical map projections

Lesson ten

Perspective azimuthals

X.1 Azimuthals in general

We are now at the point where we are getting to know specific map projections. Let us start our exploration of *azimuthal projections*: Azimuthals are best discussed in a polar coordinate system. The mapped parallels are concentric full circles. The straight concurrent meridians divide them equidistantly, so the polar angle is equal to the longitude, and only the radii of the mapped parallels can be varied. Let this radius be denoted by the strictly increasing *radius function* $\rho(\delta)$, where the *colatitude* δ is the complementary angle of the latitude φ ($\delta = 90^\circ - \varphi$)! This uniquely defines the azimuthal projection (Fig. X.1):

$$\begin{aligned}x &= \rho \sin \lambda \\y &= -\rho \cos \lambda\end{aligned}$$

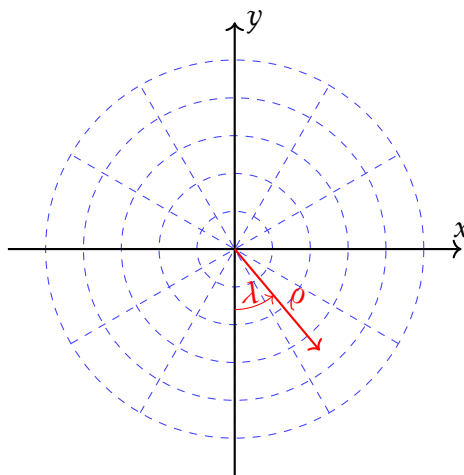


Figure X.1: Polar coordinates in azimuthals

These projections are called *azimuthal* because they preserve the azimuths of the orthodromes starting from the centre; and they are also called *zenithal*

because points at the same distance from the centre are also at the same distance on the map. Linear scales along graticule lines:

$$h = \frac{\sqrt{\left(\frac{\partial x}{\partial \varphi}\right)^2 + \left(\frac{\partial y}{\partial \varphi}\right)^2}}{R} = \frac{\sqrt{\left(\frac{d\rho}{d\varphi}\right)^2 \sin^2 \lambda + \left(\frac{d\rho}{d\varphi}\right)^2 \cos^2 \lambda}}{R}$$

$$= \frac{\sqrt{\left(-\frac{d\rho}{d\delta}\right)^2 \sin^2 \lambda + \left(-\frac{d\rho}{d\delta}\right)^2 \cos^2 \lambda}}{R} = \frac{1}{R} \frac{d\rho}{d\delta}$$

$$k = \frac{\sqrt{\left(\frac{\partial x}{\partial \lambda}\right)^2 + \left(\frac{\partial y}{\partial \lambda}\right)^2}}{R \cos \varphi} = \frac{\sqrt{\rho^2 \cos^2 \lambda + \rho^2 \sin^2 \lambda}}{R \sin \delta} = \frac{\rho}{R \sin \delta}$$

We have just taken advantage of the fact that:

$$\frac{d\rho}{d\varphi} = \frac{d\rho}{d\delta} \frac{d\delta}{d\varphi} = \frac{d\rho}{d\delta} \frac{d(90^\circ - \varphi)}{d\varphi} = -\frac{d\rho}{d\delta}$$

In general, we note that for the purpose of continuous representation at the pole, we can expect $\rho(0) = 0$. Furthermore, the colatitude δ need not be measured from the North Pole for azimuthal and conic projections, it can be measured from the South Pole. In this case, the Southern Hemisphere will be at the centre of the map.

X.2 Vertical perspective projection

Vertical perspective projections can be produced by using a central perspective projection. Denote the distance between the centre of the sphere and the focal point by fR , and the distance between the focal point and the plane by cR . The perspective projection is *tangent* if the plane touches the sphere ($c = 1 + f$), *secant* if it intersects the sphere, otherwise, it is *extern*. The ratios of the legs of the two similar right triangles in Fig. X.2 are equal:

$$\frac{R(f + \cos \delta)}{R \sin \delta} = \frac{cR}{\rho}$$

$$\rho = R \frac{c \sin \delta}{f + \cos \delta}$$

Of the vertical perspective projections, the ones with focal points outside the sphere ($|f| > 1$) are the most common. If the centre of projection and the plane are on the same side of the sphere ($f < -1$, *near-side perspective*), then the Earth is represented as it appears from above. This is similar to

X. Perspective azimuthals

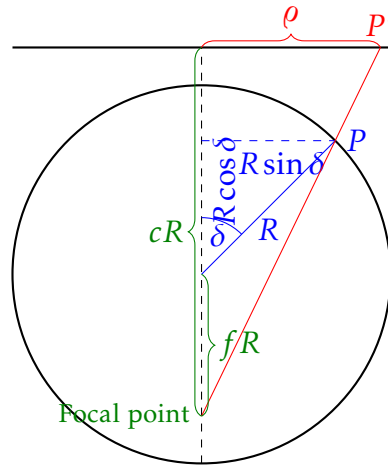


Figure X.2: The principle of the vertical perspective projection

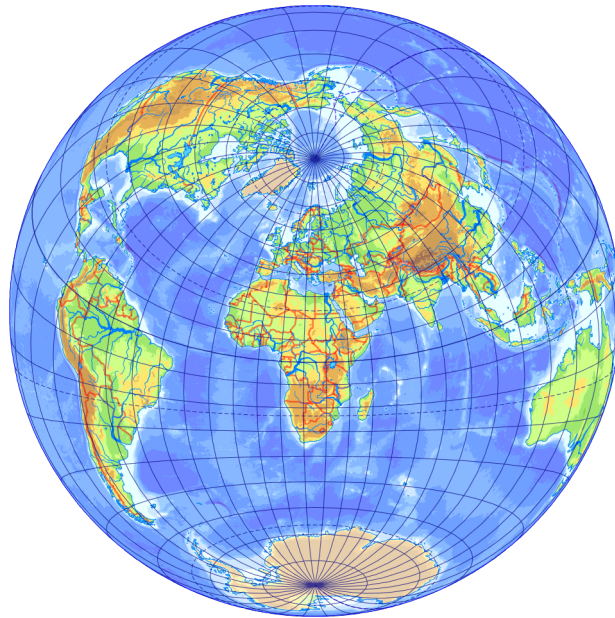


Figure X.3: Oblique far-side perspective projection

the mapping found in Google Earth. If the focal point is at the opposite side of the sphere (*far-side perspective*), it can be used to represent areas larger than a hemisphere (Fig. X.3).

Perspective azimuthals map those spherical circles whose plane contains the centre of projection into a straight line. This is easy to see since the rays from the centre of projection are in this plane. The line of intersection of the plane of the projection and that of the rays is, of course, a straight line. The images of other spherical circles are conic sections. This is also easy to prove because this time the rays between the circle and the focal point now form an oblique cone, whose planar sections are by definition conic sections.

X.3 Gnomonic projection

In the case of $f = 0$ (projection from the centre):

$$\rho = cR \tan \delta$$

This is called the *gnomonic* projection (Fig. X.4) and was created by THALES. The formula shows that the Equator can no longer be represented by it. The distortions for the tangent ($c = 1$) placement are:

$$h = \frac{1}{R} \frac{d\rho}{d\delta} = \frac{1}{\cos^2 \delta}$$

$$k = \frac{\rho}{R \sin \delta} = \frac{\tan \delta}{\sin \delta} = \frac{1}{\cos \delta}$$

At the pole $h = k = 1$, so it is true-scale, while at the Equator, the distortions are infinitely large. In between, the distortions increase rapidly, with a significant increase in areal ($hk > 1$) and angular distortion ($h \neq k$). Its distortions are very unfavourable, but it is rarely used because this projection maps spherical geodesic lines to straight lines (since the centre of projection is now in their plane). This may be of interest for communication (e.g. positioning radio towers) or navigation purposes.

The projection is also easily recognizable in the transverse and oblique aspects because its meridians are parallel or concurrent lines, and mapped parallels are conic sections.

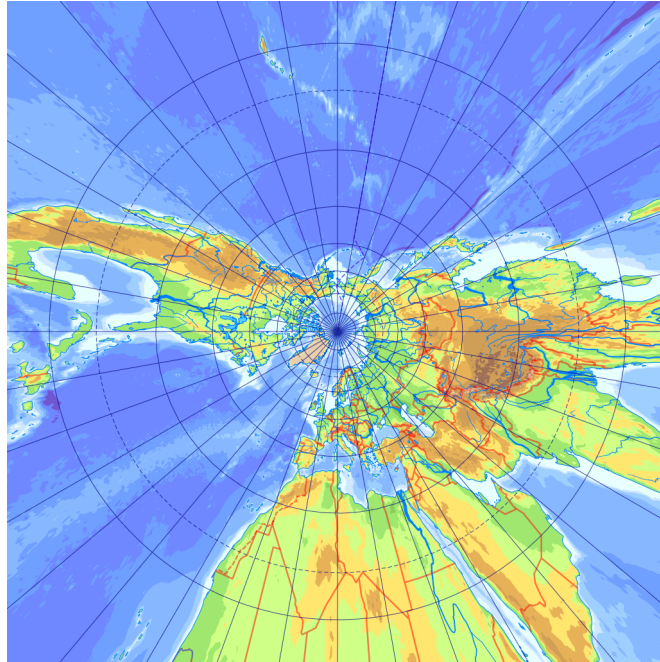


Figure X.4: Gnomonic projection

X.4 Orthographic projection

Let us consider the case $f \rightarrow \infty, c \rightarrow \infty$ by limit calculus (in this case the centre of projection is infinitely far away, the rays are parallel):

$$\rho = R \sin \delta$$

This is the *orthographic* projection, which shows the Earth as if viewed from a great distance (Fig. X.5). It was created by APOLLONIUS. Since distant celestial bodies are seen in this way when viewed through a telescope, it is a popular choice for planetary maps, especially in the transverse aspect. No area larger than a hemisphere can be represented. The distortions:

$$h = \frac{1}{R} \frac{d\rho}{d\delta} = \cos \delta$$

$$k = \frac{\rho}{R \sin \delta} = \frac{\sin \delta}{\sin \delta} = 1$$

$k = 1$, so the projection is equidistant in parallels. There is no distortion at the pole ($h = 1$), linear scale along meridians is unacceptable at the Equator ($h = 0$). The distortions increase rapidly away from the pole causing areal reduction ($hk < 1$) and angular distortion ($h \neq k$). In rotated aspects, the mapped meridians are arcs of ellipses and the parallels are displayed as arcs of ellipses or parallel lines (the latter in transverse aspect).

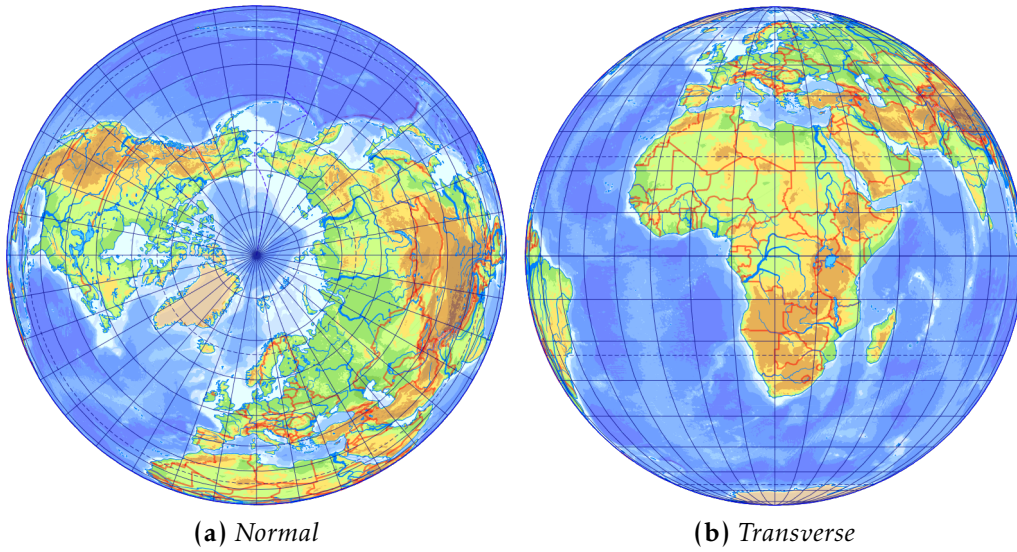


Figure X.5: Orthographic projection

X.5 Stereographic projection

The most important perspective azimuthal projection is $f = 1$, i.e. when the centre of projection is at the opposite pole. This is the *stereographic* projection (Fig. X.6):

$$\rho = Rc \frac{\sin \delta}{1 + \cos \delta} = Rc \frac{2 \sin \frac{\delta}{2} \cos \frac{\delta}{2}}{\sin^2 \frac{\delta}{2} + \cos^2 \frac{\delta}{2} + \cos^2 \frac{\delta}{2} - \sin^2 \frac{\delta}{2}} = Rc \tan \frac{\delta}{2}$$

To understand the properties of distortion, we calculate the linear scales along graticule lines:

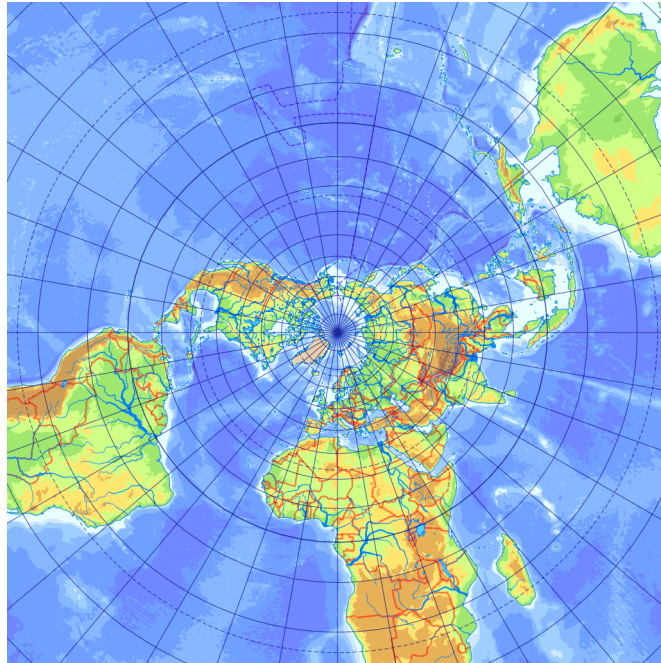
$$h = \frac{1}{R} \frac{d\rho}{d\delta} = \frac{1}{R} \frac{Rc}{2 \cos^2 \frac{\delta}{2}} = \frac{c}{2 \cos^2 \frac{\delta}{2}}$$

$$k = \frac{\rho}{R \sin \delta} = \frac{Rc \tan \frac{\delta}{2}}{2R \sin \frac{\delta}{2} \cos \frac{\delta}{2}} = \frac{c}{2 \cos^2 \frac{\delta}{2}}$$

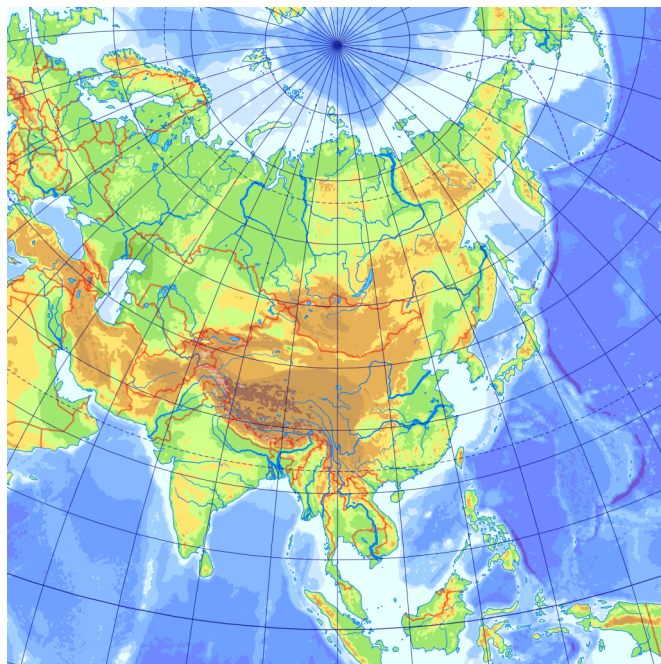
$h = k$, i.e. the stereographic projection is conformal. In addition, the every spherical circle in this projection is either a circle or a straight line, i.e. the projection *preserves circles*. The procedure of the proof can be followed in Fig. X.7:

Take an arbitrary circle on the surface of the sphere. The figure shows the vertical section of the sphere that is perpendicular to the plane of the circle. We have seen earlier that if the plane of the circle contains the focal point

X. Perspective azimuthals



(a) *Normal*



(b) *Oblique (for Asia)*

Figure X.6: *Stereographic projection*

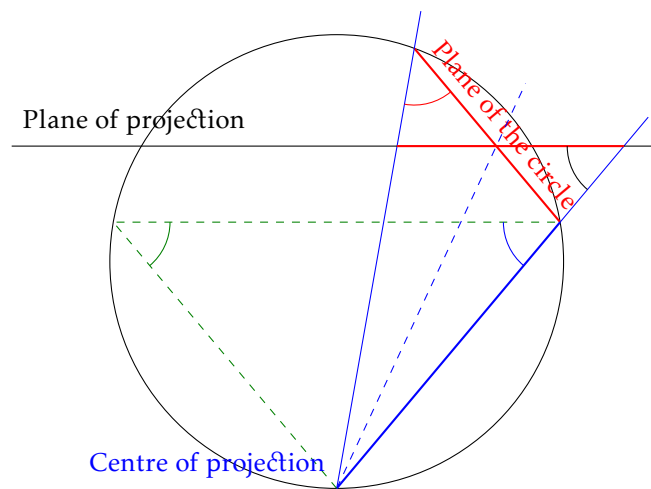


Figure X.7: *The stereographic projection preserves circles*

then its mapped image is straight in all perspective azimuthal projections; we will now consider only circles in a general position. Each point of the circle is connected to the focal point by a ray, forming an oblique cone (blue). The plane of projection cuts out a conic section. The red and green angles are the same because they are inscribed angles of the same thick blue chord. The green and blue angles are equal because of symmetry, while the blue and black are corresponding angles, so all four angles are equal.

The blue oblique cone is symmetrical to the plane marked by the blue dashed line because it is the angle bisector of the aperture. Since the vertical positioning of the plane of projection does not affect the preservation of circles (since it is only a uniform scaling), it can be positioned without loss of generality to contain the intersection line of the plane of the original circle and the symmetry plane of the oblique cone (which is perpendicular to the plane of the figure). Since the red and black angles are the same, the plane of the circle and the plane of the projection are mirror images of each other in the blue dashed plane. So the mapped image marked in red on the plane of projection can also be produced as a mirror image of the original circle, so it is also a circle, of course. This completes the proof.

This projection was known to the ancient Egyptians and was used in star maps. Today it is used, among other things, on meteorological maps where measurement of angles is important. The isocols of the projection are circles centred on the pole, i.e. it is the least distorted conformal projection for circular regions according to CHEBYSHEV's theorem. Therefore, it is often found in transverse (e.g. conformal maps of hemispheres) and oblique aspects for nearly circular areas. Because of its advantageous properties,

X. Perspective azimuthals

this mapping is widely used despite the fact that the South Pole is mapped to infinity.

The $c = 2$ (tangent) version is true-scale at the North Pole ($h = k = 1$), and distortions increase rapidly away from it. Let the plane intersect the sphere in the secant parallel δ_s ! Then:

$$c = 1 + \cos \delta_s = \sin^2 \frac{\delta_s}{2} + \cos^2 \frac{\delta_s}{2} + \cos^2 \frac{\delta_s}{2} - \sin^2 \frac{\delta_s}{2} = 2 \cos^2 \frac{\delta_s}{2}$$

Substituting back into the formula for h and k and looking at $\delta = \delta_s$, we find no distortion ($h = k = 1$), i.e. the secant parallel of the secant stereographic projection is true-scale.* Note that c is just a scaling factor in the projection, so the secant stereographic projection can always be obtained by reducing the corresponding tangent projection.

Derivation of the oblique tangent stereographic projection ($c = 2$):

$$\begin{aligned} \rho &= 2R \frac{\sin \delta'}{1 + \cos \delta'} = 2R \frac{\cos \varphi'}{1 + \sin \varphi'} \\ x &= \rho \sin \lambda' = 2R \frac{\cos \varphi' \sin \lambda'}{1 + \sin \varphi'} \\ &= -2R \frac{\sin(\lambda - \lambda_o) \cos \varphi}{1 + \sin \varphi \sin \varphi_o + \cos \varphi \cos \varphi_o \cos(\lambda - \lambda_o)} \\ y &= -\rho \cos \lambda' = -2R \frac{\cos \varphi' \cos \lambda'}{1 + \sin \varphi'} \\ &= -2R \frac{\sin \varphi \cos \varphi_o - \cos \varphi \sin \varphi_o \cos(\lambda - \lambda_o)}{1 + \sin \varphi \sin \varphi_o + \cos \varphi \cos \varphi_o \cos(\lambda - \lambda_o)} \end{aligned}$$

The derivation of the inverse projection formulæ is given in App. H.

The graticule of an oblique stereographic projection is easily identified by its conformality and preservation of circles: the mapped graticule lines in each aspect are complete circles or straight lines, which always intersect at right angles.

* Although, unfortunately, the literature on map projections sometimes states uninformedly the opposite, perspective projections are usually not true-scale in the secant parallel, this is just a special property of the stereographic projection!

Lesson eleven

Non-perspective azimuthals

XI.1 Azimuthal equidistant

Let us develop a map projection equidistant in meridians ($h = 1$)!

$$\begin{aligned}\frac{1}{R} \frac{d\rho}{d\delta} &= 1 \\ \int d\rho &= R \int d\delta \\ \rho &= R\widehat{\delta} + d\end{aligned}$$

The constant of integration $d = 0$ because at the pole $\rho = 0$. This is the *azimuthal equidistant projection* (Fig. XI.1). Despite it is also named after POSTEL, this projection was not invented by him: ancient Egyptians had already used it for star maps. The linear scale along parallels:

$$k = \frac{\rho}{R \sin \delta} = \frac{\widehat{\delta}}{\sin \delta}$$

At the North Pole ($\delta = 0$), k is obtained by L'HÔPITAL's rule:

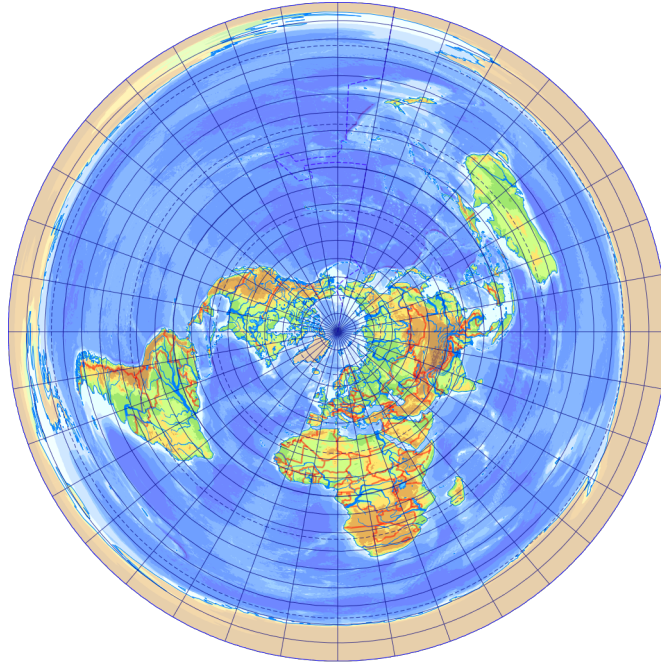
$$\lim_{\delta \rightarrow 0} k = \lim_{\delta \rightarrow 0} \frac{\widehat{\delta}}{\sin \delta} = \lim_{\delta \rightarrow 0} \frac{1}{\cos \delta} = 1$$

At the North Pole, the projection is distortion-free ($h = k = 1$), at the South Pole the denominator of k is zero, the distortion is thus infinitely large, and distortions increase gradually between the two.

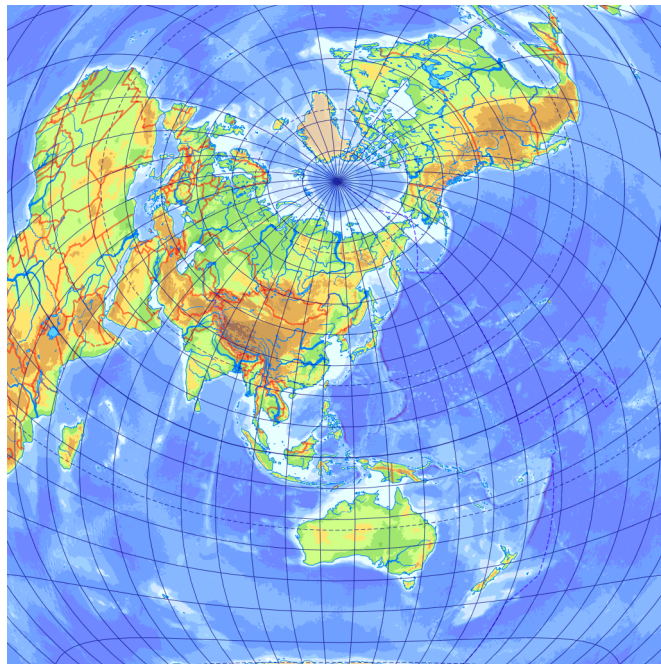
The isocols are circles, since k is a function of δ only, while h is constant. Although an azimuthal projection with a more favourable distortion is known, its formulæ are very complicated, and it does not deviate spectacularly from this projection in areas smaller than a hemisphere. Therefore, if neither conformality nor equivalency is required, this mapping is recommended as a rule of thumb for nearly circular areas.

In the oblique aspect, the metapole of the projection will be undistorted and the metameridians radiating from it will be azimuthal and equidistant.

XI. *Non-perspective azimuthals*



(a) *Normal*



(b) *Oblique (centred on North Korea)*

Figure XI.1: *Azimuthal equidistant projection*

This is advantageous, for example, for applications in communication. It is also advantageous that the concentric circles centred on the metapole are metaparallels, which map to equidistant concentric circles. For example, if one wants to represent the areas that North Korea's missile of a given range can hit, one simply needs to use this projection in the correct aspect, since in this way circles centred on North Korea are mapped to circles of true radii. This latter feature is also advantageous when, for example, flights departing from a particular airport are to be shown.

The eastern and western hemispheres are also circular areas, and the transverse aspect of this projection is used to represent them side by side, especially in atlases. Derivation using the transverse formulæ at the end of Sec. V.3:

$$\begin{aligned}\rho &= R\widehat{\delta}' = R\arccos \cos \delta' = R\arccos \sin \varphi' = R\arccos(\cos \varphi \cos \lambda) \\ x &= \rho \sin \lambda' = R\arccos(\cos \varphi \cos \lambda) \frac{\sin \lambda \cos \varphi}{\sqrt{1 - \cos^2 \varphi \cos^2 \lambda}} \\ y &= -\rho \cos \lambda' = R\arccos(\cos \varphi \cos \lambda) \frac{\sin \varphi}{\sqrt{1 - \cos^2 \varphi \cos^2 \lambda}}\end{aligned}$$

The graticule of the transverse and oblique azimuthal equidistant is difficult to recognize but if the graticule of a regional map is formed by complex lines, parallels intersect the central meridian at equal intervals, and the distortions are small in the centre of the map and larger at the edges then one can suspect it. In the transverse aspect, the spacing of meridians is also uniform along the Equator.

XI.2 LAMBERT azimuthal equal-area

Let us also make an equal-area variant ($hk = 1$)! Let the constant of integration be $R^2 + d/2$!

$$\begin{aligned}\frac{1}{R} \frac{d\rho}{d\delta} \frac{\rho}{R \sin \delta} &= 1 \\ \int \rho d\rho &= R^2 \int \sin \delta d\delta \\ \frac{\rho^2}{2} &= -R^2 \cos \delta + R^2 + \frac{d}{2} = -R^2 \left(\cos^2 \frac{\delta}{2} - \sin^2 \frac{\delta}{2} - 1 \right) + \frac{d}{2} \\ \rho &= \sqrt{-2R^2 \left(1 - \sin^2 \frac{\delta}{2} - \sin^2 \frac{\delta}{2} - 1 \right) + d} = 2R \sin \frac{\delta}{2}\end{aligned}$$

XI. Non-perspective azimuthals

In the last step, we took advantage of the fact that at the pole $\rho = 0$, which can only be the case if $d = 0$. The result is the *LAMBERT azimuthal equal-area projection*, known since 1772^{*} (Fig. XI.2).

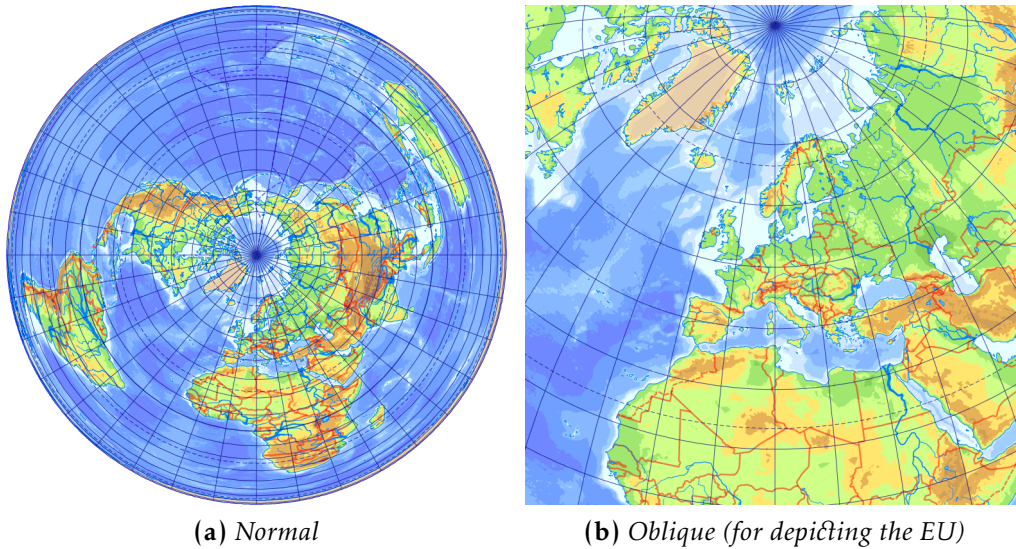


Figure XI.2: *LAMBERT azimuthal equal-area projection*

Linear scales along graticule lines:

$$h = \frac{1}{R} \frac{d\rho}{d\delta} = \cos \frac{\delta}{2}$$

$$k = \frac{\rho}{R \sin \delta} = \frac{2 \sin \frac{\delta}{2}}{2 \sin \frac{\delta}{2} \cos \frac{\delta}{2}} = \frac{1}{\cos \frac{\delta}{2}}$$

At the North Pole, $h = k = 1$, i.e. the projection is distortion-free. At the South Pole the distortions are infinitely large, since $h = 0$ and $k \rightarrow \infty$. The isocols follow parallels because h and k are independent of the longitude. Therefore, the projection can be recommended for equal-area representations of nearly circular areas. The official maps of the European Union are drawn in an oblique LAMBERT azimuthal equal-area, centred on 52° N, 10° E.

^{*} The Swiss mathematician LAMBERT was primarily concerned with physical and mathematical problems, with only a marginal interest in the theory of map projections. He wrote only one article on the subject but revolutionized the field. Five of his seven new projections (equal-area azimuthal, conic, and cylindrical; conformal conic and pseudocylindrical; transverse conformal and equal-area cylindrical) are still among the most widely used ones. He was the first to seek conformal and equal-area mappings by solving the differential equations $h = k$ and $hk = 1$, which are also used in this note.

This projection is also used to represent the eastern and western hemispheres in transverse aspect. Derivation:

$$\begin{aligned}\rho &= 2R \sin \frac{\delta'}{2} = R\sqrt{2} \sqrt{\sin^2 \frac{\delta'}{2} + \cos^2 \frac{\delta'}{2} - \cos^2 \frac{\delta'}{2} + \sin^2 \frac{\delta'}{2}} \\ &= R\sqrt{2} \sqrt{1 - \cos \delta'} = R\sqrt{2 - 2 \sin \varphi'} = R\sqrt{2 - 2 \cos \varphi \cos \lambda} \\ x &= \rho \sin \lambda' = R\sqrt{2 - 2 \cos \varphi \cos \lambda} \frac{\sin \lambda \cos \varphi}{\sqrt{1 - \cos^2 \varphi \cos^2 \lambda}} \\ &= R \frac{\sqrt{2(1 - \cos \varphi \cos \lambda)} \sin \lambda \cos \varphi}{\sqrt{(1 - \cos \varphi \cos \lambda)(1 + \cos \varphi \cos \lambda)}} = R \frac{\sqrt{2} \sin \lambda \cos \varphi}{\sqrt{1 + \cos \varphi \cos \lambda}} \\ y &= -\rho \cos \lambda' = R\sqrt{2 - 2 \cos \varphi \cos \lambda} \frac{\sin \varphi}{\sqrt{1 - \cos^2 \varphi \cos^2 \lambda}} \\ &= R \frac{\sqrt{2} \sin \varphi}{\sqrt{1 + \cos \varphi \cos \lambda}}\end{aligned}$$

This projection is even more difficult to recognize from its graticule in rotated aspects. The best clue is that there is a significant angular distortion at the edges of the map, and the spacing of parallels on the central meridian becomes slightly denser towards the edge of the map.

XI.3 GINZBURG'S scheme

GINZBURG noticed that the radius functions of azimuthals used frequently follow a single pattern:

$$\rho = dR \sin \frac{\delta}{d} \quad \text{or} \quad \rho = dR \tan \frac{\delta}{d}$$

The orthographic and equal-area mappings fit the series of sines, with $d = 1$ for the former and $d = 2$ for the latter. The *tangent* gnomonic and stereographic projections are included in the series of tangents where d is 1 and 2, respectively. At first glance, the azimuthal equidistant seems to be out of the pattern, but in fact it fits both series. We can prove its fit into the formula with sine by L'HÔPITAL'S rule:

$$\lim_{d \rightarrow \infty} R d \sin \frac{\delta}{d} = R \lim_{d \rightarrow \infty} \frac{\sin \frac{\delta}{d}}{\frac{1}{d}} = R \lim_{d \rightarrow \infty} \frac{-\frac{\delta}{d^2} \cos \frac{\delta}{d}}{-\frac{1}{d^2}} = R\widehat{\delta}$$

The limit of the formula with tangent can be computed similarly and also results in $R\widehat{\delta}$. That is, this projection emerges from both formulæ if d is chosen to be infinitely large.

XI. Non-perspective azimuthals

GINZBURG was primarily concerned with the series with sine and in 1957 he proposed the use of variant $d = 3$:

$$\rho = 3R \sin \frac{\delta}{3}$$

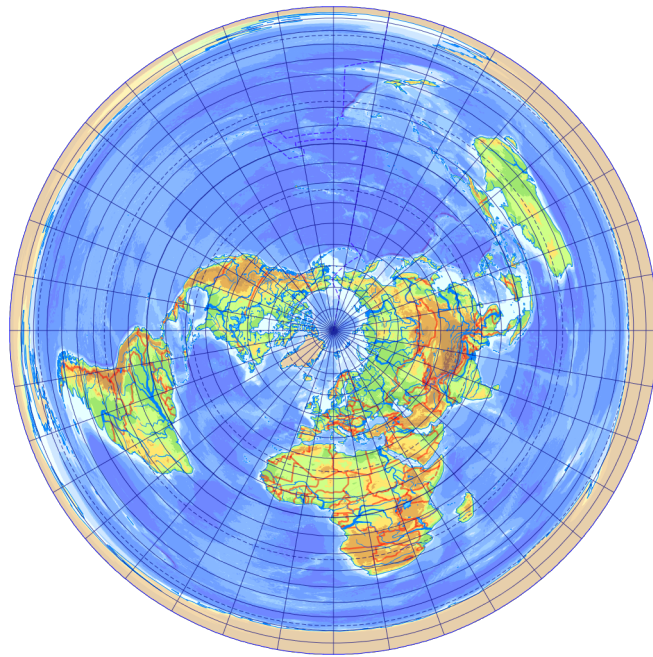


Figure XI.3: *GINZBURG's azimuthal projection*

This is GINZBURG's azimuthal (Fig. XI.3), which has very small distortions (even more favourable than the azimuthal equidistant in terms of finite length distortions), it is aphylactic, but has a very low areal distortion. GINZBURG also recommended version $d = 1.5$, which resembles the spherical shape of the Earth.

XI.4 Ellipsoidal azimuthals

The linear scales along graticule lines of azimuthals based on an ellipsoid are as follows:

$$h = -\frac{1}{M(\Phi)} \frac{d\rho}{d\Phi}$$
$$k = \frac{\rho}{N(\Phi) \cos \Phi}$$

The azimuthal equidistant is obtained from the solution of the equation $h = 1$:

$$\rho = \int_{90^\circ}^{\Phi} M(\Phi) d\Phi$$

For the azimuthal equal-area, we have to solve the equation $hk = 1$ and the constant of integration can be expressed from the requirement of $\rho = 0$ at the pole:

$$\rho = a\sqrt{1-e^2} \left(\frac{1}{1-e^2} + \frac{1}{2e} \ln \frac{1+e}{1-e} - \frac{\sin \Phi}{1-e^2 \sin^2 \Phi} - \frac{1}{2e} \ln \frac{1+e \sin \Phi}{1-e \sin \Phi} \right)^{1/2}$$

For an azimuthal conformal mapping, the constant of integration d in the function obtained by solving the equation $h = k$ is arbitrary:

$$\rho = d \tan \left(45^\circ - \frac{\Phi}{2} \right) \left(\frac{1+e \sin \Phi}{1-e \sin \Phi} \right)^{e/2}$$

If linear scale c is prescribed at the pole, then:

$$d = \frac{2ca}{\sqrt{1-e^2}} \left(\frac{1+e}{1-e} \right)^{e/2}$$

This projection is applied by NATO to the polar regions as UPS (Universal Polar Stereographic) with $c = 0.994$ chosen on the reference frame WGS84. To avoid negative coordinates, a false easting and a false northing of 2000 km must be added to both coordinates. Please note that, unlike the sphere, the ellipsoidal azimuthal conformal projection is not perspective, so the name stereographic is misleading!* The UPS projection is used up to latitude 84° in the Northern Hemisphere and latitude 80° in the Southern Hemisphere instead of the UTM zones.

For the reference frame of an ellipsoid of revolution, the metacoordinate system is not defined, so there are two methods to obtain an oblique projection: the first is called *double mapping*, in which case we first project onto an auxiliary sphere, rotate the graticule on the sphere, and finally apply

* Remember that the term *secant* can only be applied to perspective projections, so even though the UPS contains a scaling and therefore a true-scale parallel, it is not a secant projection (despite what much of the literature claims), but rather, correctly speaking, a *reduced* one!

the map projection in the spherical form. The other option is to arbitrarily select some distortion characteristics of the spherical map projection so that these conditions, when applied to the ellipsoid, uniquely define the formulæ of the projection. Thus, we obtain direct ellipsoid-to-plane formulæ. Below, we will look at both methods for determining oblique ellipsoidal azimuthal projections.

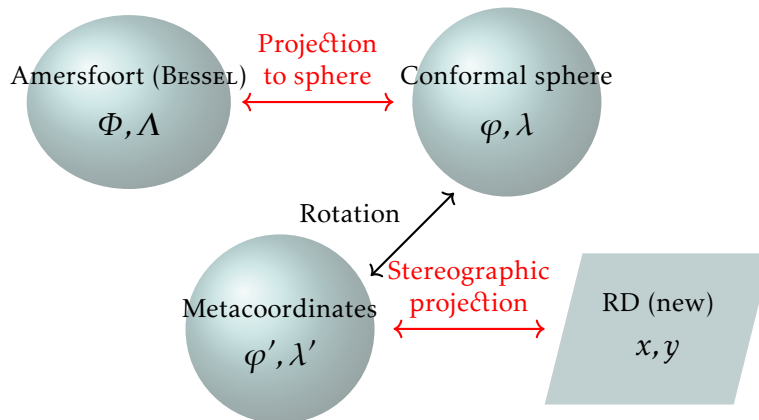


Figure XI.4: *Amersfoort projection in the Netherlands*

The *Amersfoort* projection (Fig. XI.4) on Dutch topographic maps uses method of double mapping. The reference frame is the Amersfoort Datum based on the BESSEL ellipsoid. The auxiliary sphere chosen is the Gaussian conformal sphere (Sec. IX.3), the true-scale parallel is the latitude of the fort in the town Amersfoort. The oblique stereographic projection with its metapole on Amersfoort is then applied. Finally, the coordinate axes are shifted so that there are no negative coordinates and the vertical coordinate is always greater than the horizontal. Since only conformal mappings were used, the result is conformal.

The Amersfoort projection is significant from a Hungarian point of view because it is very similar to our old stereographic projection. The only difference in principle is that the true-scale parallel of the auxiliary sphere does not pass through the origin of the projection in the old Budapest and Marosvásárhely stereographic systems. If your GIS does not support the Hungarian stereographic projection, feel free to use the Amersfoort projection instead, reparameterized to the origin Gellérthegy. The error of the transformation will then be around centimetres, which is sufficient for most practical applications. You may read more about old Hungarian systems in App. F.

The other method is used by the ROUSSILHE projection. We know that in the spherical tangent stereographic projection, points of the central

XI. Non-perspective azimuthals

meridian are mapped to $y = 2R \tan(s/2R)$, where s is the distance from the metapole. We generalize this to the ellipsoid of revolution by interpreting the distance s along the meridian on the ellipsoid, while substituting the radius of the osculating sphere ($\sqrt{M(\Phi_0)N(\Phi_0)}$) at the origin of the projection for the radius R . The resulting intervals of intersections along the central meridian and conformality together clearly define the projection. Since the projection requires trigonometric functions and elliptic integrals defined over complex numbers, it is approximated in practice by several series.

ROUSSILHE projection is found today, for example, in Romania called Stereo70 centred near Braşov, translated and reduced. A similar projection was used until recently by the Poles, dividing the country into five separately mapped zones, four of which were represented in this mapping.

Lesson twelve

Perspective & equal-area cylindricals

XII.1 General formulæ

In *cylindrical projections*, parallels and meridians appear as parallel straight lines perpendicular to each other. The vertical coordinate, therefore, depends only on the latitude, which is a strictly increasing and often odd function to have symmetry. The axis x usually coincides with the mapped Equator. The condition of equal spacing implies that the horizontal coordinate is in direct proportion to the longitude (Fig. XII.1). Let the coefficient of proportionality be cR !

$$x = cR\widehat{\lambda}$$
$$y = f(\varphi)$$

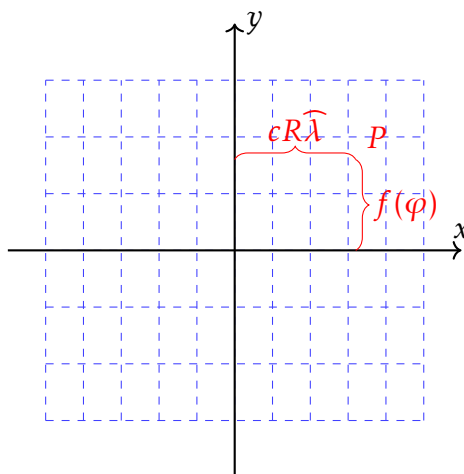


Figure XII.1: Coordinates in cylindrical projections

XII. Perspective & equal-area cylindricals

Let us write down the linear scales along the graticule:

$$h = \frac{\sqrt{\left(\frac{\partial x}{\partial \varphi}\right)^2 + \left(\frac{\partial y}{\partial \varphi}\right)^2}}{R} = \frac{\sqrt{0^2 + \left(\frac{dy}{d\varphi}\right)^2}}{R} = \frac{1}{R} \frac{dy}{d\varphi}$$

$$k = \frac{\sqrt{\left(\frac{\partial x}{\partial \lambda}\right)^2 + \left(\frac{\partial y}{\partial \lambda}\right)^2}}{R \cos \varphi} = \frac{\sqrt{(cR)^2 + 0^2}}{R \cos \varphi} = \frac{c}{\cos \varphi}$$

Examining the formula for k , we can see that latitude $\pm\varphi_s$ is equidistant if $c = \cos \varphi_s$.

XII.2 Central cylindrical projection

To derive the perspective cylindrical (or *central cylindrical*) projection, see Fig. XII.2. The circumference of the base of the cylinder is equal to the change in the coordinate x between the longitudes ± 180 , i.e. $cR2\pi = 2R\pi \cos \varphi_s$. From this, the radius of the cylinder is $cR = R \cos \varphi_s$, so $\pm\varphi_s$ is just the two secant parallels of the cylinder.

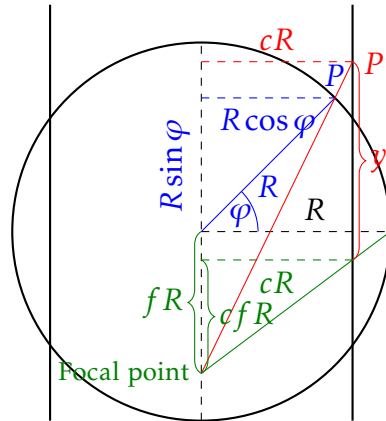


Figure XII.2: *The principle of the central cylindrical projection*

Let the distance of the focal point from the centre be fR ! Then the ratio of the legs of the similar right triangles with green hypotenuse (illustrating the mapping of the Equator) is the same, so the vertical leg of the smaller

XII. Perspective & equal-area cylindricals

triangle is necessarily cfR . From the ratio of the legs of similar right triangles with red hypotenuse:

$$\frac{y + cfR}{cR} = \frac{R(f + \sin \varphi)}{R \cos \varphi}$$
$$y = cR \left(\frac{f + \sin \varphi}{\cos \varphi} - f \right)$$

The distortions of perspective cylindricals are highly unfavourable (Fig. XII.3). The projection is *aphylactic* ($h \neq k$ and $hk \neq 1$). Perspective cylindricals are found almost exclusively in Russian atlases.

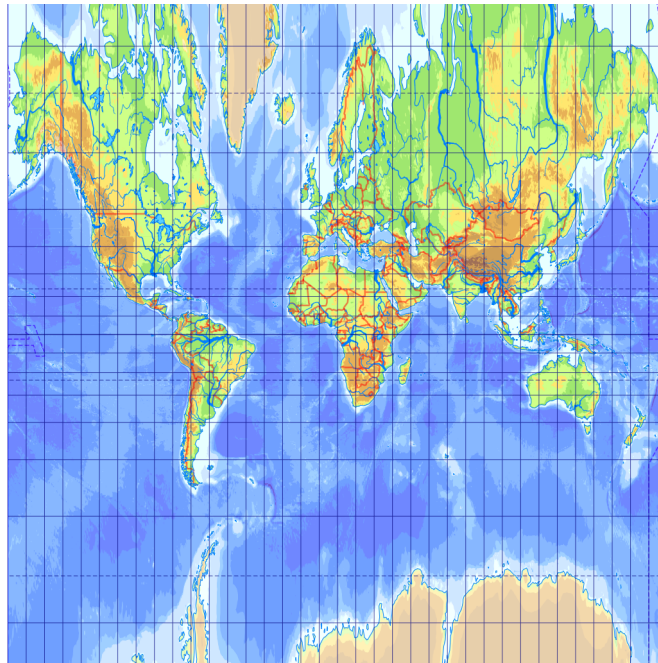


Figure XII.3: Central cylindrical projection

XII.3 Quasi-perspective cylindricals

Among cylindrical and conic projections, we can also consider mappings as perspective in a broad sense in which each meridian is projected from a separate focal point. The centre of projection is in a line perpendicular to the generatrix of the developable surface corresponding to the meridian currently being mapped and passing through the centre of the reference frame, and changes position in a rotationally symmetrical manner with the meridians during the mapping process. These are the *quasi-perspective*

XII. Perspective & equal-area cylindricals

projections. In this course, we will explore two quasi-perspective mappings (Fig. XII.4).

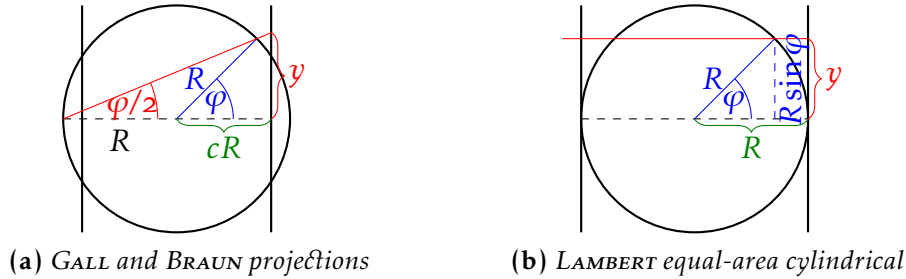


Figure XII.4: Major quasi-perspective cylindricals

In the first case, let the centre of projection be at the equatorial point opposite to the meridian, as in the stereographic projection. The red inscribed angle shown in the figure is half of the blue central angle. The tangent of the inscribed angle:

$$\tan \frac{\varphi}{2} = \frac{y}{R + cR}$$

$$y = R(1 + c) \tan \frac{\varphi}{2}$$

In cylindrical projections, the linear scale along parallels is $k = c/\cos \varphi$. The linear scale along meridians is:

$$h = \frac{1}{R} \frac{dy}{d\varphi} = \frac{1 + c}{2 \cos^2 \frac{\varphi}{2}} = \frac{1 + c}{\sin^2 \frac{\varphi}{2} + \cos^2 \frac{\varphi}{2} + \cos^2 \frac{\varphi}{2} - \sin^2 \frac{\varphi}{2}} = \frac{1 + c}{1 + \cos \varphi}$$

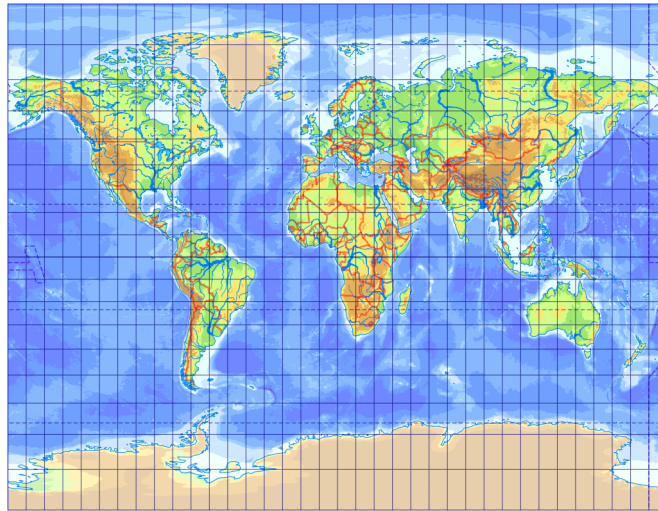
That is, unlike the stereographic projection, the mapping is *aphylactic* ($h \neq k$ and $hk \neq 1$), but a property that is reminiscent of the stereographic projection is that the secant parallels are exceptionally true-scale (if $\varphi = \varphi_s$ and $c = \cos \varphi_s$, then $h = k = 1$).

The projection was first derived by the Scottish cartographer GALL in 1855 with the secant parallel $\varphi_s = \pm 45^\circ$, so the variant $c = \sqrt{2}/2$ is named after him. The tangent ($c = 1$) version was independently created by BRAUN in 1867.

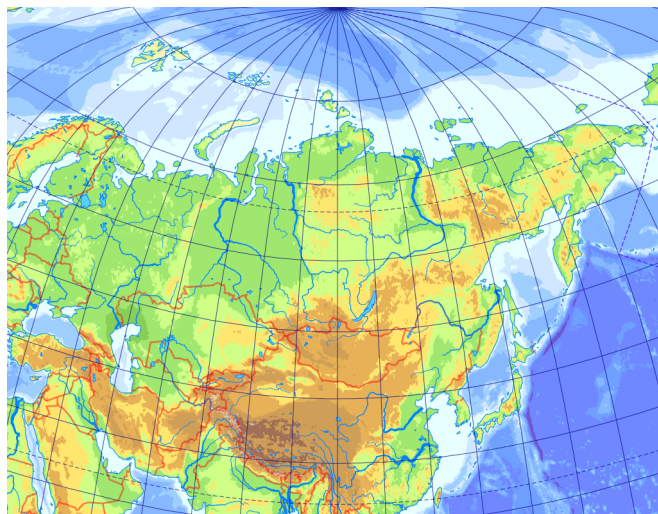
Although it gives a rather pleasing representation, it is extremely rare to come across it. Its use could be considered, for example, in time-zone maps where no special distortion conditions are needed, but meridian convergence is to be eliminated.

As is the case with perspective projections in general, such mappings are primarily found in Russian atlases, sometimes with $\varphi_s = \pm 30^\circ$ for world

XII. Perspective & equal-area cylindricals



(a) Normal



(b) Oblique (for the former USSR) following SOLOVYOV

Figure XII.5: GALL projection

XII. Perspective & equal-area cylindricals

maps. Quasi-perspective projections were also used in oblique aspect to represent the Soviet Union (Fig. XII.5).

Our next quasi-perspective projection is obtained by placing the centre of projection infinitely far away, as in the case of the orthographic projection. Then the rays will be parallel. Let the cylinder be tangential, i.e., of radius R ($c = 1$)! As shown in Fig. XII.4:

$$y = R \sin \varphi$$

Distortions of the projection:

$$h = \frac{1}{R} \frac{dy}{d\varphi} = \cos \varphi$$

$$k = \frac{c}{\cos \varphi} = \frac{1}{\cos \varphi}$$

Notice that $hk = 1$, so we have an equal-area projection. This is the LAMBERT equal-area cylindrical projection (1772). Is this the only equal-area cylindrical, or are there others among the non-perspective projections?

XII.4 Equal-area cylindricals

To answer our question, we solve the equation $hk = 1$:

$$\begin{aligned} \frac{1}{R} \frac{dy}{d\varphi} \frac{c}{\cos \varphi} &= 1 \\ \int dy &= \frac{R}{c} \int \cos \varphi d\varphi \\ y &= \frac{R}{c} \sin \varphi + d \end{aligned}$$

The constant of integration d is just a translation, so it can be ignored, and c is the cosine of the equidistant parallel. If it is 0° ($c = 1$), then we get the LAMBERT equal-area cylindrical, but otherwise, we get additional non-perspective projections as a solution. The distortions:

$$\begin{aligned} h &= \frac{1}{R} \frac{dy}{d\varphi} = \frac{\cos \varphi}{c} \\ k &= \frac{c}{\cos \varphi} \end{aligned}$$

Apart from the unsurprising equivalency, we can see that the parallel $\pm\varphi_s$ is true-scale, because here $h = k = 1$. Such parallels are called *standard*

XII. Perspective & equal-area cylindricals

parallels of the projection. At the pole, h is zero, while k is infinitely large, so the angular distortions are infinite. In 1910, BEHRMANN proposed $\varphi_s = \pm 30^\circ$ ($c = \sqrt{3}/2$). He found its average angular distortion over the whole Earth to be the most favourable among possible equal-area cylindricals (Fig. XII.6).

In 1967, the German historian PETERS proposed the variant $\varphi_s = \pm 45^\circ$ ($c = \sqrt{2}/2$), known as the GALL–PETERS projection. It is still used relatively often recently, although its angular distortions are disturbingly large.*

Numerous other equal-area cylindricals are known under various names, differing only in the choice of standard parallels. The creators usually named these projections after themselves. The graticule of equal-area cylindricals can be recognized by denser spacing of parallels near the edge.

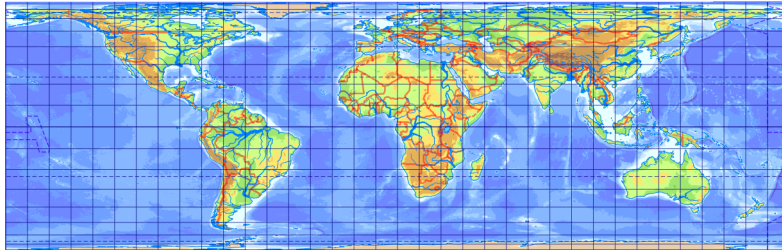
* The GALL–PETERS projection is a typical example of a recurring phenomenon, where laymen who do not know map projections reinvent the wheel. In 20th century American cartography, it was common for world maps (whether school atlases or wall maps) to be presented in the MERCATOR projection described in the next lesson. This is an inappropriate choice of projection because at high latitudes there is considerable areal distortion, while the conformal property is rarely advantageous for a map intended for indoor use. This does not mean that this projection is bad in itself but rather that we can make good use of its conformality on a medium to large-scale map of the (meta)equatorial region intended for field use (e.g. a hiking map).

However, PETERS made a political issue out of it. He claimed that the imperialist superpower states were deliberately producing distorted maps that made developed countries look larger than the more miserable regions of Africa and South America. PETERS claimed that the maps were lying and that only his depiction of the Earth correctly represented it. His demagogic lobbying was successful and despite fierce protests from professionals, he succeeded in getting official maps of various UN agencies to be edited in his projection.

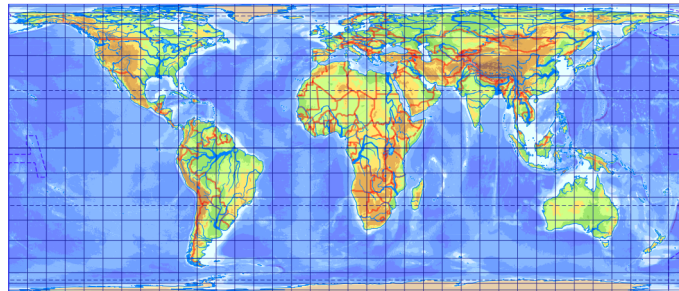
From a professional point of view, PETERS's claims are, to put it mildly, debatable. His assumption that only an equal-area mapping can correctly represent the Earth is so-so, but that his projection was the first equivalent projection in the world is ridiculous. He was not even the first to invent the mapping he promoted, but the Scottish cartographer GALL did it as early as 1855. And the angular distortions are small along the 45° latitude of developed regions, whereas he flattens the countries around the Equator like a pancake so that the distortions are greatest precisely where PETERS claims to favour.

Unfortunately, the tabloid media is still picking up on this topic, and you can nowadays also find articles like 'Maps lie to us'. As a result, there was an article a few years ago that Boston schools should be required to teach using GALL–PETERS maps in schools because it is fair to the former colonies.

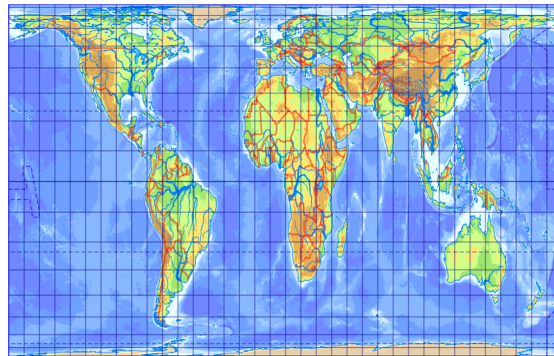
XII. Perspective & equal-area cylindricals



(a) LAMBERT equal-area cylindrical



(b) BEHRMANN projection



(c) GALL-PETERS projection

Figure XII.6: Equal-area cylindricals

Lesson thirteen

Other cylindrical projections

XIII.1 Equidistant cylindricals

Develop a cylindrical projection with equidistant meridians ($h = 1$)!

$$\frac{1}{R} \frac{dy}{d\varphi} = 1$$
$$\int dy = R \int d\varphi$$
$$y = R\widehat{\varphi} + d$$

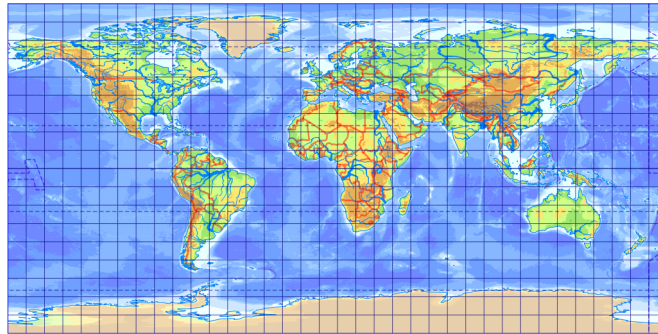
The constant of integration d results only in a translation again, so we ignore it. Due to the equidistant meridians, we have $h = 1$, while in all cylindrical projections, $k = c/\cos \varphi$ (since $x = cR\widehat{\lambda}$). Knowing that $c = \cos \varphi_s$, it is easy to see that latitude $\pm\varphi_s$ is true-scale, i.e., a standard parallel ($h = k = 1$). At the pole, k is infinitely large, less than one between standard parallels, and increases away from them.

The projection of the choice $c = 1$ (true-scale Equator) is called the *Plate Carrée projection* (Fig. XIII.1) due to the shape of its graticule and was possibly created by ERATOSTHENES. Most GIS software displays data in this projection if no projection is specified. Note, however, that if you do not specify a map projection, the software interprets the coordinates in degrees, whereas if you explicitly set the Plate Carrée projection, everything is expressed in metres.

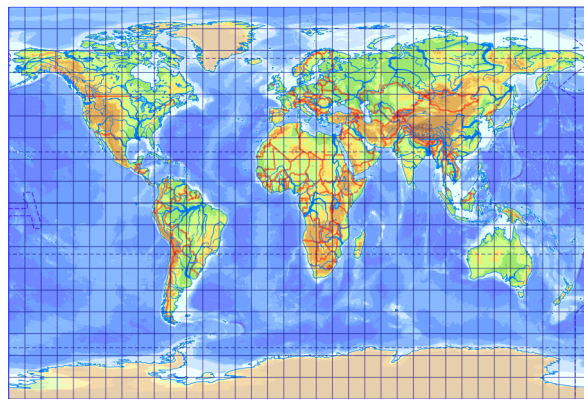
By choosing c appropriately, other standard parallels can be selected for the equidistant cylindricals (*equiarectangular projection*). This form of the projection was first used by MARINOS, who chose the true-scale latitude through the island of Rhodes.

Since k is symmetrical about the Equator in all cylindrical map projections, and h also has this symmetry in most of the mappings we have learned so far, we can conclude that the isocols of cylindrical projections are usually also symmetrical about the Equator. Hence, it follows that this family of projections should be applied to long regions that are symmetrical

XIII. Other cylindrical projections



(a) Plate Carrée projection



(b) Equirectangular projection ($\varphi_s = \pm 42^\circ$)

Figure XIII.1: *Equidistant cylindricals*

about the Equator. If the map's theme requires neither equivalency nor conformality, then it is worth using this projection because GYÖRFFY has shown that there is no lower distortion cylindrical mapping to represent a spherical belt that is symmetrical about the Equator than an equidistant one. Although the choice of a cylindrical projection to represent the entire Earth is acceptable only in rare cases, FRANČULA recognized that in this case, the standard parallel should be chosen approximately at latitude $\pm 42^\circ$ to minimize distortion.

In transverse aspect:

$$x = cR\widehat{\lambda}' = cR \arctan \frac{\sin \lambda'}{\cos \lambda'} = cR \arctan(-\sin \lambda \cot \varphi)$$

$$y = R\widehat{\varphi}' = R \arcsin(\cos \varphi \sin \lambda)$$

In this aspect, and with $c = 1$, we know this mapping as the CASSINI projection (Fig. XIII.2), described by the famous French geodesist in 1745.

XIII. Other cylindrical projections

Its distortions are favourable in the surroundings of the metaequator (a bimeridian), therefore the spherical lunes to be mounted on a globe model were made in this projection.

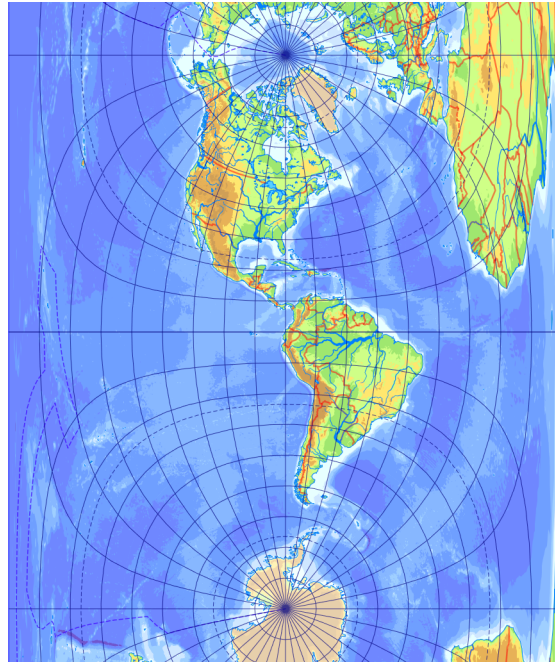


Figure XIII.2: *CASSINI projection for the Americas*

XIII.2 MERCATOR projection

For the conformal version ($h = k$), the antiderivative of $1/\cos \varphi$ was obtained from Sec. III.3:

$$\begin{aligned}\frac{1}{R} \frac{dy}{d\varphi} &= \frac{c}{\cos \varphi} \\ \int dy &= cR \int \frac{1}{\cos \varphi} d\varphi \\ y &= cR \ln \tan\left(45^\circ + \frac{\varphi}{2}\right) + d\end{aligned}$$

This is the **MERCATOR** projection (Fig. XIII.3), originally created by the Dutch cartographer **KREMER** in 1569.* The poles are mapped to infinity.

* It can be suspected that this projection has a much older origin, but its construction was forgotten during the Middle Ages. From the beginning, portolan charts were copied from base maps drawn in a strikingly similar map projection. Furthermore, distances between the latitudes on **ETZLAUB**'s compass of 1511 follow the **MERCATOR** projection almost exactly.

XIII. Other cylindrical projections

The projection is recognizable by parallels spaced at increasingly greater distances as further away from the Equator. Its significance lies in the fact that it maps the loxodromes into straight lines. This is why it used to be very important in navigation: since it is also conformal, the azimuth of any loxodrome between two points can be read directly from it.

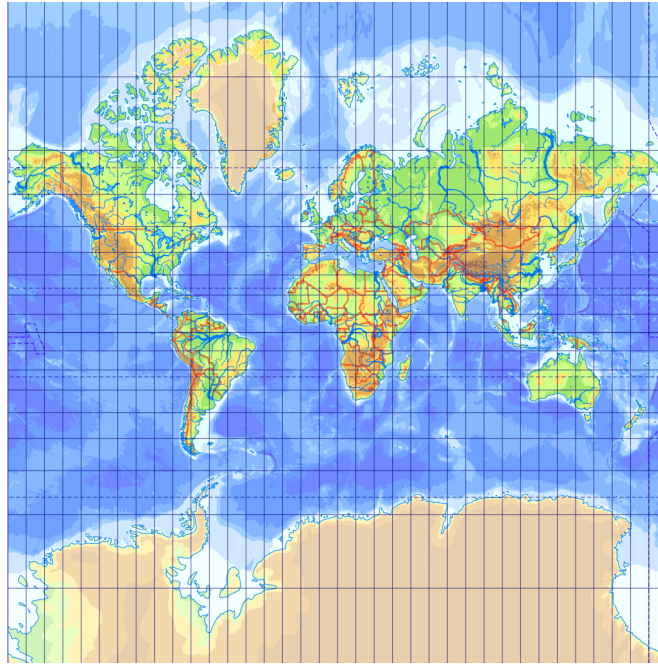


Figure XIII.3: *MERCATOR projection*

The fact that loxodromes are straight is easy to see. The special loxodromes of azimuth $\alpha = 0^\circ$ are meridians, which are always straight in cylindrical projections. Other loxodromes intersect all meridians at an angle of α because of conformality. A line that intersects meridians that appear as parallel straight lines at a constant angle can only be straight. This completes the proof.

Let us examine the distortions of the projection.

$$h = k = \frac{c}{\cos \varphi}$$

The constant c makes the map smaller or larger. For $c = 1$, the Equator is true-scale. The downscaled version ($c < 1$) may increase the size of areas with favourable distortion since it produces two distortion-free parallels, reduction of size between them and enlargement outwards, but the deviation of linear scale from unity is smaller than for $c = 1$. Downscaled

XIII. Other cylindrical projections

conformal^{*} projections (minimum of linear scale is between 0 and 1) are called *reduced* projections.[†] This projection should also be applied to long regions along the Equator based on CHEBYSHEV'S theorem since its isocols are parallel to the Equator.

A different form of the projection should be used to express it after the rotation of the graticule:

$$\begin{aligned}
 y &= cR \ln \tan \left(45^\circ + \frac{\varphi'}{2} \right) = cR \ln \sqrt{\frac{2 \sin^2 \left(45^\circ + \frac{\varphi'}{2} \right)}{2 \cos^2 \left(45^\circ + \frac{\varphi'}{2} \right)}} \\
 &= \frac{cR}{2} \ln \frac{\sin^2 \left(45^\circ + \frac{\varphi'}{2} \right) + \cos^2 \left(45^\circ + \frac{\varphi'}{2} \right) + \sin^2 \left(45^\circ + \frac{\varphi'}{2} \right) - \cos^2 \left(45^\circ + \frac{\varphi'}{2} \right)}{\cos^2 \left(45^\circ + \frac{\varphi'}{2} \right) + \sin^2 \left(45^\circ + \frac{\varphi'}{2} \right) + \cos^2 \left(45^\circ + \frac{\varphi'}{2} \right) - \sin^2 \left(45^\circ + \frac{\varphi'}{2} \right)} \\
 &= \frac{cR}{2} \ln \frac{1 - \cos(90^\circ + \varphi')}{1 + \cos(90^\circ + \varphi')} = \frac{cR}{2} \ln \frac{1 + \sin \varphi'}{1 - \sin \varphi'}
 \end{aligned}$$

This is advantageous because we already have a formula for $\sin \varphi'$ and can substitute it without modification. We also use the conversion $\widehat{\lambda}' = \arctan \tan \lambda'$. Instead of the latitude of the metapole φ_o , we will substitute the latitude of the intersection between the metaequator and the prime meridian φ_c (see Sec. V.3).

$$\begin{aligned}
 x &= cR \arctan \tan \lambda' = cR \arctan \frac{\sin \lambda}{\tan \varphi \sin \varphi_c - \cos \lambda \cos \varphi_c} \\
 y &= \frac{cR}{2} \ln \frac{1 + \sin \varphi \cos \varphi_c - \cos \varphi \sin \varphi_c \cos \lambda}{1 - \sin \varphi \cos \varphi_c + \cos \varphi \sin \varphi_c \cos \lambda}
 \end{aligned}$$

The derivation of the inverse projection formulæ can be found in App. H.

^{*} While conformal projections remain conformal after downscaling, the same is not true for equal-area and equidistant mappings, so the term *reduced* is meaningful only for conformal projections.

[†] Unfortunately, many people refer to the *reduced* version of the MERCATOR projection as a secant projection, and to the standard parallels as secant parallels. This is misleading, as this projection is *not perspective* and we used neither a secant cylinder nor a central projection to derive it, we just did some maths. The consequence of this incorrect use of terminology is that properties of the stereographic projection is generalized erroneously to all mappings. Widespread but easily disprovable misconceptions are that secant projections can always be obtained by reducing the corresponding tangent projection and that secant lines are always distortion-free, with reduction of size between them and enlargement elsewhere.

XIII. Other cylindrical projections

The transverse **MERCATOR** projection is called the **GAUSS-SCHREIBER** projection, although it was actually first derived by **LAMBERT**. It is considered to be a conformal projection with a favourable distortion for areas along a meridian. Its graticule is similar to that of the **CASSINI** projection, distinguished from it by the fact that in the **CASSINI** projection the meridians are placed along the Equator evenly, whereas in the **GAUSS-SCHREIBER** projection the meridians cross the Equator at increasingly greater distances away from the Prime meridian (Fig. XIII.4).

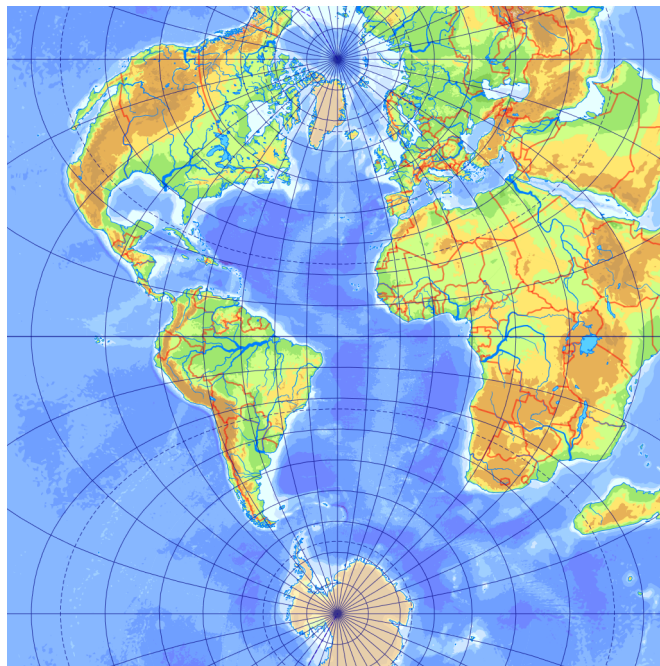


Figure XIII.4: *GAUSS-SCHREIBER* projection for the Atlantic Ocean

XIII.3 Rarely occurring cylindricals

Although the **MERCATOR** projection is not really favourable for world maps, it is still overused today. A problem is that the image of the poles is at infinity, which means that the projection has to be arbitrarily truncated at a bounding latitude. There has been a demand for mappings that resemble the **MERCATOR** projection, but the poles are not mapped into infinity.

Among the quasi-perspective cylindricals, **BRAUN** found a version with the centre of projection in the plane of the Equator, two-fifths spherical radii away from the axis of revolution. Although this mapping is very similar in appearance to the **MERCATOR** projection, it is not the same, since it is not conformal, nor is the image of the pole at infinity. This research

XIII. Other cylindrical projections

demonstrates that MERCATOR's projection is indeed not possible to develop as a perspective mapping.*

Somewhat more popular is the MILLER projection, published in 1942, which multiplies the latitude by four-fifths before applying the MERCATOR projection ($c = 1$) and then divides the vertical coordinate by the same number after the mapping:

$$y = \frac{5R}{4} \ln \tan \left(45^\circ + \frac{2\varphi}{5} \right)$$

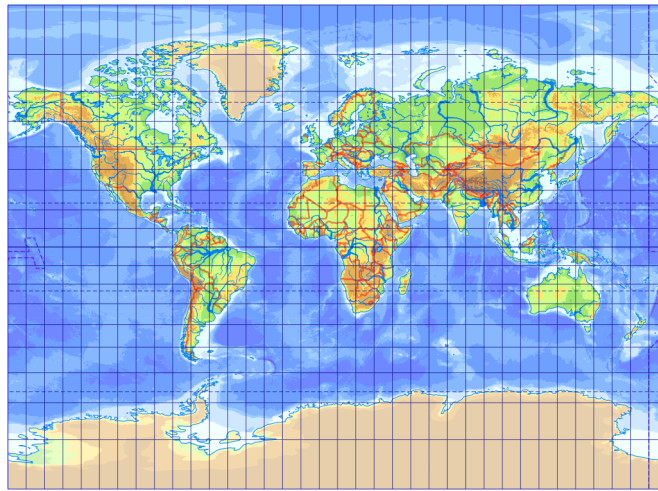


Figure XIII.5: *MILLER projection*

This projection, rarely used in atlases and wall maps, is *aphylactic* and, unlike the MERCATOR projection, can be used to represent the poles (Fig. XIII.5).

* Although this statement seems obvious, it is unfortunately not: A few years ago, for example, a postage stamp was issued in Germany under the title '500. Geburtstag MERCATOR', showing this mapping as a quasi-perspective projection.

Lesson fourteen

Cylindricals for the ellipsoid of revolution

XIV.1 Cylindricals in normal aspect

In cylindrical map projections using an ellipsoid as the reference frame, the constant c , which determines the spacing of the meridians, takes a different form. Accordingly:

$$x = c\widehat{\Lambda}$$

Consequently, the linear scales along the graticule lines of cylindricals are:

$$h = \frac{1}{M(\Phi)} \frac{dy}{d\Phi}$$
$$k = \frac{c}{N(\Phi)\cos\Phi}$$

That is, latitudes $\pm\Phi_s$ will be equidistant if $c = N(\Phi_s)\cos\Phi_s$.

The cylindrical projection equidistant in meridians is given by the solution of the equation $h = 1$:

$$y = \int_{0^\circ}^{\Phi} M(\Phi) d\Phi$$

For the equal-area cylindrical, we solve the equation $hk = 1$ and the constant of integration can be omitted because it only causes a vertical translation:

$$y = a^2 \frac{1-e^2}{2c} \left(\frac{\sin\Phi}{1-e^2\sin^2\Phi} - \frac{1}{2e} \ln \frac{1-e\sin\Phi}{1+e\sin\Phi} \right)$$

For the conformal cylindrical, the constant of integration in the function obtained by solving the equation $h = k$ can also be omitted:

$$y = c \ln \left[\tan \left(45^\circ + \frac{\Phi}{2} \right) \left(\frac{1-e\sin\Phi}{1+e\sin\Phi} \right)^{e/2} \right]$$

XIV.2 CASSINI–SOLDNER projection

The CASSINI–SOLDNER projection is a generalization of the CASSINI projection (transverse Plate Carrée projection) to an ellipsoid of revolution. The CASSINI projection is equidistant in the central meridian coinciding with the metaequator and in the perpendicular metameridians. We want to keep this for the ellipsoid of revolution so that the central meridian remains equidistant and the geodesic lines perpendicular to it are mapped to straight lines perpendicular to it, along which there is also equidistance. These conditions clearly define the projection over most parts of the ellipsoid of revolution.*

This mapping was created by SOLDNER in 1810. The first topographic mappings in Europe were developed in this projection before the spread of modern conformal projections. The practical computation of coordinates can be done by solving geodetic problems on an ellipsoid (Sec. V.4) or by MUGNIER's approximate series, which demands less computation power. The latter is only reliable in the narrow environment of the central meridian, but since this is typically the only place where this projection is useful anyway, this is the form typically used in GIS.

XIV.3 The Pseudo Mercator

The *Pseudo Mercator* is the favourite map projection of on-line map providers. What is the ideal projection for a zoomable on-line map?

- Whatever part I zoom in on, North should always be up. That is, it should be a cylindrical projection.
- Whatever part I look at, there should be locally no noticeable distortion. Maps showing local similarity transformations are conformal, so only the MERCATOR projection remains.
- Keep the computational complexity of the formulæ simple! Spherical formulæ require fewer resources on the server than complex ellipsoidal formulæ.

For the aforementioned conditions, the spherical conformal cylindrical was selected. To project the ellipsoidal data onto a sphere with as little computation as possible, the Google auxiliary sphere (Sec. IX.3, Fig. XIV.1) was chosen. Since this auxiliary sphere is aphyllactic, the Pseudo Mercator is not a conformal projection in a strict sense either, but its angular distortion is very small (nowhere more than half a degree). The deviation between

* In a small area opposite the central meridian, this definition is ambiguous, but since this projection will not be used at a large distance from the central meridian anyway, this is not a practical problem.

XIV. Cylindricals for the ellipsoid of revolution

the true conformal cylindrical and the Pseudo Mercator is of the order of 10 km.



Figure XIV.1: The Pseudo Mercator projection

The projection was first used by Google Maps, launched in 2005, and became a de-facto standard. Since it is not suitable for world maps, it is now only used at higher zoom levels in Google Maps, but it is still used in the background for storing data and alternative map providers still display their world maps in this projection.

XIV.4 GAUSS–KRÜGER projection

Create a conformal projection that maps a selected meridian with no distortion and its surroundings with little distortion. In the case of a spherical reference frame, the problem is straightforward. We know that the MERCATOR projection is conformal and maps the Equator without distortion. Let us rotate the metacoordinate system into a transverse aspect, i.e. let the metapole fall on the Equator! The metaequator then falls on the bimeridian at $\pm 90^\circ$ from the metapole. By applying the MERCATOR projection to the metacoordinates, this bimeridian will be undistorted and the whole projection will be conformal, so the solution is the GAUSS–SCHREIBER projection.

The situation is not so simple for the ellipsoid of revolution. Since we defined the metagratidule on a sphere, we would have to convert the ellipsoid to an auxiliary sphere. As we want to preserve conformality, only the conformal sphere would be an option. However, a double mapping of a conformal sphere and a transverse MERCATOR projection would not be true-scale in the central meridian, since the conformal sphere can only have a selected latitude without distortion. Therefore, only a projection *directly from the ellipsoid of revolution to a plane* is suitable.

It may sound surprising, but if you define the distortions of a conformal projection along a single arbitrary smooth curve, it clearly defines the entire projection.* In the present case, the equidistancy of the central meridian is

* The reason lies deep in mathematical analysis. A conformal mapping between two map planes parametrized by complex numbers can only be established by a function that is differentiable over an open subset of the complex plane (Sec. XXIX.1).

XIV. Cylindricals for the ellipsoid of revolution

predefined, i.e. this and the conformality define a single projection. The final result can be written in this form:^{*}

$$\begin{aligned} x &= A_0(\Phi) + A_2(\Phi)(\widehat{\Delta\Lambda})^2 + A_4(\Phi)(\widehat{\Delta\Lambda})^4 + \dots \\ y &= A_1(\Phi)\widehat{\Delta\Lambda} + A_3(\Phi)(\widehat{\Delta\Lambda})^3 + A_5(\Phi)(\widehat{\Delta\Lambda})^5 + \dots \end{aligned}$$

The formulæ for the first two coefficients are simple:

$$\begin{aligned} A_0(\Phi) &= \int_0^\Phi M(\Phi) d\Phi \\ A_1(\Phi) &= N(\Phi) \cos \Phi \end{aligned}$$

The recursive formulæ for other coefficients A_i ($i = 2, 3, \dots$):

$$A_i = \frac{(-1)^{i-1}}{i} \frac{N(\Phi) \cos \Phi}{M(\Phi)} \frac{dA_{i-1}}{d\Phi}$$

The mapping was formulated by GAUSS, while the series for practical application was computed by KRÜGER in 1912, and is therefore known as the GAUSS–KRÜGER projection. The series converges only for small $\Delta\Lambda$, and LEE’s formulæ containing elliptic functions can be applied far away from the central meridian. Popular GIS software compute with series, so the mapping can only be displayed correctly in the vicinity of ca. 10° from the central meridian. Do not blindly trust the image of farther parts!

Although the projection looks similar to the transverse conformal cylindrical, it is in fact not quite the same. For example, the conformal cylindrical projection maps the two opposite points of the sphere into infinity, whereas the GAUSS–KRÜGER projection maps the entire ellipsoid into a finite shape (Fig. XIV.2). Although we would not do this from a strictly mathematical point of view, we classify it in the family of cylindricals due to its derivation.

We use this mapping to represent the narrow environment of a central meridian. For topographic purposes, we divide the Earth into 6° wide ellipsoidal lunes, known as *zones*, denoted by numbers starting from meridian -180° (Fig. XIV.3). Zones are further divided into 4° wide *bands*, denoted by capital letters starting from the Equator.

The official projection of the Warsaw Pact was the GAUSS–KRÜGER projection system. The datum S42 (also known as Pulkovo) based on the

^{*} The complicated derivation is based on a series expansion of elliptic integrals defined over the complex plane.

XIV. Cylindricals for the ellipsoid of revolution

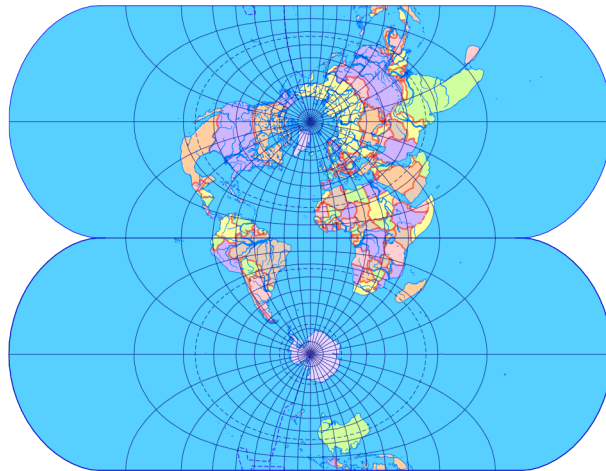


Figure XIV.2: *GAUSS-KRÜGER projection of the ellipsoid WGS84*

KRASOVSKIY ellipsoid was chosen as the reference frame. In Hungary, from the beginning of the Soviet occupation until the accession to NATO, military cartography (and for a short time, civil cartography) used this system.* For geodetic purposes, several countries (mostly in Eastern Europe, but also in Austria, Germany and the southern Slavic countries) use this projection, but the distortions increase rapidly away from the central meridian, so we also see 2° or 3° wide zones. A slightly modified version is the official projection of British and Irish cartography.

* The introduction of the projection in Hungary was not without its problems: the incoming Soviet commanders expected the army to immediately survey and map the territory of the country in the GAUSS-KRÜGER projection. As soon as the soldiers handed over the first maps of the Tiszahát region, the Soviets immediately tried to match them with their own map of Transcarpathia, but there was a gap of about 100 m between them! Naturally, a scandal broke out immediately, and the Soviets accused the Hungarians of sabotage. All that really happened, of course, was that the Soviets did not say what reference frame they were using. The Hungarians had already used the GAUSS-KRÜGER projection during World War II, because the German army used it in all its battlegrounds. The Hungarians were happy, because the base points had already been converted to this system. Yes, but the Germans then defined this mapping for a BESSEL ellipsoid with the datum RDN₁₉₄₀! Of course, they could explain to the Soviets afterwards about the discrepancy between the KRASOVSKIY and the BESSEL ellipsoids or about datum conversions, the 'competent' Soviet comrades were very good at everything... Let this story remain as a reminder that without a geodetic datum the description of a map projection is never complete!

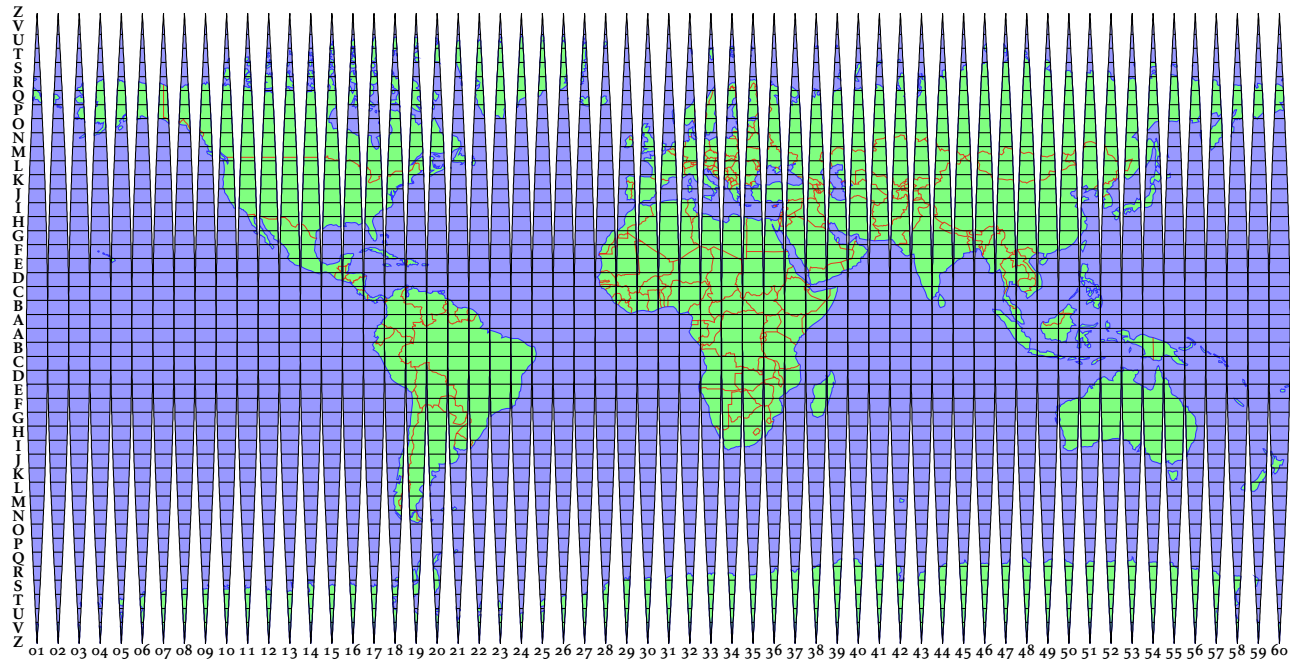


Figure XIV.3: Zones and bands of the GAUSS-KRÜGER projection

XIV.5 The systems of NATO

NATO also developed its own projection system. It uses two types of projection: the *Universal Transverse Mercator (UTM)* between 80° S and 84° N, which is not a MERCATOR projection, and the *Universal Polar Stereographic (UPS)*, which is not stereographic (Sec. XI.4), at the poles.

The UTM projection actually applies the formulæ of the GAUSS–KRÜGER projection system to the ellipsoid WGS84, but with a reduction of 0.9996 for better distortions. As a result, the distortions are more favourably distributed: two lines almost parallel to the central meridian will be free of distortion, with a reduction of length between them and an increase in length outside them. To prevent negative horizontal coordinates, a false easting of 500 km is used. In the Southern Hemisphere, a false northing of 10 000 km is also applied so that the vertical coordinate is also positive. The bands of UTM are 8° wide and are denoted by letters starting with C at latitude 80° S, but the letters I and O are omitted. Hungary is in zones T and U. The northernmost band, X, is 12° wide.

Topographic maps of Southern Europe and the Scandinavian countries are all drawn in UTM, but there are slight irregularities in the zones near Norway. Since NATO accession (the 1990s), Hungarian military topography has been using UTM zones 33 and 34, bounded by the meridian 18° near Veszprém.

To avoid the need to report three numbers (zone, x , y) to define a location, NATO has developed a military geocode system called *Military Grid Reference System (MGRS)*. The first two digits of the reference are the zone (in the case of the UPS, this is omitted, of course), followed by the designation of the band.

This is followed by the letter indicating a column: between the coordinates 100 km and 900 km, zones are divided into 8 columns, each 100 km wide. The letters are repeated for each three zones: A-H, J-R and S-Z, from west to east, I and O are omitted. The third letter marks the row. Rows are also 100 km wide, their designation starts with A for odd zones and F for even zones, increasing in both directions from the Equator. Letters I, O, W, X, Y and Z are omitted for the rows, so after reaching the letter V, the designation starts again with A, the letters are recurring at every 2000 km. In the UPS, a grid of 100×100 km is also used, but letters D, E, M, N, V and W are omitted for columns so that no UTM and UPS squares of the same letter are next to each other, only I and O are omitted for rows. The designation of the 100×100 km squares for Hungary is shown in Fig. XIV.4.

Last come the digits of the coordinates, first x , then y . Since the designation of rows and columns gives the coordinate unambiguously up to

XIV. Cylindricals for the ellipsoid of revolution

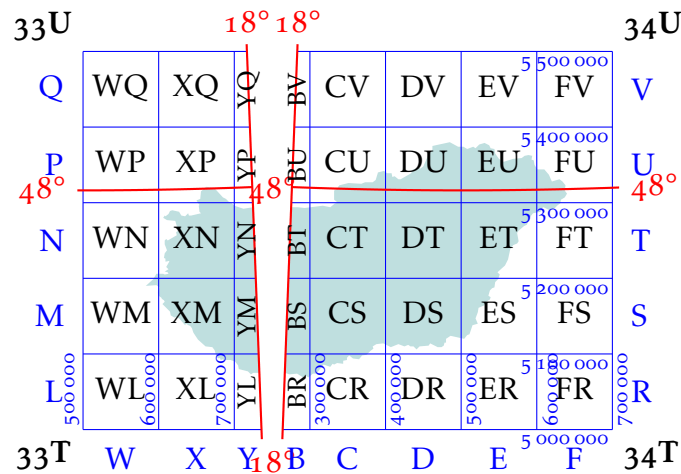


Figure XIV.4: MGRS in Hungary

the place value of 100 000, only the remaining 5 digits are written. If less precision is required, it is possible to write fewer digits, in which case the coordinates are truncated. For example, the tram stop Petőfi híd, budai hídű is located under the coordinates UTM 34T 353755 5259967, while the MGRS reference with accuracy of 100 m is 34TCT537599.

XIV.6 ROSENMUND and HOTINE projections

Like the stereographic projection, the MERCATOR projection is often used in oblique aspect with reference frame as an ellipsoid of revolution. We do not have direct ellipsoid-to-plane formulæ because it is not possible to represent a general geodesic line as an equidistant line in an ellipsoidal conformal projection. We, therefore, resort to a double mapping.

In 1903, the Swiss ROSENMUND developed the following projection: in a first step, he transformed the ellipsoid of revolution into a Gaussian conformal sphere of very low distortion. The standard parallel of the auxiliary sphere is the latitude of the Bern Observatory. In the second step, the spherical oblique MERCATOR projection is used ($c = 1$, i.e. the mapped metaequator is true-scale), the intersection of the metaequator and the prime meridian on the sphere is again the Bern Observatory. The modern Swiss topographic projection differs from this in that it uses a uniform scaling and applies a translation against the negative coordinates on the coordinate axes. Since all transformations (Fig. XIV.5) were conformal, their succession was also a conformal mapping.

XIV. Cylindricals for the ellipsoid of revolution

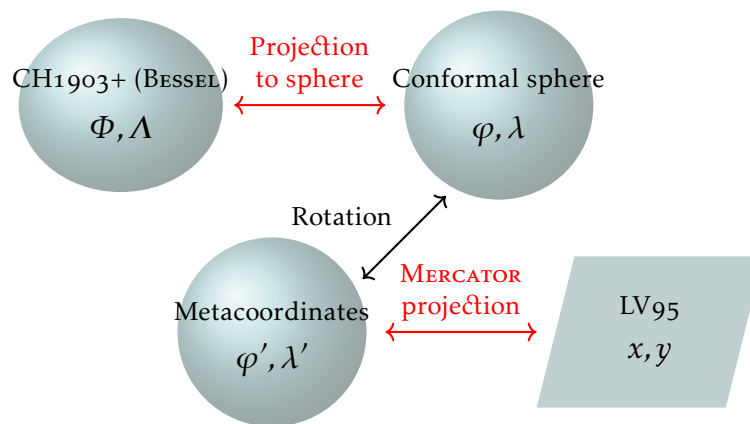


Figure XIV.5: ROSENMUND projection in Switzerland

This mapping is very similar to the Hungarian official map projection (EOV), which:

- Uses the datum HD72 based on ellipsoid IUGG67.
- The ellipsoidal latitude of the standard parallel on the Gaussian auxiliary sphere is $\Phi_s = 47^\circ 10'$.
- The spherical latitude of the metaequator is $47^\circ 6'$.
- The coordinates of the cylindrical map were multiplied by 0.999 93 (*reduced projection*), yielding two true-scale metaparallels. The distribution of the distortions is thus more favourable: there is a reduction of the length between the two distortion-free lines and an increase in length outside them. The only areas where the linear scale exceeds the required value of 1 : 10 000 are near Torna and Zemplén and in the Ormánság region.
- The coordinate axes are unusual: x points to the North and y to the East. To avoid negative signs, they have been shifted by 200 km to the South and 650 km to the West. Thus, in Hungary, the vertical coordinates are less than 400 km, the horizontal coordinates are always greater than this (Fig. XIV.6).

Introduced in 1975, the EOV is used often in Hungary: except for military topographic and geological maps, almost all map databases in Hungary use this system. The most important application is the EOTR, which is a series of topographic maps covering the whole territory of Hungary in this system.

The EOV implementation of popular open-source GIS is not accurate because it approximates it with the ROSENMUND projection. The only difference, as we have seen, is that the standard parallel of the Gaussian auxiliary sphere is not parametrizable, but coincides with the latitude of

XIV. Cylindricals for the ellipsoid of revolution

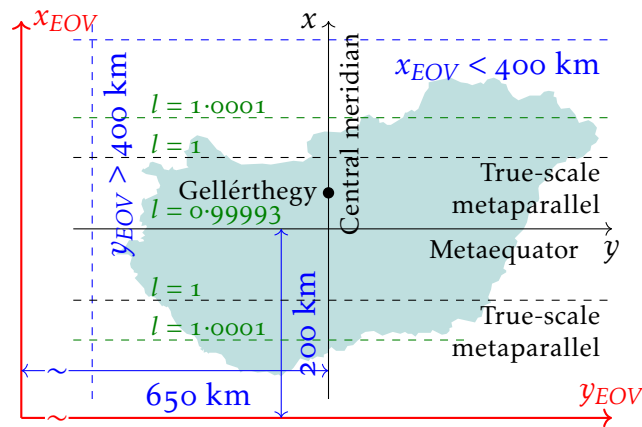


Figure XIV.6: The EOVS coordinate system

the metaequator. The error is of the order of cm.

In 1946, British geodesist HOTINE used a surface of revolution shaped like a turnip (*aposphere*) instead of a Gaussian sphere as an intermediate surface for the conformal double projection. This surface has a constant Gaussian curvature, i.e. a distortion-free projection can be constructed between the aposphere and the sphere (Sec. VI.1). The projection between the aposphere and the plane employs a conformal mapping that maps a geodesic line of the aposphere to a straight true-scale line. HOTINE's and ROSENMUND's formulæ theoretically give exactly the same projection, but because of the different derivation, HOTINE's projection must be parametrized differently. This projection was developed to represent Malaysia, which is located along two oblique geodesic lines. This projection can also be used to approximate the EOVS if ROSENMUND's projection is not supported by the software.

Lesson fifteen

Aphylactic conic projections

XV.1 Conic projections

In *conic projections*, the images of meridians are concurrent straight lines and the images of parallels are concentric arcs of circles perpendicular to them. Because of their equal spacing, the angle formed by the meridians is in direct proportion to the difference in longitude. For this reason, conic map projections differ from azimuthal projections only in that the polar angle is $n\lambda$ (Fig. XV.1). Together with the *cone constant* $0 < n < 1$ (ratio of the angle between mapped meridians to their difference in longitude), we are still free to choose a strictly increasing radius function ρ . The conversion between polar and Cartesian coordinates:

$$\begin{aligned}x &= \rho \sin(n\lambda) \\ y &= -\rho \cos(n\lambda)\end{aligned}$$

The conic projection is *pointed-polar* if $\rho = 0$ at $\delta = 0$, otherwise it is *flat-polar*. When calculating the linear scales along graticule lines, we use the relation found in Sec. X.1, namely $d\rho/d\varphi = -d\rho/d\delta$:

$$\begin{aligned}h &= \frac{\sqrt{\left(\frac{\partial x}{\partial \varphi}\right)^2 + \left(\frac{\partial y}{\partial \varphi}\right)^2}}{R} = \frac{\sqrt{\left(-\frac{d\rho}{d\delta}\right)^2 \sin^2(n\lambda) + \left(-\frac{d\rho}{d\delta}\right)^2 \cos^2(n\lambda)}}{R} = \frac{1}{R} \frac{d\rho}{d\delta} \\ k &= \frac{\sqrt{\left(\frac{\partial x}{\partial \lambda}\right)^2 + \left(\frac{\partial y}{\partial \lambda}\right)^2}}{R \cos \varphi} = \frac{\sqrt{\rho^2 n^2 \cos^2(n\lambda) + \rho^2 n^2 \sin^2(n\lambda)}}{R \sin \delta} = \frac{\rho n}{R \sin \delta}\end{aligned}$$

* In order to get simple formulæ, we assume here that the origin is at the centre of the mapped parallels. In geodesic practice, however, to avoid excessive numbers for coordinates, we place the horizontal axis at the tangent of some freely chosen *central parallel*. The colatitude of the central parallel is most often chosen as $\delta_m = \arccos n$, which usually coincides with the equidistant parallel in conic maps with one equidistant parallel, and lies between the equidistant parallels if the conic projection has two of them.

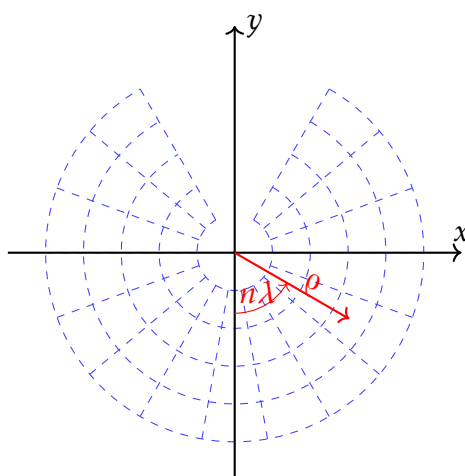


Figure XV.1: Polar coordinates in conic map projections

XV.2 Perspective conics

To derive perspective conic projections, see Fig. XV.2. Denote half the aperture of the cone with σ ! Then we can see that the radius of the mapped parallels before rolling out is $\rho \sin \sigma$ from the right triangle of hypotenuse ρ . That is, the circumference of the mapped parallel on the cone is $2\pi\rho \sin \sigma$. Developing the cone, the radius of the parallel rolled out to an arc becomes ρ and the central angle will be $n2\pi$. Since the development of the cone is an isometry, the arc of the circle has the same length as the circumference of the original circle:

$$\begin{aligned} n2\pi\rho &= 2\pi\rho \sin \sigma \\ n &= \sin \sigma \end{aligned}$$

Thus, in perspective conics, the descriptive meaning of the cone constant n is the sine of half the cone's aperture.

As usual, let the centre of projection be at a distance of fR from the centre of the sphere, while the apex of the cone is placed at a distance of cR from the centre of projection. The distance marked by the red brace and the vertical leg of the right triangle of hypotenuse ρ ($\rho \cos \sigma$) together give just cR , of which the distance highlighted by the brace is $cR - \rho \cos \sigma$. The two right triangles of the red hypotenuses are similar, their aspect ratios are the same:

$$\frac{\rho \sin \sigma}{R \sin \delta} = \frac{cR - \rho \cos \sigma}{R(f + \cos \delta)}$$

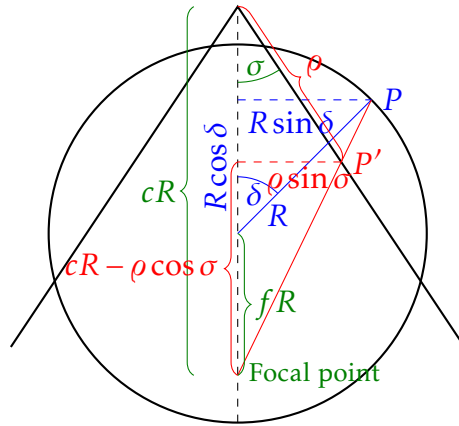


Figure XV.2: The principle of perspective conics

$$\left[\frac{\sin \sigma}{R \sin \delta} + \frac{\cos \sigma}{R(f + \cos \delta)} \right] \rho = \frac{c}{f + \cos \delta}$$

$$\frac{f \sin \sigma + \sin \sigma \cos \delta + \cos \sigma \sin \delta}{R \sin \delta (f + \cos \delta)} \rho = \frac{c}{f + \cos \delta}$$

$$\rho = \frac{c R \sin \delta}{f \sin \sigma + \sin(\sigma + \delta)}$$

Perspective conics are even rarer than perspective cylindricals. This is because they are aphylactic ($h \neq k$ and $hk \neq 1$), their distortions are very unfavourable (Fig. XV.3). Perspective conics are pointed-polar*, their only benefit is that their tangent versions will provide the basis for the construction of polyconic projections in Sec. XXVI.1.†

Consider Fig. XV.4. The two acute angles of a right triangle are each other's complementary angles, so $\sigma = 90^\circ - \delta_s$. Also, by formulating the tangent of δ_s , the radius ρ_s of the tangent parallel can be calculated:

$$\rho_s = R \tan \delta_s$$

$$n = \sin \sigma = \cos \delta_s$$

* Except for the case $f = -1$.

† As among cylindrical projections, there are quasi-perspective projections among conic projections. In these, the centre of projection is located on the plane perpendicular to the generatrix of the cone and passing through the centre of the sphere. For example, from the opposite point of the sphere, one can project in a manner similar to stereographic projection, while from an infinite distance, one can project with parallel rays in a manner similar to orthographic projection. (The latter is not the same as the conic projection with equidistant parallels, because the parallel rays are not vertical this time, but oblique!) Quasi-perspective conics are flat-polar, neither of them has special distortions, so they are of no practical use.

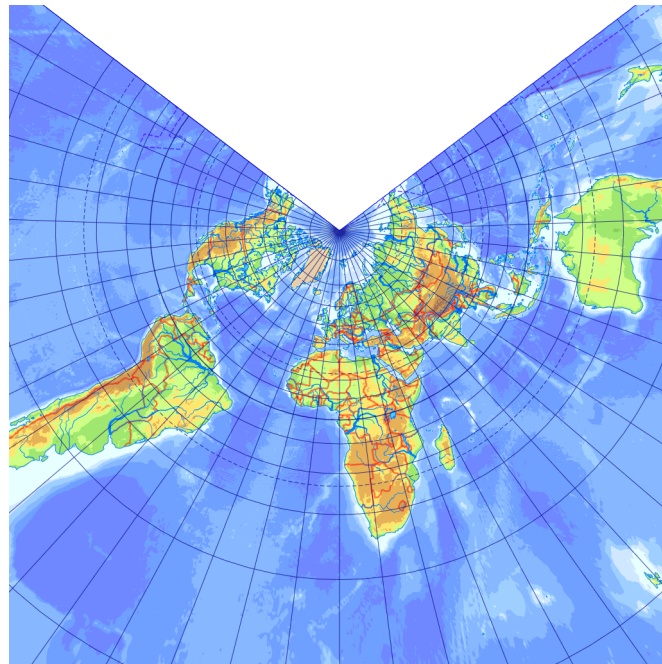


Figure XV.3: *Perspective conic*

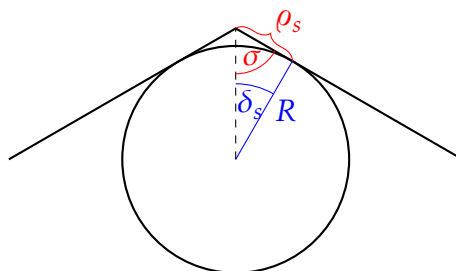


Figure XV.4: *Tangent perspective conic projection*

After formulating the linear scales along graticule lines, it can be seen that $h = k = 1$ at the tangent parallel, i.e. it is true-scale.* Surprisingly, we will find that these three properties hold for non-perspective conic projections with one standard parallel.

XV.3 Conic projection with equidistant parallels

Place the centre of projection infinitely far away, i.e. the rays should be parallel vertical lines. Then $f \rightarrow \infty$ and $c \rightarrow \infty$. In the denominator of the

* This is a non-trivial statement, and for secant perspective conics, it is not even true for secant parallels.

radius function, it is insignificant to add $\sin(\sigma + \delta)$ to the infinitely large number. Since f and c are equally infinite, they can be simplified. The vertical positioning of the cone does not change the projection because of the parallel rays, so it can be considered tangent without loss of generality. In this case, the relation $\sin \sigma = \cos \delta_s$ is applied:

$$\begin{aligned}\rho &= \frac{R \sin \delta}{\cos \delta_s} \\ n &= \cos \delta_s \\ h &= \frac{1}{R} \frac{d\rho}{d\delta} = \frac{\cos \delta}{\cos \delta_s} \\ k &= \frac{\rho n}{R \sin \delta} = \frac{R \sin \delta \cos \delta_s}{\cos \delta_s R \sin \delta} = 1\end{aligned}$$

Since $k = 1$, the projection is equidistant in parallels. It is unsuitable to represent an area larger than a hemisphere. Apart from its theoretical interest, it has no practical use (Fig. XV.5).

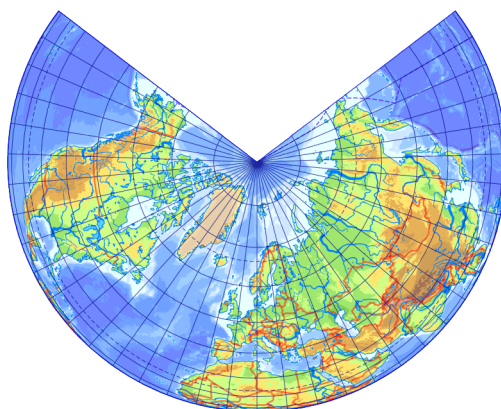


Figure XV.5: Conic projection with equidistant parallels

XV.4 Equidistant conic

Among the non-perspective conics, the derivation of the projection equidistant in meridians ($h = 1$) is straightforward:

$$\begin{aligned}\frac{1}{R} \frac{d\rho}{d\delta} &= 1 \\ \int d\rho &= R \int d\delta \\ \rho &= R\delta + Rd\end{aligned}$$

The constant of integration d characterizes the radius of the pole-line, and the two parameters (n, d) allow for one or two equidistant parallels. Let δ_1 and δ_2 be equidistant! For these two parallel circles, write the equation $k = 1$:

$$\frac{R(\widehat{\delta}_{1,2} + d)n}{R \sin \delta_{1,2}} = 1$$

That is

$$\begin{aligned} n(\widehat{\delta}_1 + d) &= \sin \delta_1 \\ n(\widehat{\delta}_2 + d) &= \sin \delta_2 \end{aligned}$$

Subtracting the two equations from each other:

$$\begin{aligned} n(\widehat{\delta}_1 - \widehat{\delta}_2) &= \sin \delta_1 - \sin \delta_2 \\ n &= \frac{\sin \delta_1 - \sin \delta_2}{\widehat{\delta}_1 - \widehat{\delta}_2} \end{aligned}$$

Dividing the two equations by each other:

$$\begin{aligned} \frac{\widehat{\delta}_1 + d}{\widehat{\delta}_2 + d} &= \frac{\sin \delta_1}{\sin \delta_2} \\ (\widehat{\delta}_1 + d) \sin \delta_2 &= (\widehat{\delta}_2 + d) \sin \delta_1 \\ \widehat{\delta}_1 \sin \delta_2 - \widehat{\delta}_2 \sin \delta_1 &= d(\sin \delta_1 - \sin \delta_2) \\ d &= \frac{\widehat{\delta}_1 \sin \delta_2 - \widehat{\delta}_2 \sin \delta_1}{\sin \delta_1 - \sin \delta_2} \end{aligned}$$

Note that at the equidistant parallels $k = 1$ and everywhere $h = 1$, i.e. the equidistant latitudes are also true-scale standard parallels ($h = k = 1$). At other latitudes:

$$k = \frac{\rho n}{R \sin \delta} = \frac{(\widehat{\delta} + d)n}{\sin \delta}$$

Substituting $\delta = 0$ into the formula above, we obtain that the distortion at the pole is infinite. The exception is if $d = 0$ (the projection is pointed-polar) because then we get a limit of type $\widehat{\delta}/\sin \delta$, which approaches 1, so $k = n$. At the South Pole ($\delta = 180^\circ$), the term also diverges to infinity, so k necessarily has a minimum somewhere, and increases towards the poles. If we have two standard parallels, it follows that between them $k < 1$, and $k > 1$ outwards.

XV. Aphylactic conic projections

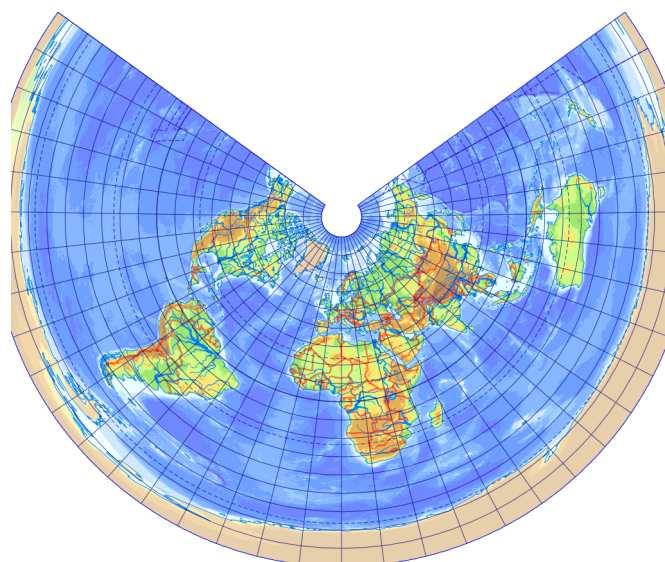
This mapping is called the *equidistant conic* (Fig. XV.6) and is attributed to DE L'ISLE, although he was not the first to use it. This mapping is one of the most favourable projections for areas extending along parallels (its isocols run along parallels) so, a more favourable conic projection is not worth using because of the complexity of the calculations. The projection can be recognized by the even spacing of the parallels. It is most commonly used for middle latitudes, but in theory, there is nothing to stop the two standard parallels being in different hemispheres. It is advisable to pick the standard parallels close to the edges of the area rather than the centre.

Special cases of projection are obtained by the special choice of $\delta_{1,2}$. If $\delta_2 = 0$, i.e. taken at the pole, then substituted back into the equations:

$$n = \frac{\sin \delta_1 - 0}{\widehat{\delta_1} - 0} = \frac{\sin \delta_1}{\widehat{\delta_1}}$$

$$d = \frac{\widehat{\delta_1} 0 - 0 \sin \delta_1}{\sin \delta_1 - 0} = 0$$

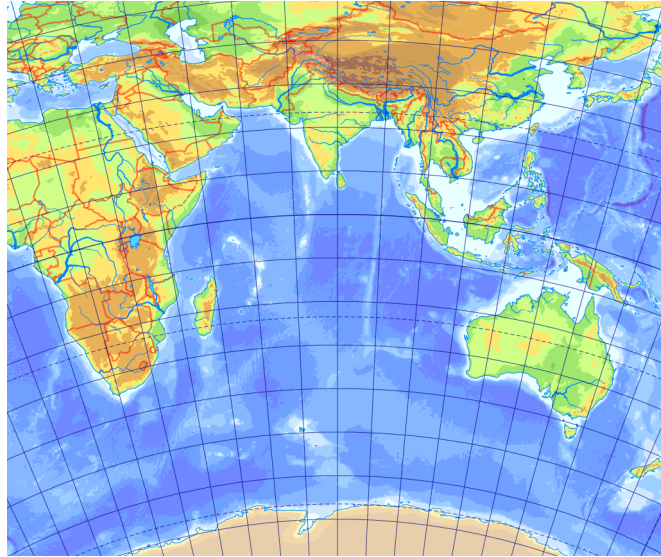
Thus, we obtain a pointed-polar conic. Interestingly, the pole is not true-scale at the same time: although $h = 1$, $k = n$ emerged at the pole. The resulting angular distortion is visible to the naked eye: the meridians do not form true angles at the pole. This variant is the work of the Russian chemist MENDELEYEV, and is not actually used in practice.



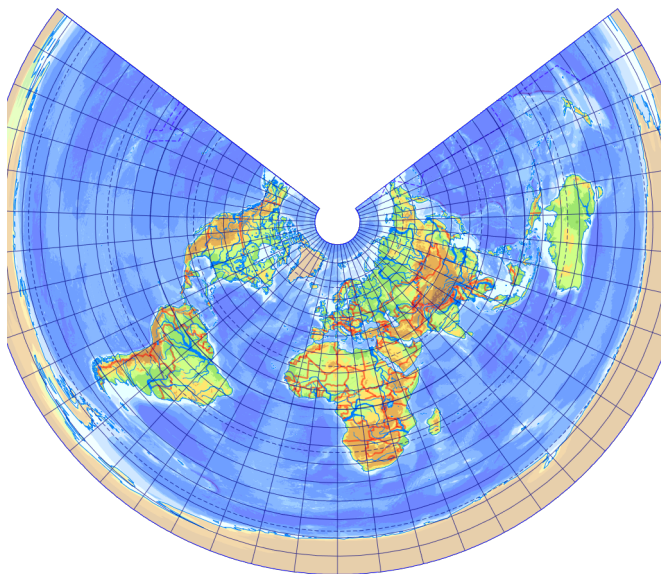
(a) *Equidistant conic*

Figure XV.6: *Conic projections with equidistant meridians*

XV. *Aphylactic conic projections*



(b) *Equidistant conic for the Indian Ocean*



(c) *PTOLEMY I projection*

Figure XV.6: *(contd.)*

Let us consider the version where the two standard parallels coincide ($\delta_1 = \delta_2 = \delta_s$). Since the direct substitution leads to divisions of type o/o, we only substitute δ_s for δ_2 , and write $\delta_s + \Delta\delta$ for δ_1 temporarily, then let $\Delta\delta$ approach zero and apply L'HÔPITAL's rule:

$$n = \lim_{\Delta\delta \rightarrow 0} \frac{\sin(\delta_s + \Delta\delta) - \sin \delta_s}{(\widehat{\delta_s + \Delta\delta}) - \widehat{\delta_s}} = \lim_{\Delta\delta \rightarrow 0} \frac{\cos(\delta_s + \Delta\delta)}{1} = \cos \delta_s$$

$$d = \lim_{\Delta\delta \rightarrow 0} \frac{(\widehat{\delta_s + \Delta\delta}) \sin \delta_s - \widehat{\delta_s} \sin(\delta_s + \Delta\delta)}{\sin(\delta_s + \Delta\delta) - \sin \delta_s}$$

$$= \lim_{\Delta\delta \rightarrow 0} \frac{\sin \delta_s - \widehat{\delta_s} \cos(\delta_s + \Delta\delta)}{\cos(\delta_s + \Delta\delta)} = \tan \delta_s - \widehat{\delta_s}$$

From the above formulæ, it can be seen that, just like the case of tangent perspective conics, the radius of the standard parallel is just $R \tan \delta_s$ and the cone constant is $\cos \delta_s$. We call this mapping the *PTOLEMY I* projection.*

If both parallels approach the pole ($\delta_s = 0$), the above formulæ give $n = 1$ and $d = 0$, i.e. $\rho = R\widehat{\delta}$, so we get the azimuthal equidistant, in which the pole becomes true-scale.

It is exciting to consider the case $\delta_2 = 180^\circ - \delta_1$. Then $n = 0$ is obtained, i.e. the mapped meridians are parallel. Moreover, since the denominator of d is zero and the numerator is not zero, $d \rightarrow \infty$, i.e. the parallel circles have infinite radii and are therefore parallel lines. Ultimately, we have the equidistant cylindrical. This shows that the conic projections are a transition between azimuthals and cylindricals.

* We find this projection in *Geographica*, his work written in the 2nd century, which laid the foundations for cartography.

Lesson sixteen

Equal-area & conformal conic mappings

XVI.1 ALBERS equal-area conic

First, the equal-area conic ($hk = 1$) is calculated. Let the constant of integration be $R^2/n + R^2d/2n$!

$$\begin{aligned} \frac{1}{R} \frac{d\rho}{d\delta} \frac{\rho n}{R \sin \delta} &= 1 \\ \int \rho d\rho &= \frac{R^2}{n} \int \sin \delta d\delta \\ \frac{\rho^2}{2} &= -\frac{R^2}{n} \cos \delta + \frac{R^2}{n} + \frac{R^2 d}{2n} \\ \rho^2 &= \frac{R^2}{n} \left(-2 \cos^2 \frac{\delta}{2} + 2 \sin^2 \frac{\delta}{2} + 2 \cos^2 \frac{\delta}{2} + 2 \sin^2 \frac{\delta}{2} + \frac{2d}{2} \right) \\ \rho &= \frac{R}{\sqrt{n}} \sqrt{4 \sin^2 \frac{\delta}{2} + d} \end{aligned}$$

The constant d determines the radius of the pole-line, since for the substitution $\delta = 0$, we get $\rho = R\sqrt{d/n}$. By setting n and d appropriately, one or two arbitrarily chosen parallels may be equidistant.* Let our two equidistant parallels be δ_1 and δ_2 ! At these latitudes $k = 1$, so $k^2 = 1$. Take

* Conic projections with two standard parallels are often called secant conics in the literature, and there are beautiful illustrations of cones intersecting the sphere in two circles. This is a very illustrative explanation, with only one flaw: it is absolutely false. Such conic maps, when rolled to form a cone, will not happen to have the true-scale parallels where the cone intersects the sphere. In addition, these projections may not always be obtained by uniform scaling of the version with one standard parallel, so the term reduced should also be avoided for not conformal projections.

XVI. Equal-area & conformal conic mappings

the formula ρ^2 not from the final solution, but from the third line of the derivation above.

$$\frac{\rho^2 n^2}{R^2 \sin^2 \delta_{1,2}} = 1$$

$$2 \left(-\frac{R^2}{n} \cos \delta_{1,2} + \frac{R^2}{n} + \frac{R^2 d}{2n} \right) n^2 = R^2 \sin^2 \delta_{1,2}$$

That is, after simplifying by R^2 :

$$n(2 - 2 \cos \delta_1 + d) = \sin^2 \delta_1$$

$$n(2 - 2 \cos \delta_2 + d) = \sin^2 \delta_2$$

Subtracting the two equations from each other:

$$n(2 \cos \delta_2 - 2 \cos \delta_1) = \sin^2 \delta_1 - \sin^2 \delta_2$$

$$n = \frac{1 - \cos^2 \delta_1 - 1 + \cos^2 \delta_2}{2(\cos \delta_2 - \cos \delta_1)}$$

$$= \frac{(\cos \delta_2 + \cos \delta_1)(\cos \delta_2 - \cos \delta_1)}{2(\cos \delta_2 - \cos \delta_1)} = \frac{\cos \delta_1 + \cos \delta_2}{2}$$

The first equation of the system of equations:

$$n(2 - 2 \cos \delta_1) + nd = \sin^2 \delta_1$$

$$nd = \sin^2 \delta_1 - \frac{2(1 - \cos \delta_1)(\cos \delta_1 + \cos \delta_2)}{2}$$

Before calculating further, note that:

$$\cos \delta = \cos^2 \frac{\delta}{2} - \sin^2 \frac{\delta}{2} = \cos^2 \frac{\delta}{2} + \sin^2 \frac{\delta}{2} - \sin^2 \frac{\delta}{2} - \sin^2 \frac{\delta}{2} = 1 - 2 \sin^2 \frac{\delta}{2}$$

This makes it easy to get the final result:

$$d = \frac{\sin^2 \delta_1 - (1 - \cos \delta_1)(\cos \delta_1 + \cos \delta_2)}{n}$$

$$= \frac{\sin^2 \delta_1 - (1 - \cos \delta_1) \left(1 - 2 \sin^2 \frac{\delta_1}{2} + 1 - 2 \sin^2 \frac{\delta_2}{2} \right)}{n}$$

$$= \frac{\sin^2 \delta_1 - 2 \left(1 - 1 + 2 \sin^2 \frac{\delta_1}{2} \right) \left(1 - \sin^2 \frac{\delta_1}{2} - \sin^2 \frac{\delta_2}{2} \right)}{n}$$

$$= \frac{4 \sin^2 \frac{\delta_1}{2} \cos^2 \frac{\delta_1}{2} - 4 \sin^2 \frac{\delta_1}{2} \left(\cos^2 \frac{\delta_1}{2} - \sin^2 \frac{\delta_2}{2} \right)}{n}$$

$$= \frac{4 \sin^2 \frac{\delta_1}{2} \left(\cos^2 \frac{\delta_1}{2} - \cos^2 \frac{\delta_1}{2} + \sin^2 \frac{\delta_2}{2} \right)}{n} = \frac{4 \sin^2 \frac{\delta_1}{2} \sin^2 \frac{\delta_2}{2}}{n}$$

This mapping is called the *ALBERS equal-area conic* (Fig. XVI.1). Although he published the projection as early as 1805, we rarely see it until the

XVI. Equal-area & conformal conic mappings

middle of the 20th century. Its popularity is now on the rise, especially in the USA. Let us examine the distortions!

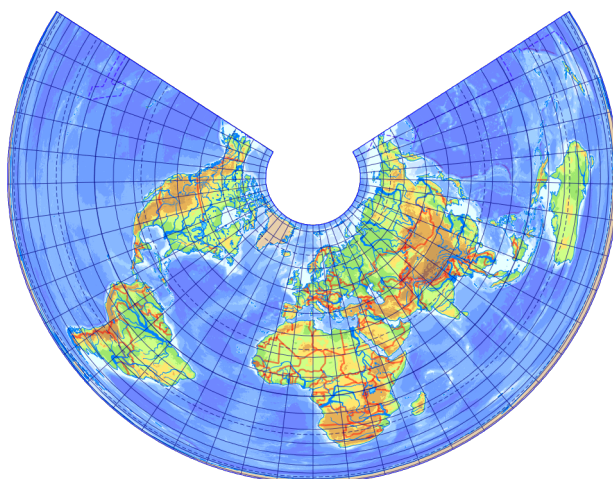
$$h = \frac{1}{R} \frac{d\rho}{d\delta} = \frac{\frac{4 \times 2}{2} \sin \frac{\delta}{2} \cos \frac{\delta}{2}}{2\sqrt{n} \sqrt{4 \sin^2 \frac{\delta}{2} + d}} = \frac{\sin \delta}{\sqrt{n} \sqrt{4 \sin^2 \frac{\delta}{2} + d}}$$

$$k = \frac{\rho n}{R \sin \delta} = \frac{\sqrt{n}}{\sin \delta} \sqrt{4 \sin^2 \frac{\delta}{2} + d}$$

This time, the equidistant parallels are also standard parallels, because here $k = 1$ and $h = 1/k = 1$ due to equivalency. At the poles, the numerator of h and the denominator of k are zero, so the former is zero and the latter tends to infinity. Again, the case $d = 0$ is exception, because then we can simplify by $2 \sin \delta/2$ so that at the North Pole $h = 1/\sqrt{n}$ and $k = \sqrt{n}$. Apart from this pointed-polar case, it can be seen that since k is infinitely large at the poles and the projection has two standard parallels, $h < 1$ and $k > 1$ outward from the standard parallels, so the objects are stretched in the east-west direction. On the other hand, between the two standard parallels, where $h > 1$ and $k < 1$, the stretching is in the north-south direction. This helps us to recognize the projection: the parallels in the middle of the map cross the meridians less densely than at the bottom and top of the map.

Special cases will also be of interest. If $\delta_2 = 0$, i.e. at the pole, then:

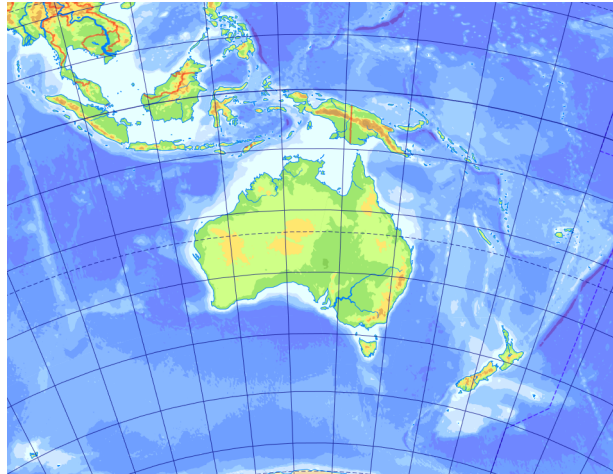
$$n = \frac{\cos \delta_1 + 1}{2} = \frac{\cos^2 \frac{\delta_1}{2} - \sin^2 \frac{\delta_1}{2} + \sin^2 \frac{\delta_1}{2} + \cos^2 \frac{\delta_1}{2}}{2} = \cos^2 \frac{\delta_1}{2}$$



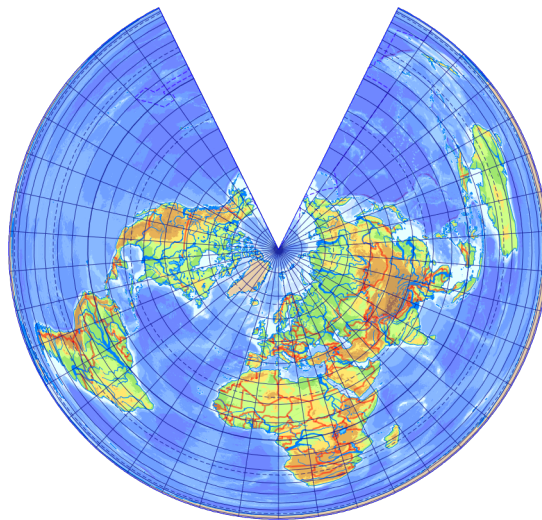
(a) ALBERS equal-area conic

Figure XVI.1: Equal-area conics

XVI. Equal-area & conformal conic mappings



(b) ALBERS projection for Australia



(c) LAMBERT equal-area conic

Figure XVI.1: (contd.)

XVI. Equal-area & conformal conic mappings

$$d = \frac{4 \sin^2 \frac{\delta_1}{2} \times 0}{n} = 0$$

This pointed-polar conic projection ($d = 0$) is called *LAMBERT equal-area conic* and has been known since 1772. Contrary to our expectation, the pole is not true-scale because $h = 1/\sqrt{n}$ and $k = \sqrt{n}$, so angular distortion is present. This is logical since mapped meridians cannot arrive at the pole at their true angle.

Let us now construct a flat-polar equal-area conic with only one standard parallel! This can be easily done by substituting $\delta_1 = \delta_2 = \delta_s$, this time no limit calculus is needed:

$$n = \frac{\cos \delta_s + \cos \delta_s}{2} = \cos \delta_s$$

$$d = \frac{4 \sin^2 \frac{\delta_s}{2} \sin^2 \frac{\delta_s}{2}}{n} = \frac{4 \sin^4 \frac{\delta_s}{2}}{\cos \delta_s}$$

Substituting back and applying a sufficient amount of trigonometric identities, it can be seen that, less and less surprisingly, the radius of the standard parallel becomes again $R \tan \delta_s$.

If both standard parallels are placed at the pole ($\delta_s = 0$), the result of the above formulæ is $n = 1$ and $d = 0$, i.e. we get the LAMBERT azimuthal equal-area. If $\delta_2 = 180^\circ - \delta_1$, then $n = 0$ and $d \rightarrow \infty$, giving a limit to the family of equal-area cylindricals.

XVI.2 LAMBERT conformal conic

Only the conformal version ($h = k$) is left. In the derivation, the constant of integration is $\ln d + \ln R$.

$$\frac{1}{R} \frac{d\rho}{d\delta} = \frac{\rho n}{R \sin \delta}$$

$$\int \frac{1}{\rho} d\rho = n \int \frac{1}{\sin \delta} d\delta$$

$$\ln \rho = n \ln \tan \frac{\delta}{2} + \ln d + \ln R$$

$$\rho = dR \tan^n \frac{\delta}{2}$$

This time, the parameter d denotes a uniform scaling, the projection is in any case pointed-polar.* The South Pole is mapped to infinity. This time

* In general, there is no flat-polar conformal projection, unless the pole at infinity is considered to be a pole-line.

XVI. Equal-area & conformal conic mappings

again, two equidistant parallels can be set by choosing n and d appropriately. Let δ_1 and δ_2 be the equidistant parallels! Here, let $k = 1$! From this:

$$\frac{\rho n}{R \sin \delta_{1,2}} = 1$$

$$ndR \tan^n \frac{\delta_{1,2}}{2} = R \sin \delta_{1,2}$$

Thus:

$$nd \tan^n \frac{\delta_1}{2} = \sin \delta_1$$

$$nd \tan^n \frac{\delta_2}{2} = \sin \delta_2$$

Dividing the two equations by each other:

$$\frac{\tan^n \frac{\delta_1}{2}}{\tan^n \frac{\delta_2}{2}} = \frac{\sin \delta_1}{\sin \delta_2}$$

$$n \left(\ln \tan \frac{\delta_1}{2} - \ln \tan \frac{\delta_2}{2} \right) = \ln \sin \delta_1 - \ln \sin \delta_2$$

$$n = \frac{\ln \sin \delta_1 - \ln \sin \delta_2}{\ln \tan \frac{\delta_1}{2} - \ln \tan \frac{\delta_2}{2}}$$

d cannot be expressed in such a nice form, but it can be expressed from either of the two equations:

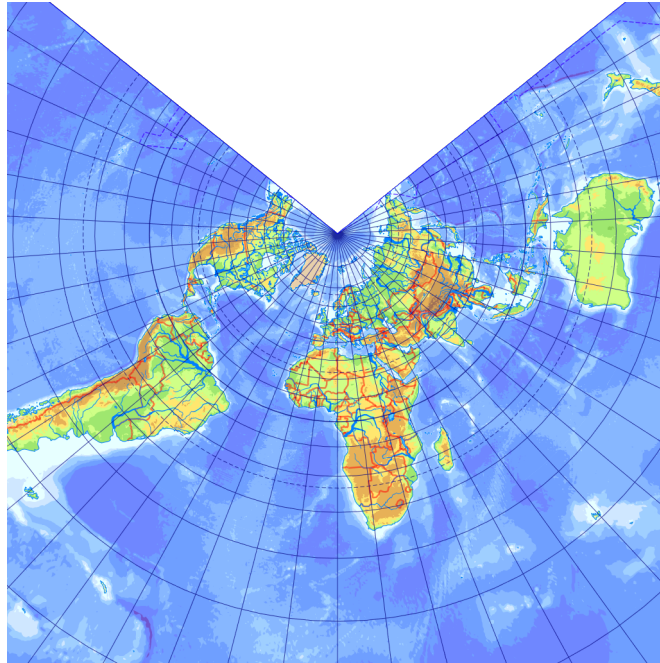
$$d = \frac{\sin \delta_1}{n \tan^n \frac{\delta_1}{2}} = \frac{\sin \delta_2}{n \tan^n \frac{\delta_2}{2}}$$

The mapping is called the *LAMBERT conformal conic* or the *LAMBERT-GAUSS* projection (Fig. XVI.2), and like LAMBERT's other projections, it was published in 1772. As it received little attention at first, its authorship remained unknown for a long time, and several scientists of map projections, including GAUSS, created it independently. How do the distortions of projection arise?

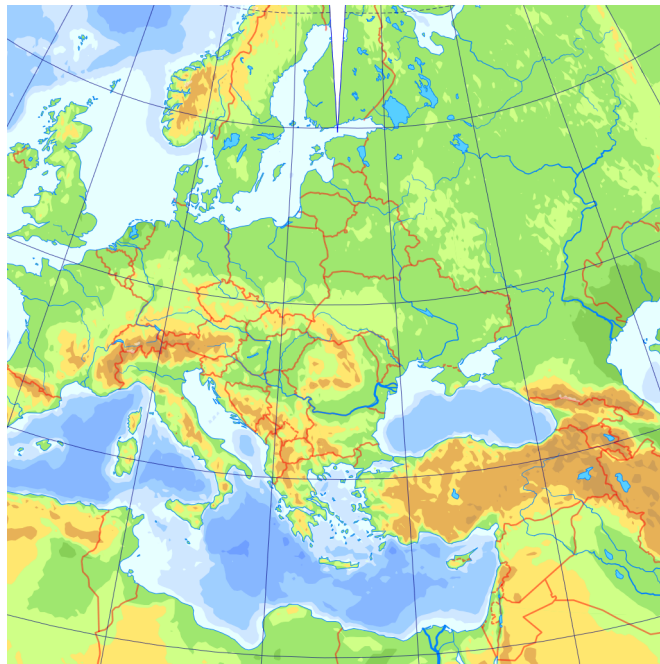
$$h = \frac{1}{R} \frac{d\rho}{d\delta} = \frac{dn \tan^{n-1} \frac{\delta}{2}}{2 \cos^2 \frac{\delta}{2}} = \frac{nd}{2 \sin^{1-n} \frac{\delta}{2} \cos^{1+n} \frac{\delta}{2}}$$

$$k = \frac{\rho n}{R \sin \delta} = \frac{nd \tan^n \frac{\delta}{2}}{2 \sin \frac{\delta}{2} \cos \frac{\delta}{2}} = \frac{nd}{2 \sin^{1-n} \frac{\delta}{2} \cos^{1+n} \frac{\delta}{2}}$$

XVI. Equal-area & conformal conic mappings



(a) LAMBERT conformal conic



(b) Křovák projection

Figure XVI.2: Conformal conics

XVI. Equal-area & conformal conic mappings

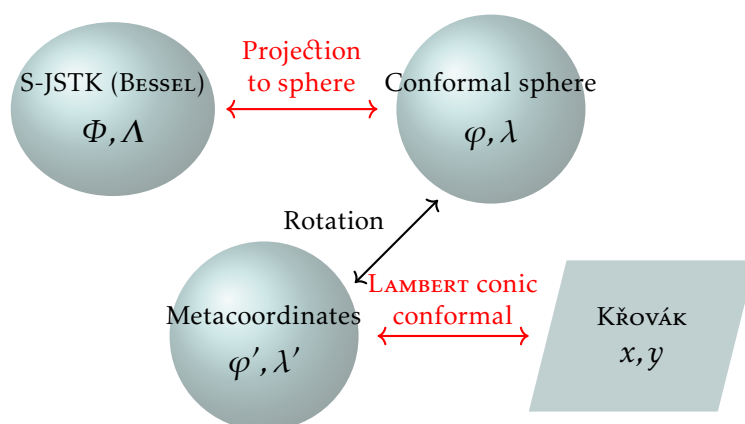


Figure XVI.3: Křovák projection in Czechia and Slovakia

Interestingly, at the North Pole, the mapping is not conformal, since the meridians do not meet at their true angles. We can see from the formula that at both poles $h = k \rightarrow \infty$, i.e. the distortions are infinitely large.* Since they are of finite magnitude between the two poles, there is a minimum somewhere between the two equidistant parallels. Thus, between the two equidistant parallels $h = k < 1$, away from them $h = k > 1$. This helps to recognize projection: the mapped parallels in the middle of the map intersect the mapped meridians more densely than at the northern and southern edges of the map. The equidistant parallels are now also standard parallels: if $k = 1$, then $h = k = 1$.

What happens if $\delta_1 = \delta_2 = \delta_s$? The division cannot be done in the formula n , so again we resort to the trick $\delta_1 = \delta_s + \Delta\delta$, as $\Delta\delta \rightarrow 0$. Again, we can calculate the limit using L'HÔPITAL's rule.

* An interesting property of conformal projections is the *singularity*. It is known from the analysis of complex numbers that a mapping is conformal if and only if the $\mathbb{C} \rightarrow \mathbb{C}$ (complex) function describing it is differentiable. However, discontinuities necessarily appear in the projections, so our function here is not continuous and therefore cannot be differentiable. Therefore, the mapping at the endpoints of the discontinuities (and sometimes elsewhere, but even then only at isolated points) is necessarily singular, not differentiable. Conformal projections exhibit three types of singularity:

The mapped point may be at infinity, in which case the conformality is not definable (for example, the South Pole in the stereographic projection). The point may have infinitely large distortions ($l \rightarrow \infty$ or very rarely $l = 0$), the conformality is lost at this single point (see the North Pole in the projection we are discussing). It is rare that a line bifurcates without a break at a point, in which case the conformality is preserved (turn to Fig. XIV.2 and you will find points on the GAUSS-KRÜGER projection where the Equator divides into two branches).

XVI. Equal-area & conformal conic mappings

$$\begin{aligned}
 n &= \lim_{\Delta\delta \rightarrow 0} \frac{\ln \sin(\delta_s + \Delta\delta) - \ln \sin \delta_s}{\ln \tan \frac{\delta_s + \Delta\delta}{2} - \ln \tan \frac{\delta_s}{2}} \\
 &= \lim_{\Delta\delta \rightarrow 0} \frac{\frac{\cos(\delta_s + \Delta\delta)}{\sin(\delta_s + \Delta\delta)}}{\frac{1}{2 \tan \frac{\delta_s + \Delta\delta}{2} \cos^2 \frac{\delta_s + \Delta\delta}{2}}} = \frac{\cot \delta_s}{\frac{1}{2 \sin \frac{\delta_s}{2} \cos \frac{\delta_s}{2}}} = \cos \delta_s
 \end{aligned}$$

It still holds that:

$$d = \frac{\sin \delta_s}{n \tan^n \frac{\delta_s}{2}}$$

Once again, as $n = \cos \delta_s$, is the radius of the standard parallel $R \tan \delta_s$? If we substitute it back into the radius function, then it will indeed come out.

Since d is just a scaling, you can get any versions with two standard parallels by reducing the projection with one standard parallel of the same cone constant. Therefore, in GIS, it is common that the projection is not parametrized by the two standard parallels, but by a single parallel and a reduction factor.

The LAMBERT–GAUSS projection is preferred by international aviation because, besides its conformality, it displays orthodromes shorter than 3000 km as almost straight lines. The *World Aeronautical Chart (WAC)* also uses an ellipsoidal version of this projection for datum WGS84, but most aeronautical charts are also produced in this projection. It is also used as a projection for topographic maps in many countries, especially in the French culture. It should be used for medium latitudes, for areas extending along a parallel, because its isocols are arcs of circles.

In Czechia and Slovakia, the oblique aspect of this projection is still used in a double projection known as the Křovák projection (Fig. XVI.3). The reason for this is that the former Czechoslovakia (today's Czechia, Slovakia, and Transcarpathia of Ukraine) had a curved shape. They were looking for a projection with isocols following this shape. Thus this projection was chosen. Since the area is not located along a parallel but is rotated, a graticule rotation is required. This was done in the usual way, by double mapping. A conformal sphere is calculated based on the BESSEL ellipsoid and the graticule is rotated so that the metapole is near Helsinki. The conformal conic is characterized by the metaparallel δ_s and a reduction factor so that the distortions meet the geodetic requirements almost everywhere in the country. A similar projection was used in their national atlas to represent Japan, which has a shape like a banana.

XVI. Equal-area & conformal conic mappings

What happens if you move one of the standard parallels to the pole ($\delta_2 \rightarrow 0$)? In this case, to overcome the quotient of the logarithms of zero, we repeat L'HÔPITAL'S rule with δ_2 as an independent variable:

$$n = \lim_{\delta_2 \rightarrow 0} \frac{\ln \sin \delta_1 - \ln \sin \delta_2}{\ln \tan \frac{\delta_1}{2} - \ln \tan \frac{\delta_2}{2}} = \lim_{\delta_2 \rightarrow 0} \frac{-\frac{\cos \delta_2}{\sin \delta_2}}{-\frac{1}{2 \tan \frac{\delta_2}{2} \cos^2 \frac{\delta_2}{2}}} = \lim_{\delta_2 \rightarrow 0} \cos \delta_2 = 1$$

Contrary to our previous experience, we did not get a pointed-polar conic (since the conformal projection was already pointed-polar), but it was enough to place one of the standard parallels in the pole to get an azimuthal projection ($n = 1$). But is not that the right way? After all, unlike the azimuthal equal-area or equidistant, we could choose a standard parallel for the stereographic projection, which is distortion-free. Thus, if you place one of the standard parallels of the projection at the pole, the other parallel will be the secant parallel of the stereographic projection. In the pole, of course, conformality is then restored, but equivalency is lost because the stereographic projection is only distortion-free at the standard parallel.

The other limit is $\delta_2 = 180^\circ - \delta_1$, which leads by simple substitution to $n = 0$, i.e. the MERCATOR projection.

XVI.3 Ellipsoidal conic projections

The linear scales along graticule lines in conic projections for an ellipsoid are as follows:

$$h = -\frac{1}{M(\Phi)} \frac{d\rho}{d\Phi}$$

$$k = \frac{\rho n}{N(\Phi) \cos \Phi}$$

The equidistant conic projection is obtained from the solution of the equation $h = 1$ (d is a constant of integration):

$$\rho = d + \int_{90^\circ}^{\Phi} M(\Phi) d\Phi$$

The equal-area conic is obtained by solving the equation $hk = 1$:

$$\rho = a \frac{\sqrt{1-e^2}}{\sqrt{n}} \sqrt{d - \frac{\sin \Phi}{1-e^2 \sin^2 \Phi} - \frac{1}{2e} \ln \frac{1+e \sin \Phi}{1-e \sin \Phi}}$$

XVI. Equal-area & conformal conic mappings

We get the conformal conic by solving the equation $h = k$:

$$\rho = d \tan^n \left(45^\circ - \frac{\Phi}{2} \right) \left(\frac{1 + e \sin \Phi}{1 - e \sin \Phi} \right)^{ne/2}$$

Expressing the constants from two standard parallels leads to lengthy formulæ, but for all versions with a single standard parallel, $n = \sin \Phi_s$, and the radius of the standard parallel is $N(\Phi_s) \cot \Phi_s$, which is similar to spherical maps.

Lesson seventeen

Applied theory of map projections

XVII.1 Can distortion be useful?

Up until now, we have been struggling to keep the distortions of map projections under control. However, there are times when distortion is an advantage. Fig. XVII.1 shows such a map. It shows the results of an old election in Germany. If our map did not contain distortion, it would be hard to tell that the party in red was the winner, since typically only a few major cities (Berlin, Hamburg, and the Saxon industrial cities) were won. If the map editor were to show the area with slight distortions, it would look as if the party with the most rural voters, the one in khaki, had won overwhelmingly. The map editor rightly compensated for this by plotting the constituencies by population rather than by actual area.

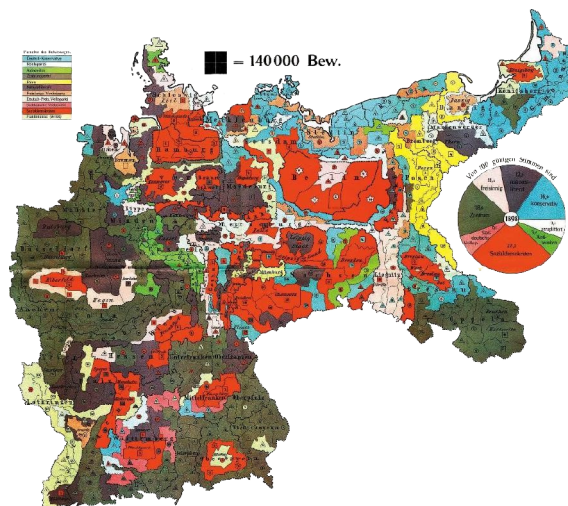


Figure XVII.1: Example of a distorted cartogram

Such representations are called *distorted cartograms*. They can be considered a special kind of map projections in a broad sense. The distortion can be adjusted according to some quantitative measure, but we can also choose, for example, to plot the distance of objects from a given point

according to the travel time from the centre. A special kind of distorted cartogram is the underground map, where the distance depends on the number of stations travelled through. There is a variety of software for creating classical cartograms distorted by quantitative data, such as ScapeToad.

XVII.2 The focus of map projections

In large cities, streets and places of interest (pictograms) are often very densely concentrated in the centre of the city, so the data density is too high; while in the suburbs there are fewer landmarks to represent in a unit area. For this reason, it might be a good decision to use a different map scale in the city centre than in the outer districts. This problem is addressed by the *hyperboloid projection* used in FALK's urban maps. It takes its name from the fact that the kilometre grid lines appear as hyperbolæ. They can also be recognized by the fact that the map scale is shown as an interval (Fig. XVII.2). Projections, in which the linear scale is deliberately increased at the centre, are called *focused projections*.

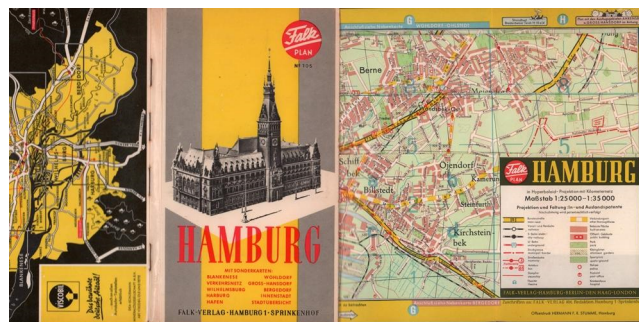


Figure XVII.2: Map of a town in hyperboloid projection

The mathematics of the mapping is a trade secret, but the Israeli cartographer KADMON got a very similar (perhaps exactly the same) map with the following train of thought: let the centre of the coordinate system be at the centre of the city where the linear scale is l_0 ! In distance ρ_p from this, we want a linear scale of $l_p < l_0$. For these two points, we fit a linear function:

$$l = \frac{l_p - l_0}{\rho_p} \rho + l_0$$

XVII. Applied theory of map projections

On the other hand, l is the infinitesimal new length divided by the old length:

$$l = \frac{d\rho'}{d\rho}$$

$$\frac{d\rho'}{d\rho} = \frac{l_p - l_o}{\rho_p} \rho + l_o$$

$$\int d\rho' = \int \frac{l_p - l_o}{\rho_p} \rho + l_o d\rho$$

$$\rho' = \frac{l_p - l_o}{2\rho_p} \rho^2 + l_o \rho$$

With this method, the scale varies continuously. Hungarian cartographer SZIKLÓSI proposed a method where the centre of the map is magnified with a lens while the edges are left unchanged. This is advantageous if the outer districts are not to be distorted.

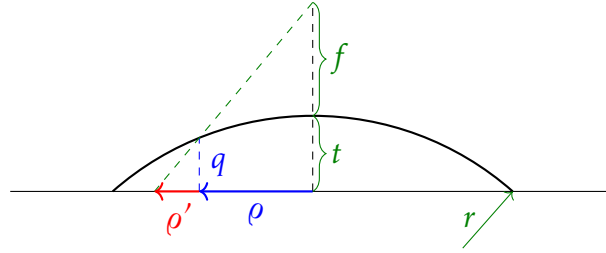


Figure XVII.3: Creating a focused map using a lens

The centre of the circle of radius r shown in Fig. XVII.3 is at distance $r - t$ from the plane of projection. Thus, the equation of the circle is:

$$(q + r - t)^2 + \rho^2 = r^2$$

$$q = \sqrt{r^2 - \rho^2} - r + t$$

The ratio of the sides of two similar triangles in the figure is equal:

$$\frac{\rho'}{f + t} = \frac{\rho' - \rho}{q}$$

$$\rho' \left(\sqrt{r^2 - \rho^2} - r + t \right) = (f + t) \rho' - (f + t) \rho$$

$$\rho' \left(f - \sqrt{r^2 - \rho^2} + r \right) = (f + t) \rho$$

$$\rho' = \frac{(f + t) \rho}{f + r - \sqrt{r^2 - \rho^2}}$$

This transformation leaves intact the parts of the map that are not covered by the lens.

XVII.3 Map projections and GIS

When applying a projection in GIS, it is always necessary to specify the reference frame and the mapping unambiguously. This is quickly identified by the *EPSG number*, behind which the type of projection, its parameters and the reference frame with its placement are stored in a database. Some important EPSG numbers:

4326 Datum WGS84, geographic coordinates
 3857 Pseudo Mercator / datum WGS84
 23700 EOVS / datum HD72
 32633 / 32634 UTM zones 33 / 34 / datum WGS84

In the QGIS application, when you apply a projection for the first time, a dialogue box will pop up asking you which transformation to choose. If there are three parameters in the parameter set, then it will use the MOLODENSKIY transform, if there are seven parameters, then it will use the more accurate HELMERT transform (Sec. VI.4). Sometimes, for a given datum, there may be several very different parameter sets, in which case what usually happens is that the difference between them is negligible in a horizontal sense, but there will be significant differences in the result in the vertical sense. When converting 3D data, particular care must be taken (see also App. D)!

As an example, the case of the EOVS is shown in Fig. XVII.4. The transformation one (in the pop-up) has seven parameters but is not recommended because of its inaccuracy as described. The selected transformation four (read in the main window) has three parameters.

If a map projection cannot be found in the GIS software, it is typically possible to specify a new map projection. While in GlobalMapper this means filling in a simple dialogue box, in other software this is possible using the WKT format. As an example, let us look at the definition of the EOVS in ArcGIS software:

```
PROJCS["HD72_EOV",
  GEOGCS["GCS_HD72",
    DATUM["D_Hungarian_1972",
      SPHEROID["GRS_1967",6378160,298.247167427],
      TOWGS84[52.17,-71.82,-14.9,0,0,0,0]],
    PRIMEM["Greenwich",0],
    UNIT["Degree",0.017453292519943295]]],
```

XVII. Applied theory of map projections

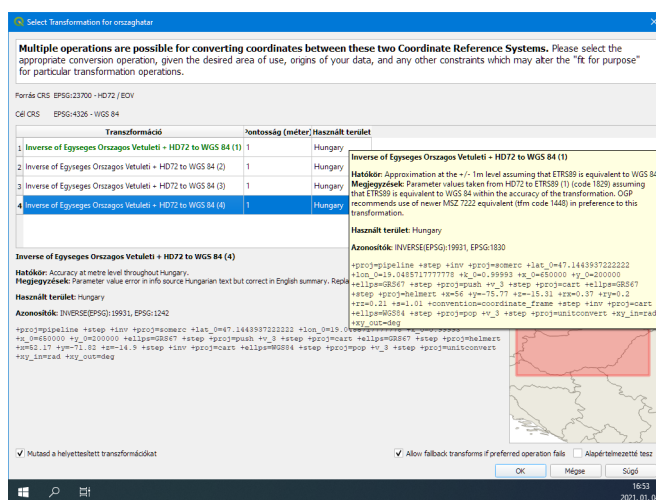


Figure XVII.4: Setting the transformation in QGIS

```
PROJECTION["Hotine_Oblique_Mercator_Azimuth_Center"],
PARAMETER["latitude_of_center",47.1443937222222],
PARAMETER["longitude_of_center",19.0485717777778],
PARAMETER["azimuth",90],
PARAMETER["scale_factor",0.99993],
PARAMETER["false_easting",650000],
PARAMETER["false_northing",200000],
UNIT["Meter",1],
AXIS["Y",EAST],
AXIS["X",NORTH]]
```

It can be seen that ArcGIS derives the datum HD72 in the setting TOWGS84 using the three-parameter form of MOLODENSKIY based on the ellipsoid IUGG67. The mapping is approximated by the HOTINE projection (Sec. XIV.6) with appropriate parametrization. The advantage of the format WKT is that one can specify the mapping precisely, but it is also lengthy. In open-source software, it is possible to use the more compact format PROJ.4, in which there is fewer possibility to define the projection precisely, but this does not usually sacrifice the accuracy required in GIS. An example is the definition of the EOJ in QGIS:

```
+proj=somerc +lat_0=47.1443937222222
+lon_0=19.0485717777778 +k_0=0.99993 +x_0=650000
+y_0=200000 +ellps=GRS67 +towgs84=52.684,-71.194,-13.975,
-0.312,-0.1063,-0.3729,1.0191 +units=m +no_defs
```

This time, `towgs84` contains seven parameters, so it uses a HELMERT transform.* `somerc` is an abbreviation for Swiss Oblique MERCATOR, i.e. the ROSENMUND projection (Sec. XIV.6). Abbreviations of some projections in PROJ.4:

aea ALBERS Equal-Area
aeqd Azimuthal EQUiDiStant
eqdc EQUiDiStant Conic
laea LAMBERT Azimuthal Equal-Area
lcc LAMBERT Conformal Conic
longlat No projection, geographic coordinates
tmerc GAUSS–KRÜGER projection

Using our knowledge, georeference a map in the Budapest stereographic system (App. F) as an example! Unfortunately, this projection is not supported by QGIS, we have to teach it. The mapping is similar to the Amersfoort projection (Sec. XI.4), coded `sterea`. The reference is the BESSEL ellipsoid, on which the regional datum HD1863 is based, whose placement was calculated by TIMÁR using both three and seven parameters. We use the latter parameter set because it gives a more accurate result. The latitude and longitude of the midpoint Gellérthegy can be found in the literature, the false easting and northing are 500 km. From this, the required definition in format PROJ.4:

```
+proj=sterea +lat_0=47d29'9.6380" +lon_0=19d3'7.5533"
+k=1 +x_0=500000 +y_0=500000 +ellps=bessel +towgs84=595.75,
121.09,515.50,8.2270,-1.5193,-5.0121,-2.6729 +units=m
+no_defs
```

By typing this into the QGIS custom projection dialogue box, the georeferencing can be done (Fig. XVII.5). In the example, a map in the Budapest stereographic system was transformed into the Pseudo Mercator projection for comparison to the OpenStreetMap database. Since the horizontal position of the more accurately measured inhabited areas is the same on both maps, the slightly different roads are due to inaccuracies and drawing errors of the topographic survey. Our georeferencing, therefore, achieved the desired accuracy.

XVII.4 Georeferencing

When georeferencing a map, the GIS software will usually ask you, after selecting the control points, which method to use to calculate the projected

* A grid shift (Sec. VI.4) could be set with the parameter `+nadgrids`.

XVII. Applied theory of map projections

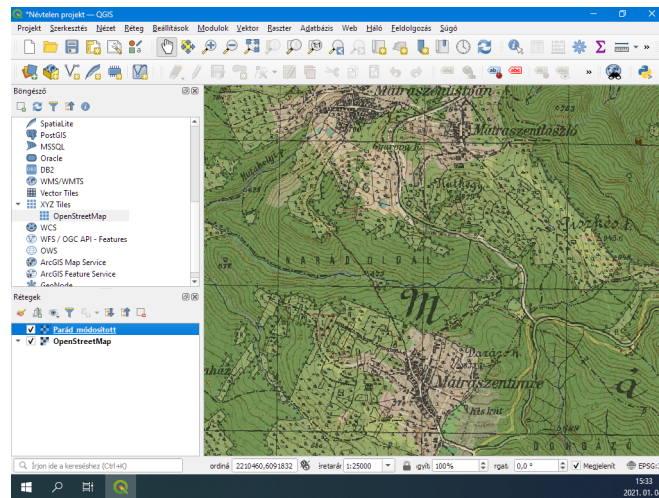


Figure XVII.5: Comparison of OSM and an old topographic map

coordinates of the other points. Unfortunately, the nomenclature of the methods is not intuitive. Let us denote the pixel coordinates of the image by x, y and the corresponding projected coordinates by x', y' !

The method called linear *in GIS* does not resample the image, but only writes the spatial resolution. This corresponds to the equations $x' = ax + b$ and $y' = cy + d$. This only gives acceptable results if the map is not rotated, so it is only good for digital (not for scanned) maps. It requires two control points. For scanned maps, the map sheet is usually rotated, so this must be taken into account. This is what the *HELMERT transform* is for:

$$\begin{aligned} x' &= px + qy + c \\ y' &= -qx + py + d \end{aligned}$$

Here, c and d are the translations, and if the angle of rotation is δ and the scaling factor is s , then $p = s \cos \delta$ and $q = s \sin \delta$. This method also requires at least two control points. This is a similarity, so it preserves angles and straight lines.

If, for example, the paper of an old map sheet has a different stretch in the direction of fibres than perpendicular to it, similarity will not give a good result. A transformation called linear *in mathematics*, which is called Polynomial₁ in QGIS, and Affine in Global Mapper and ArcGIS, scales differently depending on the direction. It requires three control points, is not conformal, but preserves the parallel straight lines:

$$\begin{aligned} x' &= a_1x + a_2y + a_0 \\ y' &= b_1x + b_2y + b_0 \end{aligned}$$

XVII. Applied theory of map projections

In aerial photography, it happens that the camera angle is skew, this is corrected by the *projective transform*. GlobalMapper lacks it, but other programs know it. It also preserves straight lines, but angles and parallel lines are lost. Formulæ for this method, which requires at least four control points:

$$x' = \frac{a_1x + a_2y + a_0}{c_1x + c_2y + 1}$$
$$y' = \frac{b_1x + b_2y + b_0}{c_1x + c_2y + 1}$$

If the projection of the georeferenced map cannot be determined in any way, it is possible to estimate coordinates using higher degree polynomials. This will be expanded in Sec. [XVIII.3](#).

Lesson eighteen

Transformations between reference systems

XVIII.1 Transform via the reference frame

We are given a point in a coordinate system. How can we find the same point in a different coordinate system? It is inaccurate but quick to read if you have a map with both systems printed. In multi-zone systems of projections, the coordinates of the neighbouring zone are often indicated on the map frame by ticks near the zone boundaries to speed up the calculation.

The applicability of the more accurate methods depends on whether the two projections use the same or different reference frames (Fig. XVIII.1). In the case of the same base surface, reprojection can be performed exactly. The projected coordinates are transformed back to the reference frame using the *inverse* formulæ of the projection, and then the mapped point in the second system is obtained using the formulæ of the other projection. This method can be applied, for example, between the zones of the GAUSS-KRÜGER projection. It is also appropriate between UTM zones and UPS. It is important that the reference frame is the same, so you cannot convert from UTM to GK, for example.

For different reference frames, only approximate methods can be used. In this case, it still makes sense to calculate the coordinates on the reference frame, but the difference between the two datums must be corrected by a MOLODENSKIY or HELMERT transform (Sec. VI.4). The parameters of the transformations can be determined on the basis of control points whose coordinates and heights above the ellipsoid are known for both datums. The MOLODENSKIY transform, which gives an accuracy of about 5-20 m, requires a single control point, whereas the HELMERT transform, which typically gives an accuracy of 0.5-2 m, requires at least three such points. Therefore, despite the lower accuracy, the 3 parameter method of MOLODENSKIY is still popular today, and even has an abridged formula that does not require the calculation of 3D Cartesian coordinates. Another, less popular method

XVIII. Transformations between reference systems

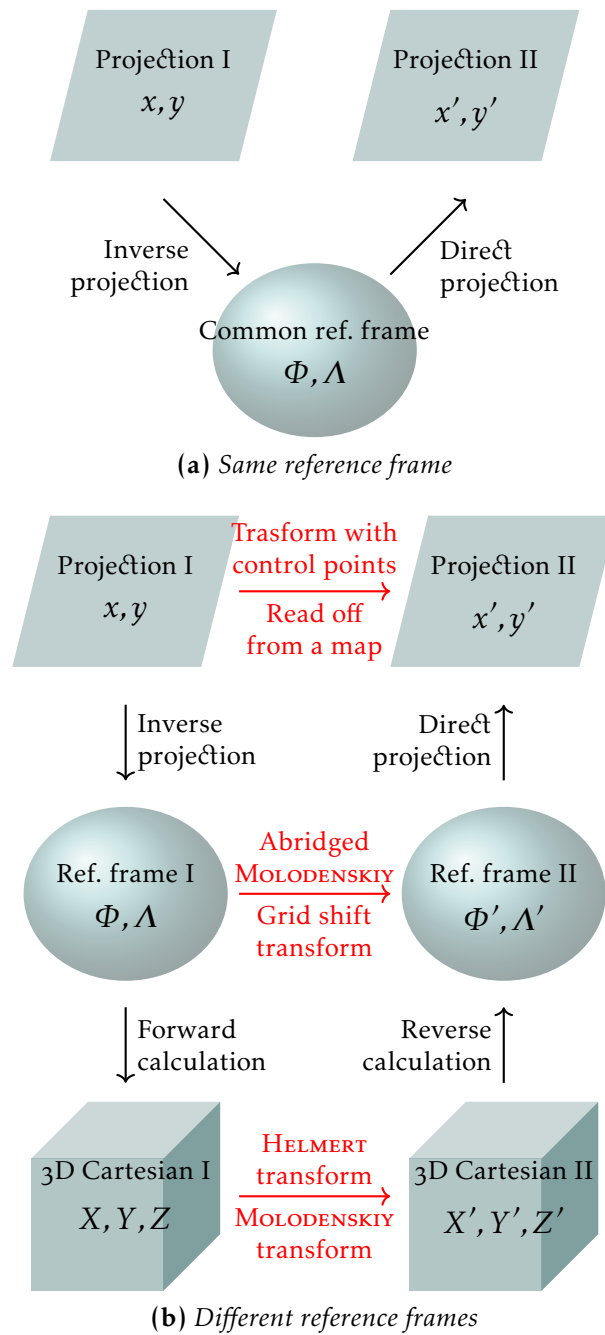


Figure XVIII.1: Possible transforms between coordinate systems

XVIII. Transformations between reference systems

uses a *grid shift* raster to store the local differences between the geographic coordinates.

XVIII.2 Transform with control points

Since it is not possible to convert between two different datums in a standard way, the question arises whether the new coordinates x', y' can be estimated directly from the old coordinates x, y using a pair of functions $x'(x, y)$ and $y'(x, y)$. Suppose that the new coordinate depends almost linearly on the old one:

$$\begin{aligned}x' &= a + bx + cy \\y' &= d + ex + fy\end{aligned}$$

We have six unknown parameters denoted by a to f . Each control point known in both systems yields two equations according to the relation above. So we need six equations, or three control points. For now, let us write down only the three equations for coordinate x' :

$$\begin{aligned}x'_1 &= a + bx_1 + cy_1 \\x'_2 &= a + bx_2 + cy_2 \\x'_3 &= a + bx_3 + cy_3\end{aligned}$$

This is a system of linear equations in three variables, which can be solved by any standard method:

$$\begin{pmatrix} 1 & x_1 & y_1 \\ 1 & x_2 & y_2 \\ 1 & x_3 & y_3 \end{pmatrix} \begin{pmatrix} a \\ b \\ c \end{pmatrix} = \begin{pmatrix} x'_1 \\ x'_2 \\ x'_3 \end{pmatrix}$$

From the equations containing y' , the remaining three coefficients can be derived in the same way:

$$\begin{pmatrix} 1 & x_1 & y_1 \\ 1 & x_2 & y_2 \\ 1 & x_3 & y_3 \end{pmatrix} \begin{pmatrix} d \\ e \\ f \end{pmatrix} = \begin{pmatrix} y'_1 \\ y'_2 \\ y'_3 \end{pmatrix}$$

Now, for any new pair x, y , we can estimate the coordinate pair x', y' using the previous parameters, marking the estimated coordinates with a hat:

$$\begin{aligned}\hat{x}' &= a + bx + cy \\ \hat{y}' &= d + ex + fy\end{aligned}$$

And what can we do if we have more than three control points? Then we can take into account the higher degree terms in the original coordinates

XVIII. Transformations between reference systems

x, y . Calculating up to n^{th} degree terms, we first compute only coordinate x' (assuming that x' is a smooth function of x and y):

$$x' = a_{00} + a_{10}x + a_{01}y + a_{20}x^2 + a_{11}xy + a_{02}y^2 + \dots = \sum_{i=0}^n \sum_{j=0}^{n-i} a_{ij}x^i y^j$$

Expanding the sums, we see that there are $m = (n+1)(n+2)/2$ unknown coefficients a_{ij} , so we need this number of control points. So we can use 6 control points for the second degree, 10 for the third degree and 15 for the fourth degree approximation. Increasing the number of powers improves accuracy for a while, but you cannot get blood out of a turnip: very high-degree polynomials may bend suddenly, and the measurement errors in our dataset can be magnified to an unintended extent. In general, it makes sense to go up till the fourth degree, which alone can provide a very good accuracy of decimetres over a part of a country. The solution for coefficients a_{ij} is provided by a linear system of equations:

$$\begin{pmatrix} 1 & x_1 & y_1 & x_1^2 & x_1 y_1 & \dots & y_1^n \\ 1 & x_2 & y_2 & x_2^2 & x_2 y_2 & \dots & y_2^n \\ 1 & x_3 & y_3 & x_3^2 & x_3 y_3 & \dots & y_3^n \\ 1 & x_4 & y_4 & x_4^2 & x_4 y_4 & \dots & y_4^n \\ 1 & x_5 & y_5 & x_5^2 & x_5 y_5 & \dots & y_5^n \\ \vdots & \vdots & \vdots & \vdots & \vdots & \ddots & \vdots \\ 1 & x_m & y_m & x_m^2 & x_m y_m & \dots & y_m^n \end{pmatrix} \begin{pmatrix} a_{00} \\ a_{10} \\ a_{01} \\ a_{20} \\ a_{11} \\ \vdots \\ a_{0n} \end{pmatrix} = \begin{pmatrix} x'_1 \\ x'_2 \\ x'_3 \\ x'_4 \\ x'_5 \\ \vdots \\ x'_m \end{pmatrix}$$

The other coordinate can be described by a similar formula:

$$y' = b_{00} + b_{10}x + b_{01}y + b_{20}x^2 + b_{11}xy + b_{02}y^2 + \dots = \sum_{i=0}^n \sum_{j=0}^{n-i} b_{ij}x^i y^j$$

The coefficients b_{ij} can be obtained from the same control points by substituting b_{ij} for a_{ij} and y'_i for x'_i in the system of equations. This procedure is called the *polynomial transformation*.

XVIII.3 The method of least squares

It is rare that we have exactly 3, 6, 10, or 15 control points. In such cases, we can make some sort of selection, for example, we can discard the most outlying measurements, but we may also try to get an average set of parameters taking all our points into account. Assume that our points are

XVIII. Transformations between reference systems

subject to *normally distributed* errors!* In this case, the maximum likelihood parameter set a_{ij} is provided by the *method of least squares*. Let x' be the actual coordinate x in the new system, \hat{x}' the estimated one!

We want to obtain the estimated values such that the error of the estimate for our m number of control points is minimal. We define the error of the estimate by squaring the difference between the actual coordinate x'_k of the k^{th} control point and the coordinate \hat{x}'_k estimated by the transformation (the absolute value is not apt because it is not differentiable), and then summing them for each point:

$$\sum_{k=1}^m (\hat{x}'_k - x'_k)^2 \rightarrow \min$$

The above expression is minimal if its derivative with respect to all a_{ij} is zero:

$$\begin{aligned} \frac{\partial \sum_{k=1}^m (\hat{x}'_k - x'_k)^2}{\partial a_{ij}} &= \sum_{k=1}^m 2(\hat{x}'_k - x'_k) \frac{\partial \hat{x}'_k}{\partial a_{ij}} = 0 \\ \sum_{k=1}^m \hat{x}'_k x_k^i y_k^j &= \sum_{k=1}^m x'_k x_k^i y_k^j \\ \sum_{k=1}^m (a_{00} + a_{10}x_k + a_{01}y_k + \dots) x_k^i y_k^j &= \sum_{k=1}^m x'_k x_k^i y_k^j \\ a_{00} \sum_{k=1}^m x_k^i y_k^j + a_{10} \sum_{k=1}^m x_k^{i+1} y_k^j + a_{01} \sum_{k=1}^m x_k^i y_k^{j+1} + \dots &= \sum_{k=1}^m x'_k x_k^i y_k^j \end{aligned}$$

We have a linear system of equations for a_{ij} -s, since i and j can take any value. The system of equations to be solved in the form of a matrix equation:

$$\begin{pmatrix} m & \sum x_k & \sum y_k & \sum x_k^2 & \sum x_k y_k & \dots & \sum y_k^n \\ \sum x_k & \sum x_k^2 & \sum x_k y_k & \sum x_k^3 & \sum x_k^2 y_k & \dots & \sum x_k y_k^n \\ \sum y_k & \sum x_k y_k & \sum y_k^2 & \sum x_k^2 y_k & \sum x_k y_k^2 & \dots & \sum y_k^{n+1} \\ \sum x_k^2 & \sum x_k^3 & \sum x_k^2 y_k & \sum x_k^4 & \sum x_k^3 y_k & \dots & \sum x_k^2 y_k^n \\ \sum x_k y_k & \sum x_k^2 y_k & \sum x_k y_k^2 & \sum x_k^3 y_k & \sum x_k^2 y_k^2 & \dots & \sum x_k y_k^{n+1} \\ \vdots & \vdots & \vdots & \vdots & \vdots & \ddots & \vdots \\ \sum y_k^n & \sum x_k y_k^n & \sum y_k^{n+1} & \sum x_k^2 y_k^n & \sum x_k y_k^{n+1} & \dots & \sum y_k^{2n} \end{pmatrix} \begin{pmatrix} a_{00} \\ a_{10} \\ a_{01} \\ a_{20} \\ a_{11} \\ \vdots \\ a_{0n} \end{pmatrix} = \begin{pmatrix} \sum x'_k \\ \sum x'_k x_k \\ \sum x'_k y_k \\ \sum x'_k x_k^2 \\ \sum x'_k x_k y_k \\ \vdots \\ \sum x'_k y_k^n \end{pmatrix}$$

By writing b_{ij} instead of a_{ij} and y'_k instead of x'_k , coordinate y can be estimated in the same way using the expressions \hat{x}'_k in terms of b_{ij} . This

* The measurement errors are indeed usually approximately normally distributed after the systematic errors are removed.

XVIII. Transformations between reference systems

method slightly improves the achievable accuracy, but the accuracy of the transformation is greatly degraded in the case of outliers with erroneous values.

Although often more accurate than traditional datum transformations, GIS systems do not usually support control point transforms between projections, but only during georeferencing, which is typically implemented using the least squares method described here, even though higher degree polynomials would make sense primarily for conversions between different projections.

In the case of the *HELMERT transform* as described in Sec. XVII.4, the formulæ for x' and y' already have common coefficients, so the least squares minimization for the two coordinates must be done simultaneously. (Note that we have two equations for each point, so the four unknowns require at least two control points.)

$$\sum_{k=1}^m (\hat{x}'_k - x'_k)^2 + (\hat{y}'_k - y'_k)^2 \rightarrow \min$$

Where:

$$\begin{aligned}\hat{x}' &= px + qy + a \\ \hat{y}' &= -qx + py + b\end{aligned}$$

Derived with respect to parameter $t \in \{a, b, p, q\}$:

$$\frac{\partial \sum_{k=1}^m (\hat{x}'_k - x'_k)^2 + (\hat{y}'_k - y'_k)^2}{\partial t} = \sum_{k=1}^m 2 \left[(\hat{x}'_k - x'_k) \frac{\partial \hat{x}'_k}{\partial t} + (\hat{y}'_k - y'_k) \frac{\partial \hat{y}'_k}{\partial t} \right] = 0$$

From this, substituting each of the four parameters for t gives four equations:

$$\begin{aligned}\sum_{k=1}^m (px_k + qy_k + a - x'_k) \mathbf{1} &= 0 \\ \sum_{k=1}^m (-qx_k + py_k + b - y'_k) \mathbf{1} &= 0 \\ \sum_{k=1}^m (px_k + qy_k + a - x'_k) x_k + (-qx_k + py_k + b - y'_k) y_k &= 0 \\ \sum_{k=1}^m (px_k + qy_k + a - x'_k) y_k + (-qx_k + py_k + b - y'_k) (-x_k) &= 0\end{aligned}$$

XVIII. Transformations between reference systems

Expanding the parentheses and rearranging into a linear system of equations:

$$\begin{pmatrix} m & 0 & \sum x_k & \sum y_k \\ 0 & m & \sum y_k & \sum -x_k \\ \sum x_k & \sum y_k & \sum x_k^2 + y_k^2 & 0 \\ \sum y_k & \sum -x_k & 0 & \sum x_k^2 + y_k^2 \end{pmatrix} \begin{pmatrix} a \\ b \\ p \\ q \end{pmatrix} = \begin{pmatrix} \sum x'_k \\ \sum y'_k \\ \sum x'_k x_k + y'_k y_k \\ \sum x'_k y_k - y'_k x_k \end{pmatrix}$$

The former transformation has the important advantage of being a similarity transform, i.e. it preserves angles, but it is of little use for a conversion between two different conformal projections because it does not model the areal distortion that varies from place to place. The polynomial transformation is flexible for our area, but it distorts the angles between the two systems. The advantages of both methods are combined in the *complex polynomial transformation*, which is based on considering the planar coordinates as the real and imaginary parts of a so-called *complex number*, i.e. we introduce the notations $z = y + ix$ and $z' = y' + ix'$, where $i^2 = -1$. From the analysis of complex numbers, it is known that the conformality of the transformation implies the differentiability of the function $z'(z)$, and, vice versa, that differentiable complex functions are conformal (Sec. XXIX.1). Therefore, a relation between two arbitrary conformal projections can be established by a differentiable function $\mathbb{C} \rightarrow \mathbb{C}$, which can be approximated to any precision by a polynomial:

$$\hat{z}' = a_0 + a_1 z + a_2 z^2 + a_3 z^3 + \dots = \sum_{i=0}^n a_i z^i$$

If we require $\sum (\hat{z}'_k - z'_k)^2$ to be minimal for our control points, we obtain the linear system of equations below, which requires at least $n + 1$ control points for an n^{th} degree approximation. Since both the unknowns and the coefficients are complex numbers, it is important to implement the algorithm in an environment that is capable of dealing with complex numbers, such as the Python programming language.

$$\begin{pmatrix} m & \sum z_k & \sum z_k^2 & \dots & \sum z_k^n \\ \sum z_k & \sum z_k^2 & \sum z_k^3 & \dots & \sum z_k^{n+1} \\ \sum z_k^2 & \sum z_k^3 & \sum z_k^4 & \dots & \sum z_k^{n+2} \\ \vdots & \vdots & \vdots & \ddots & \vdots \\ \sum z_k^n & \sum z_k^{n+1} & \sum z_k^{n+2} & \dots & \sum z_k^{2n} \end{pmatrix} \begin{pmatrix} a_0 \\ a_1 \\ a_2 \\ \vdots \\ a_n \end{pmatrix} = \begin{pmatrix} \sum z'_k \\ \sum z'_k z_k \\ \sum z'_k z_k^2 \\ \vdots \\ \sum z'_k z_k^n \end{pmatrix}$$

In the practice of GIS, coordinates are most often transformed back to the reference frame, then into 3D Cartesian coordinates, and finally from

XVIII. Transformations between reference systems

this the 3D Cartesian coordinates are estimated for the other datum. A major difficulty of this method is that it requires the ellipsoidal height of the control points. The simplest is the *MOLODENSKIY transform*, which is, in fact, just a translation:

$$\begin{pmatrix} x' \\ y' \\ z' \end{pmatrix} = \begin{pmatrix} \Delta x \\ \Delta y \\ \Delta z \end{pmatrix} + \begin{pmatrix} x \\ y \\ z \end{pmatrix}$$

From the equation above, it follows directly that the value of the parameters $\Delta x, \Delta y, \Delta z$ for one control point is the difference between the coordinates of the point in the two systems. By the method of least squares, the average of these coordinate differences becomes the value of the parameters for several control points.

The more complex *HELMERT transform in three dimensions* (sometimes referred to as *BURŠA–WOLF transform*) also takes into account three rotation parameters and one scaling parameter. Since the angles of rotation $\sigma_x, \sigma_y, \sigma_z$ are small, we use the approximations $\sin \sigma \approx \widehat{\sigma}$, $\cos \sigma \approx 1$, and $\sigma_i \sigma_j \approx 0$. Then the product of the rotation matrices is:

$$\begin{aligned} & \begin{pmatrix} 1 & 0 & 0 \\ 0 & \cos \sigma_x & \sin \sigma_x \\ 0 & -\sin \sigma_x & \cos \sigma_x \end{pmatrix} \begin{pmatrix} \cos \sigma_y & 0 & -\sin \sigma_y \\ 0 & 1 & 0 \\ \sin \sigma_y & 0 & \cos \sigma_y \end{pmatrix} \begin{pmatrix} \cos \sigma_z & \sin \sigma_z & 0 \\ -\sin \sigma_z & \cos \sigma_z & 0 \\ 0 & 0 & 1 \end{pmatrix} \\ & \approx \begin{pmatrix} 1 & 0 & 0 \\ 0 & 1 & \widehat{\sigma}_x \\ 0 & -\widehat{\sigma}_x & 1 \end{pmatrix} \begin{pmatrix} 1 & 0 & -\widehat{\sigma}_y \\ 0 & 1 & 0 \\ \widehat{\sigma}_y & 0 & 1 \end{pmatrix} \begin{pmatrix} 1 & \widehat{\sigma}_z & 0 \\ -\widehat{\sigma}_z & 1 & 0 \\ 0 & 0 & 1 \end{pmatrix} \\ & \approx \begin{pmatrix} 1 & 0 & 0 \\ 0 & 1 & \widehat{\sigma}_x \\ 0 & -\widehat{\sigma}_x & 1 \end{pmatrix} \begin{pmatrix} 1 & \widehat{\sigma}_z & -\widehat{\sigma}_y \\ -\widehat{\sigma}_z & 1 & 0 \\ \widehat{\sigma}_y & 0 & 1 \end{pmatrix} \approx \begin{pmatrix} 1 & \widehat{\sigma}_z & -\widehat{\sigma}_y \\ -\widehat{\sigma}_z & 1 & \widehat{\sigma}_x \\ \widehat{\sigma}_y & -\widehat{\sigma}_x & 1 \end{pmatrix} \end{aligned}$$

The scaling then is a multiplication by a scalar, while the translation adds the corresponding vector:

$$\begin{pmatrix} x' \\ y' \\ z' \end{pmatrix} = \begin{pmatrix} \Delta x \\ \Delta y \\ \Delta z \end{pmatrix} + (1 + s) \begin{pmatrix} 1 & \widehat{\sigma}_z & -\widehat{\sigma}_y \\ -\widehat{\sigma}_z & 1 & \widehat{\sigma}_x \\ \widehat{\sigma}_y & -\widehat{\sigma}_x & 1 \end{pmatrix} \begin{pmatrix} x \\ y \\ z \end{pmatrix}$$

It can be seen that for the determination of the seven unknowns, we have three equations for each control point, but even for three control points the system of equations becomes overdetermined, so the calculation of the parameters is only possible by estimation, e.g. by the method of least

XVIII. Transformations between reference systems

squares. After substituting $a = (1 + s)\widehat{\sigma}_x$, $b = (1 + s)\widehat{\sigma}_y$, $c = (1 + s)\widehat{\sigma}_z$, and $d = 1 + s$ and avoiding the very lengthy derivation:

$$\begin{pmatrix} m & 0 & 0 & 0 & \sum -z_k & \sum y_k & \sum x_k \\ 0 & m & 0 & \sum z_k & 0 & \sum -x_k & \sum y_k \\ 0 & 0 & m & \sum -y_k & \sum x_k & 0 & \sum z_k \\ 0 & \sum z_k & \sum -y_k & \sum y_k^2 + z_k^2 & \sum -x_k y_k & \sum -x_k z_k & 0 \\ \sum -z_k & 0 & \sum x_k & \sum -x_k y_k & \sum x_k^2 + z_k^2 & \sum -y_k z_k & 0 \\ \sum y_k & \sum -x_k & 0 & \sum -x_k z_k & \sum -y_k z_k & \sum x_k^2 + y_k^2 & 0 \\ \sum x_k & \sum y_k & \sum z_k & 0 & 0 & 0 & \sum x_k^2 + y_k^2 + z_k^2 \end{pmatrix} \begin{pmatrix} \Delta x \\ \Delta y \\ \Delta z \\ a \\ b \\ c \\ d \end{pmatrix} = \begin{pmatrix} \sum x'_k \\ \sum y'_k \\ \sum z'_k \\ \sum y'_k z_k - z'_k y_k \\ \sum z'_k x_k - x'_k z_k \\ \sum x'_k y_k - y'_k x_k \\ \sum x'_k x_k + y'_k y_k + z'_k z_k \end{pmatrix}$$

Tab. XVIII.1 shows the parameter set of transformations in Hungary from some datums to the WGS84 one. Be careful, because in this lecture notes the coordinate frame has been rotated, but some GIS software rotate the position vector of the point instead. In such a case, the signs of the rotations must be reversed! The inverse transformation can be approximated well by inverting the sign of each parameter.

Table XVIII.1: Datum parameters for Hungary

Datum	Δx (m)	Δy (m)	Δz (m)	σ_x (")	σ_y (")	σ_z (")	s (ppm)
HD72	52.684	-71.194	-13.975	0.3120	0.1063	0.3729	1.0191
S42/83	-5.38	-91.75	-86.23	-0.988	-0.700	0.652	2.273
S42/58	17.20	-84.03	-60.97	-1.085	-0.682	0.473	-3.185
RDN1940	566.54	108.25	487.93	-2.2867	-2.6409	1.5194	-0.7365
HD1863	595.75	121.09	515.50	-8.2260	1.5193	5.0121	-2.6729

Third module

Non-conical map projections

Lesson nineteen

Theory of non-conical projections

XIX.1 The shape of the graticule

Recall from Sec. VI.6 that conical projections satisfy all the following properties:

- The mapped meridians are parallel or concurrent straight lines.
- Parallels are mapped to concentric circles, arcs of circles or parallel straight lines.
- Mapped graticule lines are perpendicular everywhere.
- Meridians divide the mapped parallels evenly.

If at least one of the conditions in the list above is not met, a *non-conical projection* is obtained. These projections are divided into subgroups according to the mapped image of the graticule. In contrast to conical projections, in non-conical projections, we do not always require the concentricity of the mapped parallels. They must only satisfy our general expectation that map projections are bijective mappings. It only follows that the mapped parallels must not intersect. For this reason, if our projection still has concentric parallels, we consider them special, and use the prefix *pseudo-* for their families. Mappings with non-concentric circular parallels will be denoted by the prefix *poly-* (Fig. XIX.1):

- If the mapped parallels are complete concentric circles, our projection is *pseudoazimuthal*. A *polyazimuthal* mapping is similar but its parallels are not concentric.
- Among *pseudoconic* projections, the parallels are mapped into concentric arcs of circles. Projections with non-concentric parallels are called *polyconic*, but some of them may also be grouped as *pseudopolyconic* (the distinction between these two groups is discussed in Sec. XXVI.1).
- If the mapped parallels are parallel straight lines, then we speak of a *pseudocylindrical* mapping.
- Projections that do not belong to any of the above groups are called *miscellaneous* projections.

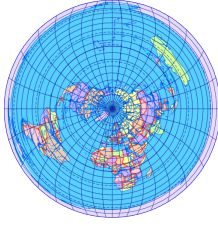
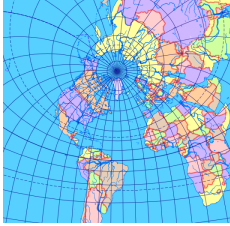
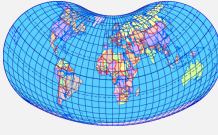

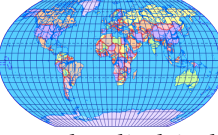
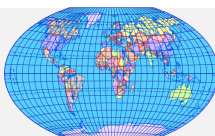
Parallels	Concentric	Non-concentric
Circles	 Pseudoazimuthal	 Polyazimuthal
Arcs	 Pseudoconic	 (Pseudo)polyconic
Straight	 Pseudocylindrical	—
Other	 Miscellaneous	

Figure XIX.1: Classification of non-conical projections according to the shape of the graticule

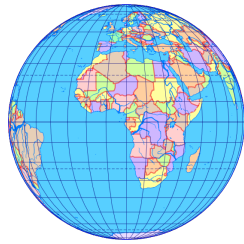
Since the perpendicularity of the mapped graticule is not required among non-conical projections, mappings with perpendicular graticule are identified as *rectangular*. This corresponds to the statement $\cot \vartheta = 0$ and can be easily checked using the projection formulæ (Sec. VII.2). As an example, the polyazimuthal projection shown in Fig. XIX.1 is also rectangular. Not all families of non-conical projections include rectangular mappings.

It is very important to note, in order to avoid ambiguities, that our classification is strictly for projections in the *normal* aspect. Let us look at Fig. XIX.2. Although projections (a) and (c) seem to be non-conical maps, they are in fact rotated aspects of conical projections (b) and (d).

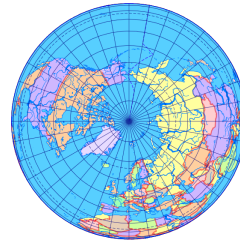
XIX.2 Seven aspects of a non-conical projection

This brings us to the question of the graticule rotation. Fig. XIX.3 shows the MOLLWEIDE projection using different rotations. The longitude of the

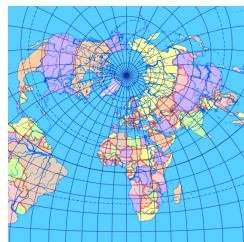
XIX. Theory of non-conical projections



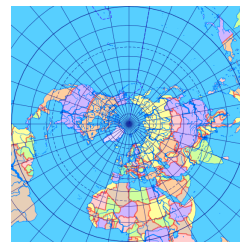
(a) Is this a pseudocylindrical map?



(b) Rather transverse orthographic!



(c) Is this a polyazimuthal map?



(d) Rather oblique stereographic!

Figure XIX.2: Conical or non-conical?

metapole λ_0 is uniform because it does not affect the image of the graticule. For conical projections, it is always assumed that the prime meridian passes through one of the poles. We could use this simplification because conical projections are rotationally symmetric, changing the prime meridian only rotates or shifts the image of the grid. In contrast, non-conical projections behave quite differently with respect to the rotation of the graticule. Canadian geodesist WRAY published these findings in 1974.*

No special phenomenon is observed in the *normal* aspect of the projection. Although the prime meridian has been changed, the mapped graticule has not. We would expect to see the same when the metapole is rotated to the Equator. But the graticule is significantly altered by the different placement of the prime meridian. Therefore, in the case $\varphi_0 = 0^\circ$, we

* The areas of more favourable distortion can be rotated to arbitrary areas in this way, just like with conical projections. Yet in practice, we almost never encounter such a projection. One reason for this is that non-conical projections give a rather unusual image when rotated. Unfortunately, another important aspect is that the literature today still often misinterprets the aspects of projections. Instead of rotating the graticule, they are typically defined by the placement of a cone or cylinder compared to a sphere, although this definition is already unintelligible in the context of non-perspective conical projections. How do we rotate the cylinder in MERCATOR projection if no cylinder is used in the derivation? This is precisely why, with this concept, the rotation of non-conical projections cannot be explained intuitively. Here is another reason why we defined cylindrical projections not by projecting onto a cylinder, but by the shape of mapped parallels.

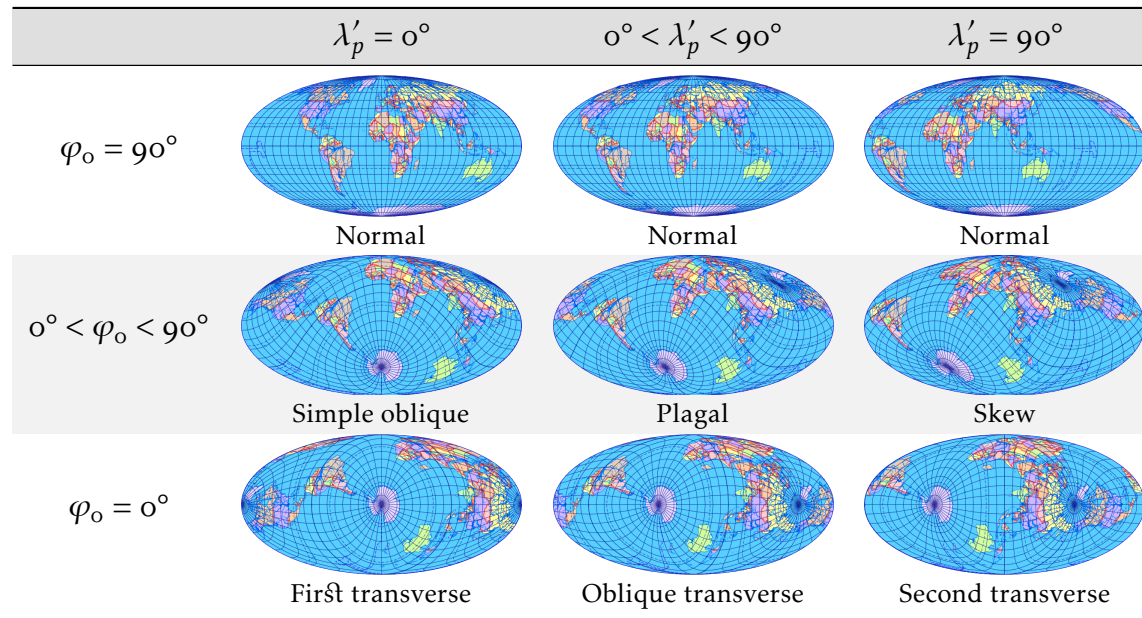


Figure XIX.3: *The MOLLWEIDE projection in different aspects*

distinguish between three aspects. In the *first transverse* one, the one of the poles is located on the vertical axis of symmetry; in the *second transverse* one, the two poles are equally far away from the axis of symmetry. In the *oblique transverse* aspect, the projection has no vertical axis of symmetry.

We can describe this formally by subtracting a prime metalongitude λ'_p from the metalongitude λ' in the projection, and thus our *prime metameridian* encloses this spherical angle λ'_p with the metameridian through the geographic pole (Fig. XIX.4)*. In the first case $\lambda'_p = 0^\circ$, in the second case $\lambda'_p = \pm 90^\circ$, while in the general case it is any other value.

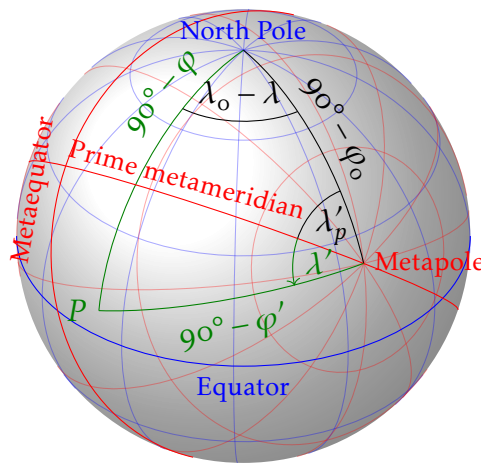


Figure XIX.4: Prime metameridian in plagal aspect

We see similar results when the metapole is placed neither on the Equator nor at the pole, but somewhere else. In this case, if one of the poles is on the vertical axis of symmetry, then our aspect is *simple oblique* ($\lambda'_p = 0^\circ$), if $\lambda'_p = \pm 90^\circ$, then it is *skew* (some projections have central symmetry in this aspect). If neither of these special cases is fulfilled, then we speak of a *plagal* aspect based on the Greek word plagios, which means oblique.

Returning to Fig. XIX.2, we find an interesting problem. For example, if we forget that projection (a) is a transverse orthographic one, we might easily think that we are dealing with a normal aspect pseudocylindrical projection. Considering the mapping (a) as a map projection in its own right, its first transverse aspect would just reproduce the graticule (b). Now then, can (a) be considered as a normal and (b) as a first transverse aspect

* What we are really saying here is that any arbitrary spatial rotation of any object can be described by three angles. Here, the spatial rotation of the graticule is given by the coordinates φ_0 and λ_0 of the metapole and the prime metameridian λ'_p

of a pseudocylindrical map? Not at all, since they are rather the aspects of an azimuthal map. WRAY gave two rules of thumb for such cases:

- The normal aspect of a projection is always the one, in which the projection formulæ can be reduced to a simpler form. The mapping (b) can be defined by the equation $\rho = R \sin \delta$, while mapping (a) requires longer expressions.
- Among the possible aspects of a projection, the one, in which the mapped graticule has the largest degree of symmetry, is always considered normal. The graticule (a) is symmetric only about the vertical and horizontal axes, while projection (b) has complete rotational symmetry.

Of course, these rules of thumb do not always give clear results. For example, none of the normal, first and second transverse aspects of the LITTELOW projection (Sec. XXVII.1) have simpler formulæ and none of them exhibit greater symmetry. In such a case, we are forced to consider the first described form of the projection as the normal aspect.

XIX.3 Map distortions

The distortions of non-conical projections are essentially determined by whether their graticule is rectangular. Since all conformal projections are also rectangular, conformal mappings are found only among rectangular projections. Thus, the equations $\cot \vartheta = 0$ and $h = k$ must be satisfied simultaneously to speak of conformal projections. For this reason, for a long time only a few conformal maps were found among non-conical projections. However, among miscellaneous projections, a clever modification of the conformality condition leads to a variety of conformal mappings (see Sec. XXIX.1). Nevertheless, it is safe to say that conformal non-conical projections are almost never encountered in practice.

In the case of rectangular projections, $\sin \vartheta = 1$, so the formula for areal scale is still $p = hk$ *. However, in other non-conical projections, the graticule lines are not principal directions of the mapping, so the maximal and minimal linear scales a and b do not correspond to the linear scale along the graticule lines. In this case, we have to use the formula $p = ab = hk \sin \vartheta$. This is not much more complicated than the one of conical projections, so it is not difficult to find equal-area projections.

The linear scales of non-conical projections can be computed using the general formulæ of Tissot's distortion theory. Among aphyllactic conical projections, the mappings equidistant in meridians showed a balance in

* Map projections that are rectangular and equal-area at the same time are called *EULER projections*.

their angular and areal distortions, while among non-conical projections we find that we can balance the two types of distortion well in mappings with an equidistant central meridian.

XIX.4 Application of non-conical projections

The oldest known non-conical mapping is the PTOLEMY II projection, which is a pseudoconic projection. He created it to achieve lower distortion than in his conic one. Since then, many such mappings have been created. Many of them are more favourable than the conic projections, but only if they are used wisely.

For areas of extent less than 3500 km, it is easy to find conical projections, in which distortions are not detectable with the naked eye. In such cases, there is no point in bothering with the more complex non-conical projections unless our goal is engineering precision. Since in small-scale maps of large areas, the ~ 20 km difference between the sphere and the ellipsoid of revolution is typically below the cartographic accuracy of the map, the projections will be derived for a sphere as the reference frame. Only on old topographic maps should you expect to find a projection with a reference frame as an ellipsoid.

Note here that in the case where there is no ellipsoidal version of a mapping, the vast majority of GIS software simply drop the ellipsoidal coordinates into the spherical formulæ; exactly as we have seen with the Pseudo Mercator. QGIS very often inaccurately handles map projections also in this respect.

If we had done so now, specific distortions (e.g. conformality or equivalency) would have been lost, with noticeable errors at larger scales. On a world map, of course, this is not a problem. ArcGIS can be made to apply the correct auxiliary sphere (e.g. the authalic sphere for an equal-area mapping) to some projections in hidden, barely understandable menu items, and this is a fair solution. Using an auxiliary sphere, you can apply a non-conical projection at a larger scale, although the practical usefulness of this is questionable, since non-conical projections are rather applied at very small scales.

The distortions of conical projections are usually unacceptable for areas larger than a hemisphere. In such cases (unless the theme requires, for example, the elimination of meridian convergence, or you insist on a rectangular map frame), choose a non-conical projection! For a hemisphere (because of its circular shape), azimuthal projections are the best, and for continents and oceans, both conical and non-conical projections are suitable. For smaller areas, experience has shown that many non-conical

XIX. Theory of non-conical projections

mappings, although much better than traditional conical mappings, do not provide breakthrough improvements. Take care, as the correct choice of projections requires a great deal of expertise. It is not difficult to fall into the mistake of choosing a mapping with a less favourable distortion pattern than the conical projection recommended for that area.

When choosing a map projection, consider not only the theme of the map but also the target audience, and this is especially true for non-conical projections! A reader with better abstraction skills will have no difficulty in reading a more complex graticule, but printing a plagal aspect non-conical projection in a school atlas would be a bad prank. For a map intended for younger readers, or even for purely aesthetic reasons, consider using rectangular projections, which resemble the spherical graticule with its right angles. Note that the main advantage of rectangular projections is lost when the aspect is rotated!

Experience has shown that the interpretation of the pole-line is straightforward only for skilled readers. Avoid the use of flat-polar maps on educational world maps, but even for press maps, think before choosing a flat-polar projection for your world map! Flat-polar projections with more favourable distortions are acceptable for geographic atlases or thematic maps, and also feel free to use them on maps where the pole-line is outside the map frame.

Never use a flat-polar projection in a rotated aspect if the pole-line appears within the map frame. And if the pole-line is curved, absolutely do not! The reader can easily understand the reason for this based on Fig. XIX.5:

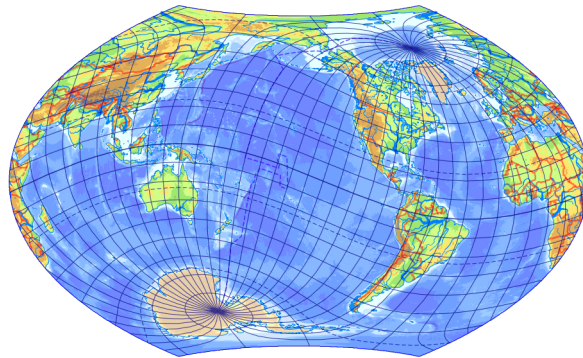


Figure XIX.5: *It has favourable distortions at most areas, yet not the best choice*

Lesson twenty

Earlier pseudocylindrical maps

XX.1 Distortions of pseudocylindricals

The projections, in which the images of the parallels are parallel straight lines, are called *pseudocylindrical projections*. In addition, we often expect the projection to be symmetric about the Equator. This already shows that this family of projections is used to represent large areas (e.g. the entire surface of the Earth, the Pacific Ocean) symmetric about the Equator. Pseudocylindrical projections map the spherical zones of the Earth onto horizontal bands, making them well suited for representing thematics depending on latitude (e.g. climate, vegetation cover). Pseudocylindrical mappings are further divided into the families of pseudocylindricals with sinusoidal, elliptical, circular, straight and other meridians, based on their characteristic shape of mapped meridians.

The vertical coordinate does not depend on the longitude and is of the form $y(\varphi)$, or in other words $\partial y/\partial \lambda = 0$. Due to symmetry, y is an odd, strictly increasing function. The horizontal coordinate depends on both parameters, is in the form of $x(\varphi, \lambda)$, it is an even function of φ and an odd, strictly increasing function of λ .

Compared to the general formulæ, k and $\cot \vartheta$ can be simplified by substituting $\partial y/\partial \lambda = 0$.

$$k = \frac{\sqrt{\left(\frac{\partial x}{\partial \lambda}\right)^2 + \left(\frac{\partial y}{\partial \lambda}\right)^2}}{R \cos \varphi} = \frac{1}{R \cos \varphi} \frac{\partial x}{\partial \lambda}$$
$$\cot \vartheta = \frac{\frac{\partial x}{\partial \varphi} \frac{\partial x}{\partial \lambda} + \frac{\partial y}{\partial \varphi} \frac{\partial y}{\partial \lambda}}{\frac{\partial y}{\partial \varphi} \frac{\partial x}{\partial \lambda} - \frac{\partial x}{\partial \varphi} \frac{\partial y}{\partial \lambda}} = \frac{\partial x}{\partial \varphi} \bigg/ \frac{\partial y}{\partial \varphi}$$

In rectangular projections, $\cot \vartheta = 0$, i.e. $\partial x/\partial \varphi = 0$. However, this would imply that the mapped meridians are vertical lines, so we would get into the family of cylindrical projections. Finally, we can state that *there is no rectangular pseudocylindrical, and hence conformal ones do not exist either*.

XX. Earlier pseudocylindrical maps

Let us recall the following formula from Sec. VII.3 and substitute $\partial y/\partial \lambda = 0$ into it!

$$p = \frac{\frac{\partial y}{\partial \varphi} \frac{\partial x}{\partial \lambda} - \frac{\partial x}{\partial \varphi} \frac{\partial y}{\partial \lambda}}{R^2 \cos \varphi} = \frac{1}{R^2 \cos \varphi} \frac{dy}{d\varphi} \frac{\partial x}{\partial \lambda}$$

We know that $p = hk \sin \vartheta$. Let us substitute the previously obtained formulæ for k and p into this to express the yet unknown h :

$$\frac{1}{R^2 \cos \varphi} \frac{dy}{d\varphi} \frac{\partial x}{\partial \lambda} = h \frac{1}{R \cos \varphi} \frac{\partial x}{\partial \lambda} \sin \vartheta$$

$$h = \frac{dy}{d\varphi} \frac{1}{R \sin \vartheta}$$

Is there an equal-area pseudocylindrical mapping? Let us examine the equation $p = 1$!

$$\frac{1}{R^2 \cos \varphi} \frac{dy}{d\varphi} \frac{\partial x}{\partial \lambda} = 1$$

$$\frac{\partial x}{\partial \lambda} = R^2 \frac{\cos \varphi}{\frac{dy}{d\varphi}}$$

Since on the right-hand side of the equation there are only functions of φ , it is clear that the derivative in the left-hand side is also independent of λ . If the derivative of x is constant with respect to λ , then x is a linear function of λ . To make practical use of it, we may say that *there exist equal-area pseudocylindrical projections, but the parallels of such mappings are always evenly divided by the mapped meridians (the parallels have constant scale).*

XX.2 Globular projections

With the great geographical discoveries, the world opened up and soon the first world atlases were published. The demand for world maps was immediate. At that time, contrary to recent negative trends, mapmakers knew that the MERCATOR projection was only suitable for navigational maps, so they sought other projections. The first non-conical projections showed the Earth divided into two hemispheres side-by-side in two maps. The hemisphere is circular when viewed from afar, so it is obvious to represent the map in a circular frame. Non-conical projections that represent the hemisphere in a circular contour are called *globular projections*.

The origin of the first globular projections is a matter of debate, but some sources claim that Arabic scholars had globular projections before

Europeans as early as around 1000 AD. At the dawn of the modern age, atlas makers tried to lower distortions with newer and newer graticule networks, of which there are countless variants. The parallels of some globular projections are mapped to arcs of circles, so in the modern classification they are more properly classified as pseudopolyconic projections (see Sec. XXVII.2). The globular projections have by now been superseded by transverse azimuthal projections of more favourable distortions patterns for hemisphere maps.

The two most common globular projections are named after APÍAN. In addition to the circular frame, they both have horizontal straight lines for parallels and equidistant Equator and central meridian. The first projection is probably the work of VESPUCCI, who identified America as a continent in the early 16th century. It uses circular meridians. The exact origin of the second projection is disputed, but it is likely not the development of APÍAN. It maps meridians to semi-ellipses.

The mapped meridians are therefore arcs of circles in the APÍAN I projection. Their centres are located on axis x due to symmetry. The equation of a circle centred at $(d, 0)$ (Fig. XX.1) is:

$$(x - d)^2 + y^2 = \rho^2$$

Since the Equator is equidistant, we must have $x = R\widehat{\lambda}$ on the horizontal axis (i.e., substituting $y = 0$):

$$\begin{aligned} (R\widehat{\lambda} - d)^2 &= \rho^2 \\ d &= R\widehat{\lambda} - \rho \end{aligned}$$

Because of the equidistant central meridian, the mapped image of the North Pole is at distance $R\pi/2$ from the mapped Equator. All arcs pass through the point of the Pole, so the equations of the circles must hold true for the substitution $x = 0$ and $y = R\pi/2$:

$$\begin{aligned} (-d)^2 + \left(R\frac{\pi}{2}\right)^2 &= \rho^2 \\ (\rho - R\widehat{\lambda})^2 + \left(R\frac{\pi}{2}\right)^2 - \rho^2 &= 0 \\ R^2\widehat{\lambda}^2 - 2R\widehat{\lambda}\rho + R^2\left(\frac{\pi}{2}\right)^2 &= 0 \\ \rho &= R\frac{\widehat{\lambda}^2 + \left(\frac{\pi}{2}\right)^2}{2\widehat{\lambda}} \end{aligned}$$

From the equidistant central meridian:

$$y = R\widehat{\varphi}$$

Substituting this and the equation $d = R\widehat{\lambda} - \rho$ back into the equation of the circle:

$$\begin{aligned} (x - R\widehat{\lambda} + \rho)^2 + (R\widehat{\varphi})^2 &= \rho^2 \\ x - R\widehat{\lambda} + \rho &= \pm \sqrt{\rho^2 - R^2\widehat{\varphi}^2} \\ x &= R\widehat{\lambda} - \rho \pm \sqrt{\rho^2 - R^2\widehat{\varphi}^2} \end{aligned}$$

The symmetry of the projection is guaranteed if the sign \pm is positive in the Eastern Hemisphere and negative in the Western Hemisphere. By calculating h , it can be concluded that the scale along parallels is not constant (Fig. XX.3), so the projection is certainly not equal-area.

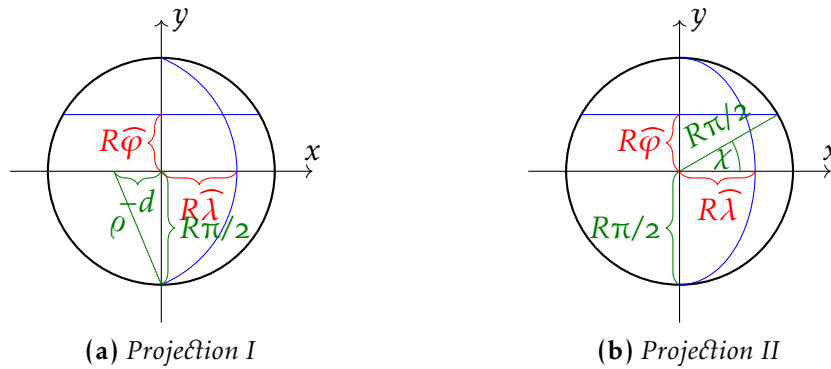


Figure XX.1: The construction of the APIAN projections

The meridians of the APIAN II projection are mapped to semi-ellipses, their semi-axes fall on the axes x and y . The vertical semi-axis of the ellipses is $R\pi/2$ due to the equidistant central meridian, and their horizontal semi-axis is $R\widehat{\lambda}$ due to the equidistant Equator. Thus, the equation of the ellipses is:

$$\frac{x^2}{(R\widehat{\lambda})^2} + \frac{y^2}{(R\frac{\pi}{2})^2} = 1$$

The central meridian is equidistant:

$$y = R\widehat{\varphi}$$

Substituting this back:

$$\frac{x^2}{R^2 \widehat{\lambda}^2} = 1 - \frac{R^2 \widehat{\varphi}^2}{R^2 \left(\frac{\pi}{2}\right)^2}$$

$$x = R \widehat{\lambda} \sqrt{1 - \left(\frac{2\widehat{\varphi}}{\pi}\right)^2}$$

Let us examine the distortions of the projection.

$$k = \frac{1}{R \cos \varphi} \frac{\partial x}{\partial \lambda} = \frac{1}{\cos \varphi} \sqrt{1 - \left(\frac{2\widehat{\varphi}}{\pi}\right)^2}$$

The parallels have therefore constant scale. Is the projection equal-area?

$$h = \frac{dy}{d\varphi} \frac{1}{R \sin \vartheta} = \frac{1}{\sin \vartheta}$$

$$\cot \vartheta = \frac{\partial x / \partial \varphi}{dy / d\varphi} = \frac{-4 \widehat{\lambda} \widehat{\varphi}}{\pi^2 \sqrt{1 - \left(\frac{2\widehat{\varphi}}{\pi}\right)^2}}$$

$p = hk \sin \vartheta \neq 1$, so the projection is *aphylactic*. As can be seen in Fig. XX.2, the projection is pointed-polar, but its pole does not have that cusped shape common to conical projections, but meridians have a more aesthetically pleasing smooth shape.

Globular projections are no longer used in modern cartography, but there are many derivatives of the APRIAN II projection, which are still popular today. These all have elliptic meridians, and we will get to know them during the module. For easier calculation of these derivative projections, we use a parameter χ instead of the latitude φ , which is defined by the equation $\sin \chi = 2\widehat{\varphi}/\pi$ as shown in Fig. XX.1. The projection formulæ then take the following simpler form:

$$x = R \widehat{\lambda} \sqrt{1 - \sin^2 \chi} = R \widehat{\lambda} \cos \chi$$

$$y = R \frac{\pi}{2} \sin \chi$$

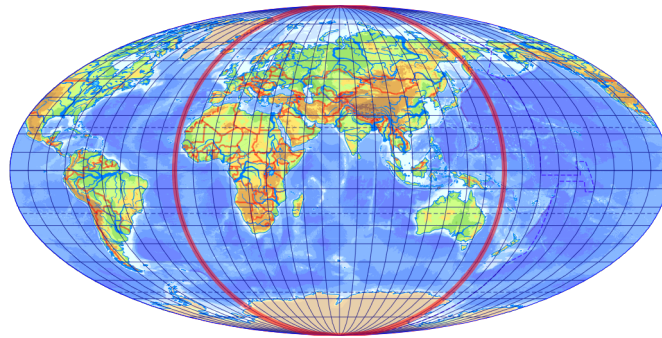


Figure XX.2: APiAN II projection (globular projection is in red)

XX.3 Extended globular projections

Of course, there was also a demand for a continuous representation of the entire surface of the globe in early world atlases. Although the APiAN II projection is designed to represent only the hemisphere, the formulæ of the projection can be extended to the entire surface of the sphere in unchanged form. Thus we obtain a projection representing the Earth in an elliptical frame, with the hemisphere in the middle being the original globular projection (Fig. XX.2).

The formulæ of the APiAN I projection could also be applied to the full globe, but the resulting projection would be unreasonably distorted. The 16th century Italian cartographer AGNESE therefore extended the projection to longitudes $|\lambda| > 90^\circ$ with circles of radius $R\pi/2$, which is the same size as the original circular frame. The Equator is still equidistant. The formulæ of the projection are the same as for the APiAN I projection, except that for $|\lambda| > 90^\circ$, $\rho = \pm R\pi/2$ is substituted.

This projection can be identified if we observe that, although it is flat-polar, the hemisphere in the centre of the map (which is in fact in the APiAN I projection) is still pointed-polar (Fig. XX.3). This projection was erroneously attributed to ORTELIUS, who applied it in his world atlas.

XX.4 Sinusoidal projection

Create a pseudocylindrical projection that is equidistant in central meridian and in all parallels. From the equidistant central meridian, it follows that:

$$y = R\widehat{\varphi}$$

On the other hand, $k = 1$:

$$\frac{1}{R \cos \varphi} \frac{\partial x}{\partial \lambda} = 1$$

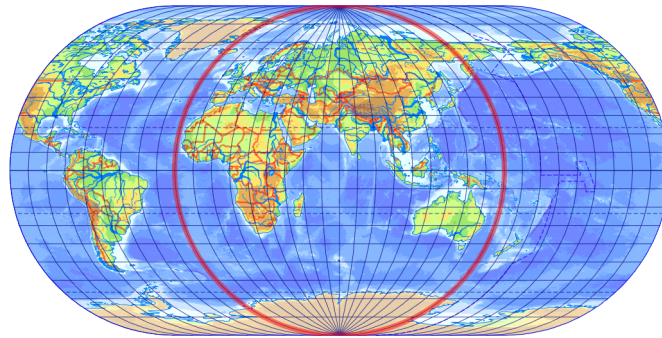


Figure XX.3: ORTELIUS projection (APIAN I projection is in red)

$$\int dx = R \int \cos \varphi d\lambda$$

$$x = R\widehat{\lambda} \cos \varphi + f(\varphi)$$

The symmetry about the central meridian can only be satisfied if the constant of integration $f(\varphi)$ is 0, so we can safely omit it. How do the distortions evolve?

$$h = \frac{dy}{d\varphi} \frac{1}{R \sin \vartheta} = \frac{1}{\sin \vartheta}$$

$$\cot \vartheta = \frac{\partial x}{\partial \varphi} \bigg/ \frac{dy}{d\varphi} = -\widehat{\lambda} \sin \varphi$$

Our mapping is equal-area, because $hk \sin \vartheta = 1$. The distortions are favourable at the Equator and at the central meridian ($h = k = 1$ and $\cot \vartheta = 0$). Farther away from them, $\cot \vartheta$ starts to increase very rapidly, causing catastrophic angular distortions (Fig. XX.4). The lesson is that if we try to completely eliminate too many distortions at once, one of the ignored distortion features will always increase significantly.

This mapping was devised by the French cartographer COSSIN at the end of the 16th century, but it is sometimes called as MERCATOR–SANSON or SANSON–FLAMSTEED projection.* Since its meridians are affine images of a sine wave, its most frequently used name is the *sinusoidal projection*.

Because of its locally favourable distortions, it is rarely used to represent continents at low latitudes in an equal-area form. Its isocols are reminiscent of hyperbolæ, so it would be good for cross-shaped areas, but in

* MERCATOR, by the way, has nothing to do with this projection; it is attributed to him because HONDIUS depicted the Earth in this projection in the world atlas he bought from MERCATOR and continued to sell as the MERCATOR Atlas.

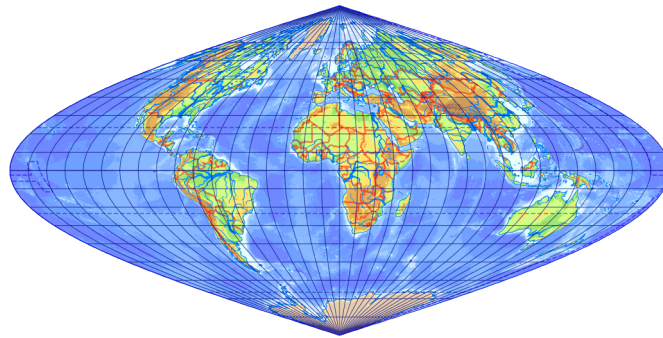


Figure XX.4: *Sinusoidal projection*

practice few such areas occur. Its practical significance is that it will be the base of modern sinusoidal projections, which will have a similar shape of meridians.

Since this projection has also been used for regional maps, an ellipsoidal variant also exists. It is defined under the same conditions as the spherical one. From the equidistant central meridian:

$$y = \int_0^{\Phi} M(\Phi) d\Phi$$

From the equidistant parallels:

$$x = N(\Phi) \widehat{\Lambda} \cos \Phi$$

The ellipsoidal variant also turns out to be equal-area.

Lesson twenty-one

Aphylactic pseudocylindrical projections

XXI.1 Loximuthal projection

Sometimes the map's theme requires interesting distortion patterns. In 1935, the German cartographer SIEMON found a solution to the problem of showing the length and direction of shipping routes from a particular port. If the ships had travelled along orthodromes, the azimuthal equidistant projection would have been correct in oblique aspect. SIEMON was looking for a projection with similar properties, but for loxodromes. *Azimuthal* projections are called so because the orthodromes (metameridians) starting from the metapole enclose their true angles on the map. Since this projection is azimuthal with respect to the loxodromes starting from the origin, the American cartographer TOBLER called it the *loximuthal projection*.

The port must be located on the meridian $\lambda_s = 0^\circ$. This is not a constraint, because the central meridian of a mapping can always be changed arbitrarily. The latitude of the starting point is φ_s . The azimuth α and the length s of rhumb lines are taken from Sec. III.3:

$$\tan \alpha = \frac{\widehat{\lambda} - \widehat{\lambda}_s}{\ln \tan\left(45^\circ + \frac{\varphi}{2}\right) - \ln \tan\left(45^\circ + \frac{\varphi_s}{2}\right)}$$
$$s = R \frac{\widehat{\varphi} - \widehat{\varphi}_s}{\cos \alpha}$$

This gives the projection formulæ in polar coordinates. Converted to Cartesian coordinates:

$$y = s \cos \alpha = R \frac{\widehat{\varphi} - \widehat{\varphi}_s}{\cos \alpha} \cos \alpha = R(\widehat{\varphi} - \widehat{\varphi}_s)$$

XXI. Aphylactic pseudocylindrical projections

From this, it can be seen that the resulting projection belongs to the family of pseudocylindrical mappings. The other coordinate:

$$\begin{aligned}
 x &= s \sin \alpha = R \frac{\widehat{\varphi} - \widehat{\varphi}_s}{\cos \alpha} \sin \alpha = R(\widehat{\varphi} - \widehat{\varphi}_s) \tan \alpha \\
 &= R \frac{\widehat{\lambda}(\widehat{\varphi} - \widehat{\varphi}_s)}{\ln \tan\left(45^\circ + \frac{\varphi}{2}\right) - \ln \tan\left(45^\circ + \frac{\varphi_s}{2}\right)}
 \end{aligned}$$

This formula leads to a division by zero if $\varphi = \varphi_s$. In this case, however, the loxodrome connecting the two points is a parallel of azimuth 90° and length $x = R\widehat{\lambda} \cos \varphi_s$. The projection leads to a division by infinity at the two poles, so $x \rightarrow \infty$, i.e. the projection is pointed-polar even though it does not appear to be.

The horizontal coordinate is a linear function of λ , so the parallels of the projection have constant scale. The central meridian and the latitude φ_s are loxodromes passing through the origin, so they are also equidistant. If $\varphi_s \neq 0$, the projection image is asymmetric about the Equator (Fig. XXI.1). This projection is aphylactic because $hk \sin \vartheta \neq 1$.

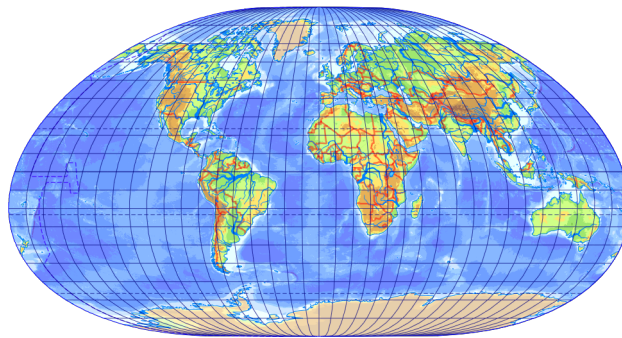


Figure XXI.1: Loximuthal projection for Lisbon

XXI.2 Blended projections

We have learned through our explorations in the field of map projections that every mapping has its weak points. The sinusoidal projection, for example, gives a very good representation of the equatorial region, but higher latitudes suffer from very severe angular distortion. This area is stretched in the north-south direction. On the other hand, the Plate Carrée projection is also favourable around the Equator, and at high latitudes it dilates the map content in the east-west direction. If we could somehow combine the advantages of these two projections, we would expect that at

XXI. Aphylactic pseudocylindrical projections

high latitudes the distortions of the two projections would nicely cancel each other out.

A *blended projection* of mappings A and B is a mapping developed by the average of the two projections and a rescaling c :

$$\begin{aligned}x &= c \frac{x_A + x_B}{2} \\y &= c \frac{y_A + y_B}{2}\end{aligned}$$

Blended projections may retain many properties of the original projections. The mapped graticule resembles both initial projections. If the two projections had a common equidistant line, it will have a constant scale in the new projection (equidistant if $c = 1$). The blended projection, however, does not preserve the conformal or equal-area property of the initial projections, so blended projections will be aphylactic by themselves. An equal-area blended projection may be produced using the method described in Sec. XXII.1. The idea of the blended projections is attributed to ECKERT, who produced six projections by this method in 1906.

Let us blend the **sinusoidal** and the **Plate Carrée** projection.

$$\begin{aligned}x &= c \frac{R\widehat{\lambda} \cos \varphi + R\widehat{\lambda}}{2} = cR \frac{\widehat{\lambda}}{2} (1 + \cos \varphi) \\y &= c \frac{R\widehat{\varphi} + R\widehat{\varphi}}{2} = cR\widehat{\varphi}\end{aligned}$$

By substituting $\lambda = \pm 180^\circ$ into the formula for x , we see that the length of the pole-line ($cR\pi$) is half the length of the Equator ($2cR\pi$). Substituting $\varphi = \pm 90^\circ$ into the equation for y shows that the length of the central meridian ($cR\pi$) is also half the length of the Equator.

Choose the constant c such that the total area of the projection equals the surface of the sphere. Such mappings are not equal-area, but they are expected to reduce areal distortions. The area of the map may be decomposed into a square of side $cR\pi$ and two sinusoids of base $cR\pi$ and height $cR\pi/2$. The area of a sinusoid of height H and base B :

$$\int_0^B H \sin \frac{\pi x}{B} dx = -\frac{HB}{\pi} \cos \frac{\pi B}{B} + \frac{HB}{\pi} \cos \frac{0\pi}{B} = \frac{2HB}{\pi}$$

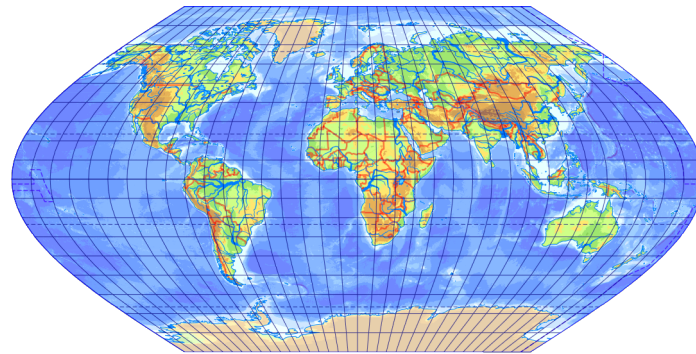
So the area of the square is $c^2R^2\pi^2$, the area of the sinusoids is $c^2R^2\pi$. Since the sum of the three areas is equal to the surface area $4R^2\pi$ of the

XXI. Aphyllactic pseudocylindrical projections

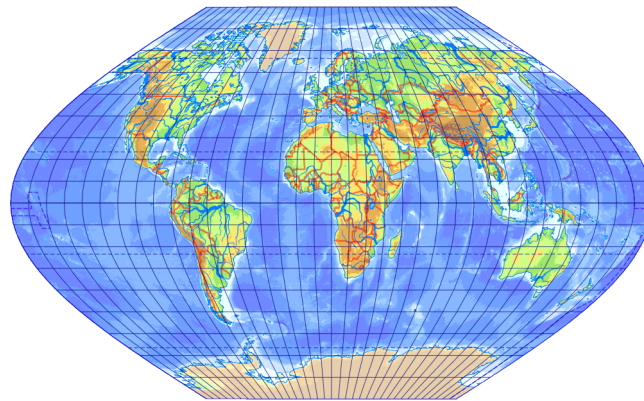
sphere:

$$c^2 R^2 \pi^2 + 2c^2 R^2 \pi = 4R^2 \pi$$

$$c = \frac{2}{\sqrt{\pi + 2}}$$



(a) ECKERT V projection



(b) WINKEL I projection

Figure XXI.2: Blended projections with sinusoidal meridians

The distortions are:

$$h = \frac{dy}{d\varphi} \frac{1}{R \sin \vartheta} = \frac{c}{\sin \vartheta}$$

$$k = \frac{1}{R \cos \varphi} \frac{\partial x}{\partial \lambda} = \frac{c}{2} \frac{1 + \cos \varphi}{\cos \varphi}$$

$$\cot \vartheta = \frac{\partial x}{\partial \varphi} \bigg/ \frac{dy}{d\varphi} = -\frac{\widehat{\lambda}}{2} \sin \varphi$$

This mapping is called the ECKERT V projection, it is aphyllactic (Fig. XXI.2). In German speaking lands, it is sometimes used as a projection on world maps.

XXI. *Aphylactic pseudocylindrical projections*

The equal total area of the blended projection and the surface of the sphere can be ensured not only by rescaling. If both original mappings have correct total area, their blended map will also have this total area, so we do not have to lose the equidistancy of the central meridian because of the rescaling. This is the basic idea behind the WINKEL I projection. The sinusoidal projection is equal-area, so its total area is guaranteed to be correct. Instead of a Plate Carrée projection, let us choose an equirectangular mapping that has correct total area.

The frame of the equirectangular projection is a rectangle of height $R\pi$ and width $2R\pi \cos \varphi_s$. Its total area is equal to the surface of the sphere if:

$$\begin{aligned} 2R^2\pi^2 \cos \varphi_s &= 4R^2\pi \\ \cos \varphi_s &= \frac{2}{\pi} \\ \varphi_s &\approx \pm 50^\circ 27' 35'' \end{aligned}$$

Thus, the projection formulæ are obtained as the average of the sinusoidal and the equirectangular (with standard parallels $\pm\varphi_s$. The length of the pole-line is ca. one third (exactly $1/\pi$ times) the length of the Equator.

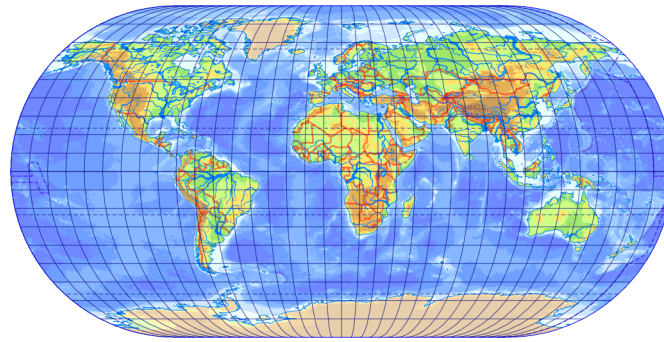
The ECKERT III projection is obtained by blending the **APIAN II** and the **Plate Carrée** projection, then rescaled in the usual way to make its total area correct:

$$\begin{aligned} x &= c \frac{R\widehat{\lambda} \cos \chi + R\widehat{\lambda}}{2} = cR \frac{\widehat{\lambda}}{2} (1 + \cos \chi) \\ y &= c \frac{R\widehat{\varphi} + R\widehat{\varphi}}{2} = cR\widehat{\varphi} = cR \frac{\pi}{2} \sin \chi \end{aligned}$$

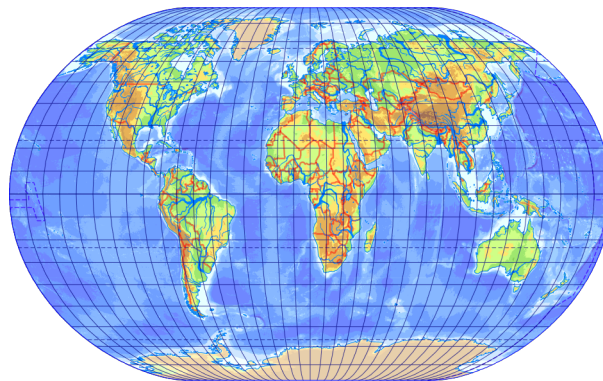
The length of both the central meridian and the pole-line ($cR\pi$) is half the length of the Equator. The mapped bounding meridians are semicircles (Fig. XXI.3). The area of the map can thus be divided into a square of side $cR\pi$ and two semicircles of radius $cR\pi/2$. Their summed area is $4R^2\pi$ for the purpose of correct total area:

$$\begin{aligned} c^2 R^2 \pi^2 + \frac{c^2 R^2 \pi^2}{4} \pi &= 4R^2\pi \\ c &= \sqrt{\frac{4}{\pi + \frac{\pi^2}{4}}} = \frac{4}{\sqrt{4\pi + \pi^2}} \end{aligned}$$

XXI. Aphylactic pseudocylindrical projections



(a) ECKERT III projection



(b) WINKEL II projection

Figure XXI.3: Blended projections with elliptical meridians

The distortions of the projection

$$h = \frac{dy}{d\varphi} \frac{1}{R \sin \vartheta} = \frac{c}{\sin \vartheta}$$

$$k = \frac{1}{R \cos \varphi} \frac{dx}{d\lambda} = \frac{c}{2} \frac{1 + \cos \chi}{\cos \varphi}$$

$$\cot \vartheta = \frac{\partial x / \partial \varphi}{dy / d\varphi} = \frac{-c \frac{\widehat{\lambda}}{2} \sin \chi \frac{d\chi}{d\varphi}}{c \frac{\pi}{2} \cos \chi \frac{d\chi}{d\varphi}} = -\frac{\widehat{\lambda}}{\pi} \tan \chi$$

On world maps created in Europe, we may see this aphylactic projection. Since in the Northern Hemisphere $\chi \leq \varphi$, the linear scales are slightly more favourable compared to the ECKERT V projection. However, at the pole, the angular distortions increase unboundedly, as can be seen from the limits $k \rightarrow \infty$ and $\cot \vartheta \rightarrow \infty$. Because of its pleasing shape, it is recommended if high latitudes are less important for the map's theme.

Again, the WINKEL II projection blends the APIAN II projection and the previously calculated equirectangular mapping of correct total area, so its pole-line is shorter. It is not known because of its complexity, although it has more favourable angular distortions than the ECKERT III projection.

XXI.3 Polyhedric projection

Divide the ellipsoid into 1° wide geographic quadrangles, then map each geographic quadrangle into planar trapezia using a pseudocylindrical mapping whose two bounding parallel circles and central meridian are equidistant, and maps all meridians to straight lines. Similar pseudocylindrical projections with straight meridians were popular at the dawn of the modern era (for a broader view see App. J). The resulting sections have different sizes in each spherical zone, so they cannot be mosaicked together in the plane, but the sheets can be folded into a polyhedron resembling a disco ball, hence this projection is called the *polyhedric projection*.

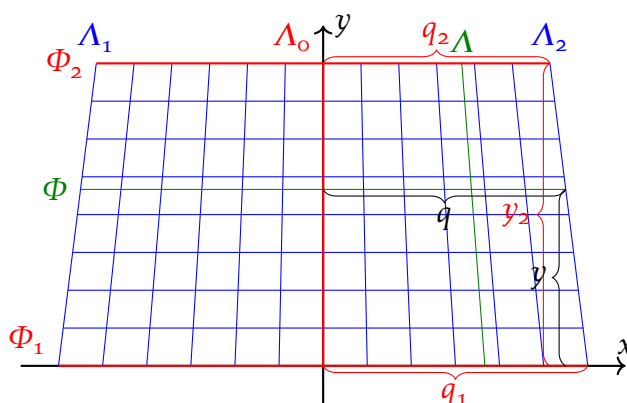


Figure XXI.4: Construction of the polyhedric projection

From the equidistant central meridian:

$$y = \int_{\Phi_1}^{\Phi} M(\Phi) d\Phi$$

From the equidistant bounding parallels, the half bases of the trapezium:

$$q_{1,2} = N(\Phi_{1,2}) \cos \Phi_{1,2} \frac{\widehat{\Lambda_2} - \widehat{\Lambda_1}}{2}$$

XXI. *Aphylactic pseudocylindrical projections*

From the legs of the two similar right triangles, as shown in Fig. XXI.4:

$$\frac{y_2}{q_1 - q_2} = \frac{y}{q_1 - q}$$

$$q = \frac{q_2 y + q_1 (y_2 - y)}{y_2}$$

Finally, the meridians divide the mapped parallel of length q proportionally:

$$x = q \frac{\widehat{\Lambda} - \widehat{\Lambda}_0}{\frac{\widehat{\Lambda}_2 - \widehat{\Lambda}_1}{2}}$$

$$= (\widehat{\Lambda} - \widehat{\Lambda}_0) \frac{N(\Phi_2) \cos \Phi_2 \int_{\Phi_1}^{\Phi} M(\Phi) d\Phi + N(\Phi_1) \cos \Phi_1 \int_{\Phi}^{\Phi_2} M(\Phi) d\Phi}{\int_{\Phi_1}^{\Phi_2} M(\Phi) d\Phi}$$

This projection, suggested by the Prussian military officer LICHTENSTERN, was used in many European countries (e.g. Germany, Austro-Hungarian Empire, Russia) for military topographic maps before World War I. In Hungary, we find it on the maps of the third military survey. It is also called the MÜFFLING projection. The projection is aphylactic, but the areal distortion is very small (the bounding parallels are locally equal-area).

This projection is not supported by modern GIS technology, so we need to approximate the nature of the projection while georeferencing. The ellipsoidal version of the sinusoidal projection is equidistant not only in the two bounding parallels, but in all parallels. Its meridians are not straight, but sinusoidal, however, their curvature can be neglected within such a small area. Thus, this projection approximates the polyhedral projection well with an error of 20 m at most, so the inaccuracy is below the cartographic accuracy of the sections.

Lesson twenty-two

Auxiliary angles in equal-area mappings

XXII.1 ECKERT'S equal-area mappings

The projections discussed so far have all been aphyllactic, with one exception. We would therefore need a method that somehow produces an equal-area projection from our aphyllactic mapping. This is the purpose of the *method of auxiliary angles*, whose result is:

- The map frame and mapped meridians remain unchanged.
- From an aphyllactic projection, an equal-area projection is obtained.
- Among the basic properties of the graticule, only the placement of the parallels is changed and therefore, among other things, the pole-line or the pole-point is preserved.

We already know from Sec. XX.1 that the parallels of equal-area pseudocylindricals have constant scale. Therefore, the present method works only for such pseudocylindrical projections, whose parallels have constant scale. Another condition is that the total area of the initial mapping is correct, otherwise it would not be possible to construct an equal-area mapping in the given map frame. The latter is not a problem, since any the total area of the projection can be made correct by a scaling.*

Since we do not want to change the mapped meridians, it follows that we will only modify the latitudes with an odd, differentiable function $\psi(\varphi)$. We want to preserve the frame of the projection, hence $\psi(90^\circ) = 90^\circ$. We also expect the function to be strictly increasing so that the map does not

* Nothing illustrates the generality of the method better than the fact that in the mid-20th century, many people produced equal-area pseudocylindrical projections using it. Due to the labour-intensive nature of the task, only the three most important ones are listed here, but there are also equal-area mappings with parabolic meridians (CRASTER projection), various pointed-polar and flat-polar projections with meridians as conic sections (PUTNINŠ projections) and mappings with a remarkably short pole-line (MCBRYDE-THOMAS projections). These are typically used in western cartography. The paradigm of the era was that a good map was equal-area, and therefore aphyllactic projections were hardly ever produced during this period.

XXII. Auxiliary angles in equal-area mappings

bend under itself. We then substitute the auxiliary angle ψ for φ in the formulæ of the original projection. This method can be considered as a special case of the graticule renumbering transformation described in the next lesson. The general formulæ are somewhat complicated, so it is more comprehensible to demonstrate the method on a certain map projection. The ECKERT V projection comes to mind, which has correct total area, its parallels have constant scale, but is not equal-area. Let us substitute ψ for φ in the original formulæ.

$$\begin{aligned}x &= cR \frac{\widehat{\lambda}}{2} (1 + \cos \psi) \\y &= cR \widehat{\psi} \\c &= \frac{2}{\sqrt{\pi + 2}}\end{aligned}$$

In Fig. XXII.1, we can see that the mapped spherical zone of latitude ψ can be decomposed into a blue rectangle and two red areas under a cosine wave. The area of the rectangle is not a problem, because its width is $cR\pi$ and its height is y , i.e. $cR\widehat{\psi}$, and the area is the product of these two values. The area under the cosine wave is more exciting because we have to integrate. In addition, the height of the cosine wave is not unity, but $cR\pi/2$, so we have to multiply the integral by that. Since in the vertical direction, the cosine wave reaches zero not at $\pi/2$ but at $cR\pi/2$, we multiply the integral by cR to take this into account:

$$cR \int_{0^\circ}^{\psi} \frac{cR\pi}{2} \cos \psi \, d\psi = \frac{c^2 R^2 \pi}{2} \sin \psi - 0$$

The surface area of a spherical zone is $2R^2\pi(\sin \varphi_2 - \sin \varphi_1)$, the formula known from Sec. II.2 simplifies to $2R^2\pi \sin \varphi$ between the Equator and latitude φ . If the projection is equal-area, then the summed areas of the blue rectangle and the two red areas under the cosine waves should give just the same:

$$\begin{aligned}c^2 R^2 \left(\pi \widehat{\psi} + 2 \frac{\pi}{2} \sin \psi \right) &= 2R^2 \pi \sin \varphi \\ \frac{4}{\pi + 2} \left(\widehat{\psi} + \sin \psi \right) &= 2 \sin \varphi\end{aligned}$$

Substituting c back, we can check that the equation is fulfilled for $\psi = \varphi = 90^\circ$, so the function satisfies our expectations. Since ψ cannot be

XXII. Auxiliary angles in equal-area mappings

expressed from the equation, it is an *implicit function*. It can be solved by numerical methods. To compute the distortions, we form the implicit derivative according to φ !

$$c^2(1 + \cos \psi) \frac{d\psi}{d\varphi} = 2 \cos \varphi$$

$$\frac{d\psi}{d\varphi} = \frac{2}{c^2} \frac{\cos \varphi}{1 + \cos \psi}$$

It can be seen that ψ is indeed strictly increasing as expected, because its derivative is positive. Using the chain rule:

$$h = \frac{dy}{d\psi} \frac{d\psi}{d\varphi} \frac{1}{R \sin \vartheta} = c \frac{2}{c^2} \frac{\cos \varphi}{1 + \cos \psi} \frac{1}{\sin \vartheta}$$

$$k = \frac{1}{R \cos \varphi} \frac{\partial x}{\partial \lambda} = \frac{c}{2} \frac{1 + \cos \psi}{\cos \varphi}$$

$$\cot \vartheta = \frac{\frac{\partial x}{\partial \psi} \frac{d\psi}{d\varphi}}{\frac{dy}{d\psi} \frac{d\psi}{d\varphi}} = \frac{\partial x}{\partial \psi} \bigg/ \frac{dy}{d\psi} = -\frac{\widehat{\lambda}}{2} \sin \psi$$

We can check that indeed $hk \sin \vartheta = 1$, so the ECKERT VI projection obtained in this way is equal-area. The formula of k has become quite complicated, so the equidistance of the central meridian is lost. Moreover, at the pole $h = 0$, i.e. in the direction of meridians, it compresses the map content unacceptably. This is compensated for by $k \rightarrow \infty$ to maintain equivalency, so the angular distortions at high latitudes are not too favourable (Fig. XXII.2). It is often found on European world maps, and is more popular than aphylactic blended projections.

Let us make an equal-area mapping from the ECKERT III projection. To make the calculation easier, we start from the simpler formulæ containing χ , substituting the auxiliary angle ψ for χ :

$$x = cR \frac{\widehat{\lambda}}{2} (1 + \cos \psi)$$

$$y = cR \frac{\pi}{2} \sin \psi$$

$$c = \frac{4}{\sqrt{4\pi + \pi^2}}$$

This time, in Fig. XXII.1, we decompose the mapped spherical zone into three different shapes. The area of the green rectangle is easy to determine, the height is now $y = cR\pi/2 \sin \psi$. The radii of the two blue circular sectors

XXII. Auxiliary angles in equal-area mappings

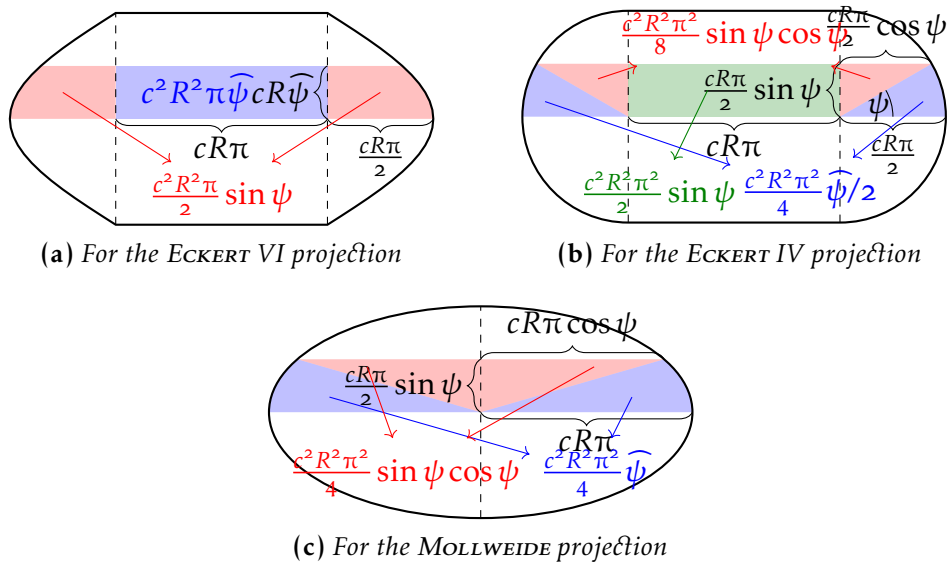


Figure XXII.1: Calculation of the auxiliary angle

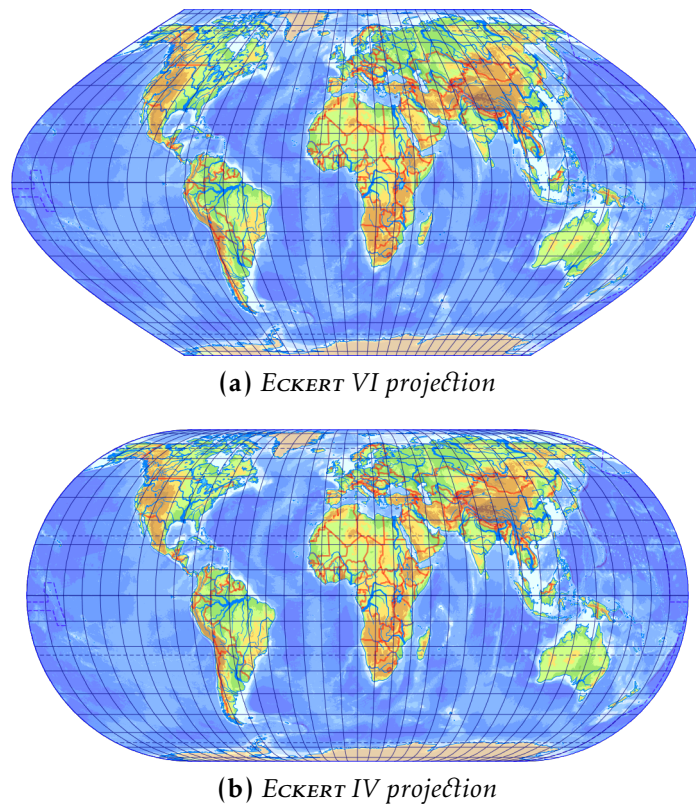


Figure XXII.2: Equal-area blended projections

XXII. Auxiliary angles in equal-area mappings

are $cR\pi/2$. Their heights are $cR\pi/2 \sin \psi$, so using the definition of sine, we find that ψ is the subtended angle of the arc. The area of the circle (i.e. the circular sector of angle 2π) is $r^2\pi$, which gives us that the area of the circular sector is proportionally $r^2\widehat{\psi}/2$. Only the two red right triangles remain. We know the vertical leg and the hypotenuse (the latter is the radius of the circular sector), so we can calculate the horizontal leg using the PYTHAGOREAN theorem. To do this, we use that $\sin^2 \psi + \cos^2 \psi = 1$. The area of a right triangle is half the product of the two legs. The projection will be equal-area if the area of the mapped spherical zone, i.e. the green rectangle, the two blue circular sectors and the two red right triangles, is exactly the surface $2R^2\pi \sin \varphi$ of the spherical zone:

$$\begin{aligned} c^2 R^2 \left(\frac{\pi^2}{2} \sin \psi + 2 \frac{\pi^2}{8} \widehat{\psi} + 2 \frac{\pi^2}{8} \sin \psi \cos \psi \right) &= 2R^2 \pi \sin \varphi \\ \frac{16}{4\pi + \pi^2} \left[\frac{\pi}{2} \sin \psi + \frac{\pi}{4} \widehat{\psi} + \frac{\pi}{8} \sin(2\psi) \right] &= 2 \sin \varphi \\ 4 \sin \psi + 2 \widehat{\psi} + \sin(2\psi) &= (4 + \pi) \sin \varphi \end{aligned}$$

Again, we have an implicit function, the equation is satisfied at the pole, so far good. Check the monotonicity using the implicit derivative of the first equation:

$$\begin{aligned} c^2 R^2 \left[\frac{\pi^2}{2} \cos \psi + \frac{\pi^2}{4} (1 + \cos^2 \psi - \sin^2 \psi) \right] \frac{d\psi}{d\varphi} &= 2R^2 \pi \cos \varphi \\ \frac{c^2 \pi}{2} \left(\cos \psi + \frac{2 \cos^2 \psi}{2} \right) \frac{d\psi}{d\varphi} &= 2 \cos \varphi \\ \frac{d\psi}{d\varphi} &= \frac{4 \cos \varphi}{c^2 \pi \cos^2 \psi + \cos \psi} \end{aligned}$$

This is indeed a positive number. The distortions:

$$\begin{aligned} h &= \frac{dy}{d\psi} \frac{d\psi}{d\varphi} \frac{1}{R \sin \vartheta} = c \frac{\pi}{2} \cos \psi \frac{4 \cos \varphi}{c^2 \pi \cos^2 \psi + \cos \psi} \frac{1}{\sin \vartheta} = \frac{2 \cos \varphi}{c} \frac{1}{1 + \cos \psi} \frac{1}{\sin \vartheta} \\ k &= \frac{1}{R \cos \varphi} \frac{\partial x}{\partial \lambda} = \frac{c}{2} \frac{1 + \cos \psi}{\cos \varphi} \\ \cot \vartheta &= \frac{\partial x}{\partial \psi} \bigg/ \frac{dy}{d\psi} = \frac{-cR \frac{\widehat{\lambda}}{2} \sin \psi}{cR \frac{\pi}{2} \cos \psi} = -\frac{\widehat{\lambda}}{\pi} \tan \psi \end{aligned}$$

Although the formulæ only prove equivalency ($hk \sin \vartheta = 1$) at a glance, the ECKERT IV projection is one of the most favourable equal-area pseudo-cylindrical mapping commonly available in GIS (Fig. XXII.2), and is the

most widely used among ECKERT's projections. For map themes requiring equivalency, it is highly recommended for world maps. The mapped meridians are semi-ellipses. The only drawback of the mapping is the pole-line and the angular distortion that increases unbounded at high latitudes ($h = 0, k \rightarrow \infty$, and $\cot \vartheta \rightarrow \infty$). ECKERT's equal-area projections were also published in 1906.

XXII.2 MOLLWEIDE projection

The APIAN II projection cannot be converted directly into an equal-area projection, because the method only works for projections of correct total area. However, if the projection is slightly reduced by a constant c , its total area can be made correct. The frame of the APIAN II projection is an ellipse of semi-major axis $R\pi$ and semi-minor axis $R\pi/2$. After reduction, both semi-axes are multiplied by c . The area of the ellipse is the product of the two semi-axes and π , which is equal to the surface $4R^2\pi$ of the sphere:

$$\frac{c^2 R^2 \pi^3}{2} = 4R^2 \pi$$

$$c = \frac{2\sqrt{2}}{\pi}$$

By multiplying the formulæ with this constant, the method of auxiliary angles can be performed. Again, we substitute ψ into the formulæ containing χ :

$$x = cR\widehat{\lambda} \cos \psi$$

$$y = cR\frac{\pi}{2} \sin \psi$$

This time, we are already familiar with finding the auxiliary angle. Fig. XXII.1 shows that the mapped spherical zone can be decomposed into two red right triangles and two blue shapes. The legs of the red right triangle are given by the projection formulæ x and y , the former with the substitution $\lambda = 180^\circ$. We notice immediately that the dimensions of the blue and red figures differ from that of the ECKERT IV projection only in that everything is now doubled in the horizontal direction, so their areas are therefore doubled. The sum of the areas is again $2R^2\pi \sin \varphi$:

$$c^2 R^2 \left(2 \frac{\pi^2}{4} \widehat{\psi} + 2 \frac{\pi^2}{4} \sin \psi \cos \psi \right) = 2R^2 \pi \sin \varphi$$

$$\frac{8}{\pi^2} \left[\frac{\pi}{2} \widehat{\psi} + \frac{\pi}{4} \sin(2\psi) \right] = 2 \sin \varphi$$

$$2\widehat{\psi} + \sin(2\psi) = \pi \sin \varphi$$

XXII. Auxiliary angles in equal-area mappings

By substituting 90° , the equation is fulfilled. The derivative of the implicit function is calculated from the first equation of the previous derivation:

$$\begin{aligned} c^2 R^2 \frac{\pi^2}{2} (1 + \cos^2 \psi - \sin^2 \psi) \frac{d\psi}{d\varphi} &= 2R^2 \pi \cos \varphi \\ \frac{c^2 \pi}{2} 2 \cos^2 \psi \frac{d\psi}{d\varphi} &= 2 \cos \varphi \\ \frac{d\psi}{d\varphi} &= \frac{2 \cos \varphi}{c^2 \pi \cos^2 \psi} \end{aligned}$$

The derivative is positive.

$$\begin{aligned} h &= \frac{dy}{dx} \frac{d\psi}{d\varphi} \frac{1}{R \sin \vartheta} = c \frac{\pi \cos \psi}{2 \sin \vartheta} \frac{2 \cos \varphi}{c^2 \pi \cos^2 \psi} = \frac{\cos \varphi}{c \cos \psi} \frac{1}{\sin \vartheta} \\ k &= \frac{1}{R \cos \varphi} \frac{dx}{d\lambda} = c \frac{\cos \psi}{\cos \varphi} \\ \cot \vartheta &= \frac{dx}{d\psi} \Big/ \frac{dy}{d\psi} = \frac{-cR\widehat{\lambda} \sin \psi}{cR\frac{\pi}{2} \cos \psi} = -2 \frac{\widehat{\lambda}}{\pi} \tan \psi \end{aligned}$$

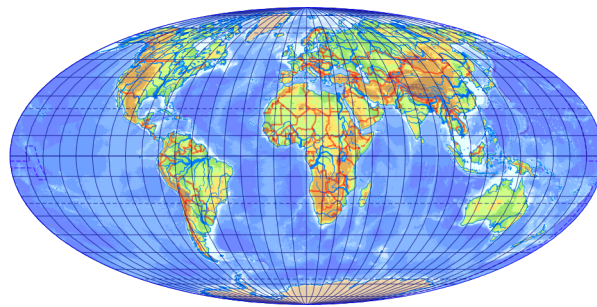
From the formulæ, it can be seen that the projection is equal-area. At the Equator, $k \approx 0.9003$, from there on, k increases, reaching the value 1 (equidistant along the parallel) at latitude $\varphi \approx \pm 40.7367^\circ$. Its angular distortions are very large (Fig. XXII.3).

This mapping was created by the German MOLLWEIDE in 1805, but only became widespread when the French BABINET began to popularize it as the *homolographic projection*. It used to be popular, but is now less often used because of its unfavourable distortions.* The projection is pointed-polar, its meridians are smooth at the pole, which makes it particularly suitable for graticule rotation.† The *Atlantis projection* published in 1948, in the atlases of the Scottish cartographer BARTHOLOMEW, is in fact this mapping in an oblique transverse aspect ($\varphi_0 = 0^\circ$, $\lambda_0 = 60^\circ$, $\lambda'_p = -135^\circ$).

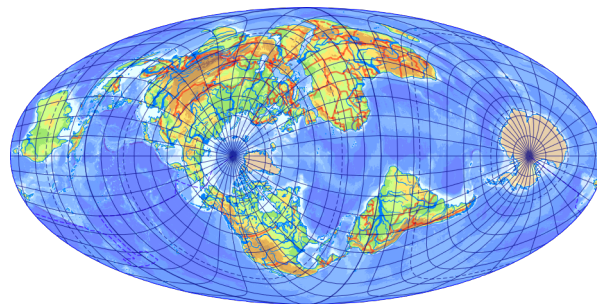
* Rarely, this projection is transformed by stretching (with a factor d in the horizontal direction and $1/d$ in the vertical direction to preserve areas), for example, to have a circular outline (TOBLER projection) or to have an equidistant Equator (BROMLEY projection).

† It is hard work for anyone who tries to do a graticule rotation in GIS software! In general, ArcGIS does not know rotated non-conical projections, it mostly supports this only among conical projections. In theory, QGIS can rotate any known projection if `+proj=ob_tran +o_proj=code` is substituted for `+proj=code` in the projection definition. However, it is no good doing this, because practically our lines turn jumbled in vector layers, rasters are drawn with no-data stripes.

XXII. Auxiliary angles in equal-area mappings



(a) Normal aspect



(b) Atlantis projection (oblique transverse, for the Atlantic Ocean)

Figure XXII.3: MOLLWEIDE projection

Lesson twenty-three

Renumbering the graticule

XXIII.1 The method 'Umbeziffern'

Both the sinusoidal and APIAN II projections have favourable distortions near the centre of the map, while near the map frame they are rather unfavourable. WAGNER and SIEMON came up with the idea in the 1930s: they used only the favourable parts of the projections and represented the whole Earth in it. Their method has no accepted term in English, it is usually referred to as *Umbeziffern* (German word for renumbering).

The idea is to substitute the renumbered latitude ψ for φ and the renumbered longitude ζ for λ in the projection formulæ. Since we want to preserve the characteristics of the original graticule, it is important that parallels remain parallels and meridians remain meridians. This can be achieved by making ψ a function of φ only, and ζ a function of λ only. Of course, the functions are strictly increasing and differentiable.

Consider the simplest renumbering:

$$\begin{aligned}\psi &= m\varphi \\ \zeta &= n\lambda\end{aligned}$$

If $m, n < 1$, then the above transformation will result in using only a small fraction of the original projection. Since this will also reduce the total area of our map, we will restore the original scale by a factor of $1/\sqrt{mn}$. WAGNER did not use the parameters n and m directly, but instead used the ratio between the length of the central meridian and that of the Equator (p) and the ratio between the length of the pole-line and that of the Equator (q). These are derived from the bounding latitude $\widehat{\psi}_B = m\pi/2$ and longitude $\widehat{\zeta}_B = n\pi$, since the Pole and the 180° meridian will be mapped to these values. For two projections, we show how m and n can be obtained given p and q :

For the sinusoidal projection:

$$p = \frac{y(\psi_B)}{x(o, \zeta_B)} = \frac{R\widehat{\psi}_B}{R\widehat{\zeta}_B} = \frac{m\frac{\pi}{2}}{n\pi} = \frac{m}{2n}$$

$$q = \frac{x(\psi_B, \zeta_B)}{x(o, \zeta_B)} = \frac{R\widehat{\zeta}_B \cos \psi_B}{R\widehat{\zeta}_B} = \cos\left(m\frac{\pi}{2}\right)$$

$$m = \frac{2}{\pi} \arccos q$$

$$n = \frac{\arccos q}{\pi p}$$

For the APIAN II projection:

$$p = \frac{y(\psi_B)}{x(o, \zeta_B)} = \frac{R\widehat{\psi}_B}{R\widehat{\zeta}_B} = \frac{m\frac{\pi}{2}}{n\pi} = \frac{m}{2n}$$

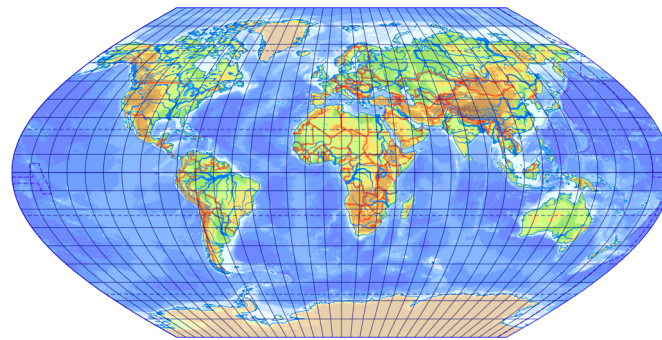
$$q = \frac{x(\psi_B, \zeta_B)}{x(o, \zeta_B)} = \frac{R\widehat{\zeta}_B \sqrt{1 - \left(\frac{2\widehat{\psi}_B}{\pi}\right)^2}}{R\widehat{\zeta}_B} = \sqrt{1 - m^2}$$

$$m = \sqrt{1 - q^2}$$

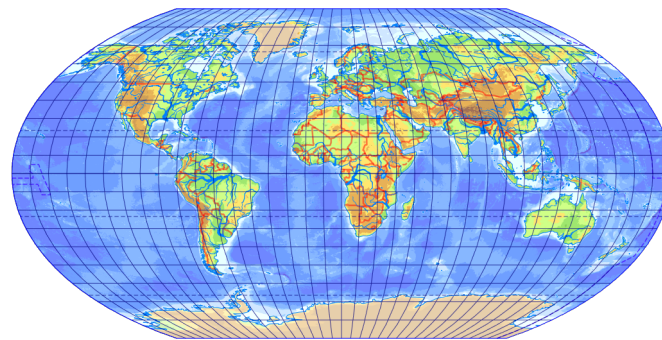
$$n = \frac{\sqrt{1 - q^2}}{2p}$$

The WAGNER III projection is a renumbered sinusoidal projection with the choice $p = q = 1/2$ (i.e., $m = n = 2/3$), while the WAGNER VI projection is a renumbered APIAN II projection by choosing $p = q = 1/2$ (i.e., $m = n = \sqrt{3}/2$). These aphylactic mappings and ECKERT's projections are like peas in a pod, but the formers retain the equidistant central meridian.* An important difference is that the meridians of the renumbered graticules consist only of the middle sections of the sinusoidal or elliptic arcs, and are therefore less curved than in the blended projections (Fig. XXIII.1). These projections are almost never encountered, but their principle helps to understand a popular Russian projection.

* To distribute the distortions more favourably, the projection may be subjected to a stretching of factor d in the direction of the Equator. This will still preserve the equidistancy of the central meridian, but another latitude will be equidistant instead of the Equator.



(a) WAGNER III projection



(b) WAGNER VI projection

Figure XXIII.1: Projections modified by the *Umbeziffern*

XXIII.2 KAVRAYSKIY VII projection

If you are looking for an aphyllactic pseudocylindrical projection, and nothing matters except the balance of distortions, choose the KAVRAYSKIY VII projection: It is the least distorted of all the well-known pseudocylindrical mappings. The projection is defined by four conditions:

- The mapped parallels are divided by meridians proportionally.
- Meridians are arcs of ellipses, but the mapped meridians $\pm 120^\circ$ are arcs of circles.
- Its pole-line is half as long as the Equator.
- It is equidistant in the central meridian.

From the first two conditions, we can see that we have to cut the corresponding piece from the APIAN II projection using the *Umbeziffern*. In this projection, the meridians $\pm 90^\circ$ are mapped to arcs of circles. To transform longitude $\pm 120^\circ$ here, we renumber meridians by $n = 90^\circ/120^\circ = 3/4$. By the third condition, $q = 1/2$, i.e., by using the formulæ of WAGNER, $m = \sqrt{1 - q^2} = \sqrt{3}/2$. Because of the fourth condition, WAGNER's proposed

scaling by $1/\sqrt{mn}$ will not be correct. Instead, we seek a scaling factor that restores the vertical axis. Since the latitudes have been shrunk by a factor of m , the length of the central meridian is restored by a scaling factor of $1/m = 2/\sqrt{3}$. The formulæ of the projection are therefore:

$$\begin{aligned} x &= \frac{R}{m} \widehat{\zeta} \sqrt{1 - \left(\frac{2\widehat{\psi}}{\pi}\right)^2} = \frac{R}{m} n \widehat{\lambda} \sqrt{1 - \left(\frac{2m\widehat{\varphi}}{\pi}\right)^2} \\ &= R \frac{6}{4\sqrt{3}} \widehat{\lambda} \sqrt{1 - \left(\frac{2\sqrt{3}\widehat{\varphi}}{2\pi}\right)^2} = R \frac{\sqrt{3}}{2} \widehat{\lambda} \sqrt{1 - \left(\frac{\sqrt{3}\widehat{\varphi}}{\pi}\right)^2} \\ y &= \frac{R}{m} \widehat{\psi} = \frac{R}{m} m \widehat{\varphi} = R \widehat{\varphi} \end{aligned}$$

Calculate the distortions as well.

$$\begin{aligned} h &= \frac{dy}{d\varphi} \frac{1}{R \sin \vartheta} = \frac{1}{\sin \vartheta} \\ k &= \frac{1}{R \cos \varphi} \frac{\partial x}{\partial \lambda} = \frac{\sqrt{3}}{2} \frac{\sqrt{1 - \left(\frac{\sqrt{3}\widehat{\varphi}}{\pi}\right)^2}}{\cos \varphi} \\ \cot \vartheta &= \frac{\partial x / \partial \varphi}{\partial y / \partial \varphi} = \frac{\sqrt{3}}{2} \widehat{\lambda} \frac{-\frac{3\widehat{\varphi}}{\pi^2}}{\sqrt{1 - \left(\frac{\sqrt{3}\widehat{\varphi}}{\pi}\right)^2}} \end{aligned}$$

Aside from the inconvenience of $k \rightarrow \infty$ in the pole-line, we have a very favourable projection.* Its only flaw is that KAVRAYSKIY published it in Russian in 1939, so it could not be widespread in most of the world due to language barriers, and can be found mostly in atlases of Eastern Europe and the former Soviet states. The original derivation did not use the Umbeziffern, but was described independently. It is very suitable as a world map (Fig. XXIII.2), if you want to represent geographical zones in horizontal stripes (e.g. climate zones).

* Of the well-known pseudocylindrical projections, this projection is among the least distorted ones. But how does the least possible distorted pseudocylindrical mapping look like? We do not know much about this, only that GYÖRFFY realized that the best pseudocylindrical is equidistant in the central meridian. Well, that is not much information, considering that the unfavourable sinusoidal projection also has an equidistant central meridian...

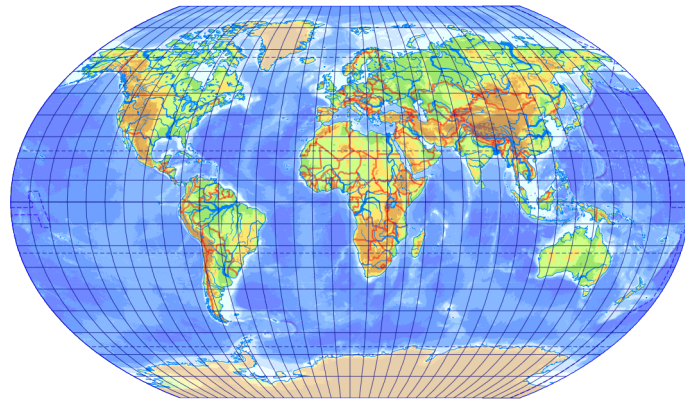


Figure XXIII.2: KAVRAYSKIY VII projection

XXIII.3 The WAGNER transform

We already have a renumbering that preserves the equidistant central meridian and uses only the favourable parts of the projection. There is also one that creates an equal-area map but fills the entire map frame. Could we develop such an *Umbeziffern* transformation that uses only the favourable, central parts of an equal-area projection, and the result is still equal-area? Since a pseudocylindrical mapping can only be equal-area if its parallels have constant scale, we must preserve this. The new longitude is therefore a linear function of the old one:

$$\zeta = n\lambda$$

The projection can only remain equal-area if the mapped surface of any spherical zone is in direct proportion to the old one after renumbering. Reduce each spherical zone by a factor m . The new surface of the spherical zone ($2R^2\pi \sin \psi$) must be equal to m times the old surface ($2R^2\pi \sin \varphi$):

$$\begin{aligned} 2R^2\pi \sin \psi &= m2R^2\pi \sin \varphi \\ \psi &= \arcsin(m \sin \varphi) \end{aligned}$$

This idea was developed by SIEMON, and then WAGNER used it to form equal-area projections, hence the *Umbeziffern* that preserves equivalency is also called the *WAGNER transform*.^{*} If $m, n < 1$, we will use again the middle

^{*} WAGNER also created maps with small ($p < 1.2$) areal distortion up to latitudes of 60° . This was achieved by using the *Umbeziffern* $\psi = \arcsin[m_1 \sin(m_2 \varphi)]$ and $\zeta = n\lambda$. These are the WAGNER II and V projections. It can be seen that the more m_2 deviates from 1, the more the projection deviates from equivalency, so the areal distortions can be controlled.

part cut from the projection (Fig. XXIII.3). The projection is not equal-area yet, because the areas have been reduced by a factor of n while renumbering the longitudes, and by a factor of m while renumbering the latitudes. The areas have thus been rescaled by a factor of mn , so we need to magnify them back by the factor $1/mn$. The areas are proportional to the square of the scaling factor, so a scaling factor of $1/\sqrt{mn}$ restores the area.*

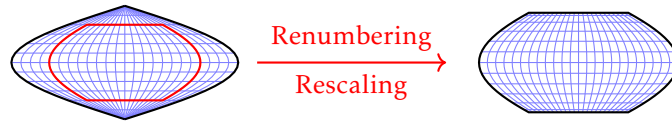


Figure XXIII.3: The substance of the Umbeziffern

Again, WAGNER gave the ratio between the length of the central meridian and that of the Equator (p) and the ratio between the length of the pole-line and that of the Equator (q) as parameters. Let us see again for two projections how they are obtained from the latitude $\widehat{\psi}_B = \arcsin m$ and the longitude $\widehat{\zeta}_B = n\pi$!

For the sinusoidal projection:

$$p = \frac{y(\psi_B)}{x(o, \zeta_B)} = \frac{R\widehat{\psi}_B}{R\widehat{\zeta}_B} = \frac{\arcsin m}{n\pi}$$

$$q = \frac{x(\psi_B, \zeta_B)}{x(o, \zeta_B)} = \frac{R\widehat{\zeta}_B \cos \psi_B}{R\widehat{\zeta}_B} = \cos \arcsin m = \sqrt{1 - m^2}$$

$$m = \sqrt{1 - q^2}$$

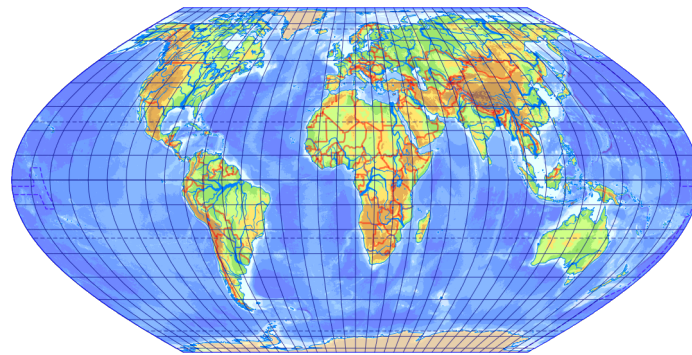
$$n = \frac{\arcsin \sqrt{1 - q^2}}{\pi p}$$

For the MOLLWEIDE projection, you have to do some tricks because it already has a renumbered latitude. Therefore, ψ_B is expressed in terms of q and then m is obtained from the implicit function:

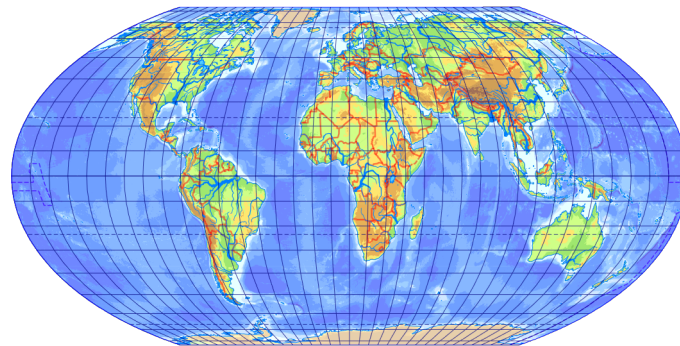
$$q = \frac{x(\psi_B, \zeta_B)}{x(o, \zeta_B)} = \frac{cR\widehat{\zeta}_B \cos \psi_B}{cR\widehat{\zeta}_B} = \cos \psi_B$$

$$p = \frac{y(\psi_B)}{x(o, \zeta_B)} = \frac{cR\frac{\pi}{2} \sin \psi_B}{cR\widehat{\zeta}_B} = \frac{\frac{\pi}{2} \sqrt{1 - q^2}}{n\pi} = \frac{\sqrt{1 - q^2}}{2n}$$

* Naturally, the area is preserved if we then stretch the projection by a factor d in the horizontal direction and a factor $1/d$ in the vertical direction, which is another way to fine-tune the distortions.



(a) KAVRAYSKIY VI projection (WAGNER I projection)



(b) WAGNER IV projection

Figure XXIII.4: Equal-area projections using the Umbezziffen

$$2\widehat{\psi}_B + \sin(2\psi_B) = m\pi \sin 90^\circ$$

$$m = \frac{2 \arccos q + \sin(2 \arccos q)}{\pi}$$

$$n = \frac{\sqrt{1 - q^2}}{2p}$$

Because of its complexity, the WAGNER transformed MOLLWEIDE projection is not used, although it gives a surprisingly pleasing picture despite being equal-area. The choice $p = q = 1/2$ is the WAGNER IV projection, which has very favourable distortions as shown in Fig. XXIII.4; the other choices were called *MOLLWEIDE series* by WAGNER.

The *MERCATOR series*, i.e. the WAGNER transformed sinusoidal (or *MERCATOR-SANSON*) projection is more important from a practical point of view. From the condition $p = q = 1/2$, we get $m = \sqrt{3}/2$, $n = 2/3$, and $1/\sqrt{mn} = \sqrt[4]{3}$, i.e. the projection formulæ:

$$\begin{aligned}
 x &= \frac{R\widehat{\zeta}}{\sqrt{mn}} \cos \psi = \frac{Rn\widehat{\lambda}}{\sqrt{mn}} \sqrt{1 - \sin^2 \psi} \\
 &= \frac{Rn\widehat{\lambda}}{\sqrt{mn}} \sqrt{1 - m^2 \sin^2 \varphi} = R \frac{2\sqrt[4]{3}}{3} \widehat{\lambda} \sqrt{1 - \frac{3}{4} \sin^2 \varphi} \\
 y &= \frac{R\widehat{\psi}}{\sqrt{mn}} = \frac{R \arcsin \sin \psi}{\sqrt{mn}} = \frac{R \arcsin(m \sin \varphi)}{\sqrt{mn}} = R \sqrt[4]{3} \arcsin\left(\frac{\sqrt{3}}{2} \sin \varphi\right)
 \end{aligned}$$

KAVRAYSKIY discovered this projection in 1936, while WAGNER discovered it in 1932, so it is called both the KAVRAYSKIY VI and the WAGNER I projection. It is very often found as equal-area world maps in the former Eastern Bloc countries. The projection should not be confused with the ECKERT VI projection, whose meridians are complete sinusoids, not just two-thirds from their middle. In the KAVRAYSKIY VI projection, the meridians are therefore less curved. Following URMAYEV's suggestion, members of the MERCATOR series also appear on Soviet ocean maps with a different choice of m and n .

XXIII.4 Composite projections

Some projections show more favourable distortions around the Equator, while others show more favourable distortions at higher latitudes. For example, the sinusoidal projection maps the Equator distortion-free, but is less applicable at high latitudes, where other projections are preferable. Could not a projection be created that shows each area separately in its corresponding projection and then the parts are stitched together? If a projection has piecewise projection formulæ for different parts of the Earth, the mapping is called a *composite projection*.

The American cartographer GOODE published his idea of the *homolosine projection* in 1923: let us plot the low latitudes in the sinusoidal projection, and the high latitudes in the MOLLWEIDE (homolographic) projection for both hemispheres! Of course, the expectation is that the two projections should fit on the bounding latitude. We know that the sinusoidal projection is equidistant in all parallels, but in the MOLLWEIDE projection is equidistant only at latitudes $\varphi_B \approx \pm 40.7367^\circ$. It already follows that the two projections can only fit at these two latitudes. Thus, in the GOODE projection, we use the sinusoidal projection at latitudes $-40.7367^\circ < \varphi < 40.7367^\circ$, and MOLLWEIDE projection at latitudes higher than this.

In order to align the parts, the MOLLWEIDE projection must be shifted slightly vertically towards the Equator. In the sinusoidal projection, the bounding latitude is mapped to $y_S = R\widehat{\varphi}_B$, while the MOLLWEIDE projection

maps it to $y_M = \sqrt{2}R \sin \psi_B$, where the auxiliary angle ψ_B is given by the implicit function (Sec. XXII.2) as 32.6893° . From this, the shift is $\Delta y = y_S - y_M \approx -0.05280R$.

GOODE also suggested that since the projection is only favourable in the neighbourhood of the central meridian, each continent should be mapped using its own central meridian. As shown in Fig. XXIII.5, the different meridians result in that the parts are connected to each other only along the Equator and that there are discontinuities in the oceans. Mappings using different central meridians for different longitudes are known as *interrupted projections*.

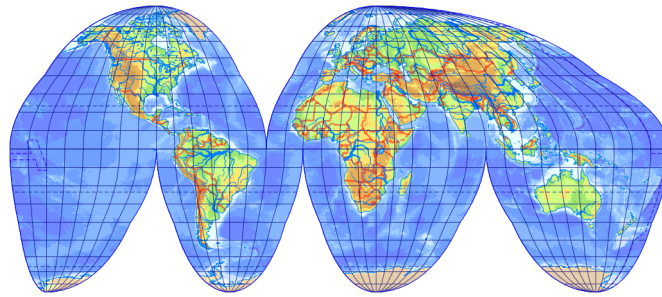


Figure XXIII.5: *GOODE projection*

In the GOODE projection, the middle parts of the mapped meridians are sinusoids, the outside parts are arcs of ellipses. At the bounding parallels, the meridians are cusped, which is not æsthetic to say the least. The projection is made up of equal-area projections, and is therefore also equivalent. The distortions of interrupted projections are generally significantly better than those of usual projections, but the increased number of cuts makes it difficult to perceive the contiguity of adjacent areas.* They are unsuitable for maps of global relationships or geopolitical conditions. Discontinuities should always be placed so as to have the least possible impact on the map's theme. Accordingly, GOODE has created an oceanic version, with the central meridians in the middle of the oceans and the cuts running mostly across continents.

As the GOODE projection is still unfavourable in its uninterrupted form, Hungarian cartographer ÉRDI-KRAUSZ improved the idea in 1968. He widened the area of the central zone to the bounding latitude $\varphi_B = \pm 60^\circ$ or $\pm 70^\circ$. In this zone, he applied the a WAGNER transformed sinusoidal

* Of course, any other projection can be used as an interrupted projection instead of the GOODE projection. A common example is the BOGGS projection, a blended projection of the sinusoidal and MOLLWEIDE projections modified with auxiliary angles to make it equal-area.

projection found in Sec. XXIII.3. ÉRDI-KRAUSZ chose the values $p = 0.4$ and $q = 0.6$. This gives $m = 0.8$ and $n = \arcsin(0.8)/(0.4\pi)$.

In the MOLLWEIDE projection, the length of the bounding parallel is shorter than in the WAGNER transformed sinusoidal projection. To fit the parts, the MOLLWEIDE projection needs to be enlarged. The scaling factor is given by the original lengths of the corresponding parallels: $c \approx 1.188719$ for $\varphi_B = 60^\circ$ and $c \approx 1.387333$ for $\varphi_B = 70^\circ$. The MOLLWEIDE projection must be shifted in the vertical direction also in this projection to align them together. If $\varphi_B = 60^\circ$, $0.285475R$ must be subtracted from the y coordinate, and $0.583282R$ if $\varphi_B = 70^\circ$.

The ÉRDI-KRAUSZ projection does not ensure the smooth join of meridians, but this is less obvious than in the GOODE projection (Fig. XXIII.6). Former cartographers used to blot out the cusp with loose strokes.* The mapping is composed of equal-area projections, but the parts using the MOLLWEIDE projection had to be enlarged to fit. Since the final projection would then no longer be equal-area, two nominal scales and scalebars were added to the maps: one for low latitudes and one for high latitudes.

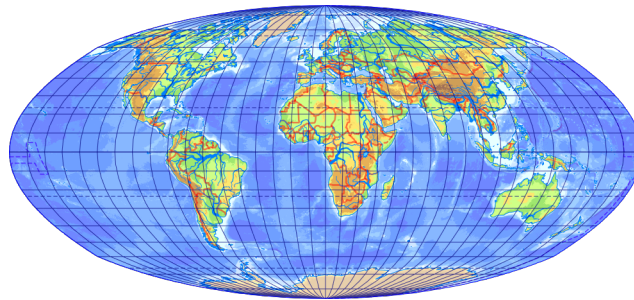


Figure XXIII.6: ÉRDI-KRAUSZ projection

This projection is common in Hungarian world atlases, but is barely known abroad. It can be recommended for pointed-polar world maps of economic or other map themes requiring equivalency. This mapping is not typically supported by GIS software.

* In 2002, JUHÁSZ showed that with a slight modification of the projection formulæ, this cusp can be eliminated mathematically, and his solution also eliminates the different scale, so it can be considered as equal-area in a strict sense. In 2004, GEDE further developed the solution by discovering a set of projections and selecting the one with the most favourable distortion, which, despite being equal-area, exhibits relatively low angular distortion.

Lesson twenty-four

Modern pseudocylindrical maps

XXIV.1 The BARANYI projections

In the middle of the 20th century, equal-area world maps were all the rage. During this period, newer and newer equal-area projections were developed, and not equivalent world maps were considered outdated. This was crowned by PETERS's map projection that ignored angular distortions. This became a hot potato in the cartographic community, so they began to construct aphyllactic mappings that favourably represented the shape of the continents. These graticules were drawn by people less skilled in mathematics, so they were typically published in the form of constructions describing the map. In other cases, the graph paper positions of the intersection points of graticule lines were given in tabular form. This was not a problem at the time, as the cartographic content of each geographical quadrangle was plotted manually anyway. Digital cartography, however, requires exact formulæ for mapping; so these must be subsequently provided as an approximation if such a mapping is applied.

Among the developers of such maps, BARANYI deserves special mention, who published a number of projections in 1968. These all aimed to represent the shape of the continents faithfully. His maps have also received some international attention for their favourable distortions. He published his graticules in the form of constructions.

The frame of the BARANYI II projection consists of arcs smoothly connected at $\varphi_B = 70^\circ$. The Equator is equidistant, the length of the central meridian is 0.7 times that of the Equator. On the central meridian, distances of parallels increase as an arithmetic progression so that latitude 70° divides the central meridian in the ratio 13 : 5. All parallels have constant scale. Based on this description, KARSAY and GYÖRFFY gave an approximate

formula:^{*}

$$x = \frac{\widehat{\lambda}}{\pi} \times \begin{cases} (R\pi - r_1 + r_1 \cos \chi) & \text{if } |\varphi| \leq \varphi_B \\ r_2 \sin \zeta & \text{if } |\varphi| > \varphi_B \end{cases}$$

$$y = R \left(0.95 |\widehat{\varphi}| + 0.005 \frac{180}{\pi} \widehat{\varphi}^2 \right) \text{sign } \varphi$$

The radius of the lateral arcs is $r_1 \approx 1.84466R$, that of the lower and upper arcs is $r_2 \approx 4.39461R$. χ and ζ can be calculated from these relations (derivation in App. K):

$$r_1 \sin \chi = y$$

$$r_2 \cos \zeta = r_2 - 0.7R\pi + y$$

In the BARANYI projections, the meridians pass through the pointed pole without break. The mapping is aphyllactic, the angular distortions are severe near the map frame, just as the areal distortions around the poles (Fig. XXIV.1). It is therefore recommended for thematics concentrating on lower latitudes. It has been used mainly for world maps in Hungarian historical atlases.

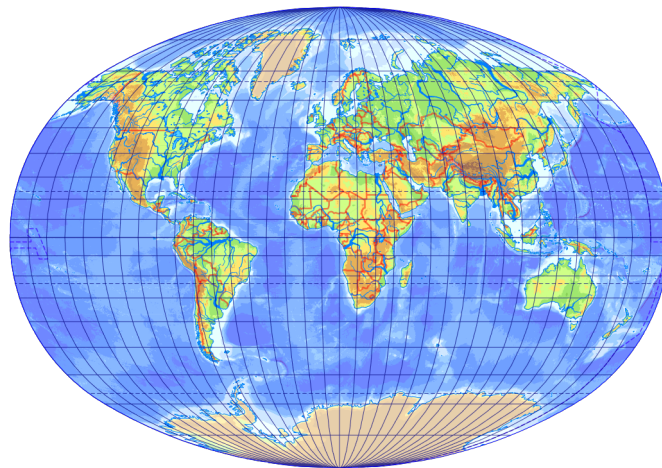


Figure XXIV.1: BARANYI II projection

The description of the BARANYI IV projection does not give any guidance on how the distances on the reference frame relate to the map scale units.

^{*} The BARANYI projections are not supported by ArcGIS, and older open source programs used VOXLAND's approximation formulæ, which differ slightly from those known in the Hungarian literature. The BARANYI projections have disappeared from QGIS into thin air.

XXIV. Modern pseudocylindrical maps

Therefore, we will start from the assumption that there is no distortion at the intersection of the Equator and the central meridian.

The map frame is formed by four arcs of circles, just as in projection II. The radius of the lateral arcs is $r_1 = 100$ units. The length of the central meridian is 222 units and that of the Equator is 368 units. By geometric considerations, the radius of the lower and upper arcs $r_2 \approx 426.23$ can be calculated from the smooth connection of the arcs. BARANYI has divided the central meridian unevenly. The middle latitudes (30° – 60°) are magnified, here the distance between the round (10°) parallels is 13 units, at lower and higher latitudes it is only 12 units. GYÖRFFY fitted a polynomial of degree nine to the values, which proved effective. The round (10°) meridians cross the Equator at 2×12 , 4×11 , 8×10 , and finally 4×9 units, respectively; the other parallels are divided in the same proportion. GYÖRFFY approximated the nature of this decrease by a logarithm.

The framing arcs join at about 96.63 units from the horizontal axis, which, when compared with the positioning of the parallels, gives $\varphi_B \approx \pm 78.07^\circ$. Since the radii of the arcs are different, a different function will give the length of the parallels on either side of the bounding parallel. The approximate formulæ are given by GYÖRFFY:

$$y = R(\widehat{\varphi} + 0.073880\widehat{\varphi}^3 - 0.0538964\widehat{\varphi}^5 + 0.01560242\widehat{\varphi}^7 - 0.001639406\widehat{\varphi}^9)$$

$$x = \frac{\ln(1 + 0.11679|\widehat{\lambda}|)}{0.31255} \operatorname{sign} \lambda \times \begin{cases} (1.22172R + \sqrt{2.115393R^2 - y^2}) & \text{if } |\varphi| \leq \varphi_B \\ \sqrt{38.4308R^2 - (4.58448R + |y|)^2} & \text{if } |\varphi| > \varphi_B \end{cases}$$

BARANYI intended his projection for economic maps by enlarging the middle latitudes, since most of the map symbols are placed in this zone. The areas beyond the polar circles and in the Pacific Ocean are severely distorted, but the lands are shown with very faithful shapes and favourable distortions (Fig. XXIV.2). For this reason, it was popular in the Hungarian atlas cartography for a long time. Because it is pointed-polar, it was often used as world maps of school atlases. If equivalency is not a requirement, it can be used as a world map. Since it is not supported by the vast majority of GIS packages, it has recently disappeared undeservedly, replaced by less favourable flat-polar projections.

BARANYI did not develop an interrupted projection in the fashion of that time. At MÁRTON'S request, however, he allowed to produce an interrupted

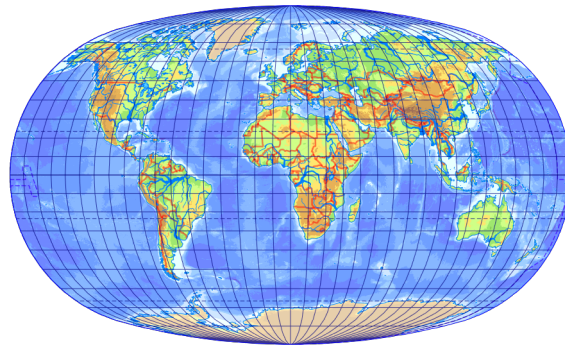


Figure XXIV.2: *BARANYI IV projection*

version of his projection IV. The purpose of the *interrupted BARANYI projection* is to show the world ocean, i.e., unlike the original BARANYI projections, lower distortions are placed in the oceans rather than on land. The projection was designed by MÁRTON, with approximate formulæ subsequently provided by GYÖRFFY. The projection was finalized in 2004.

The projection is composed of two BARANYI IV projections. The left part of the map retains the original central meridian at 10° E. This section shows the Atlantic and Indian Oceans (between 100° W and 100° E). The right part of the map shows the Pacific Ocean (between 140° W and 60° W) with a central meridian of 160° W. For the right side, $3.036131R$ must be added to the coordinate x to connect them. As shown in Fig. XXIV.3, the Americas (between 100° W and 60° W) are shown in both parts.

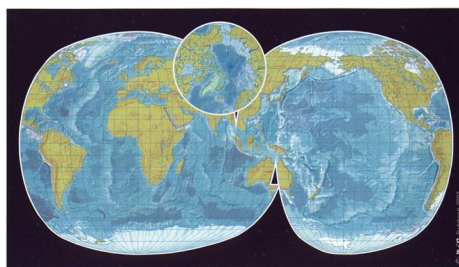


Figure XXIV.3: *Interrupted BARANYI projection (by MÁRTON)*

Between the two parts, there is a 40° wide transition zone, which is connected to the right side in the Northern Hemisphere and to the left side in the Southern Hemisphere. The area around Tasmania (south of 35° S and west of 150° E) is repeated* in the transition zone. In the transition zone, y

* Although the interrupted BARANYI projection is not the only one that represents certain parts of the area more than once, GIS packages are unable to use such projections.

is equal to that of the BARANYI IV projection, x is formulated as follows (x_l is the bounding x coordinate of the left projection substituting $\Delta\lambda = 90^\circ$, x_r is the boundary of the right projection substituting $\Delta\lambda = -60^\circ$):

$$x = \begin{cases} x_r + \left[0.332949 \left(\widehat{\lambda} + \frac{\pi}{3} \right) + 0.0123215 \left(\widehat{\lambda} + \frac{\pi}{3} \right)^2 \right] & \text{if } 0 \leq \varphi \leq \varphi_B \\ \times \left(1.22172R + \sqrt{2.115393R^2 - y^2} \right) & \\ x_r + \left[0.332949 \left(\widehat{\lambda} + \frac{\pi}{3} \right) + 0.0123215 \left(\widehat{\lambda} + \frac{\pi}{3} \right)^2 \right] & \text{if } \varphi > \varphi_B \\ \times \sqrt{38.4308R^2 - (4.58448R + |y|)^2} & \\ x_l + \left[0.315744 \left(\widehat{\lambda} - \frac{\pi}{2} \right) + 0.0123215 \left(\widehat{\lambda} - \frac{\pi}{2} \right)^2 \right] & \text{if } -\varphi_B \leq \varphi < 0 \\ \times \left(1.22172R + \sqrt{2.115393R^2 - y^2} \right) & \\ x_l + \left[0.315744 \left(\widehat{\lambda} - \frac{\pi}{2} \right) + 0.0123215 \left(\widehat{\lambda} - \frac{\pi}{2} \right)^2 \right] & \text{if } \varphi < -\varphi_B \\ \times \sqrt{38.4308R^2 - (4.58448R + |y|)^2} & \end{cases}$$

The Arctic Ocean is depicted on an inset map in the azimuthal equidistant projection. The mapped North Pole is translated to $x = 1.379854R$, $y = 1.055924R$. The frame of the inset is a circle of radius 32° , or $r = 0.558505R$, centred at 81° N, 90° W (i.e. $x = 1.240775R$, $y = 1.055924R$).

This aphyllactic projection is mainly found in oceanography textbooks and theses on oceans prepared at Eötvös Loránd University.

XXIV.2 Projections given by tables

At the same time as BARANYI, ROBINSON, who was employed at the Rand McNally company, developed his graticule following exactly the same principles. He reported the map (also known as the *orthophanic projection*) in a tabular form, so most software use some form of interpolation. BEINEKE'S

There is no way to program multiple representation. That is why such projections are only viable in Corel, their future is questionable.

approximate formula is much simpler and satisfactory for small-scale mapping purposes:

$$x = R \left(2.6666 - 0.3670\widehat{\varphi}^2 - 0.1500\widehat{\varphi}^4 + 0.0379\widehat{\varphi}^6 \right) \frac{\widehat{\lambda}}{\pi}$$

$$y = R \left(0.96047\widehat{\varphi} - 0.00857|\widehat{\varphi}|^{6.4100} \operatorname{sign} \varphi \right)$$

The projection in Fig. XXIV.4, is aphyllactic, reminiscent of the BARANYI IV projection.* Its major drawback is that it achieves similar distortion characteristics by using a flat-polar map. It is still very popular in the US, and for many years, National Geographic maps were produced in this projection.

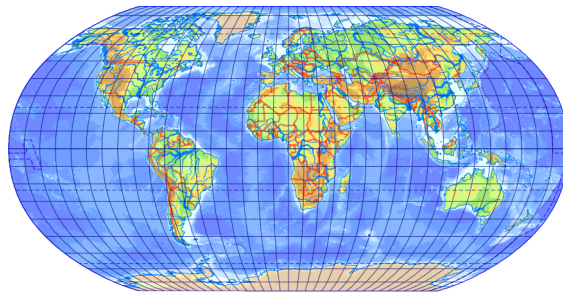


Figure XXIV.4: ROBINSON projection

The idea of ROBINSON and BARANYI was that the perception of projection distortion is subjective, and therefore subjective methods are needed to achieve favourable distortions. Although a number of studies since then have shown that the shape accuracy of continents is mathematically well-defined, it is still popular today to create projections by bypassing mathematics. The advent of the application Flex Projector has contributed significantly to the proliferation of new projections.

It is an interactive application where you can control the map with sliders. In addition to the image of the projection, the display also shows its distortions. In this way, countless interested people have been able to create (and name after themselves) new graticules. Some of them are now

* There was certainly a big quarrel when the publications appeared! Although BARANYI had published his projections as early as 1968, ROBINSON did not do so until 1974, and did not even mention BARANYI. BARANYI accused ROBINSON of plagiarism, but he claimed that he had already created his projection in 1963, and maps had been published in that projection; he therefore claimed the first place, and accused BARANYI of plagiarism. In the absence of evidence, it was never clarified who had created the first hand-drawn projection.

XXIV. Modern pseudocylindrical maps

supported by ArcGIS and QGIS. Most of the new projections are cylindrical or pseudocylindricals, but miscellaneous projections have also been created with this program. Although it is possible to create a pointed-polar map in it, the trendy mappings are all flat-polar. An example is PATTERSON's *Natural Earth* projection from 2007, for which ŠAVRIČ provided an approximate formula.

Even an *equal-area* projection was created in Flex Projector by PATTERSON, JENNY and ŠAVRIČ in 2018 called *Equal Earth*, which tries to mimic the ROBINSON projection (Fig. XXIV.5)*. An approximate mathematical description is known for it, ensuring the equivalency of the mapping.

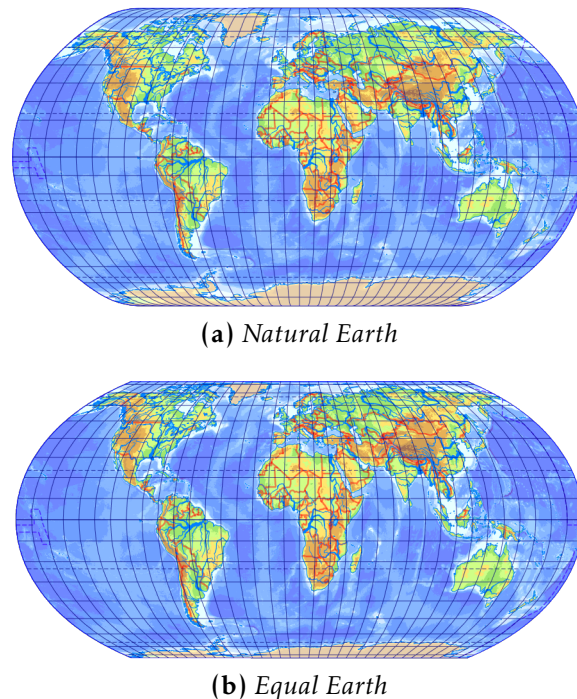


Figure XXIV.5: Maps designed in Flex Projector

Compared to the previous ones, the method of URMAYEV is closer to maths. He arbitrarily prescribed distortions at certain points on the map. From this, he obtained a system of non-linear second-order differential equations, which he solved approximately: he plotted the estimated graticule on graph paper and manually adjusted the drawing until the distortions returned by

* PATTERSON's intention *even a few years ago* was to offer a better equal-area projection than the GALL-PETERS projection. Because, yes, there are still people promoting this mapping today.

XXIV. Modern pseudocylindrical maps

cartometry were close to the expected ones. The method was widely used in the Soviet Union, most notably by GINZBURG's maps.

The GINZBURG VIII projection, created in 1949, is a pseudocylindrical mapping in which the Soviet Union is expected to have low distortion (Fig. XXIV.6). There is no angular distortion and 50% areal exaggeration at 50° N, 80° E. At latitude 28°, we expect no areal distortion, and at the intersection of the Equator and the bounding meridian, we prescribe 25% decrease. GINZBURG approximated this with the following formulæ:^{*}

$$x = R \left(1 - \frac{\widehat{\varphi}^2}{6.16} \right) \left(0.87 \widehat{\lambda} - \frac{|\widehat{\lambda}|^4 \text{sign } \lambda}{1049.95} \right)$$

$$y = R(\widehat{\varphi} + \widehat{\varphi}^3/12)$$

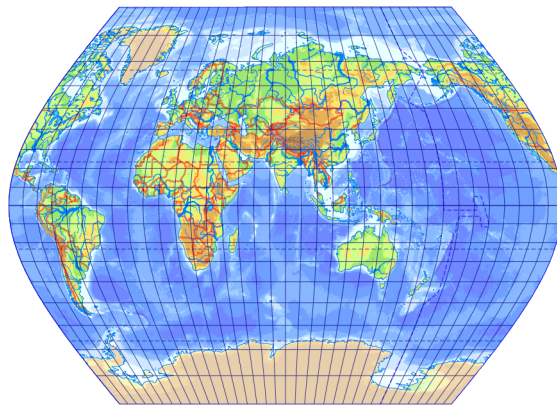


Figure XXIV.6: GINZBURG VIII projection

The mapping is aphylactic, its meridians are dense near the map frame. It was favoured by Russian cartography. Due to the cut of America, the map was continued beyond the bounding meridian, but the poles were truncated.

^{*} The formulæ used in QGIS are incorrect!

Lesson twenty-five

Pseudoconic & pseudoazimuthal mappings

XXV.1 Map projections with circular parallels

Parallels in *pseudoazimuthal*, *pseudoconic*, and *polyconic* mappings are mapped to circles or arcs of circles. We also expect reflection symmetry about axis y , so the centres of these circles fall on axis y . These projections are described using the polar coordinate system usual in conic projections, but note two differences! First, the centres of the mapped parallels are not fixed, their distance from the axis x is described by a function $c(\varphi)$, so the origin of the polar coordinates moves depending on the latitude. Second, since the meridians are neither necessarily straight nor necessarily evenly spaced, the polar angle can be an arbitrary function $\varepsilon(\varphi, \lambda)$ (due to symmetry, odd and strictly increasing in λ). The radii of parallels are still given by the radius function $\rho(\varphi)$. Fig. XXV.1 shows that the general mapping formulæ are:

$$\begin{aligned}x &= \rho \sin \varepsilon \\y &= c - \rho \cos \varepsilon\end{aligned}$$

Let us examine the distortions of such projections.

$$\begin{aligned}k &= \frac{\sqrt{\left(\frac{\partial x}{\partial \lambda}\right)^2 + \left(\frac{\partial y}{\partial \lambda}\right)^2}}{R \cos \varphi} = \frac{\sqrt{\rho^2 \cos^2 \varepsilon \left(\frac{\partial \varepsilon}{\partial \lambda}\right)^2 + \rho^2 \sin^2 \varepsilon \left(\frac{\partial \varepsilon}{\partial \lambda}\right)^2}}{R \cos \varphi} = \frac{\rho}{R \cos \varphi} \frac{\partial \varepsilon}{\partial \lambda} \\ \cot \vartheta &= \frac{\frac{\partial x}{\partial \varphi} \frac{\partial x}{\partial \lambda} + \frac{\partial y}{\partial \varphi} \frac{\partial y}{\partial \lambda}}{\frac{\partial y}{\partial \varphi} \frac{\partial x}{\partial \lambda} - \frac{\partial x}{\partial \varphi} \frac{\partial y}{\partial \lambda}} \\ &= \frac{\left(\frac{d\rho}{d\varphi} \sin \varepsilon + \rho \cos \varepsilon \frac{\partial \varepsilon}{\partial \varphi}\right) \rho \cos \varepsilon \frac{\partial \varepsilon}{\partial \lambda} + \left(\frac{dc}{d\varphi} - \frac{d\rho}{d\varphi} \cos \varepsilon + \rho \sin \varepsilon \frac{\partial \varepsilon}{\partial \varphi}\right) \rho \sin \varepsilon \frac{\partial \varepsilon}{\partial \lambda}}{\left(\frac{dc}{d\varphi} - \frac{d\rho}{d\varphi} \cos \varepsilon + \rho \sin \varepsilon \frac{\partial \varepsilon}{\partial \varphi}\right) \rho \cos \varepsilon \frac{\partial \varepsilon}{\partial \lambda} - \left(\frac{d\rho}{d\varphi} \sin \varepsilon + \rho \cos \varepsilon \frac{\partial \varepsilon}{\partial \varphi}\right) \rho \sin \varepsilon \frac{\partial \varepsilon}{\partial \lambda}}\end{aligned}$$

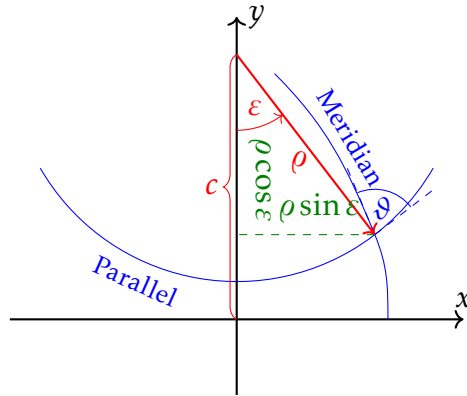


Figure XXV.1: Polar coordinates in pseudoconics and polyconics

$$\begin{aligned}
 & \rho \frac{\partial \varepsilon}{\partial \lambda} \left(\rho \frac{\partial \varepsilon}{\partial \varphi} \cos^2 \varepsilon + \frac{dc}{d\varphi} \sin \varepsilon + \rho \frac{\partial \varepsilon}{\partial \varphi} \sin^2 \varepsilon \right) = \frac{\rho \frac{\partial \varepsilon}{\partial \varphi} + \frac{dc}{d\varphi} \sin \varepsilon}{\rho \frac{\partial \varepsilon}{\partial \lambda} \left(\frac{dc}{d\varphi} \cos \varepsilon - \frac{d\rho}{d\varphi} \cos^2 \varepsilon - \frac{d\rho}{d\varphi} \sin^2 \varepsilon \right)} = \frac{\frac{dc}{d\varphi} \cos \varepsilon - \frac{d\rho}{d\varphi}}{\frac{dc}{d\varphi} \cos \varepsilon - \frac{d\rho}{d\varphi}}
 \end{aligned}$$

The linear scale in the direction of meridians can be calculated by the general formula $h = \sqrt{(\partial x / \partial \varphi)^2 + (\partial y / \partial \varphi)^2} / R$, but after performing the derivations we obtain unmanageably long formulæ. Therefore, we resort to a trick. First, we express the areal scale p . Notice that the numerator of p is the same as the denominator of $\cot \vartheta$, so we do not need to re-derive it, we can substitute the denominator we just transformed!

$$\begin{aligned}
 p &= \frac{\frac{\partial y}{\partial \varphi} \frac{\partial x}{\partial \lambda} - \frac{\partial x}{\partial \varphi} \frac{\partial y}{\partial \lambda}}{R^2 \cos \varphi} = \frac{\rho \frac{\partial \varepsilon}{\partial \lambda} \left(\frac{dc}{d\varphi} \cos \varepsilon - \frac{d\rho}{d\varphi} \cos^2 \varepsilon - \frac{d\rho}{d\varphi} \sin^2 \varepsilon \right)}{R^2 \cos \varphi} \\
 &= \frac{\rho}{R^2 \cos \varphi} \frac{\partial \varepsilon}{\partial \lambda} \left(\frac{dc}{d\varphi} \cos \varepsilon - \frac{d\rho}{d\varphi} \right)
 \end{aligned}$$

But $p = hk \sin \vartheta$:

$$\begin{aligned}
 \frac{\rho}{R^2 \cos \varphi} \frac{\partial \varepsilon}{\partial \lambda} \left(\frac{dc}{d\varphi} \cos \varepsilon - \frac{d\rho}{d\varphi} \right) &= h \frac{\rho}{R \cos \varphi} \frac{\partial \varepsilon}{\partial \lambda} \sin \vartheta \\
 h &= \frac{1}{R \sin \vartheta} \left(\frac{dc}{d\varphi} \cos \varepsilon - \frac{d\rho}{d\varphi} \right)
 \end{aligned}$$

XXV.2 Pseudoconic projections

If all the parallels are concentric arcs of circles, then the non-conical mapping is classified as a *pseudoconic projection*. In these projections, c is

constant, so we can omit the term containing the derivative of c in the formula for $\cot \vartheta$:

$$\cot \vartheta = -\rho \frac{\partial \varepsilon}{\partial \varphi} \bigg/ \frac{d\rho}{d\varphi}$$

In a rectangular projection, either ρ or $\partial \varepsilon / \partial \varphi$ must be zero. In the former case the map would collapse to a single point, in the latter case the meridians would be straight, which would lead to a conic projection. Thus, *there is no rectangular, and hence no conformal mapping among pseudoconics*. Furthermore, h is also simplified:

$$h = -\frac{d\rho}{d\varphi} \frac{1}{R \sin \vartheta}$$

From this:

$$p = hk \sin \vartheta = -\frac{d\rho}{d\varphi} \frac{1}{\sin \vartheta} \frac{\rho}{\cos \varphi} \frac{\partial \varepsilon}{\partial \lambda} \frac{\sin \vartheta}{RR} = -\frac{\rho}{R^2 \cos \varphi} \frac{\partial \varepsilon}{\partial \lambda} \frac{d\rho}{d\varphi}$$

In equal-area projections, $p = 1$, so:

$$-\frac{\rho}{R^2 \cos \varphi} \frac{\partial \varepsilon}{\partial \lambda} \frac{d\rho}{d\varphi} = 1$$

$$\frac{\partial \varepsilon}{\partial \lambda} = -R^2 \frac{\cos \varphi}{\rho \frac{d\rho}{d\varphi}}$$

On the right-hand side, there are functions of φ only, i.e. the partial derivative of ε is independent of λ . This implies that ε is a linear function of λ , and *in equal-area pseudoconic mappings, the parallels are evenly divided by the meridians (parallels have constant scale)*.

Find a pseudoconic mapping that is equidistant in the central meridian and in all parallels! From the equidistant central meridian, $-d\rho/d\varphi = R$:

$$\rho = R(-\widehat{\varphi} + d) = R(d - \widehat{\varphi})$$

$k = 1$, so:

$$\frac{\rho}{R \cos \varphi} \frac{\partial \varepsilon}{\partial \lambda} = 1$$

$$\int d\varepsilon = \int \frac{\cos \varphi}{d - \widehat{\varphi}} d\lambda$$

$$\widehat{\varepsilon} = \frac{\cos \varphi}{d - \widehat{\varphi}} \widehat{\lambda} + f(\varphi)$$

The symmetry about the central meridian is satisfied if $f(\varphi) = 0$, so the constant of integration can be ignored. Substituting $\varphi = \pm 90^\circ$ we get

$\varepsilon = 0$, i.e. the projection is pointed-polar. Let us examine the distortions, remembering that $k = 1$:

$$h = -\frac{d\rho}{d\varphi} \frac{1}{R \sin \vartheta} = \frac{1}{\sin \vartheta}$$

$$\cot \vartheta = -\rho \frac{\partial \varepsilon}{\partial \varphi} \bigg/ \frac{d\rho}{d\varphi} = \frac{R(d - \widehat{\varphi}) - \sin \varphi(-\widehat{\varphi} + d) + \cos \varphi \widehat{\lambda}}{R(d - \widehat{\varphi})^2} \widehat{\lambda}$$

$$= \frac{-\sin \varphi(d - \widehat{\varphi}) + \cos \varphi \widehat{\lambda}}{d - \widehat{\varphi}}$$

Our first observation is that $hk \sin \vartheta = 1$, so we have an equal-area projection. We can also see that the central meridian is true-scale ($h = k = 1$ and $\cot \vartheta = 0$), but as we depart, angular distortion increases rapidly. Could we expect a standard parallel φ_s to be true-scale? To do so, it is sufficient to solve the equation $\cot \vartheta = 0$ at $\varphi = \varphi_s$, since then $\sin \vartheta = 1$, i.e. it is guaranteed that $h = k = 1$:

$$\frac{-\sin \varphi_s(-\widehat{\varphi}_s + d) + \cos \varphi_s \widehat{\lambda}}{-\widehat{\varphi}_s + d} \widehat{\lambda} = 0$$

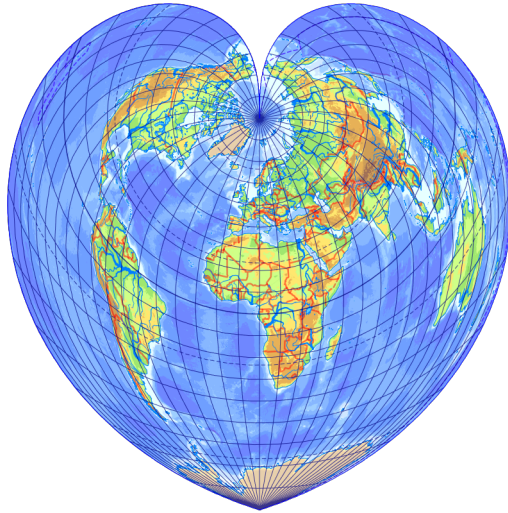
$$\cos \varphi_s = \sin \varphi_s(-\widehat{\varphi}_s + d)$$

$$d = \cot \varphi_s + \widehat{\varphi}_s$$

In other words, the projection has a standard parallel, the position of which can be controlled by choosing the constant of integration d . If $\varphi_s = 90^\circ$, i.e. $d = \pi/2$, the mapping is called the WERNER or STAB projection (Fig. XXV.2). Its exact authorship is unknown, its eponyms applied it in the early 1500s. A feature of the projection is that the Earth is represented in a shape of a heart. For $\varphi_s = 0^\circ$, $d \rightarrow \infty$, $\rho \rightarrow \infty$, i.e. the parallels are straight, and the sinusoidal projection is obtained.

By choosing φ_s differently, we are talking about the BONNE projection. It was developed gradually from the PTOLEMY II projection making more parallels equidistant in the 1400s, so it is the oldest equal-area mapping. Although it is favourable in the cross-shaped area defined by the central meridian and the standard parallel, further away the angular distortions are very unfavourable, even worse than the equal-area conic projection. Nevertheless, this mapping is overused for continental maps. The French even used it on topographic maps before the Second World War, although it is not quite conformal. They suffered with it. Due to its topographic use,

XXV. Pseudoconic & pseudoazimuthal mappings



(a) $\varphi_s = 90^\circ$ (WERNER projection)



(b) $\varphi_s = 45^\circ$

Figure XXV.2: BONNE projection

ellipsoidal formulæ are also known, which are similarly derived from the equidistant central meridian and parallels:

$$\rho = N(\Phi_s) \cot \Phi_s - \int_{\Phi_s}^{\Phi} M(\Phi) d\Phi$$

$$\widehat{\varepsilon} = \frac{N(\Phi) \cos \Phi}{\rho} \widehat{\Lambda}$$

Other pseudoconics have also been developed, which are also mostly equal-area, but almost no one knows them. These flat-polar mappings, which are not used at all, are recommended for areas of large east-west extent at middle latitudes. Some of them are also suitable for representing the whole Earth.* Unlike the BONNE projection, these have very low distortion.

XXV.3 Pseudoazimuthal projections

If the mapped parallels are complete concentric circles, then we are talking about a *pseudoazimuthal projection*. Since every parallel is mapped to a circle, the infinitesimal circle centred at the pole is also mapped to a circle. This implies that the pseudoazimuthal mappings are locally conformal at the pole. An advantage is that the representation is interrupted at only one point. In contrast to azimuthal projections, isocols have an oval shape, and are therefore chosen for areas of this shape. The projection is favourable near the pole, so we use the colatitude $\delta = 90^\circ - \varphi$ instead of the latitude in the formulæ.

Because parallels are closed in pseudoazimuthals, it is true for any λ that $\varepsilon(\delta, \lambda) = \varepsilon(\delta, \lambda + 360^\circ) - 360^\circ$ (i.e., by moving the longitude by one turn around the parallel, ε also changes one turn). Therefore, a projection can be pseudoazimuthal if angle $\varepsilon - \lambda$ is a periodic function of λ with period 360° .

Due to the concentricity of mapped parallels, we can use the simpler distortion formulæ we have seen for pseudoconic projections. From these formulæ, we have already established that, if a rectangular graticule is desired, the meridians would be straight, so *no conformal mapping is found among pseudoazimuthals*, too. From the equation for equivalency, we have found that the necessary condition for an equal-area map is that ε is a linear function of λ . However, $\varepsilon - \lambda$ can only be periodic at the same

* For example, the HILL projection, a generalization of the ECKERT IV projection, is one of the best projections for the equal-area representation of the Earth.

XXV. Pseudoconic & pseudoazimuthal mappings

time if $\varepsilon - \lambda$ is constant (or to be more precise, it is a function of δ only). Since $\varepsilon - \lambda$ is an odd function due to the requirement of symmetry, the only possible constant is $\varepsilon - \lambda = 0$. This leads to $\varepsilon = \lambda$, i.e. we found an azimuthal mapping. Because of the contradiction, *there is no equal-area pseudoazimuthal projection.*^{*}

Note that, in most cases, we expect reflection symmetry not only about the vertical axis but also about the horizontal axis among pseudoazimuthal mappings. Omitting derivation, we find that in this case, angle $\varepsilon - \lambda$ can be chosen as an odd function with period 180° .

The GINZBURG III projection is a pseudoazimuthal mapping, which uses radius function of GINZBURG's azimuthal projection (Sec. XI.3):

$$\rho = 3R \sin \frac{\delta}{3}$$

Since $\varepsilon - \lambda$ is a periodic odd function, GINZBURG proposed the formula $\widehat{\varepsilon} - \widehat{\lambda} = f(\delta) \sin(\kappa \lambda)$. If $\kappa = 1$, the period is 360° and the projection has a single symmetry; in the case of $\kappa = 2$, the period is 180° , so it is symmetrical about the horizontal axis. Substituting GINZBURG's proposal for $f(\delta)$:

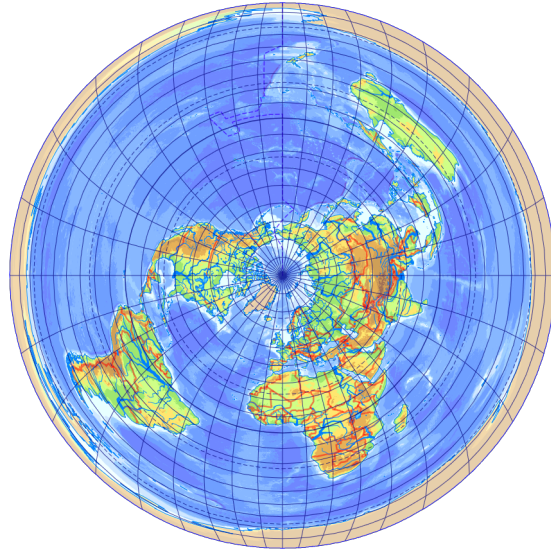
$$\widehat{\varepsilon} = \widehat{\lambda} - d \left(\frac{\delta}{\delta_B} \right)^q \sin(\kappa \lambda)$$

Here, q is 1 or 2, controlling the change in the curvature of meridians, $0.002 \leq d \leq 0.2$ is the magnitude of the curvature of meridians, and δ_B is the bounding colatitude.

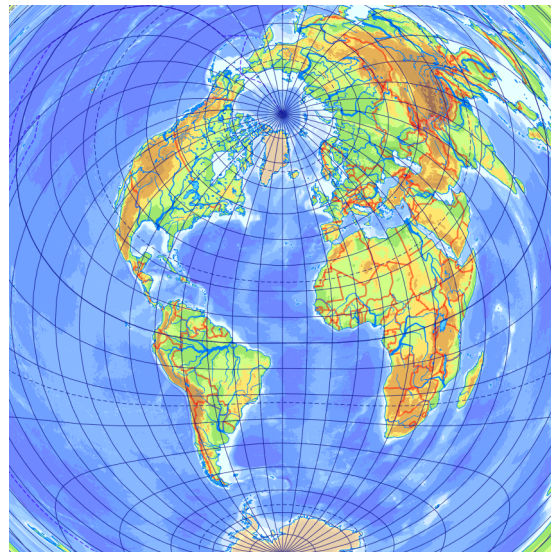
The projection was published in 1952, its isocols are oval, recommended for areas of this shape. Since it shows the vicinity of the metapole favourably, it is not commonly used in normal aspect. It is used in first transverse and simple oblique aspect on Russian maps of the Atlantic Ocean (Fig. XXV.3). On maps of the European part of Russia, we find the version equidistant in the central meridian ($\rho = R\delta$) in simple oblique aspect. It has also been used for world maps (without Antarctica) in skew aspect. Due to language barriers and complexity, it could not be widespread outside the former Eastern Bloc countries.

^{*} If we release our expectation of symmetry, it is possible to construct an equal-area pseudoazimuthal. For example, the WIECHEL projection is both equal-area and equidistant in meridians, but has no cartographic value because of its significant angular distortions and lack of symmetry.

XXV. Pseudoconic & pseudoazimuthal mappings



(a) Normal



(b) Simple oblique (Atlantic Ocean)

Figure XXV.3: GINZBURG III projection

Lesson twenty-six

Polyconic projections

XXVI.1 Properties of polyconic projections

We know that the environment of a parallel can be favourably represented in conic projections. Let us map the small environment of each parallel with a tangent perspective conic projection. By refining the infinitesimal partitions, the gaps between the conic projections become infinitely small, yielding a *polyconic projection* as a limit (Fig. XXVI.1).

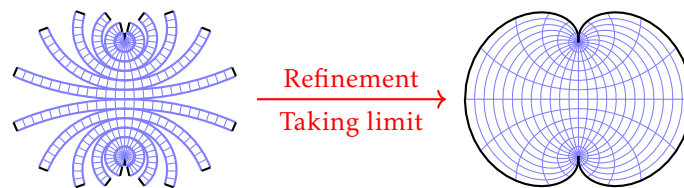


Figure XXVI.1: Origin of polyconic projections

Let us examine the resulting projection. Each parallel is mapped in its corresponding tangent perspective conic projection. In Sec. XV.2, we calculated that these mappings map the tangent parallel to an arc of radius $\rho = R \cot \varphi$, so our projection has circular parallels. In order to stitch the maps, the mapped spherical zones had to be translated vertically, so the mapped parallels are not concentric, so it is not a pseudoconic projection. On the other hand, linear scale in the direction of the meridians is unit on the tangent parallels of the perspective conic projections, so the seamlessly fitting central meridian is certainly equidistant.

Although it would follow from the derivation that the parallels are equidistant, this is not always required in practice. Similarly, the radius function can be multiplied by a constant S_n and the linear scale along the central meridian by a constant S_m to fine-tune the distortions, although these are usually chosen to be 1. Accordingly, we call *polyconic projections* those mappings in which the parallels are arcs of circles, their radii are proportional to the cotangent of the latitude, and they divide the central meridian evenly.

Expressing the same mathematically using the polar coordinates of Sec. XXV.1:

$$\begin{aligned}\rho &= S_n R \cot \varphi \\ c &= S_m R \widehat{\varphi} + \rho\end{aligned}$$

If the above condition is not satisfied by a projection that maps parallels to eccentric arcs, the mapping is classified as a *pseudopolyconic projection*. The distortions of both polyconic and pseudopolyconic projections can be computed from the general formulæ for projections with circular parallels. The polyconic projections are suitable for areas extending along a meridian. Although transverse cylindrical projections are also appropriate for this purpose, it was easier to construct the circular parallels of polyconic projections with a pair of compasses.

As polyconic projections are more commonly used on regional maps, they are rather used with an ellipsoid as the reference frame. The definition of polyconic projections is then slightly modified:

$$\begin{aligned}\rho &= S_n N(\Phi) \cot \Phi \\ c &= \rho + S_m \int_0^{\Phi} M(\Phi) d\Phi\end{aligned}$$

XXVI.2 American polyconic

Specifically, for the mapping known as the *simple*, the *ordinary*, or the *American polyconic projection*, we expect the previously mentioned equidistancy of parallels ($k = 1$):

$$\begin{aligned}\frac{\rho}{R \cos \varphi} \frac{d\varepsilon}{d\lambda} &= 1 \\ \int d\varepsilon &= \int \frac{\cos \varphi}{S_n \cot \varphi} d\lambda \\ \widehat{\varepsilon} &= \frac{\widehat{\lambda} \sin \varphi}{S_n} + f(\varphi)\end{aligned}$$

Due to the symmetry about the central meridian, the constant of integration $f(\varphi)$ is zero. The projection formulæ are indeterminate at the

Equator, but here, $y = 0$ and the from the equidistant parallels (and hence equidistant Equator), $x = R\widehat{\lambda}$. Distortions of the projection:

$$h = \frac{1}{R \sin \vartheta} \left(\frac{dc}{d\varphi} \cos \varepsilon - \frac{d\rho}{d\varphi} \right) = \frac{\left(S_m - \frac{S_n}{\sin^2 \varphi} \right) \cos \varepsilon + \frac{S_n}{\sin^2 \varphi}}{\sin \vartheta}$$

$$\cot \vartheta = \frac{\rho \frac{d\varepsilon}{d\varphi} + \frac{dc}{d\varphi} \sin \varepsilon}{\frac{dc}{d\varphi} \cos \varepsilon - \frac{d\rho}{d\varphi}} = \frac{\widehat{\lambda} \cot \varphi \cos \varphi + \left(S_m - \frac{S_n}{\sin^2 \varphi} \right) \sin \varepsilon}{\left(S_m - \frac{S_n}{\sin^2 \varphi} \right) \cos \varepsilon + \frac{S_n}{\sin^2 \varphi}}$$

Since $hk \sin \vartheta \neq 1$ and $\cot \vartheta \neq 0$, the projection is aphyllactic. The formulæ and Fig. XXVI.2 show that the distortions worsen rapidly away from the central meridian.

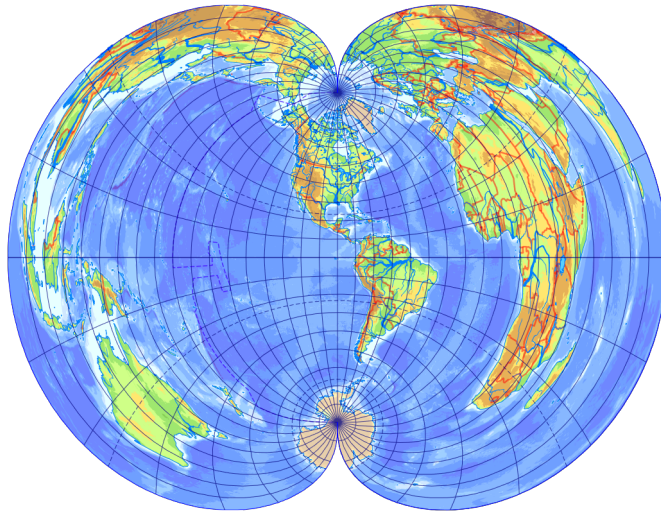
The formula for the ellipsoidal version is given by the equidistant parallels:

$$\widehat{\varepsilon} = \frac{\widehat{\Lambda} \sin \Phi}{S_n}$$

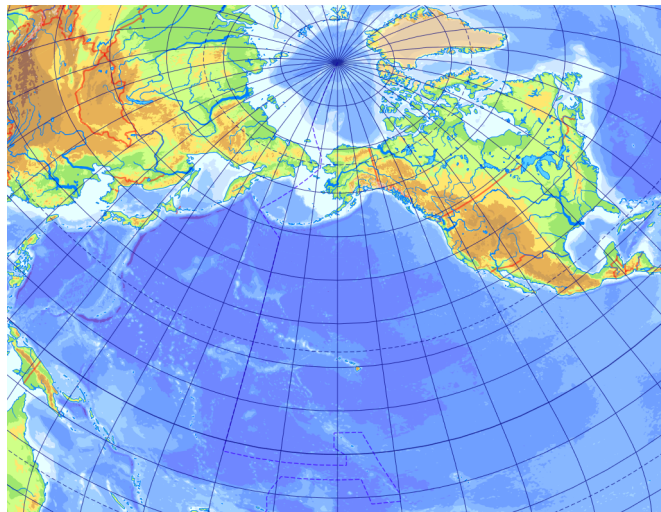
The idea of the polyconic projection was introduced in 1825 by HASSLER, a Swiss geodesist who had migrated to America. The projection quickly caught on in the USA, continental maps were produced in it, and between the two world wars it was even used for topographic maps. At DEETZ's suggestion, it appears also in oblique transverse aspect, suitable for areas of large east-west extent.

The American polyconic is similar to the *modified polyconic projection* of the French geodesist LALLEMAND, which was used for the International Map of the World with CLARKE 1880 ellipsoid as the reference frame between 1911 and 1962. Each section is mapped in its own mapping like the polyhedral projection.

For ease of construction, only the round 4° parallels bounding the sections are expected to be equidistant, with meridians running straight between them. The central meridian, unlike the polyconic projections, is not equidistant, instead the formula for c is determined by the condition that the meridians at two thirds of the bounding meridian ($\pm 2^\circ$ in the spherical zone up to $\pm 60^\circ$, $\pm 4^\circ$ up to $\pm 76^\circ$, and $\pm 8^\circ$ up to $\pm 84^\circ$) are equidistant. The hard-to-compute mathematical description of the mapping originally described as a construction is given in App. L.



(a) Normal



(b) Oblique transverse (Northern Pacific Ocean)

Figure XXVI.2: Ordinary (American) polyconic

XXVI.3 Rectangular polyconic

Our goal now is the perpendicular graticule ($\cot \vartheta = 0$):

$$\begin{aligned} \frac{\rho \frac{\partial \varepsilon}{\partial \varphi} + \frac{dc}{d\varphi} \sin \varepsilon}{\frac{dc}{d\varphi} \cos \varepsilon - \frac{d\rho}{d\varphi}} &= 0 \\ S_n R \cot \varphi \frac{\partial \varepsilon}{\partial \varphi} &= - \left(S_m R - \frac{S_n R}{\sin^2 \varphi} \right) \sin \varepsilon \\ \int \frac{1}{\sin \varepsilon} d\varepsilon &= \int \frac{S_m - \sin \varphi}{S_n \cos \varphi} - \frac{-1}{\sin^2 \varphi \cot \varphi} d\varphi \\ \ln \tan \frac{\varepsilon}{2} &= \frac{S_m}{S_n} \ln \cos \varphi - \ln \cot \varphi + \ln f(\lambda) \\ \tan \frac{\varepsilon}{2} &= f(\lambda) \cos^{\frac{S_m}{S_n}} \varphi \tan \varphi \end{aligned}$$

Here, the constant of integration $f(\lambda)$ is arbitrary. For example, let latitude φ_s be equidistant!

$$\begin{aligned} \frac{\rho}{R \cos \varphi_s} \frac{\partial \varepsilon}{\partial \lambda} &= 1 \\ \int d\varepsilon &= \int \frac{\cos \varphi_s}{S_n \cot \varphi_s} d\lambda \\ \widehat{\varepsilon} &= \frac{\sin \varphi_s}{S_n} \widehat{\lambda} \\ \tan \frac{\varepsilon}{2} &= \tan \frac{\lambda \sin \varphi_s}{2S_n} \\ f(\lambda) \cos^{\frac{S_m}{S_n}} \varphi_s \tan \varphi_s &= \tan \frac{\lambda \sin \varphi_s}{2S_n} \\ f(\lambda) &= \frac{\tan \frac{\lambda \sin \varphi_s}{2S_n}}{\cos^{\frac{S_m}{S_n}} \varphi_s \tan \varphi_s} \end{aligned}$$

The equations are indeterminate at the Equator, but here $y = 0$ and $x = 2S_n R f(\lambda)$. From this, we get that the Equator is equidistant if:

$$f(\lambda) = \frac{\widehat{\lambda}}{2S_n}$$

If the projection is rectangular, could not we choose an $f(\lambda)$ that makes the projection conformal? Unfortunately, substitution into the equation $h = k$ does not give a solution,* *there is no conformal polyconic projection.*†

This projection was used rather in its ellipsoidal form:

$$\tan \frac{\varepsilon}{2} = f(\Lambda) \sin \Phi \left[\frac{N(\Phi) \cos \Phi}{a} \right]^{\frac{S_m}{S_n} - 1}$$

Where the mapping obtained by choosing $S_m = S_n = 1$ and $f(\Lambda) = \widehat{\Lambda}/2$ (the latter provides the equidistant Equator) is known as the *War Office projection*. This projection is also aphyllactic, with a true-scale central meridian (Fig. XXVI.3).

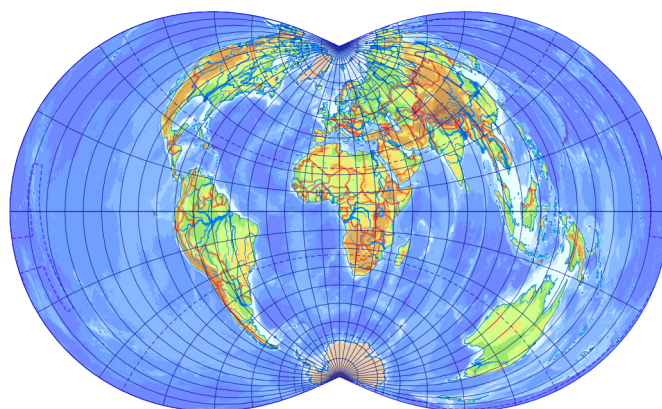


Figure XXVI.3: *War Office projection*

The War Office projection was first mentioned in the USA in 1853 as an improvement on the ordinary polyconic projection. Nevertheless, it was popularized by British military topography, hence its name. Its graticule is very easy to construct with a pair of compasses.

Canadian cartographers mapped their country in LAMBERT conformal conic projection with $\Phi_1 = 49^\circ$, $\Phi_2 = 77^\circ$. As is well known, this projection is not conformal at the pole, and at high latitudes its areal distortion approaches infinity. Therefore, another projection had to be chosen to represent the northern part of Canada ($\Phi > 80^\circ$). BOUSFIELD selected the

* However, a chosen parallel φ_s can be made conformal by this method. This idea comes from the British geodesist McCaw.

† Unfortunately, the transverse stereographic projection is also called the conformal polyconic projection. However, besides being an azimuthal mapping, it cannot be called polyconic simply because, although $\rho = \cot \varphi$ is satisfied, its central meridian is not equidistant.

rectangular polyconic projection. In order to fit the map to the adjacent parts using the conic projection, $S_n \approx 1.1164$ and $S_m \approx 1.0211$ were given, and a function $f(\Lambda)$ had to be picked that would provide the same constant linear scale $k(\Phi = 80^\circ) \approx 1.0211$ along the boundary as the conic projection. The projection formulæ of the graticule originally described as a construction were given by HAINES.

XXVI.4 Equal-area polyconic

It occurred to the German cartographer MAURER in 1935, while he was working on the taxonomy of map projections, that no equal-area polyconic projection was known. He created this mapping to solve this problem.

We assume that $p = 1$:

$$\begin{aligned} \frac{\rho}{R^2 \cos \varphi} \frac{\partial \varepsilon}{\partial \lambda} \left(\frac{dc}{d\varphi} \cos \varepsilon - \frac{d\rho}{d\varphi} \right) &= 1 \\ \int \frac{S_n R \cot \varphi}{R^2 \cos \varphi} \left[\left(S_m R - \frac{S_n R}{\sin^2 \varphi} \right) \cos \varepsilon + \frac{S_n R}{\sin^2 \varphi} \right] d\varepsilon &= \int d\lambda \\ \left(\frac{S_m S_n}{\sin \varphi} - \frac{S_n^2}{\sin^3 \varphi} \right) \sin \varepsilon + \frac{S_n^2}{\sin^3 \varphi} \widehat{\varepsilon} &= \widehat{\lambda} + f(\varphi) \end{aligned}$$

ε cannot be expressed from the equation above, we have an implicit function. The constant of integration $f(\varphi)$ is zero, otherwise the symmetry of the projection would not be guaranteed.

The projection shown in Fig. XXVI.4 is not only rather difficult to compute, it is among the worst possible choices for a world map, but it is surprisingly favourable for representing narrow areas extending along a meridian. It is interesting that along the Equator, expression of coordinate x requires the solution of a cubic equation ($x^3/6S_n R^2 + S_m x - R\widehat{\lambda} = 0$).

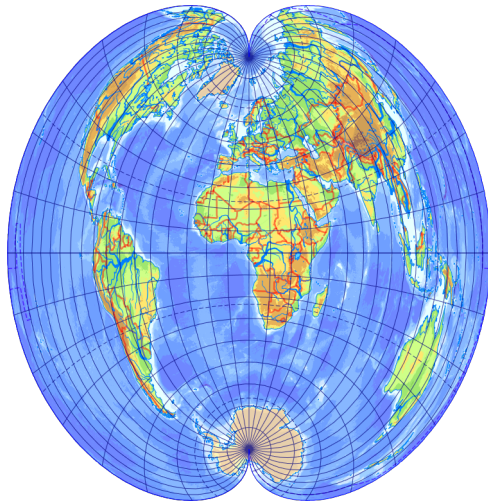


Figure XXVI.4: *Equal-area polyconic*

Lesson twenty-seven

Pseudopolyconic projections

XXVII.1 LAGRANGE projection

Let us start with the MERCATOR projection equidistant along the Equator! Reduce the map by a scale factor κ , then project it back to the sphere using the inverse MERCATOR projection. On the new sphere, the latitude is denoted by ψ and the longitude by ζ :

$$\ln \tan\left(45^\circ + \frac{\psi}{2}\right) = \kappa \ln \tan\left(45^\circ + \frac{\varphi}{2}\right)$$
$$\zeta = \kappa \lambda$$

It can be seen that the parallels are mapped to parallels on the new sphere, while meridians are also mapped to meridians. If $\kappa < 1$, then the map will not fill the entire surface of the new sphere. Nevertheless, the mapping is conformal, since both the MERCATOR projection, its inverse, and the scaling are conformal.* From the formula above, ψ can be expressed, but in practice the following equivalent formula is used instead:

$$\psi = \arcsin \frac{(1 + \sin \varphi)^\kappa - (1 - \sin \varphi)^\kappa}{(1 + \sin \varphi)^\kappa + (1 - \sin \varphi)^\kappa}$$

One can consider this transformation as a conformal variant of the *Umbeziffern* on the sphere. That is, if we substitute the renumbered coordinates ψ and ζ for φ and λ in a conformal projection, the mapping remains

* According to an anecdote, GILBERT created a conformal globe that used $\kappa = 1/2$ to represent the surface of the globe on a hemisphere so that each continent was represented twice on the entire globe. It is said that he regularly teased colleagues who came to see him to check if they noticed anything unusual about the globe, but almost no one noticed anything despite the large areal distortions of the transformation.

XXVII. Pseudopolyconic projections

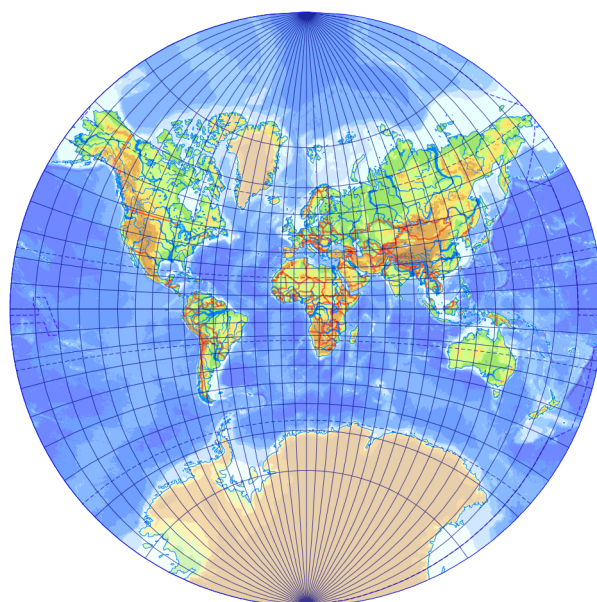
conformal. As an example, let us choose the transverse stereographic projection. Substitute $\varphi_0 = 0^\circ$ in the formula from Sec. X.5 and then renumber the graticule:

$$x = \frac{2R}{\kappa} \frac{\sin \zeta \cos \psi}{1 + \cos \psi \cos \zeta}$$

$$y = \frac{2R}{\kappa} \frac{\sin \psi}{1 + \cos \psi \cos \zeta}$$

Here, the division by κ is not necessary, only the reduction in areas due to the scaling of the MERCATOR projection was compensated by scaling it back. Since the stereographic projection preserves circles, the renumbered graticule lines (which do not wrap around the entire sphere due to the renumbering) are mapped to arcs of circles. The set of projections that map all the graticule lines to arcs of circles is called the *LAGRANGE projection family*. They were significant because it was easy to construct them with a pair of compasses. Since the mapped parallels are usually not concentric in such projections, and their radius function is not proportional to the cotangent of the latitude, they belong to the pseudopolyconic projections.

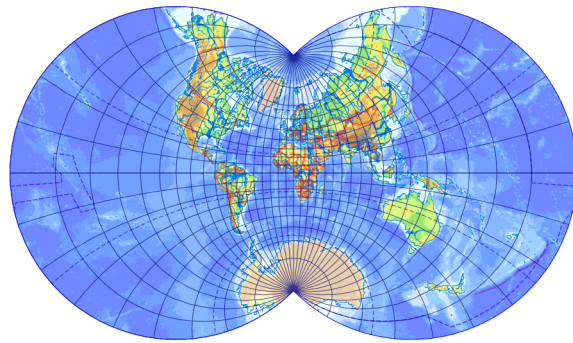
The particular mapping just derived is called the *LAGRANGE projection*. Its significance is that it is the only existing conformal pseudopolyconic



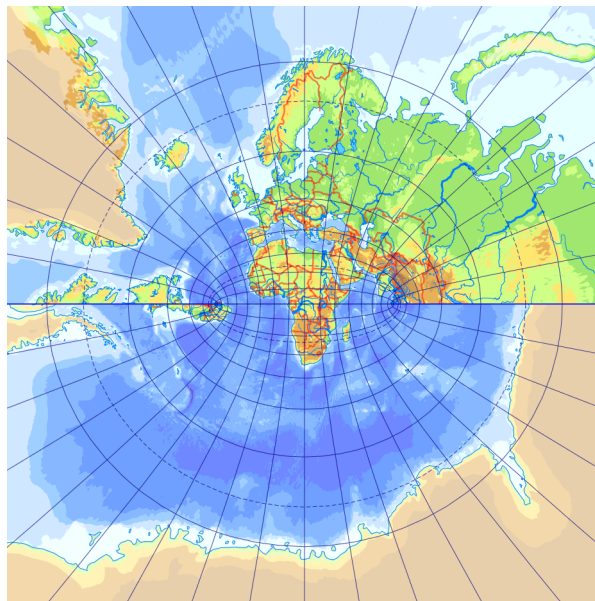
(a) $\kappa = 1/2$

Figure XXVII.1: *LAGRANGE projection*

XXVII. Pseudopolyconic projections



(b) $\alpha = 3/4$



(c) $\alpha = 2$, second transverse (LITROW projection)

Figure XXVII.1: (contd.)

projection.* The projection is not conformal at the poles, the mapped angle formed by the meridians starting here is κ times the original difference in longitude; the linear scale here is infinite for $\kappa < 1$ and zero for $\kappa > 1$. For $\kappa = 1$, the renumbering does not change anything, so the projection remains transverse stereographic. The choice $\kappa = 1/2$ represents the Earth in a circle (Fig. XXVII.1). The projection was derived by LAMBERT in 1772 and generalized for the ellipsoid by the French mathematician LAGRANGE in 1779. The ellipsoidal version of the projection is easily obtained by choosing the ellipsoidal MERCATOR projection instead of the spherical one, but after rescaling, projecting back to a sphere by using the spherical inverse. The version $\kappa = 2$ in second transverse aspect (mapped parallels are confocal ellipses, mapped meridians are hyperbolæ) is called the LITTRON projection[†] after the Austrian astronomer who created it, and has been known since 1833.

XXVII.2 Maps with circular graticule

Let us examine the general formulæ of the LAGRANGE projection family. The mapped parallels are eccentric circles, their radius is ρ , and their centre is on the positive half of the axis y at a distance c . The radius of the mapped meridians is r , their centre is on the axis x at coordinate d . In Fig. XXVII.3, for the right triangle bounded by the two axes and the section s :

$$s = \sqrt{c^2 + d^2}$$

$$\tan \sigma = \frac{-d}{c}$$

To calculate σ , the function `atan2` is recommended. In the red triangle, all three sides are known, so the law of cosines can be written for the angles

* This claim has been proved by ADAMS, and is omitted because of the complexity of the derivation. In fact, if we allow a vertical translation in the MERCATOR projection before projecting back, the mapping can be further generalized: the conformality and the circular shape of the graticule lines are preserved, but the another parallel is mapped to a straight line instead of the Equator.

[†] The LITTRON projection is a real curiosity. Although we have derived it as the second transverse aspect of another projection, its formulæ ($x = R \sin \lambda / \cos \varphi$, $y = R \cos \lambda \tan \varphi$) are no more complicated than that of the normal aspect. So which aspect is normal? Since LITTRON first derived the one shown in the figure, we can legitimately consider it as normal and the LAGRANGE projection of choice $\kappa = 2$ as the first transverse of the LITTRON projection. But then we can no longer classify it as a pseudopolyconic projection, because in normal aspect, its graticule lines are ellipses and hyperbolæ!

XXVII. Pseudopolyconic projections

$\sigma + \varepsilon$ and μ . Since $\mu = 90^\circ - (\sigma + \zeta)$, we can write $\sin(\sigma + \zeta)$ instead of $\cos \mu$. From these, we can easily express the unknown angles ε and ζ :

$$\begin{aligned} r^2 &= s^2 + \rho^2 - 2s\rho \cos(\sigma + \varepsilon) \\ \varepsilon &= \pm \arccos \frac{s^2 + \rho^2 - r^2}{2s\rho} - \sigma \\ \rho^2 &= s^2 + r^2 - 2sr \sin(\sigma + \zeta) \\ \zeta &= \pm \arcsin \frac{s^2 + r^2 - \rho^2}{2sr} - \sigma \end{aligned}$$

From the figure, x and y can be calculated:

$$\begin{aligned} x &= \rho \sin \varepsilon \\ y &= r \sin \zeta \end{aligned}$$

The earlier such projections belonged to the globular projections known from Sec. XX.2, i.e. they mapped the hemisphere into a circular frame. For example, the NICOLOSI projection is an improvement of the APIAN I projection, in which he replaced straight parallels by arcs of circles that intersect not only the meridian but also the circumference evenly. When applied to a hemisphere, the projection has favourable distortions, approaching the transverse azimuthal equidistant, and was therefore often used before the advent of computers. When extended to a full sphere, it represents the Earth in an apple-shaped frame (Fig. XXVII.2).

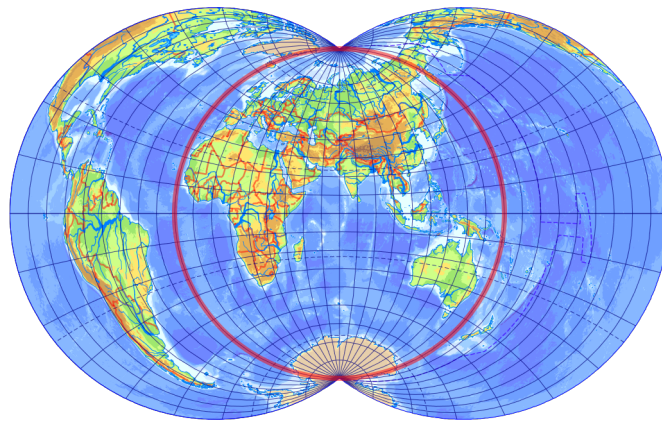


Figure XXVII.2: Nicolosi projection (globular projection is in red)

Based on the globular projections, German cartographer VAN DER GRINTEN, living in the USA, created two pseudopolyconic projections for the

XXVII. Pseudopolyconic projections

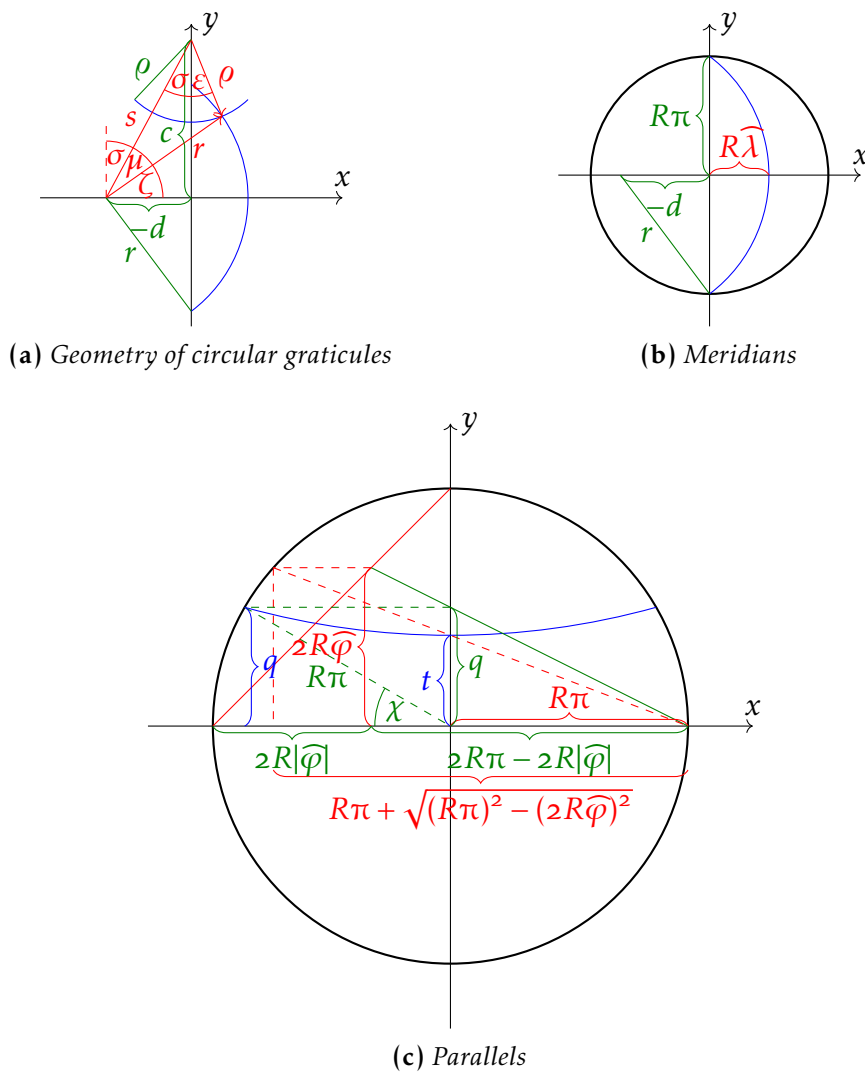


Figure XXVII.3: Construction of the VAN DER GRINTEN I projection

publisher Rand McNally.* Of these, only projection I, created in 1898, has been widely disseminated. This projection shows the entire surface of the sphere in a circular outline. Although the areal distortion of the aphylactic projection is very significant, even National Geographic used this mapping before the ROBINSON projection. Because of the large areal distortion, the map is difficult to fit on a sheet of A/4 paper, so high latitudes are often cut off, losing the only advantage, the circular frame of the projection. It is a curiosity of map projections that the rectangular map frame is often filled with repeated areas beyond longitude 180° , thus completely eliminating the only possible sense of projection.

Mapped meridians are arcs of circles centred at $(d, 0)$:

$$(x - d)^2 + y^2 = r^2$$

The frame of the projection is a circle of radius $R\pi$, the Equator is equidistant. Hence, $d = R\widehat{\lambda} - r$. Furthermore, the meridians pass through the point $(0, R\pi)$:

$$\begin{aligned} (0 + r - R\widehat{\lambda})^2 + (R\pi)^2 &= r^2 \\ r &= R \frac{\widehat{\lambda}^2 + \pi^2}{2\widehat{\lambda}} \end{aligned}$$

The parallels are mapped to arcs of circles centred at $(0, c)$:

$$x^2 + (y - c)^2 = \rho^2$$

The parallels intersect axis y at the point $y = t$, the construction of which is shown by a red dashed line in the figure. Since the framing circle has radius $R\pi$, the point $2R\widehat{\varphi}$ from axis x is $\sqrt{(R\pi)^2 - (2R\widehat{\varphi})^2}$ from axis y . Expressing the ratio between the legs of the two similar right triangles with red dashed hypotenuses, then expanding the fraction by $\pi - \sqrt{\pi^2 - (2\widehat{\varphi})^2}$:

$$\begin{aligned} \frac{t}{R\pi} &= \frac{2R\widehat{\varphi}}{R\pi + \sqrt{(R\pi)^2 - (2R\widehat{\varphi})^2}} \\ t &= R\pi \frac{2\widehat{\varphi}[\pi - \sqrt{\pi^2 - (2\widehat{\varphi})^2}]}{\pi^2 - \pi^2 + (2\widehat{\varphi})^2} = R\pi \frac{\pi - \sqrt{\pi^2 - (2\widehat{\varphi})^2}}{2\widehat{\varphi}} \end{aligned}$$

* Four projections are mentioned in the literature, but the VAN DER GRINTEN II and III projections were in fact created by BLUDAU, modifying projection I. Projection IV, like the NICOLOSI projection, maps the hemisphere into a circular frame.

XXVII. Pseudopolyconic projections

From the arrangement, $c = t + \rho$. The sine of the angle χ is $q/R\pi$, while this is also the ratio between the two legs of the smaller right triangle with a continuous green hypotenuse. Then from the two similar triangles:

$$\sin \chi = \frac{q}{R\pi} = \frac{2R\widehat{\varphi}}{2R\pi - 2R|\widehat{\varphi}|} = \frac{\widehat{\varphi}}{\pi - |\widehat{\varphi}|}$$

The parallels intersect the framing circle at $(R\pi \cos \chi, R\pi \sin \chi)$. From this, ρ can be expressed:

$$R^2\pi^2 \cos^2 \chi + (R\pi \sin \chi - t - \rho)^2 = \rho^2$$

$$\rho = \frac{t^2 - 2R\pi t \sin \chi + R^2\pi^2}{2R\pi \sin \chi - 2t}$$

Note that the inversion of the previous formula for t yields $\widehat{\varphi} = \pi^2 R t / (t^2 + R^2 \pi^2)$, which may be substituted through $\sin \chi$ to simplify the formula for ρ :

$$\rho = \frac{R^3\pi^3 - |t^3|}{2t^2} \text{sign } t$$

Once all data for the circles (c , ρ , d , r) are known, the general formulæ can be used to compute the projection, which is depicted in Fig. XXVII.4.

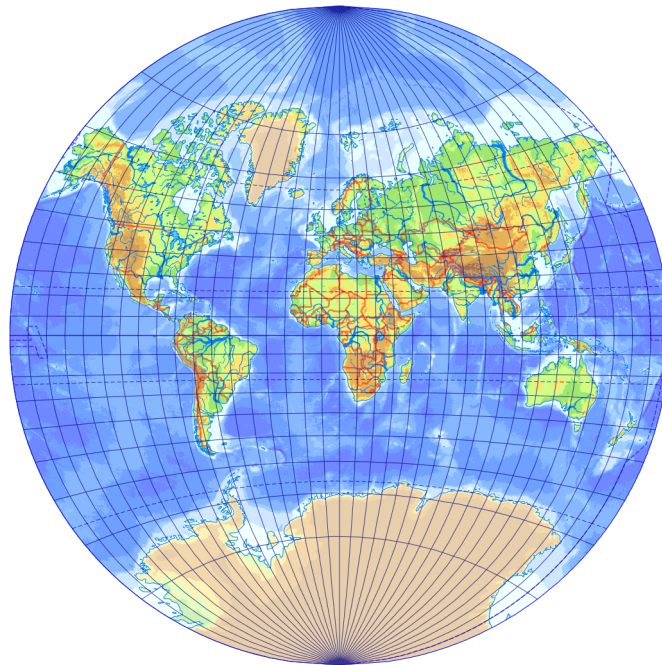


Figure XXVII.4: VAN DER GRINTEN I projection

XXVII.3 Further pseudopolyconics

Soviet cartography used pseudopolyconic projections to represent both the Soviet Union and the entire Earth. The GINZBURG IV–VII and IX projections stand out because they were widespread. These mappings were hand-drawn as described in Sec. XXIV.2, with the distortions prescribed at certain points. The projections were given in a tabular form, the approximate formulæ used today were supplied by Turkish cartographers İPBÜKER and BILDIRICI based on the calculations of the American VOXLAND.

For a better representation of the Soviet Union, the central meridian was shifted eastwards and the points of favourable distortions were defined at high latitudes (around 48–52°, depending on the version). These projections are among the most favourable ones for world maps. Their disadvantage is the unusual map frame seen in Fig. XXVII.5, which was addressed by cropping a little from the top and bottom of the map at the poles and continuing the representation beyond the bounding meridian, completely filling the rectangular map frame. They were used in encyclopædias and school atlases in the countries of the Eastern Bloc, and have been swept away by modern GIS.

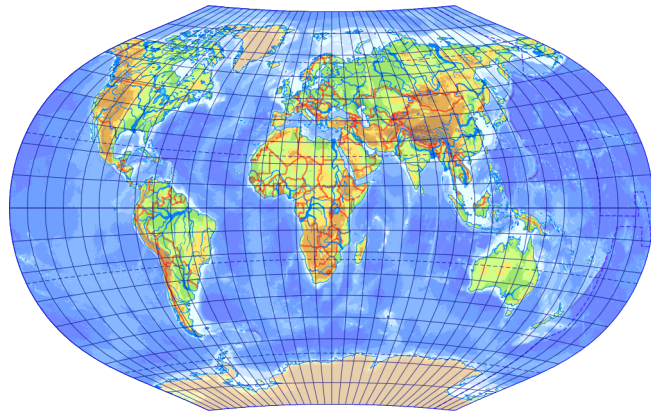
Pseudopolyconic projections also include rectangular mappings (not necessarily conformal) and equal-area projections. Their applications for regional maps of middle latitudes were investigated by GYÖRFFY and for world maps by KERKOVITS. Research has shown that this projection family is very flexible for the area to be mapped, and that their potential is still unexploited.

XXVII.4 Polyazimuthal projections

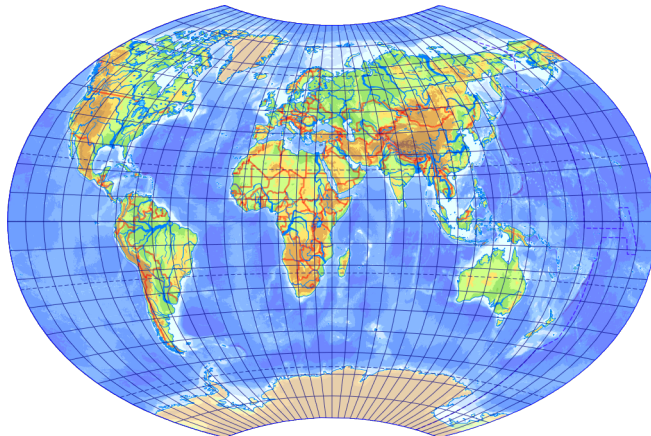
In addition to the pseudoazimuthal projections, there are also projections where the mapped parallels are full circles, but not concentric. Such projections are called *polyazimuthal*. For these projections, the general properties described in Sec. XXV.3 also hold, i.e. the conformality at the pole and the periodicity of the function $\varepsilon - \lambda$. In contrast to pseudoazimuthal mappings, there is no polyazimuthal projection which is symmetric about the horizontal axis: this would imply the concentricity of parallels. Among polyazimuthal mappings, there are equal-area and rectangular graticules, but there is no conformal one.* The definition of polyazimuthal projections was established in 1989 by the Russian cartographer TOLSTOVA, but few

* Solving the equation of conformality among polyazimuthal projections, we obtain the oblique stereographic projection, but in a complicated way. That is rather like a conical projection.

XXVII. Pseudopolyconic projections



(a) Projection V



(b) Projection VI

Figure XXVII.5: Examples of pseudopolyconics by GINZBURG

other people than the author have explored them. They can be recommended for highly asymmetrical areas at high latitudes (Fig. XXVII.6).

XXVII. Pseudopolyconic projections

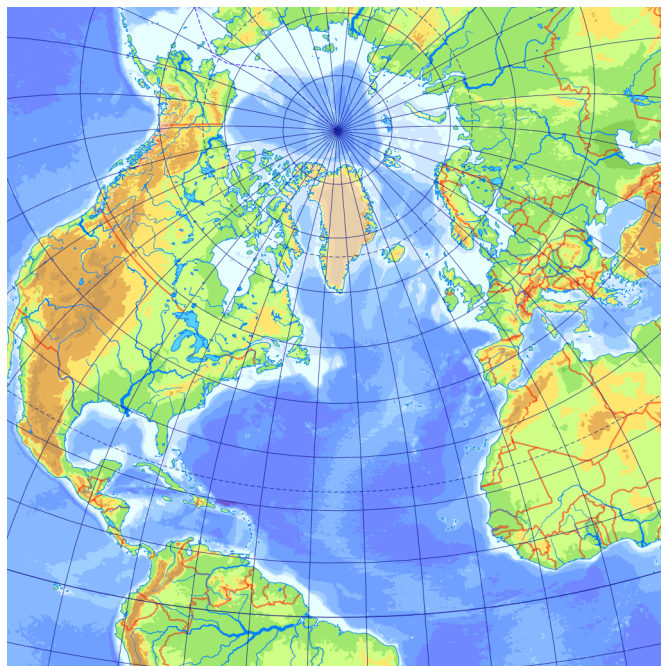


Figure XXVII.6: *Rectangular polyazimuthal projection of KERKOVITS for the Northern Atlantic Ocean*

Lesson twenty-eight

Modified azimuthal projections

XXVIII.1 AITOFF & HAMMER projections

At this point, we leave the set of projections that can be grouped according to the shape of the graticule. Mappings that do not fit into the previously established categories are simply categorized as *miscellaneous projections*. Since these projections do not have any common properties, their distortions can only be calculated using the general formulæ learned in Sec. VII.1–VIII.4. The most commonly used of such projections can all be derived from azimuthals by some previously known method (e.g., *Umbeziffern*, blended projection).

It is well known that the azimuthal equidistant has very favourable distortions for the aphyllactic representation of a circular area, including the hemisphere. However, the same mapping is obviously not used to represent the whole Earth. Since the favourable part of the *transverse* azimuthal equidistant is the hemisphere at the centre of the projection, the projection cries out for an *Umbeziffern*. The derivation and the formulæ of the transverse azimuthal equidistant can be found in Sec. XI.1:

$$x = R \arccos(\cos \varphi \cos \lambda) \frac{\sin \lambda \cos \varphi}{\sqrt{1 - \cos^2 \varphi \cos^2 \lambda}}$$
$$y = R \arccos(\cos \varphi \cos \lambda) \frac{\sin \varphi}{\sqrt{1 - \cos^2 \varphi \cos^2 \lambda}}$$

We want to map the longitude range $\pm 180^\circ$ of the entire sphere into the range $\pm 90^\circ$ of the hemisphere. This implies that instead of λ , we need to use the renumbered longitude $\zeta = \lambda/2$. At the same time, the Equator, which was originally equidistant, is now half its original length. To make the Equator longer, coordinate x is multiplied back by 2:

$$x = 2R \arccos\left(\cos \varphi \cos \frac{\lambda}{2}\right) \frac{\sin \frac{\lambda}{2} \cos \varphi}{\sqrt{1 - \cos^2 \varphi \cos^2 \frac{\lambda}{2}}}$$

XXVIII. Modified azimuthal projections

$$y = R \arccos\left(\cos \varphi \cos \frac{\lambda}{2}\right) \frac{\sin \varphi}{\sqrt{1 - \cos^2 \varphi \cos^2 \frac{\lambda}{2}}}$$

This mapping was created in 1889 by the Russian cartographer АИТОВ, who lived in France. His name spread with an incorrect transliteration, so it is known as the АИТОВ projection. Since the original mapping represented the hemisphere in a circle, after renumbering and horizontal stretching, it is transformed into an elliptical frame (Fig. XXVIII.1). The central meridian was equidistant in the azimuthal equidistant, which was not changed by the transformations because the latitudes were not renumbered. The starting point was an aphylactic projection, which was not changed by the renumbering of the graticule, and so is the present mapping. The distortions of the projection are more favourable for a world map than the similar АПИАН II projection, but this mapping is not a pseudocylindrical mapping.

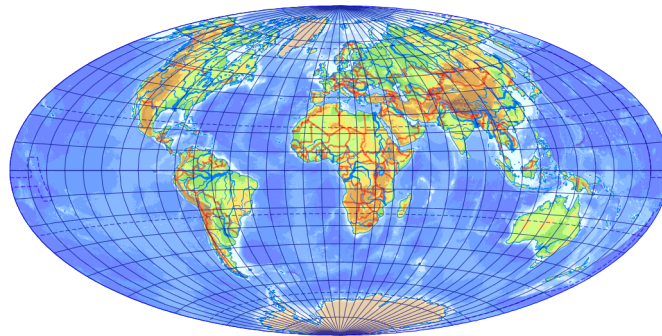


Figure XXVIII.1: АИТОВ projection

Following АИТОВ, the German geodesist HAMMER suggested in 1892 that the transverse LAMBERT azimuthal equal-area should be treated in the same way. Once again, the formulæ are taken from Sec. XI.2:

$$x = R \frac{\sqrt{2} \sin \lambda \cos \varphi}{\sqrt{1 + \cos \varphi \cos \lambda}}$$

$$y = R \frac{\sqrt{2} \sin \varphi}{\sqrt{1 + \cos \varphi \cos \lambda}}$$

We would like to preserve the equivalency, of course. It is clear that if we use the renumbering $\zeta = \lambda/2$, all areas will be reduced to their half. It follows that stretching the area of the map in either (but not both) directions by a factor of two will restore equivalency. Since the longitudes are

renumbered by compressing the map in the horizontal direction, it follows that it makes sense to stretch in the x direction.

$$x = 2R \frac{\sqrt{2} \sin \frac{\lambda}{2} \cos \varphi}{\sqrt{1 + \cos \varphi \cos \frac{\lambda}{2}}}$$

$$y = R \frac{\sqrt{2} \sin \varphi}{\sqrt{1 + \cos \varphi \cos \frac{\lambda}{2}}}$$

The combination of the renumbering and the stretching preserves areas, the HAMMER projection is equal-area. The projection is very popular, and despite being equal-area and pointed-polar, it does not have annoying levels of angular distortion. The Earth is shown in an elliptical frame similar to that of the MOLLWEIDE projection (Fig. XXVIII.2).

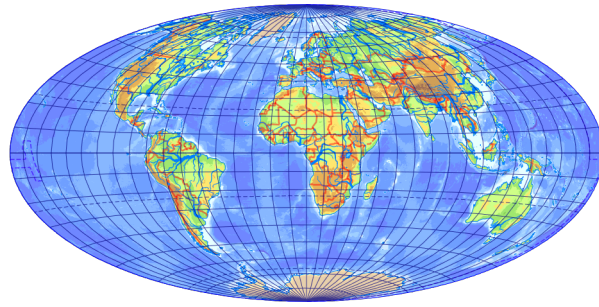
Although the bimeridians run through the pole with a cusp, and this causes a minor æsthetic problem when rotating the graticule, it is common to use this projection in simple oblique aspect. The first such application was made in 1926 by the Hungarian geographer PÉCSI, who rotated the centre of projection to latitude 25° N so the favourable distortions fell on the grain-producing countries. The projection appeared as agricultural maps of Hungarian school atlases between the two world wars and can be considered the first oblique non-conical projection in the world. Among the international examples, we may mention the *Nordic projection* of the Scottish cartographer BARTHOLOMEW, centred at 45° N, 0° E. The BRIESEMEISTER projection differs from this only in that the centre is at 10° E and, in order to obtain better angular distortions, the projection is reduced by a factor of $\sqrt{7/8}$ in the x direction, and stretched by the reciprocal in the y direction to preserve areas.

XXVIII.2 WINKEL III projection

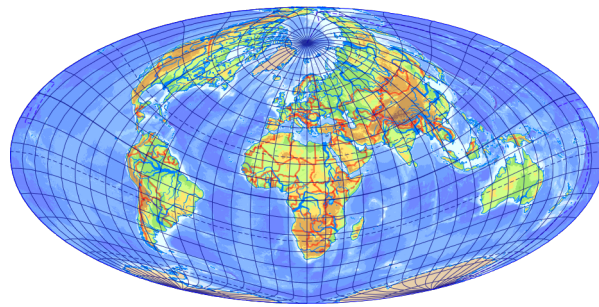
The AIRTOFF projection already shows the Earth in a quite favourable way, but at higher latitudes the angular distortion is still too large. We are reminded of how much the unfavourable sinusoidal projection could be improved by simply blending with another map. Could this also do some good with our mapping? The WINKEL III (also known as the *Tripel*) projection is the blend of the AIRTOFF projection and the equirectangular projection:

$$x = \frac{R}{2} \left[\widehat{\lambda} \cos \varphi_s + 2 \arccos \left(\cos \varphi \cos \frac{\lambda}{2} \right) \frac{\sin \frac{\lambda}{2} \cos \varphi}{\sqrt{1 - \cos^2 \varphi \cos^2 \frac{\lambda}{2}}} \right]$$

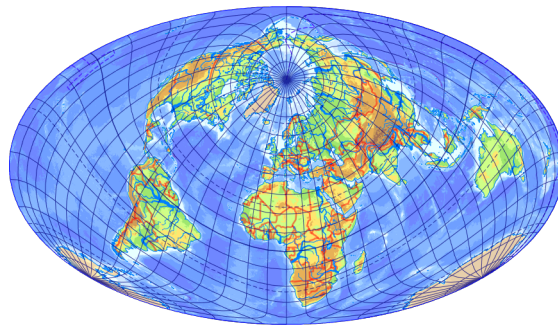
XXVIII. Modified azimuthal projections



(a) Normal



(b) Simple oblique (PÉCSI projection)



(c) Simple oblique, rescaled (BRIESEMEISTER projection)

Figure XXVIII.2: HAMMER projection

$$y = \frac{R}{2} \left[\widehat{\varphi} + \arccos \left(\cos \varphi \cos \frac{\lambda}{2} \right) \frac{\sin \varphi}{\sqrt{1 - \cos^2 \varphi \cos^2 \frac{\lambda}{2}}} \right]$$

The standard parallel φ_s of the cylindrical was proposed by WINKEL to be $\sim 50^\circ 27' 35''$, like his other projections, but in practice, the choice $\varphi_s = 40^\circ$ was adopted at BARTHOLOMEW's suggestion.

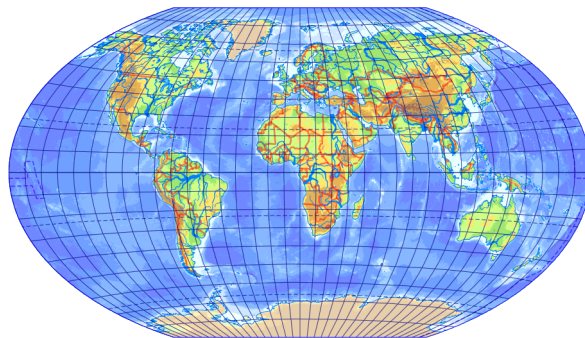


Figure XXVIII.3: WINKEL III projection ($\varphi_s = 40^\circ$)

This aphyllactic projection dates from 1921. Applied to a world map, it is the least distorted of the common projections (Fig. XXVIII.3), and is very favourable, especially for geographic maps.* This mapping started to spread rapidly first in Central Europe, and is now among the most popular projections worldwide. More recently it has displaced the ROBINSON projection on National Geographic maps. Its only drawback is being flat-polar.

XXVIII.3 WAGNER's modified azimuthals

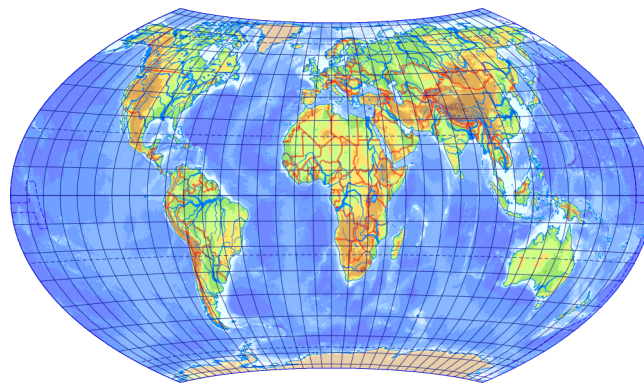
The derivation showed that the HAMMER projection can be understood as an *Umbeziffern* version of the transverse LAMBERT azimuthal equal-area. In Sec. XXIII.3, it was deduced that the equal-area WAGNER transform can be expressed in general by the functions $\psi = \arcsin(m \sin \varphi)$ and $\zeta = n\lambda$. The HAMMER projection can then be obtained by choosing $m = 1$ and $n = 1/2$. Of course, other values for n can be chosen to obtain additional equal-area

* The fact that a projection has low distortion does not mean that it should be applied everywhere. Unfortunately, this mapping is also found in time zone maps (where meridian convergence is confusing), thematic maps of global relations (where you cannot properly connect America to Asia) and school atlases (where you should not apply a flat-polar projection). That being said, rather this otherwise favourable mapping should be used beyond its merits than, for example, the VAN DER GRINTEN I projection...

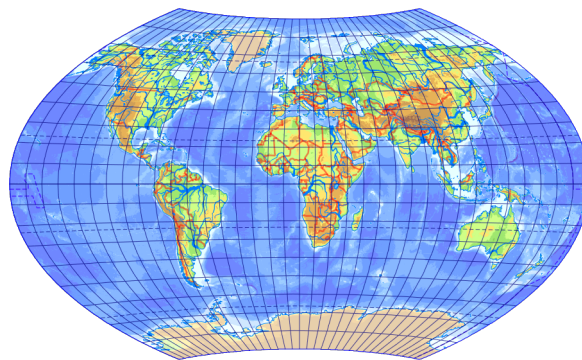
XXVIII. Modified azimuthal projections

projections. If we do not insist on pointed poles, we can choose a number less than 1 for m .

The WAGNER VII projection shown in Fig. XXVIII.4 is an equal-area mapping with very favourable distortions. WAGNER's goal was to make the length of the pole line approximately half that of the Equator, so he renumbered the latitudes so that the Pole was mapped to latitude 65° . Hence, $m = \arcsin(65^\circ)$. Furthermore, WAGNER multiplied the longitudes by $n = 1/3$. He restored equivalency as usual by multiplying both coordinates with $1/\sqrt{mn}$. The projection is one of the best among equal-area world maps, but its strong disadvantage is the concave, curved pole-line. Although it was created in the early 20th century, its popularity only started to grow in the 21st century.



(a) Projection VII



(b) Projection IX

Figure XXVIII.4: WAGNER's *Umbeziffern* transverse azimuthal projections

Similarly, for the transverse azimuthal equidistant, the AITOFF projection is not the only possibility, but here we would like to preserve the equidistant central meridian. Therefore, we use the simpler function $\psi = m\varphi$ to renumber the latitudes. In the WAGNER IX projection, the goal is to achieve

a similar appearance to the WINKEL III projection, which was popular at that time. This can be achieved by choosing $m = 7/9$ and $n = 5/18$. The stretching in the y direction is constrained by the equidistant central meridian ($1/m$), but in the x direction we choose only $0.88/n$. The projection has favourable distortions but has an unusual frame. It has a very low popularity.

XXVIII.4 Retroazimuthal mappings

The LITROW projection discussed in Sec. XXVII.1 has already been of much interest from a theoretical point of view, and we now highlight its practical usefulness. In this projection, if a point is connected to any point of the central meridian then the inclination of the section is equal to the azimuth of the orthodrome connecting the two points. While *azimuthal* projections preserve the azimuth of the orthodromes starting from the centre of projection, mappings which show the azimuth of the orthodromes going back to the centre are called *retroazimuthal projections*. Such projections are suitable for navigational (which way to turn the ship to return to the centre of projection) or telecommunicational (which way to turn the antenna to see the tower at the origin) purposes.

We see an interesting application of retroazimuthal projections in Muslim culture, where it is important to read the direction to Mecca correctly. Here again, the back azimuth of the orthodrome is sought. The problem has given rise to several projections. In the CRAIG projection, the meridians are equal-spaced vertical lines, so the azimuth to Mecca can be read with respect to any meridian (Fig. XXVIII.5). The HAMMER retroazimuthal projection is equidistant in orthodromes starting from the origin. Known retroazimuthal projections have significant distortions and, because of overlapping, generally cannot represent a large area, and are therefore only recommended for special map themes. Retroazimuthal projections can be replaced by the more favourable oblique stereographic projection, but in the latter case the back azimuth to the metapole is measured relative to the curved meridians and not to the vertical direction.

XXVIII.5 Projections of RAISZ

The flat map sheet not only distorts the surface of the Earth, but also gives the reader the false impression that the continents on the spherical surface are actually flat. However, some projections, including the orthographic one, are particularly well suited to show the three-dimensional sphere.

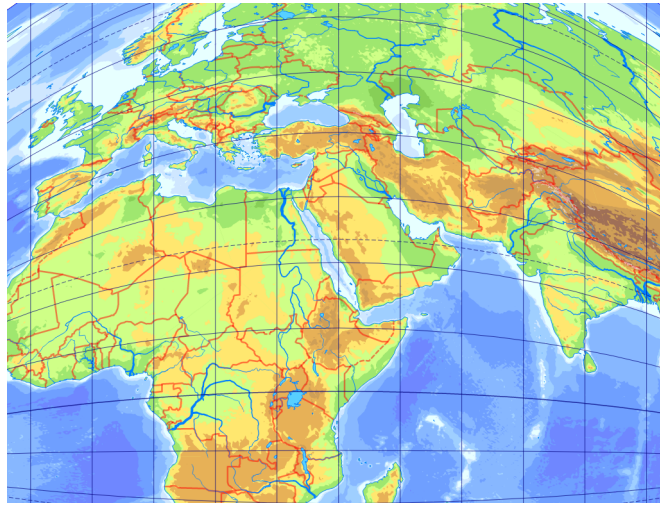


Figure XXVIII.5: *CRAIG projection centred on Mecca*

RAISZ, a Hungarian cartographer living in America, believed that the orthographic projection could be considered distortion-free, since one sees the mapped image spatially, as if looking at a globe.

A major disadvantage of orthographic projection is that it cannot represent an area larger than a hemisphere. RAISZ has resorted to a trick. He first mapped the sphere onto a variety of surfaces (e.g., very flattened ellipsoid or bean-shaped manifold). These projections had moderate distortions due to the curvature of the surface being close to that of the sphere. In a second step, the spherical surface mapped onto the manifold was presented in an oblique orthographic projection. The *Armadillo projection* became RAISZ's most popular mapping, which maps the sphere onto the surface of a degenerate torus (doughnut-shaped solid) as an intermediate surface. In the projection shown in Fig. XXVIII.6, Antarctica and New Zealand cannot be represented, all graticule lines are mapped to arcs of ellipses.

XXVIII.6 Star projections

Normal aspect azimuthals are suitable for the Northern Hemisphere, but their distortion is unacceptable in the Southern Hemisphere. Therefore, it was recommended to map parts of the Southern Hemisphere in their own projection with a different central meridian, as in the GOODE projection. The projections thus formed will have a characteristic shape of a star or a flower (Fig. XXVIII.7). In order to preserve the concentricity of the parallels, the 'petals' of the map are chosen to be a pseudoconic projection (e.g. BONNE projection). The boundary between the azimuthal and the pseudoconic

XXVIII. Modified azimuthal projections

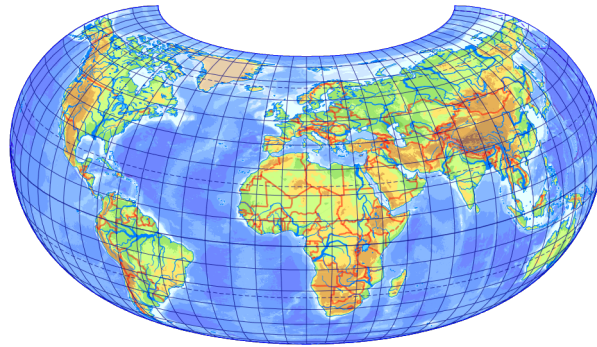


Figure XXVIII.6: *Armadillo projection*

mappings is not necessarily the Equator, and the pseudoconic projection must be modified so that the meridians are continuous at the bounding latitude.

Such projections are suitable for world maps according to their distortions, but there is a high price to pay for favourable distortions: discontinuities appear everywhere throughout the projection, and adjacent areas are moved away from each other. In general, the more discontinuities there are in a map, the more the distortions can be reduced. An important rule is to place discontinuities away from areas of interest (e.g. in the middle of oceans for an economic map). Such maps can be used with their unusual frames for decorative and eye-catching purposes, e.g. on atlas covers, wall maps, emblems, etc. Examples include the BERGHAUS, BARTHOLOMEW, and WILLIAM-OLSSON projections.

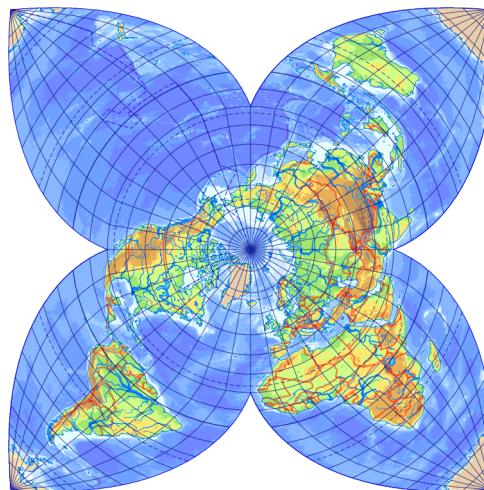


Figure XXVIII.7: *WILLIAM-OLSSON projection (equal-area)*

Lesson twenty-nine

Exotic map projections

XXIX.1 Conformal projections

So far, we have seen notably few conformal projections. Could not we discover new conformal mappings by transforming our existing conformal maps using a differentiable function $\mathbb{R}^2 \rightarrow \mathbb{R}^2$ written in the form $u(x, y), v(x, y)$?

It is known from Tissot's theory (Sec. VIII.1) that such mappings are composed of affine transformations of infinitesimal areas, i.e. if the point (x_0, y_0) is mapped to (u_0, v_0) , then the image of the point $(x_0 + \Delta x, y_0 + \Delta y)$ very close to it can be written by a local linear approximation of the function. This approximation can be decomposed into the product of the small vector $(\Delta x, \Delta y)$ and a matrix, and a translation of the resulting vector:

$$\begin{pmatrix} u \\ v \end{pmatrix} \approx \begin{pmatrix} u_0 + \frac{\partial u}{\partial x} \Delta x + \frac{\partial u}{\partial y} \Delta y \\ v_0 + \frac{\partial v}{\partial x} \Delta x + \frac{\partial v}{\partial y} \Delta y \end{pmatrix} = \begin{pmatrix} u_0 \\ v_0 \end{pmatrix} + \begin{pmatrix} \frac{\partial u}{\partial x} & \frac{\partial u}{\partial y} \\ \frac{\partial v}{\partial x} & \frac{\partial v}{\partial y} \end{pmatrix} \begin{pmatrix} \Delta x \\ \Delta y \end{pmatrix}$$

This mapping is conformal if and only if the matrix rotates all possible arms by the same angle δ (local similarity transform). That is, the matrix can be decomposed into a magnification and a rotation. It follows that the matrix must be equal to the product of a scalar and the rotation matrix of angle δ :

$$\begin{pmatrix} s \cos \delta & s \sin \delta \\ -s \sin \delta & s \cos \delta \end{pmatrix} = \begin{pmatrix} \frac{\partial u}{\partial x} & \frac{\partial u}{\partial y} \\ \frac{\partial v}{\partial x} & \frac{\partial v}{\partial y} \end{pmatrix}$$

It is clear that the equation above can only be satisfied if the main diagonal of the right matrix has identical values, while the elements of the anti-diagonal are opposite:

$$\frac{\partial u}{\partial x} = \frac{\partial v}{\partial y} \quad \text{and} \quad \frac{\partial u}{\partial y} = -\frac{\partial v}{\partial x}$$

This is known as the *CAUCHY-RIEMANN differential equation*, a necessary condition for conformal mappings. The only problem is if all four partial

derivatives are zero: although the differential equation is satisfied, the original equation can not be solved for the angle of rotation.

Planar coordinates x, y can be considered as the real and imaginary parts of a *complex number* known from higher mathematics, i.e. the original coordinates can be described by the complex number $z = y + ix$, while the new ones by $w = v + iu$, where i is the *imaginary unit*, $i^2 = -1$. Then $w(z)$ is a *complex function* $\mathbb{C} \rightarrow \mathbb{C}$. Assuming that $w(z)$ is differentiable, applying the chain rule, the formula for the derivative of sums, and $(-i) \times i = -i^2 = -(-1) = 1$:

$$\begin{aligned} \frac{\partial v}{\partial y} + i \frac{\partial u}{\partial y} &= \frac{\partial w}{\partial y} = \frac{dw}{dz} \frac{dz}{dy} = \frac{dw}{dz} \times 1 \\ \frac{\partial u}{\partial x} - i \frac{\partial v}{\partial x} &= -i \left(\frac{\partial v}{\partial x} + i \frac{\partial u}{\partial x} \right) = -i \frac{\partial w}{\partial x} = -i \frac{dw}{dz} \frac{dz}{dx} = -i \frac{dw}{dz} \times i \end{aligned}$$

That is:

$$\frac{\partial v}{\partial y} + i \frac{\partial u}{\partial y} = \frac{\partial u}{\partial x} - i \frac{\partial v}{\partial x}$$

The CAUCHY–RIEMANN differential equation follows from the equality of the real and imaginary parts. *Each conformal mapping can be generated from another conformal projection by a function that is differentiable and has a non-zero derivative on an open subset of the complex plane.* Astonishingly, any (non-constant) differentiable function can be used to transform an existing conformal projection, and the result is also conformal; indeed, all conformal mappings can be obtained from any conformal projection by using the corresponding differentiable function!*

Any smooth function can be approximated to any precision by its TAYLOR polynomial, i.e. any conformal projection can be approximated by complex polynomials.† We can approximate, for example, the projection with the lowest possible distortion, the isocols of which, following CHEBYSHEV, is known to follow the boundary of the area. In this case, it is useful to start with a well-chosen transverse or oblique stereographic map. For example, the MILLER modified stereographic projection achieves with a cubic polynomial that the isocols are oval instead of circular, and can

* Real functions that are differentiable are not necessarily differentiable as complex functions, but common ones (polynomials, trigonometric, exponential and logarithmic functions) are complex-differentiable.

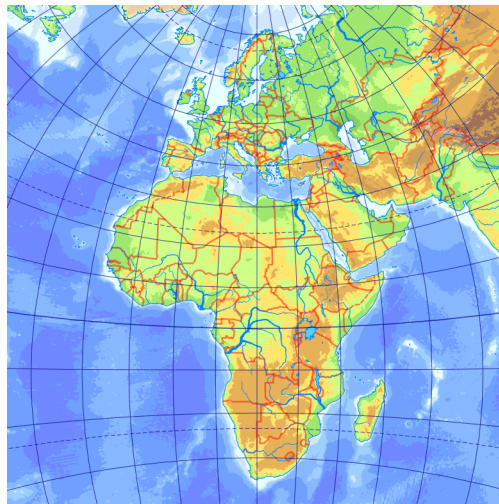
† This means that for a polynomial transformation (Sec. XVIII.3) between two conformal maps, it is preferable to use complex polynomials rather than real ones, because in this way angles are not distorted.

XXIX. Exotic map projections

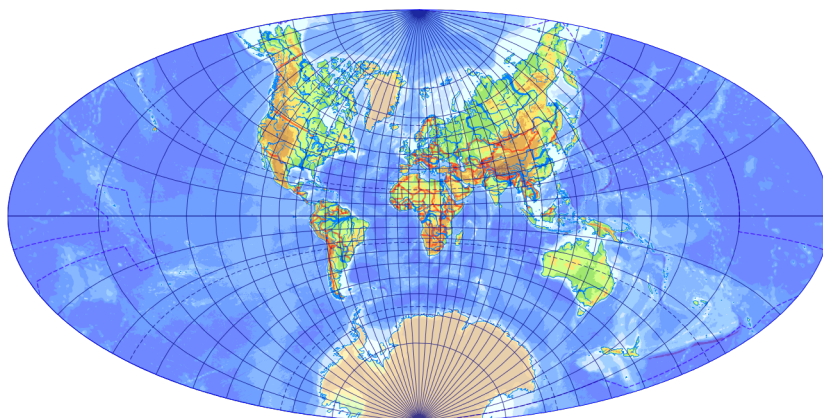
therefore be applied to such areas (e.g. Africa and Europe, Pacific Ocean). In the topographic projection of Madagascar, this method is also used to ensure that the isocols of the GAUSS–SCHREIBER projection are not vertical but follow the oblique placement of the island. Although the method has been known for a long time and provides much better projections for geodetic purposes than currently known, it is mostly rejected.*

Another application is on world maps. It is known that the sphere is mapped onto a disk by the LAGRANGE projection, and the hemisphere by the stereographic projection. German mathematician SCHWARZ introduced

* For Hungary, JUHÁSZ derived the best conformal map in this way.



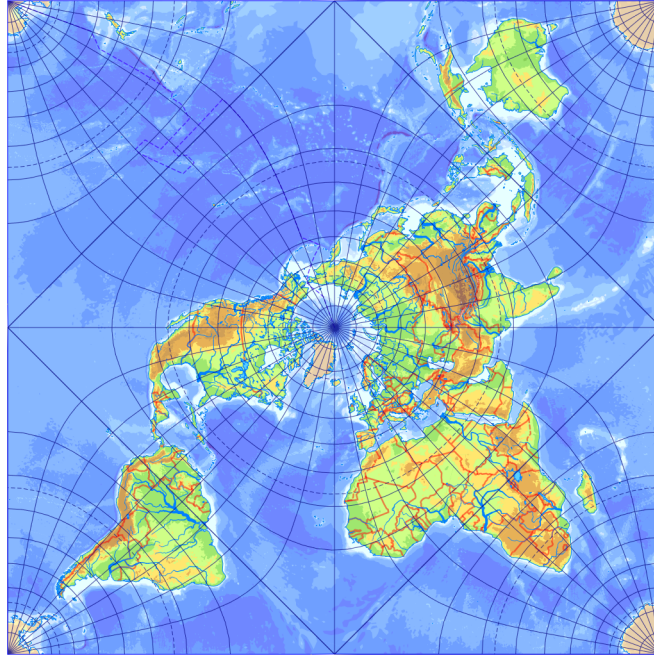
(a) MILLER modified stereographic projection



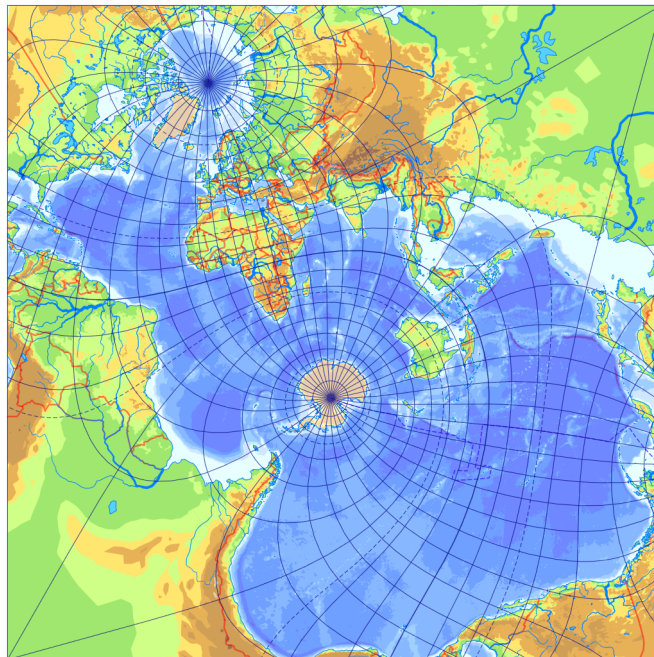
(b) LEE world in ellipse projection

Figure XXIX.1: Some conformal non-conical projections

XXIX. Exotic map projections



(c) PEIRCE projection



(d) SPILHAUS projection (plagal aspect)

Figure XXIX.1: (contd.)

the possibility of mapping the disk onto any polygon by means of certain differentiable (i.e. conformal) complex functions. Although these functions are all brain-racking elliptic integrals, in the early 20th century, the American mathematician ADAMS and in the 1970s, the New Zealander geodesist LEE conformally mapped the sphere or the hemisphere into countless shapes (e.g. rectangle, ellipse, triangle, rhombus). Fig. XXIX.1 shows the oldest such projection by PEIRCE in 1879, with the Northern Hemisphere represented as a square. The Southern Hemisphere is mapped using the same projection, but is divided into four congruent parts attached to the sides of the Northern Hemisphere. Similar mappings are useful when it is important that our map fills a certain frame.

The only thing more complicated than the foregoing is to use such projections in planal aspect. SPILHAUS created his projection to represent the world ocean in 1979. This is the ADAMS world in square projection rotated.

XXIX.2 Polyhedral projections

In the vast majority of cases, our projections map onto a plane, with a few very rare perspective projections that may map to a cylinder or a cone. However, these surfaces do not effectively approximate the shape of a sphere. Solids bounded by flat polygonal faces, also known as *polyhedra*, can be unfolded to the plane. Because of the perfect symmetry of the sphere, *regular polyhedra*, whose faces are all congruent regular polygons, are the most important for mapping applications.

In contrast to regular polygons, there are only five regular polyhedra (Fig. XXIX.2): the *tetrahedron*, consisting of four triangles; the *hexahedron* (cube), bounded by six squares; the *octahedron*, containing eight triangles; the *dodecahedron*, consisting of twelve pentagons; and the *icosahedron*, consisting of twenty triangles.

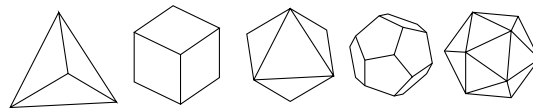


Figure XXIX.2: Regular polyhedra

Projections mapping onto a polyhedron are called *polyhedral projections*, but the term polyhedral projection is used to describe a pseudocylindrical mapping (Sec. XXI.3). Their idea comes from DÜRER. In addition to their more favourable distortions than usual mappings, they are also advantageous for making polyhedron models to replace globes. They have the disadvantage, however, that discontinuities are created when certain edges

are cut while sheets are unfolded. For polyhedral projections, we expect that the representation will not break along the edges of the polyhedron:

- The inverse images of each polyhedron face, i.e. the spherical polygons corresponding to tiling of the polyhedron, must be mapped completely filling the polyhedron face, so the bounding orthodromes are mapped to straight lines.
- The lines crossing the edges shall continue at the corresponding point on the adjacent polyhedron face.

A trivial solution to these complex conditions is the gnomonic projection, which maps all orthodromes, including the inverse images of the polyhedron edges, to straight lines. The distortions will then be significant at the polyhedron vertices. Of course, other complicated mappings can be used, such as the equal-area polyhedral projection. The previously studied complex elliptic integrals can form not only circles but also regular spherical polygons into planar polygons conformally, so ADAMS and LEE have also applied their conformal mappings to polyhedra.

The significance of the tetrahedron is that it can be formed into a rectangle by unfolding its sheets, cutting one sheet into halves and rearranging, making it convenient for printed maps, but it does not effectively approximate the sphere. The cube would be better, but its sheets are difficult to unfold favourably from a cartographic point of view. The octahedron is considered suitable because its edges lie on the Equator and on every 90° meridians. When the central meridian is chosen wisely, the polyhedron is unfolded with cuts only slightly affecting lands. This results in special butterfly-shaped maps. The idea originated from the American architect CAHILL, who produced an almost equal-area, a gnomonic, and a conformal version in 1909 (Fig. XXIX.3). The idea was later developed further by KEYES and then WATERMAN with their composite aphyllactic projections.*

The much more spherical dodecahedron can be unfolded with more cuts, and this is even more significant for the icosahedron. Still, since the icosahedron has the most faces, FULLER's *Dymaxion projection* (Fig. XXIX.4) from 1954 uses it in plagal[†] aspect. The mapping is not gnomonic, but is equidistant along the edges of the polyhedron, though due to the small

* From time to time, the spectacularly favourable distortions of polyhedral projections are rediscovered and all sorts of tabloid articles are written about them. Their authors are typically not cartographers. The media are keen to pick up on these unusual maps as if they were some sort of ground-breaking novelty and the most accurate maps possible; but the concept is nearly 500 years old, and it is important to be aware of their drawbacks (e.g. discontinuities).

[†] Even for polyhedral projections, the aspect with the simplest description is considered normal. In general, regular polyhedra are normal if the pole falls on the midpoint of any edge. Exceptions are the cube, where in the normal aspect, the pole is at the centre

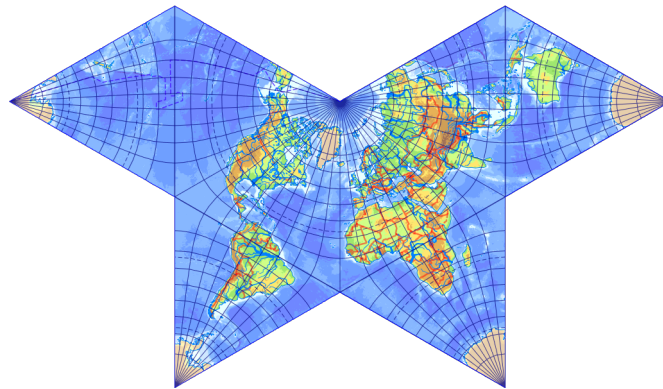


Figure XXIX.3: CAHILL conformal projection

area of the icosahedron faces, this has little effect on the map. There are no discontinuities in the continents, but this requires cutting some sheets in halves and rearranging them.

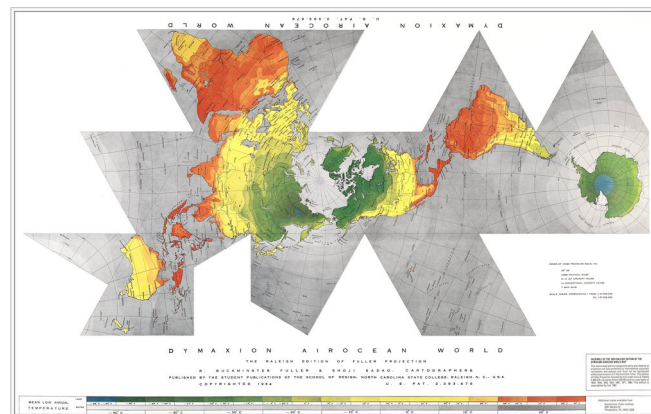


Figure XXIX.4: Dymaxion projection

XXIX.3 Projection analysis

To georeference a map, we need to know the projection of the map with all its parameters. While this information is available in the case of topographic maps, such information is shallow, if it is available at all, in

of a face, and the octahedron, where pole is mapped to a vertex in normal aspect. The transverse aspect is not defined for polyhedral projections, but aspects where the pole is mapped to a vertex or the midpoint of a face, on an edge or an angular bisector are highlighted. The name for the general aspect remains plagal.

the map surround of general maps. Determining the otherwise unknown projection of a map is called *projection analysis*.

On large- and medium-scale maps, the suitable mappings differ only slightly, so it is less important to accurately determine the projection. The application `detectproj` was developed for such cases, which uses control points to adjust the parameters of several possible projections until the projection fits the given points as best as possible. The application then plots the projections it considers most likely on the screen. Before making a final decision, it is worth taking into account the age of the map: some projections were only popular in certain eras, while others have only recently been discovered.

On small-scale maps, rare projections may occur, but the characteristics of the graticule are more visible. The Hungarian ÉRDI-KRAUSZ has grouped the most common types so that the projection of the map can be manually determined with a few measurements. The groups are shown here with GYÖRFFY's modifications:

1. Parallels are parallel straight lines, meridians are parallel straight lines.
 - (a) Equidistant meridians: If the geographical quadrangles are squares: *Plate Carrée*. If rectangles: *equirectangular*.
 - (b) The parallels are dense near the map frame: likely *equal-area cylindrical*, the standard parallel may be determined by measurements.
 - (c) The parallels are sparse near the map frame: rather *MERCATOR*, but it may also be one of the many similar perspective mappings.
2. Parallels are parallel straight lines, meridians are curved.
 - (a) The meridians are arcs of circles: If a hemisphere is in a circle: *APIAN I*, or extended to the sphere, *ORTELIUS*. The full globe is in a circle: *VAN DER GRINTEN III*.
 - (b) The meridians are arcs of ellipses, pointed-polar: equidistant central meridian: *APIAN II*. Dense parallels near the poles: *MOLLWEIDE* or for a hemisphere, *transverse orthographic*.
 - (c) The meridians are arcs of ellipses, flat-polar: meridians reach the pole with an acute angle: *KAVRAYSKIY VII*. Meridians reach the pole smooth: equidistant central meridian: *ECKERT III*. Dense parallels near the poles: *ECKERT IV*.
 - (d) The meridians consist of multiple arcs of ellipses: equally-spaced meridians: *BARANYI II*. Meridians are dense near the map frame: *BARANYI IV*.
 - (e) The meridians are sinusoids: Pointed-polar: *sinusoidal*. Flat-polar: Equidistant central meridian: *ECKERT V*. Dense parallels near the

- poles: *ECKERT VI* or *KAVRAYSKIY VI* (or any other member of the *MERCATOR* series).
- (f) The meridians consists of sinusoids and arcs of ellipses: *GOODE* or *ÉRDI-KRAUSZ*.
- (g) The meridians are straight: Can be *trapezoidal*, *COLLIGNON* or if flat-polar then *ECKERT I* or *II*. On old maps, it may also be the *polyhedric projection*.
- (h) Does not fit into any of the previous subgroups: *loximuthal*, *ROBINSON*, pseudocylindrical projections given in tabular forms, various rare equal-area pseudocylindricals (e.g. *KAVRAYSKIY V*, *CRASTER*, *PUTNINŠ*).
3. Parallels are full circles, meridians are concurrent straight lines.
- (a) Equidistant meridians: *azimuthal equidistant*.
- (b) The parallels are dense near the map frame: likely *LAMBERT*, might also be *GINZBURG's azimuthal*. If they become dense very fast: *vertical perspective*, likely *orthographic*.
- (c) The parallels are sparse near the map frame: *stereographic*. If they become sparse very fast: *gnomonic*.
4. Parallels are full circles, meridians are curved: pseudoazimuthal or polyazimuthal, extremely rare.
5. Parallels are arcs of circles, meridians are concurrent straight lines. In this group, the equidistant parallels can be determined only by measuring the radius function and the cone constant.
- (a) Equidistant meridians: *equidistant conic*.
- (b) The parallels are dense near the map frame: Pointed-polar: *LAMBERT equal-area conic*. Flat-polar: *ALBERS*.
- (c) The parallels are sparse near the map frame, pointed-polar: almost surely *LAMBERT conformal conic*, extremely rarely it can also be some perspective conic.
6. Parallels are arcs of circles, meridians are curved.
- (a) Parallels are concentric: Almost surely *BONNE* or *WERNER*, but if flat-polar, it can be some rare pseudoconic.
- (b) The radii of parallels are proportional to the cotangent of the latitude: Equidistant parallels: *ordinary polyconic*. Rectangular graticule: likely *War Office*. Straight meridians: *modified polyconic*. Parallels are sparse near the pole: *transverse stereographic*.
- (c) Does not fit into the previous ones, but equidistant Equator: The full globe is in a circle: *VAN DER GRINTEN I*. (in the rare projection *II*, the graticule is rectangular). A hemisphere is in a circle, the full sphere is apple-shaped: *NICOLOSI* or *VAN DER GRINTEN IV*. Flat-polar: *GINZBURG's pseudopolyconics*.

- (d) The Equator is not equidistant, but straight: *LAGRANGE*. The Equator is a circle: *oblique stereographic*.
- 7. Parallels are hyperbolæ, meridians are parallel straight lines: *transverse gnomonic*.
- 8. Parallels are conic sections, meridians are concurrent straight lines: *oblique gnomonic*.
- 9. Parallels are arcs of ellipses, meridians are arcs of ellipses: *oblique orthographic* or one of *RAISZ*'s projections.
- 10. Parallels are ellipses, meridians are hyperbolæ: *VON DER MÜHL* projections, most likely *LITTELOW*.
- 11. Other projections
 - (a) Equator and the central meridian are straight lines, the full globe is in an ellipse: Equidistant central meridian: *AITOFF*. Parallels are dense near the poles: *HAMMER*.
 - (b) Equator and the central meridian are straight lines, a hemisphere is in an ellipse: Equidistant central meridian: *transverse azimuthal equidistant*. Parallels are dense near the poles: *transverse LAMBERT azimuthal equidistant*.
 - (c) Equator and the central meridian are straight lines, the latter is also equidistant, pointed-polar: likely *transverse cylindrical*.
 - (d) Equator and the central meridian are straight lines, the poles are straight: *WINKEL III*.
 - (e) Equator and the central meridian are straight lines, the poles are curved: *WAGNER*-transformed azimuthals.
 - (f) Only the central meridian is straight: Some oblique projection.
 - (g) Only the Equator is straight: Transverse conic.
 - (h) No axis of symmetry: Some exotic projection, most often the *CHAMBERLIN*.

Lesson thirty

Selecting a map projection

XXX.1 Traditional methods

After learning about so many projections, how do we choose the right one? To decide, we need to consider the theme of the map, its purpose (e.g. wall map, atlas sheet, field use) and the knowledge of the expected audience.

Territorial statistical data, let it be agricultural, demographic or vegetation, should always be presented in an equal-area projection! Similarly, thematic maps about geoscience, on which professionals are expected to measure areas, in particular geological, soil, and climatic maps also require an equal-area representation. The correct presentation of the extent of countries is important on political and historical maps, but excessive angular distortion should also be avoided on such maps intended for a general audience, and therefore no equivalency is required if large areas are displayed.

Maps intended for field use (tourist, navigation, topographic, etc.) should always be conformal! To ensure measurability, we should also make particular efforts to minimize distortion of the real distances. It is also common to make measurements of directions on geophysical (geomagnetism, tectonics) and meteorological (currents, air pressure) maps, and even at the cost of large areal distortions, we should insist on conformality!

However, in the examples not mentioned above, especially for geographic maps, neither equivalency nor conformality is recommended. A well-chosen apylactic projection is always significantly more favourable than the equal-area or conformal counterpart. Among conical projections, it is difficult to find a better one than the equidistant mappings in meridians; among the non-conical projections, there is no rule of thumb, but with due care, a very favourable mapping can be found. For atlas maps, we may deviate from the above rules, because within an atlas it is desirable to show the same areas in the same projection regardless of the theme, and to choose similarly distorted mappings for different areas.

Always try to rotate the areas of favourable distortion of the projection to the most important places for the theme! For example, when presenting a long railway line or a migration, the metaequator or metaparallels should follow the path of the route. To represent effects starting from a single point (e.g. earthquake, broadcast range of a tower), the oblique azimuthal equidistant projection is suitable. For special purposes, we may need a mapping with special distortions (e.g. orthodromes appear as straight lines in the gnomonic projection, circles are mapped to circles in the stereographic projection). For time-zone maps, meridians are always needed to be mapped to parallel straight lines, and for the representation of geographical zones (agriculture, vegetation, climate) straight parallels are necessary.

The literacy of the audience is a decisive factor in deciding whether a flat-polar projection with a more favourable distortion can be used even if areas near the pole appear in the map. A lower level of education or aesthetic consideration may also be the reason for a rectangular projection. Regional maps are usually represented in a rectangular frame, but for a projection representing a hemisphere or sphere, we are forced to use the frame of the mapping. In this case, the shape of the map frame may be considered. Hemispheres are represented in a circle by azimuthal projections. The globe can also be represented in a circle (e.g. VAN DER GRINTEN I), an ellipse (e.g. MOLLWEIDE, AITOFF, HAMMER), or a square (e.g. PEIRCE). However, map frames of unusual shapes (e.g. GINZBURG's projections) should be hidden by cutting off the pole-line and repeating areas beyond the bounding meridian.

As a general rule of thumb, any conical projection is suitable for a small area if the undistorted lines pass at least partially through the area being plotted and the isocols are nearly parallel to the boundary of the area. In the case of two standard parallels, it is advisable to place them between the centre and the boundary of the area to be represented, such that they are closer to the edge.

The complex process of map projection selection is supported by manuals. GINZBURG's atlas of projection selection recommends mappings with a favourable distortion for the typical atlas maps of Russian world atlases. The distortions can be checked on the map sketches in the proposed projections using isocols. Its western counterpart is SNYDER's album, which presents the projections sequentially, with ellipses of distortion and detailed textual descriptions giving advice on their application. Based on SNYDER's guidance, ŠAVRIČ wrote the application Projection Wizard, which recommends appropriate mappings for an arbitrary geographical quadrangle. However, the latter only selects the best-known projections based on the rules of thumb described above.

XXX.2 The local distortion value

Once we have defined our requirements for the mapping, we want to choose the one with the lowest possible distortion among the candidate projections. For this purpose, it is necessary to characterize the deviation from the distortion-free state at a point of the map by some measure (hereafter referred to as *local distortion value*).

The foundations of this method were laid by the British astronomer AIRY in 1861, when he defined the *areal distortion value*, i.e. the deviation of p from 1, by the formula $\varepsilon_p^2 = (p - 1)^2 = (ab - 1)^2$. Taking squares is necessary to eliminate negative numbers, and differentiability will be important for the calculations, so the absolute value function would not be suitable. The quotient b/a to characterize the angular distortion is bounded (because if one arm of the angle falls in the 1st principal direction then $i = b/a \leq 1$). Therefore, AIRY substituted its reciprocal into the formula for *angular distortion value*: $\varepsilon_i^2 = (a/b - 1)^2$. The missing linear distortion depends not only on the location but also on the direction,* and JORDAN suggested averaging its deviation from 1 in each direction μ : $\varepsilon_l^2 = 1/(2\pi) \oint (l - 1)^2 d\mu$.

In the map, we want to minimize not only one kind of distortion but all distortions simultaneously, so to characterize this we need to introduce the concept of *total distortion value*. AIRY simply measured this by taking the arithmetic mean of the angular and areal distortion values, i.e. $\varepsilon^2 = (\varepsilon_p^2 + \varepsilon_i^2)/2 = [(ab - 1)^2 + (a/b - 1)^2]/2$. Notice that the linear distortion value is not included in the formula for the total distortion. The reason is that linear scale is algebraically related to angular and areal distortions, so they do not provide any additional information in the evaluation of map distortions. Note that while taking the average, it is not necessary to give equal weight to angular and areal distortions if their undesirability is not equal for the theme. Different weighting was suggested by KLINGATSCH. The term leading to the complicated calculations was only used by AIRY to evaluate existing projections, choosing the simpler form $\varepsilon_A^2 = [(a - 1)^2 + (b - 1)^2]/2$ to find the projection with the lowest distortion.

Although AIRY's theory still defines the evaluation of map distortion today, it has three serious shortcomings: KAVRAYSKIY complained that the formulæ do not give equal weight to increases and decreases in area. For example, among the equally distorted $p = 2$ and $p = 1/2$, the former has a

* In fact, the angular distortion would also depend on the direction of the angle arms if we did not require that one of the angle arms be the 1st principal direction of the projection.

distortion value of 1, the latter only 1/4. BAYEVA has shown that the formulæ do not measure areal and angular distortion on a comparable scale and therefore give misleading results, especially for weighted averaging. GYÖRFFY showed that AIRY's simpler total distortion actually tests completely different properties of the projection than the original version of the measure. All three shortcomings only occur in the case of large distortions, so AIRY's formulæ can be recommended for small areas.

To solve these problems, KAVRAYSKIY proposed the logarithm function for the deviation from 1, which overcomes all three shortcomings. Thus, the recommended formulæ for areal, angular, linear and total distortion values are respectively:

$$\begin{aligned}\varepsilon_p^2 &= \ln^2 p = \ln^2(ab) \\ \varepsilon_i^2 &= \ln^2 i = \ln^2 \frac{b}{a} = \ln^2 \frac{a}{b} \\ \varepsilon_l^2 &= \frac{1}{2\pi} \oint \ln^2 l \, d\mu = \frac{1}{2\pi} \oint \ln^2 \sqrt{a^2 \cos^2 \mu + b^2 \sin^2 \mu} \, d\mu \\ \varepsilon^2 &= \frac{1}{2} \left[\ln^2(ab) + \ln^2 \frac{a}{b} \right] = \ln^2 a + \ln^2 b\end{aligned}$$

The weighted average of the angular and areal distortions can be calculated also in this case.

XXX.3 The global distortion value

Unlike local distortion value, the *global distortion value* expresses the distortions of a projection over an entire area. Of course, such calculations are only worthwhile if the distortions are already visible to the naked eye due to the large extent of the area represented, or if geodetic measurements are to be made on the map. However, these two applications have quite different requirements. Geodesists want their map measurements to be free of distortion at any point, so the goodness of a projection is characterized by the *extrema* of local distortion values in the area. In contrast, for small-scale maps, locally outlying distortions (e.g. pole-line) are acceptable, but the *average* of the distortions should be minimized. The two principles were systematized by MESHCHERYAKOV. Following him, the former principle is known as the *minimax*, the latter one as the *variational*.

Distortion values of minimax type are useful in geodesy, and are thus applied primarily to conformal projections. In this case, the global distortion is the quotient of the minimal and maximal values of the linear scale. The existence of the conformal projection with minimum distortion of minimax

type is stated by CHEBYSHEV's theorem: *For any continuous region of a sphere bounded by a twice differentiable curve, there exists a conformal projection for which the ratio of the supremum and infimum of the linear scale is minimal. The distortion of this projection is constant at the boundary of the domain.* In layman's terms, the isocols of the best conformal projection run parallel to the boundary of the domain to be plotted. Although such projections are more commonly used for topographic purposes, it is interesting to note that Fig. XXX.1 shows the least distorted conformal projection of minimax type for the entire sphere. For areas of complicated shape (e.g. countries), the best mapping for topographic purposes is approximated by transforming the stereographic projection using complex polynomials (cf. Sec. XXIX.1).

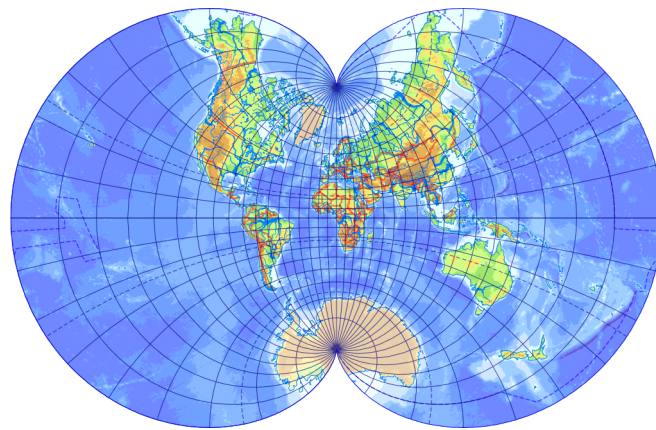


Figure XXX.1: *EISENLOHR projection*

The global distortion value of variational type is the average, i.e. the integral mean, of the local distortions over an area S :*

$$E^2 = \frac{1}{S} \iint_S \varepsilon^2 dS$$

In this formula, any local distortion value can be substituted for ε . In particular, if we substitute KAVRAYSKIY's total distortion value, we call the global distortion value the *AIRY-KAVRAYSKIY criterion*. Using the *AIRY-KAVRAYSKIY* criterion to classify the existing established projections, the most favourable mappings for world maps include the WINKEL III, BARANYI

* Some researchers believe that the distortions experienced by the map reader are not only the result of local infinitesimal distortions, but that distortions measured on finite shapes should be considered. However, algebraic relations and statistical tests show that this method does not yield a fundamentally different measure from the ones of variational type.

IV, KAVRAYSKIY VII and GINZBURG's pseudopolyconic projections, while the worst mappings include the polyconic projections, VAN DER GRINTEN's projections and the BONNE projection. If equal-area mappings are required, WAGNER-transformed projections and the ECKERT IV projection can be recommended for world mapping, while among the pointed-polar maps, the KAVRAYSKIY V and HAMMER projections are relatively preferable, but the distortion value of equal-area maps is usually higher than that of the aphyllactic ones.

The projection with the lowest global distortion value of variational type for a certain area S is called the *ideal projection*. No one has yet succeeded in solving the second-order EULER-LAGRANGE differential equation required to find the ideal projection. This does not mean that the ideal projection cannot be approximated by a power series. Thus, it is only necessary to determine the unknown coefficients of a polynomial such that the global distortion value is minimal. This can be easily found by numerical methods. An ideal projection can be interpreted not only for the whole Earth, but also for regions, in which case the distortion of the projection is minimal only for the selected area, outside which arbitrary distortions can occur.

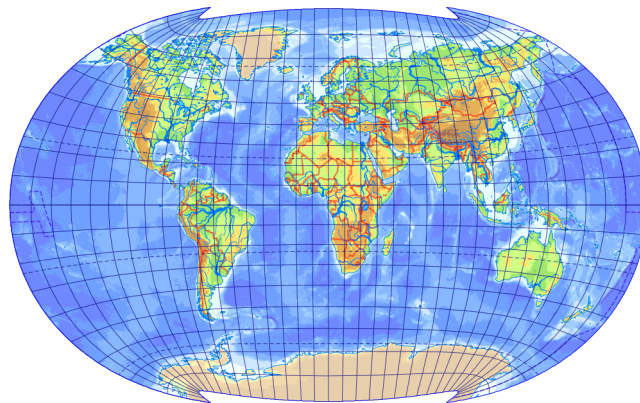


Figure XXX.2: *Approximation of the ideal projection*

As shown in Fig. XXX.2, the ideal projection of the whole Earth is not ideal for cartographic purposes. Indeed, the distortions are surprisingly good, but the map frame and the mapped graticule are very disturbing, while they can be important considerations when selecting the projection. Following MESHCHERYAKOV, the *best projection* is the mapping with the lowest global distortion value for the represented area within a set of projections defined by a prescription. The best projection according to the AIRY-KAVRAYSKIY criterion is known only among cylindrical projections (this is the equirectangular one), but according to AIRY's original, simpler

criterion, the best projection is also known among azimuthal and conic mappings (these are very complex, while for areas smaller than a hemisphere, they are hardly distinguishable from the equidistant counterparts).

Among non-conical projections, the formulæ of the best projection can only be approximated numerically by polynomials. These projections (when the unusual frame is discarded or clipped) provide unbeatable distortions for displaying the area. For example, the projection in Fig. XXVII.6 is the best rectangular polyazimuthal projection for representing the Northern Atlantic and Arctic Oceans together; Fig. XXX.3 shows the best equal-area pseudopolyconic projection for the Indian Ocean. It may be observed that the favourable parts of such projections can be concentrated in a selected area, but apart from this area distortions start to increase rapidly.

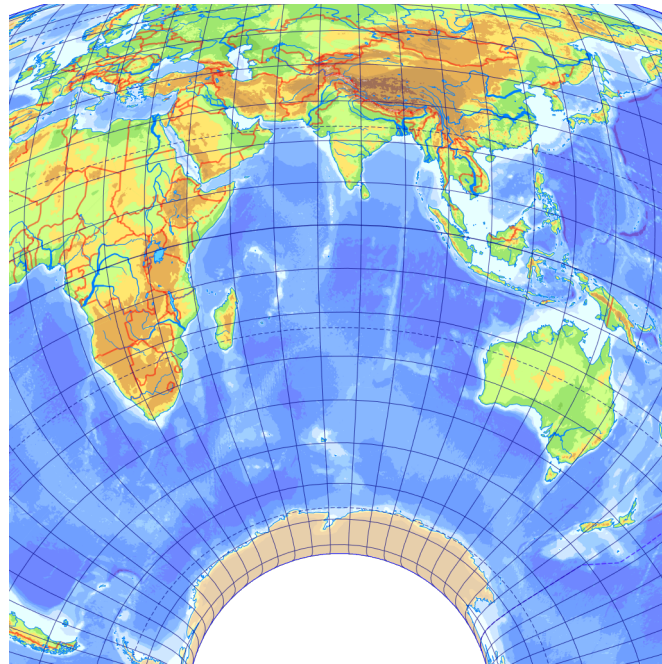


Figure XXX.3: *KERKOVITS flat-polar equal-area pseudopolyconic projection for the Indian Ocean*

XXX.4 Final thoughts

To select the projection correctly, the cartographer applies all his/her knowledge about the theory of map projection simultaneously. As you can see, there is no single recipe for finding the most appropriate mapping. Changing the projection is done with a few clicks in the appropriate program (if the desired projection is supported by the GIS), so it is worth taking the

XXX. Selecting a map projection

opportunity. Particularly for younger audience, the responsibility is great because they do not have the knowledge to correct for distortions; but a poorly chosen projection can make the interpretation of a thematic map difficult even for the best professionals.

Appendices

Appendix A

Basic mathematical relations

Below are some formulæ that can be used for the derivations in the lecture notes. The identities given here are not exhaustive, the main focus is on the identities that are important for cartographers.

Trigonometric identities

$$\sin(-\alpha) = -\sin \alpha$$

$$\cos(-\alpha) = \cos \alpha$$

$$\sin(90^\circ - \alpha) = \cos \alpha$$

$$\cos(90^\circ - \alpha) = \sin \alpha$$

$$\sin(180^\circ - \alpha) = \sin \alpha$$

$$\cos(360^\circ - \alpha) = \cos \alpha$$

$$\tan \alpha = \frac{\sin \alpha}{\cos \alpha}$$

$$\tan(180^\circ + \alpha) = \tan \alpha$$

$$\cot \alpha = \frac{1}{\tan \alpha} = \frac{\cos \alpha}{\sin \alpha}$$

$$\tan(90^\circ - \alpha) = \cot \alpha$$

$$\sin^2 \alpha + \cos^2 \alpha = 1$$

$$\tan^2 \alpha + 1 = \frac{1}{\cos^2 \alpha}$$

$$1 + \cot^2 \alpha = \frac{1}{\sin^2 \alpha}$$

$$\sin(\alpha \pm \beta) = \sin \alpha \cos \beta \pm \cos \alpha \sin \beta$$

$$\sin \alpha = \sin\left(\frac{\alpha}{2} + \frac{\alpha}{2}\right) = 2 \sin \frac{\alpha}{2} \cos \frac{\alpha}{2}$$

$$\cos(\alpha \pm \beta) = \cos \alpha \cos \beta \mp \sin \alpha \sin \beta$$

$$\cos \alpha = \cos\left(\frac{\alpha}{2} + \frac{\alpha}{2}\right) = \cos^2 \frac{\alpha}{2} - \sin^2 \frac{\alpha}{2}$$

$$1 + \cos \alpha = 2 \cos^2 \frac{\alpha}{2}$$

A. Basic mathematical relations

$$1 - \cos \alpha = 2 \sin^2 \frac{\alpha}{2}$$

$$\sin \alpha = \frac{\left(2 \sin \frac{\alpha}{2} \cos \frac{\alpha}{2}\right) / \cos^2 \frac{\alpha}{2}}{\left(\cos^2 \frac{\alpha}{2} + \sin^2 \frac{\alpha}{2}\right) / \cos^2 \frac{\alpha}{2}} = \frac{2 \tan \frac{\alpha}{2}}{1 + \tan^2 \frac{\alpha}{2}}$$

$$\cos \alpha = \frac{\left(\cos^2 \frac{\alpha}{2} - \sin^2 \frac{\alpha}{2}\right) / \cos^2 \frac{\alpha}{2}}{\left(\cos^2 \frac{\alpha}{2} + \sin^2 \frac{\alpha}{2}\right) / \cos^2 \frac{\alpha}{2}} = \frac{1 - \tan^2 \frac{\alpha}{2}}{1 + \tan^2 \frac{\alpha}{2}}$$

Logarithmic identities

$$e^{\ln a} = a$$

$$-\ln a = \ln \frac{1}{a}$$

$$\ln a + \ln b = \ln(ab)$$

$$\ln a - \ln b = \ln \frac{a}{b}$$

$$c \ln a = \ln a^c$$

$$\frac{1}{c} \ln a = \ln \sqrt[c]{a}$$

$$\operatorname{artanh} x = \frac{1}{2} \ln \frac{1+x}{1-x}$$

$$\operatorname{artanh} \sin \alpha = \ln \tan \left(45^\circ + \frac{\alpha}{2}\right)$$

$$-\operatorname{artanh} \cos \alpha = \ln \tan \frac{\alpha}{2}$$

Derivative and antiderivative functions

The table below should be used so that the function on the right is the derivative of the left one, and the left function is the antiderivative of right one with respect to variable x . After integration, a constant must be added to the result!

$\frac{d}{dx} \rightarrow$	$\leftarrow \int dx$
c	0
x	1
cx	c
x^α	$\alpha x^{\alpha-1}$
$\frac{x^{\alpha+1}}{\alpha+1}$	x^α
\sqrt{x}	$\frac{1}{2\sqrt{x}}$

A. Basic mathematical relations

e^x	e^x
$\ln x$	$\frac{1}{x}$
$\sin x$	$\cos x$
$\cos x$	$-\sin x$
$\tan x$	$\frac{1}{\cos^2 x}$
$\cot x$	$-\frac{1}{\sin^2 x}$
$\ln \tan \frac{x}{2}$	$\frac{1}{\sin x}$
$\ln \tan\left(45^\circ + \frac{x}{2}\right)$	$\frac{1}{\cos x}$
$\arcsin x$	$\frac{1}{\sqrt{1-x^2}}$
$\arccos x$	$-\frac{1}{\sqrt{1-x^2}}$
$\operatorname{arctan} x$	$\frac{1}{1+x^2}$
$\operatorname{arsinh} x$	$\frac{1}{\sqrt{1+x^2}}$
$\operatorname{arcosh} x$	$\frac{1}{\sqrt{x^2-1}}$
$\operatorname{artanh} x$	$\frac{1}{1-x^2}$

Derivative of compound functions

$$\frac{d}{dx}(f+c) = \frac{df}{dx}$$

$$\frac{d}{dx}cf = c\frac{df}{dx}$$

$$\frac{d}{dx}(f \pm g) = \frac{df}{dx} \pm \frac{dg}{dx}$$

$$\frac{d}{dx}fg = \frac{df}{dx}g + f\frac{dg}{dx}$$

$$\frac{d}{dx}\frac{f}{g} = \frac{\frac{df}{dx}g - f\frac{dg}{dx}}{g^2}$$

$$\frac{d}{dx}f[g(x)] = \frac{df}{dg}[g(x)] \times \frac{dg}{dx}(x)$$

$$\frac{df}{dx} = \frac{df}{dy} \frac{dy}{dx}$$

$$\frac{d}{dx}f^{-1} = \frac{1}{\frac{df}{dx}[f^{-1}(x)]} = \frac{dx}{df}$$

Antiderivative of compound functions

In the following formulæ, F is the antiderivative of f :

$$\begin{aligned} \int cf \, dx &= c \int f \, dx \\ \int f \pm g \, dx &= \int f \, dx \pm \int g \, dx \\ \int f(ax + b) \, dx &= \frac{1}{a}F(ax + b) + c \\ \int f^\alpha \frac{df}{dx} \, dx &= \frac{f^{\alpha+1}}{\alpha + 1} + c \\ \int \frac{\frac{df}{dx}}{f} \, dx &= \ln f + c \\ \int \frac{\frac{df}{dx}}{1 + f^2} \, dx &= \arctan f + c \\ \int \frac{\frac{df}{dx}}{1 - f^2} \, dx &= \operatorname{artanh} f + c \\ \int f[g(x)] \frac{dg}{dx} \, dx &= F[g(x)] + c \\ \int \frac{df}{dx} g \, dx &= fg - \int f \frac{dg}{dx} \, dx \end{aligned}$$

Solving a separable differential equation

If:

$$g(f)h(x) \frac{df}{dx} = 1$$

Then:

$$\int g(f) \, df = \int \frac{1}{h(x)} \, dx + c$$

Appendix B

Rare formulæ in spherical trigonometry

In this appendix, a possible derivation for theorems in spherical trigonometry that were stated without proof in Sec. III.1 is given for the interested reader. They are not discussed in the main text because they are rarely needed, but their derivation contributes to a deeper understanding of spherical geometry.

Denote the vectors from the centre of the sphere to the vertices of the triangle ABC by $\vec{A}, \vec{B}, \vec{C}$! Let \vec{A}' be the unit vector pointing in the direction of the *cross* product $\vec{B} \times \vec{C}$; i.e., draw a line through the centre of the sphere perpendicular to the plane containing side a of the spherical triangle and let the point A' be that point of intersection between the line and the sphere, which is closer to A . Use a similar construction to define points B' and C' ! The spherical triangle $A'B'C'$ is called the polar triangle of triangle ABC (Fig. B.1).

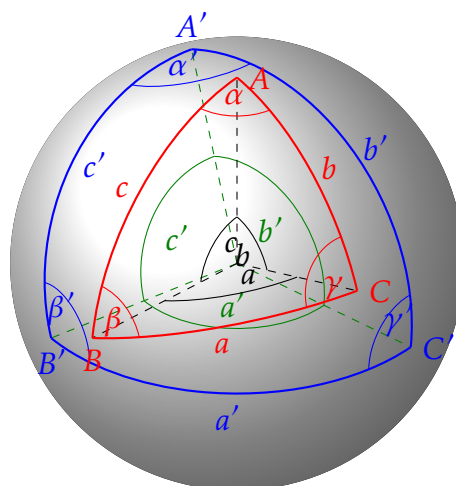


Figure B.1: Polar triangle

B. Rare formulæ in spherical trigonometry

By definition, \vec{B}' is perpendicular to the plane of side b , i.e., to both vectors \vec{A} and \vec{C} , and \vec{C}' is perpendicular to the plane of side c , i.e., to both vectors \vec{A} and \vec{B} . It follows that \vec{A} is perpendicular to both \vec{B}' and \vec{C}' , i.e. \vec{A} is perpendicular to the plane containing side a' subtended by the latter two. Similarly, the perpendicularity of \vec{B} and b' as well as \vec{C} and c' can be shown. We have now seen that the polar triangle of triangle $A'B'C'$ is the original triangle ABC .

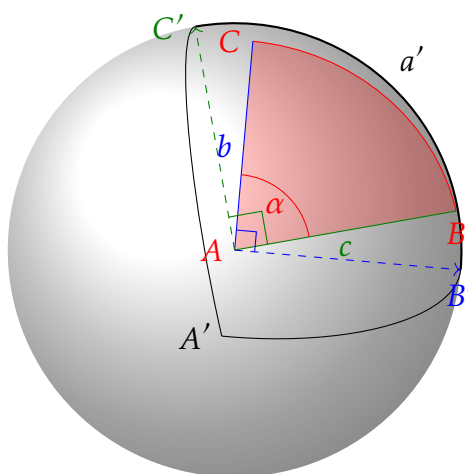


Figure B.2: The polar of angle α

In Fig. B.2, we have rotated the sphere so that the vertex A is exactly in the front. Since \vec{A} is perpendicular to the plane of side a' , from our perspective, side a' appears just on the perimeter of the mapped sphere. In the figure, the blue angle between the plane of side b and \vec{B}' and the green angle between the plane of side c and \vec{C}' are by definition right angles, but they overlap each other at angle α between the planes of the two sides. It follows that the subtended angle of a' is less than the two right angles (180°) by α . This gives $\alpha + a' = 180^\circ$. By similar reasoning, $\beta + b'$ and $\gamma + c'$ are also 180° . Since the polar of the polar triangle is the original triangle, $\alpha' + a$, $\beta' + b$, and $\gamma' + c$ also add up to 180° .

Formulate the spherical rule of cosines proved in Sec. III.1 for the polar triangle.

$$\cos c' = \cos a' \cos b' + \sin a' \sin b' \cos \gamma'$$

The corresponding sides and angles of the original and the polar triangle add up to 180° , i.e. $a' = 180^\circ - \alpha$, $\alpha' = 180^\circ - a$, $b' = 180^\circ - \beta$ etc. Substituting

B. Rare formulæ in spherical trigonometry

this:

$$\begin{aligned}\cos(180^\circ - \gamma) &= \cos(180^\circ - \alpha)\cos(180^\circ - \beta) \\ &\quad + \sin(180^\circ - \alpha)\sin(180^\circ - \beta)\cos(180^\circ - c)\end{aligned}$$

It is known that $\sin(180^\circ - \delta) = \sin \delta$ and $\cos(180^\circ - \delta) = -\cos \delta$. From this:

$$\begin{aligned}-\cos \gamma &= (-\cos \alpha)(-\cos \beta) + \sin \alpha \sin \beta(-\cos c) \\ \cos \gamma &= -\cos \alpha \cos \beta + \sin \alpha \sin \beta \cos c\end{aligned}$$

That is, we have proven the validity of *second spherical rule of cosines*. From the spherical rule of sines presented in Sec. III.1:

$$\begin{aligned}\frac{\sin c}{\sin \gamma} &= \frac{\sin a}{\sin \alpha} \\ \sin c &= \frac{\sin a \sin \gamma}{\sin \alpha}\end{aligned}$$

The spherical rule of cosines applied to both sides c and a :

$$\begin{aligned}\cos c &= \cos a \cos b + \sin a \sin b \cos \gamma \\ \cos a &= \cos b \cos c + \sin b \sin c \cos \alpha\end{aligned}$$

Applying the above rules of sines and cosines to the coloured trigonometric functions:

$$\cos a = \cos b(\cos a \cos b + \sin a \sin b \cos \gamma) + \frac{\sin b \sin a \sin \gamma \cos \alpha}{\sin \alpha}$$

The third side is cancelled from the equation. The terms containing $\cos a$ are collected on the left-hand side and then divided by $\sin a \sin b$:

$$\begin{aligned}\cos a &= \cos a \cos^2 b + \sin a \sin b \left(\cos b \cos \gamma + \sin \gamma \frac{\cos \alpha}{\sin \alpha} \right) \\ \cos a(1 - \cos^2 b) &= \sin a \sin b (\cos b \cos \gamma + \sin \gamma \cot \alpha) \\ \frac{\cos a \sin^2 b}{\sin a \sin b} &= \cos b \cos \gamma + \sin \gamma \cot \alpha \\ \cot a \sin b &= \cos b \cos \gamma + \sin \gamma \cot \alpha\end{aligned}$$

This gives the *cotangent four-part formula* we have been looking for, which creates a relationship between two sides and two angles.

B. Rare formulæ in spherical trigonometry

Note that, by choosing the two sides of the triangle differently or by swapping their order on the left-hand side and rewriting the expression on the right-hand side accordingly, there are six different forms of this equation.

Only side a and angle α can be expressed directly from the equation. If we need side b or angle γ , using relations $\sin \delta = 2 \tan(\delta/2)/[1 + \tan^2(\delta/2)]$ and $\cos \delta = [1 - \tan^2(\delta/2)]/[1 + \tan^2(\delta/2)]$ (by substituting side b or angle γ for δ) and after rearranging, we obtain a quadratic equation in $\tan(b/2)$ or $\tan(\gamma/2)$, respectively. This typically has two solutions, but sometimes it gives only one solution or no solution. In the latter case, no spherical triangle exists with the given sides and angles.

Appendix C

BORKOWSKI'S formula for the latitude

In Sec. IV.3, it was shown that:

$$z = \left[\frac{\sqrt{x^2 + y^2}}{\cos \Phi} - e^2 N(\Phi) \right] \sin \Phi$$

From this, we want to express the latitude. First note that:

$$\frac{1}{\cos^2 \Phi} = \frac{\sin^2 \Phi + \cos^2 \Phi}{\cos^2 \Phi} = \frac{\sin^2 \Phi}{\cos^2 \Phi} + \frac{\cos^2 \Phi}{\cos^2 \Phi} = \tan^2 \Phi + 1$$

Substitute the formula for the prime-vertical radius of curvature into the original equation, and then start rearranging! For simplicity, let us use the notation $r = \sqrt{x^2 + y^2}$! The point of the transformation is to remove the root sign by moving it alone to the left-hand side, then squaring both sides; remove the fractions by multiplying with the denominators, finally divide by $\cos^4 \Phi$ to transform everything to tangents.

$$\begin{aligned} \frac{z}{\sin \Phi} &= \frac{r}{\cos \Phi} - \frac{ae^2}{\sqrt{1 - e^2 \sin^2 \Phi}} \\ \frac{a^2 e^4}{1 - e^2 \sin^2 \Phi} &= \frac{r^2}{\cos^2 \Phi} - 2 \frac{rz}{\cos \Phi \sin \Phi} + \frac{z^2}{\sin^2 \Phi} \\ a^2 e^4 \cos^2 \Phi \sin^2 \Phi &= r^2 \sin^2 \Phi - r^2 e^2 \sin^4 \Phi - 2rz \cos \Phi \sin \Phi \\ &\quad + 2rze^2 \sin^3 \Phi \cos \Phi + z^2 \cos^2 \Phi - z^2 e^2 \sin^2 \Phi \cos^2 \Phi \\ a^2 e^4 \frac{\sin^2 \Phi}{\cos^2 \Phi} &= r^2 \frac{\sin^2 \Phi}{\cos^4 \Phi} - r^2 e^2 \frac{\sin^4 \Phi}{\cos^4 \Phi} - 2rz \frac{\sin \Phi}{\cos^3 \Phi} \\ &\quad + 2rze^2 \frac{\sin^3 \Phi}{\cos^3 \Phi} + \frac{z^2}{\cos^2 \Phi} - z^2 e^2 \frac{\sin^2 \Phi}{\cos^2 \Phi} \\ a^2 e^4 \tan^2 \Phi &= r^2 \tan^2 \Phi (1 + \tan^2 \Phi) - r^2 e^2 \tan^4 \Phi - 2rz \tan \Phi (1 + \tan^2 \Phi) \\ &\quad + 2rze^2 \tan^3 \Phi + z^2 (1 + \tan^2 \Phi) - z^2 e^2 \tan^2 \Phi \end{aligned}$$

C. BORKOWSKI's formula for the latitude

$$[(1 - e^2)r^2] \tan^4 \Phi + [(e^2 - 1)2rz] \tan^3 \Phi + [r^2 + z^2(1 - e^2) - a^2e^4] \tan^2 \Phi + [-2rz] \tan \Phi + z^2 = 0$$

If we introduce variable $t = \tan \Phi$, we obtain the following quartic equation for the unknown t by denoting the terms in the square brackets of the above equation by capital letters:

$$At^4 + Bt^3 + Ct^2 + Dt + E = 0$$

The solution to this quartic equation is called the FERRARI method. First, introduce a new variable $u = t + B/4A$ by substituting $t = u - B/4A$. After substitution, the equation is divided by A , the parentheses are expanded and the terms of equal degree in u are collected, and the third-degree term is eliminated:

$$u^4 + \left(\frac{-3B^2}{8A^2} + \frac{C}{A}\right)u^2 + \left(\frac{B^3}{8A^3} - \frac{BC}{2A^2} + \frac{D}{A}\right)u + \left(\frac{-3B^4}{256A^4} + \frac{B^2C}{16A^3} - \frac{BD}{4A^2} + \frac{E}{A}\right) = 0$$

The coefficients in parentheses are denoted by Greek letters:

$$u^4 + \alpha u^2 + \beta u + \gamma = 0$$

For any v , it is true that:

$$\left(u^2 + \frac{\alpha}{2} + v\right)^2 = 2vu^2 - \beta u + v^2 + \alpha v + \frac{\alpha^2}{4} - \gamma$$

This can be checked by expanding the parentheses and arranging terms on the left-hand side. In this way, v is cancelled, and the previous equation is obtained. Transforming the right-hand side further:

$$\left(u^2 + \frac{\alpha}{2} + v\right)^2 = \left(\sqrt{2vu} - \frac{\beta}{2\sqrt{2v}}\right)^2 - \frac{\beta^2}{8v} + v^2 + \alpha v + \frac{\alpha^2}{4} - \gamma$$

Since the above equation is true for any v , let us pick that v for which the green term is exactly zero. Then, denoting the red term by U and the blue term by V , $U^2 = V^2$, i.e. $U^2 - V^2 = 0$, so $(U + V)(U - V) = 0$, i.e. the next product is zero:

$$\left(u^2 + \frac{\alpha}{2} + v + \sqrt{2vu} - \frac{\beta}{2\sqrt{2v}}\right) \left(u^2 + \frac{\alpha}{2} + v - \sqrt{2vu} + \frac{\beta}{2\sqrt{2v}}\right) = 0$$

However, the product can only be zero if at least one of its factors is zero. From this we obtain two quadratic equations of u , whose two solutions

C. BORKOWSKI's formula for the latitude

will be the four solutions of the incomplete quadratic equation. Then, by definition, the four roots of u also give four solutions to t , so the quadratic equation is solved. In fact, we would have solved it if we knew what value we had chosen for v . The condition was that the green term above should be zero. Then the green term multiplied by v is also zero:

$$v^3 + \alpha v^2 + \left(\frac{\alpha^2}{4} - \gamma\right)v - \frac{\beta^2}{8} = 0$$

We have a cubic equation, which we must solve using the CARDANO formula. Let us introduce the auxiliary variable $w = v - (\alpha^2/4 + \gamma)/3$, i.e. substitute this: $v = w + (\alpha^2/4 + \gamma)/3$. Then, by expanding the parentheses and collecting terms of the same degree in w , the second-degree term is cancelled:

$$w^3 + \left[\frac{\alpha^2}{4} - \gamma - \frac{\alpha^2}{3}\right]w + \left[-\frac{\beta^2}{8} - \frac{\alpha\left(\frac{\alpha^2}{4} - \gamma\right)}{3} + \frac{2\alpha^3}{27}\right] = 0$$

In other words, denoting the constant coefficients by letters:

$$w^3 + Pw + Q = 0$$

Let $w = W + Z$! Then, by expanding the parentheses:

$$W^3 + Z^3 + (3WZ + P)(W + Z) + Q = 0$$

Since we can freely choose one of W and Z , let $3WZ + P = 0$! Then, from the equation above and our condition (all terms cubed), we get two equations:

$$\begin{aligned} W^3 + Z^3 &= -Q \\ W^3 Z^3 &= -P^3/27 \end{aligned}$$

From the above equations, it follows from VIETA's formulæ that W^3 and Z^3 are two solutions of the following quadratic equation of s :

$$s^2 + Qs - \frac{P^3}{27} = 0$$

Solving the quadratic equation:

$$s_{1,2} = W^3, Z^3 = -\frac{Q}{2} \pm \sqrt{\frac{Q^2}{4} + \frac{P^3}{27}}$$

C. BORKOWSKI's formula for the latitude

That is, since $w = W + Z$, we obtain one root of the incomplete cubic equation:

$$w = \sqrt[3]{-\frac{Q}{2} + \sqrt{\frac{Q^2}{4} + \frac{P^3}{27}}} + \sqrt[3]{-\frac{Q}{2} - \sqrt{\frac{Q^2}{4} + \frac{P^3}{27}}}$$

Our linear substitution thus returns the solution v for the original cubic equation, from which we now know v in the two quadratic equations derived from the incomplete quartic equation. Thus, we now have four solutions u to the quartic equation, from which we also have solutions for t of the original quartic equation. This is the tangent of the latitude, which we can use even to get back the height above the ellipsoid by substituting it back into the formulæ in Sec. IV.3. Let us think about the fact that this huge amount of computing is going on every second in that little GPS chip in the phone!

In fact, BORKOWSKI did not derive the quartic equation exactly in the way outlined above. The question is still an active area of research today, how to obtain a quartic equation that leads to numerically stable formulæ.

Appendix D

Vertical datums

3D spatial data are becoming increasingly important in GIS computing. Therefore, it is no longer generally satisfactory to fit data only horizontally. Thus, although altimetry and vertical coordinate systems are outside the scope of map projection theory, the definition of the reference frame of elevation data is becoming essential in addition to the projection and geodetic datum. This appendix is intended to help in understanding this.

When measuring altitude, the shape of the Earth is considered to be an ellipsoid usually only in the case of satellite navigation. This is because, on the one hand, it is difficult to measure altitude above an ellipsoid using field measurements and, on the other hand, it is not very useful, since the terrestrial ellipsoid can deviate up to 100 metres from the sea level. For this reason, the use of elevations above the ellipsoid can lead to erroneous conclusions, for example, in flood protection applications. It is therefore preferable to measure altitude relative to sea level.

Sea level is measured by tide gauges on the coast. Sea levels are recorded over a number of years to eliminate the effects of weather and tide. The average of the measured data on the tidal gauge is the *mean sea level*.

The sea level at rest is everywhere perpendicular to the local gravity, and the potential energy along the water level is constant. Surfaces along which the potential energy does not vary and is everywhere perpendicular to the force field are called *equipotential surfaces* or *level surfaces*. Level surfaces never cross each other, but their distance is not constant: since the gravity is greater at the poles than at the Equator (due to the effect of centrifugal force), the same amount of work (gaining the same amount of potential energy) will result in a smaller difference in height at the poles than at the Equator. This shows that the level surfaces are denser near the poles. The level surface that lies on the mean sea level measured on the tidal gauge is known as the *geoid* and is considered to be the shape of the Earth when measuring altitude (Fig. D.1) A curve whose tangent at each point is in the direction of gravity is called a *plumb line*.

Sea levels are affected by water temperature, salinity and currents. Therefore, the geoid fixed to a particular tidal gauge follows the mean sea level

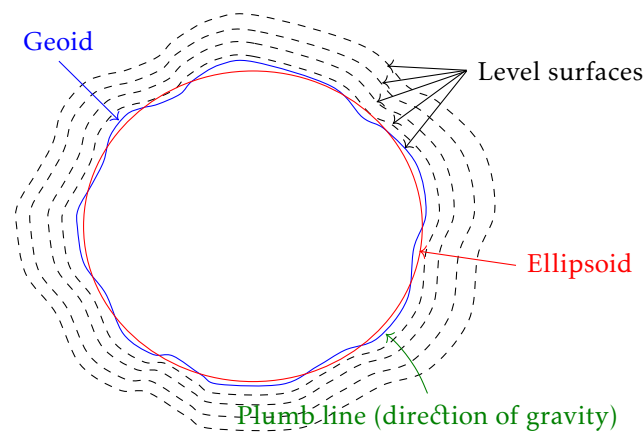


Figure D.1: The shape and the gravity field of the Earth

only loosely elsewhere in the ocean. Therefore, the level surfaces fixed to the different tidal gauges do not coincide, but the difference in height between them does not exceed one metre. In Hungary, until the 1960s, the Trieste (Adriatic height) and since then the Kronstadt (Baltic height) tidal gauges have been used as the reference. In the EU, the Amsterdam height is used when a uniform system between states is needed. Adriatic heights are 67.5 cm and Amsterdam heights are 14 cm higher than Baltic heights.

The distance along the plumb line between the geoid and our point is the *height above sea level*, denoted by H . The distance between the geoid and the ellipsoid along the normal of the ellipsoid is the *geoid undulation* n . The geoid undulation is positive if the geoid is above the ellipsoid (as it does in most parts of Europe) and negative if it runs below it (as in Fig. D.2), its value is usually between ± 100 m. The *height above the ellipsoid* (h) is also measured along the normal of the ellipsoid. The angle between the normal of the ellipsoid and the plumb line passing through our point is called the *vertical deflection*.*

* Vertical deflection is also important in horizontal systems. The *astronomical latitude* is the angle between the local horizontal and the Earth's axis of rotation (the North Star), while the *geographic latitude* is the angle between the normal of the ellipsoid and the plane of the Equator. The two latitudes are not the same because, although the Equatorial plane is perpendicular to the axis of rotation, the local horizontal and the normal of the ellipsoid are not exactly perpendicular just because of the vertical deflection. The difference is thus precisely the north-south component of the vertical deflection. Similarly, since we can determine the *astronomical longitude* with respect to the local horizontal, its deviation from the *geographic longitude* is the east-west component of the vertical deflection. It can be seen why the regional datums used for horizontal measurements in Sec. VI.4 were fitted to the geoid by minimizing the vertical deflection and not the geoid undulation.

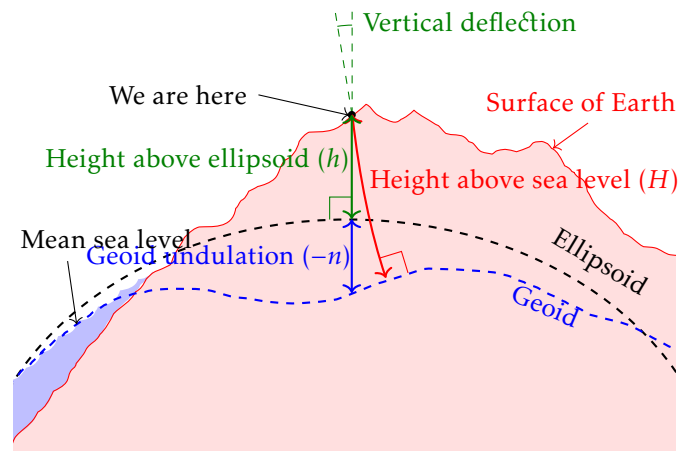


Figure D.2: Heights above sea level and above ellipsoid

The figure shows that, given the geoid undulation, the height above sea level can be estimated from the height above ellipsoid calculated in satellite navigation (Sec. IV.3):

$$H \approx h - n$$

There is no exact equality because of the vertical deflection, but the deviation is usually less than or equal to one millimetre, so in practice we do not need to take this into account (since geoid undulation is rarely known with such precision).

If you go around a closed curve and add up the differences in altitude, you would expect to get 0, since you have returned to the same point. So it would be intuitive if $\oint dH = 0$ along any closed curve. This statement would imply (as common sense would expect) that the sum of the measured height differences between two given points is independent of the path. The reality is much more complicated.

Try to determine the height H_C at the peak of the island marked by C in Fig. D.3. Because of the size of the hill, we cannot do this in one step, and it is obvious that we will not dig along the plumb line to the geoid for the sake of measurement. The group with blue rods will go straight up from point A to point C, while the group with green rods will first walk around the coast to point B (not noticing any difference in elevation, so taking the elevation of B as zero), and then level up to point C. The figure shows that the green group has measured higher altitude up to point C, and (even if neither group had made measurement errors) none of the height differences add up to the height of point C! Of course, this phenomenon is only significant at very long distances (for national surveys), but it is difficult to measure the heights of points precisely based on levelling along different routes.

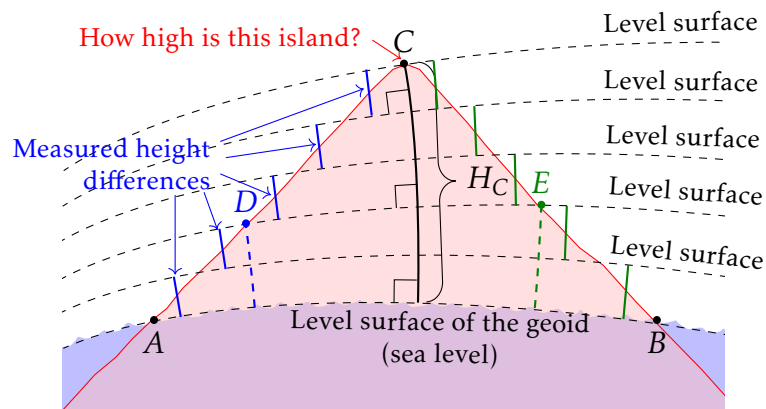


Figure D.3: Surprising properties of height measurements

Nevertheless, we can see that the points D and E are on the same level surface. This means that these two points could be on the shore of the same lake, since they are horizontal to each other. Yet the elevation of point E is higher than that of point D , i.e. water can flow *up* from point D to point E ! This is caused by the uneven gravitational field of the Earth: at point E , the level surfaces are spaced less sparsely. The height difference between different points of the water level in a mountain lake the size of Lake Geneva can be up to half metre! This can cause unpleasant surprises in case of flooding!

Therefore, for large-scale (national) surveys, it is better to measure the difference in the potential energy per unit mass (*geopotential*). The potential K is indeed independent of the measurement path, but the local gravitational acceleration g_i should always be measured in addition to the difference in height ΔH_i .

$$K = \sum_i g_i \Delta H_i$$

The measured potential is thus used to obtain the height:

$$H = \frac{K}{\bar{g}}$$

\bar{g} is the average gravitational acceleration along the plumb line, but again we will not dig down into the mountain to measure this. In the case of the traditional geometric definition of height (*orthometric height* in the literature), we attempt to model this (often used abroad), while for *normal height* we simplify the estimation of \bar{g} by assuming the Earth to have an ellipsoidal shape and uniform mass distribution. *Dynamic height* assigns

D. Vertical datums

the same height to points on the same level surface, and thus has a physical meaning. Then the value \bar{g} is chosen to be uniform regardless of location. The resulting differences are of the order of decimetres, and confusion is only problematic if engineering precision is required. However, geoid undulation can be up to 100 m, so heights above the ellipsoid should never be confused with heights above sea level!

So when entering elevation coordinates into GIS software, pay attention to their type (above ellipsoid or sea level, in the latter case, which type) and their reference frame (which ellipsoid, which sea level)! The vertical base points for Hungary are fixed to normal heights from the Kronstadt tidal gauge. The network of vertical base points is called the *vertical datum*. The conversion between the vertical datums of two countries can be done by a simple offset if centimetre accuracy is required. However, we must bear in mind that plate tectonics cause base points to shift over time, so even between vertical datums of countries using the same sea level, there may be a difference of a few centimetres over decades. To convert between elevations above ellipsoid and sea level, our software also needs a geoid model to calculate the geoid undulation.

Appendix E

Alternative derivation of TISSOT's theory

In contrast to the geometric proof presented in the note, I give an algebraic proof, because this point of view fits better to the modern approach of differential geometry. This time, Tissot's theory is proved only for a surface of revolution as the reference frame and a planar image.* First, consider a coordinate system $\Delta n, \Delta m$ at an arbitrary point on the tangent plane of the surface of revolution with the axes in the direction of the parallels and meridians of the surface of revolution. Since we are considering only the infinitely small neighbourhood of the point, we can neglect the difference between the surface of revolution and its tangent plane. The coordinates of a very close point are $(\Delta n, \Delta m)$. This can be estimated from the coordinates on the surface of revolution (due to the infinitely small distances and the differentiability of the parametric form, we can use a linear approximation):

$$\begin{aligned}\Delta n &= \frac{dn}{d\lambda} \Delta\lambda \\ \Delta m &= \frac{dm}{d\varphi} \Delta\varphi\end{aligned}$$

From this:

$$\begin{aligned}\Delta\lambda &= \frac{\Delta n}{\frac{dn}{d\lambda}} \\ \Delta\varphi &= \frac{\Delta m}{\frac{dm}{d\varphi}}\end{aligned}$$

Fig. VII.1 shows that in the plane of projection, $\Delta x = \Delta m'_x + \Delta n'_x$ and $\Delta y = \Delta m'_y + \Delta n'_y$, i.e., substituting the linear approximations obtained for

* The general proof for surfaces not of revolution is possible by examining the multiplication of so-called metric tensors.

E. Alternative derivation of Tissot's theory

them (assuming the differentiability of the map projection as indicated in Sec. VI.2):

$$\begin{aligned}\Delta x &= \frac{\partial x}{\partial \varphi} \Delta \varphi + \frac{\partial x}{\partial \lambda} \Delta \lambda \\ \Delta y &= \frac{\partial y}{\partial \varphi} \Delta \varphi + \frac{\partial y}{\partial \lambda} \Delta \lambda\end{aligned}$$

That is:

$$\begin{aligned}\Delta x &= \frac{\frac{\partial x}{\partial \varphi}}{\frac{dm}{d\varphi}} \Delta m + \frac{\frac{\partial x}{\partial \lambda}}{\frac{dn}{d\lambda}} \Delta n \\ \Delta y &= \frac{\frac{\partial y}{\partial \varphi}}{\frac{dm}{d\varphi}} \Delta m + \frac{\frac{\partial y}{\partial \lambda}}{\frac{dn}{d\lambda}} \Delta n\end{aligned}$$

Thus, the transformation between the coordinate systems $\Delta n, \Delta m$ on the surface of revolution and $\Delta x, \Delta y$ in the plane can be described perfectly by the matrix form of the two equations:

$$\begin{pmatrix} \Delta x \\ \Delta y \end{pmatrix} = \begin{pmatrix} \frac{\partial x / \frac{dm}{d\varphi}}{\frac{dn}{d\lambda}} & \frac{\partial x / \frac{dm}{d\varphi}}{\frac{dn}{d\lambda}} \\ \frac{\partial y / \frac{dm}{d\varphi}}{\frac{dn}{d\lambda}} & \frac{\partial y / \frac{dm}{d\varphi}}{\frac{dn}{d\lambda}} \end{pmatrix} \begin{pmatrix} \Delta n \\ \Delta m \end{pmatrix}$$

Suppose that the transformation above can be decomposed into a composition of a rotation by angle ν , a stretching of factor a in the horizontal and factor b in the vertical direction, and then another rotation by angle ν . The three successive transformations are formulated as a product of matrices:

$$\begin{pmatrix} \cos \nu & \sin \nu \\ -\sin \nu & \cos \nu \end{pmatrix} \begin{pmatrix} a & 0 \\ 0 & b \end{pmatrix} \begin{pmatrix} \cos \nu & \sin \nu \\ -\sin \nu & \cos \nu \end{pmatrix}$$

The product of the previous transformation matrices:

$$\begin{pmatrix} a \cos \nu \cos \nu - b \sin \nu \sin \nu & a \sin \nu \cos \nu + b \cos \nu \sin \nu \\ -a \cos \nu \sin \nu - b \sin \nu \cos \nu & -a \sin \nu \sin \nu + b \cos \nu \cos \nu \end{pmatrix}$$

E. Alternative derivation of Tissot's theory

The matrix above is assumed to describe the same transformation as the original matrix, i.e. all four elements are the same:

$$\begin{aligned} a \cos \nu \cos \nu - b \sin \nu \sin \nu &= \frac{\partial x}{\partial \lambda} \Big/ \frac{dn}{d\lambda} \\ a \sin \nu \cos \nu + b \cos \nu \sin \nu &= \frac{\partial x}{\partial \varphi} \Big/ \frac{dm}{d\varphi} \\ -a \cos \nu \sin \nu - b \sin \nu \cos \nu &= \frac{\partial y}{\partial \lambda} \Big/ \frac{dn}{d\lambda} \\ -a \sin \nu \sin \nu + b \cos \nu \cos \nu &= \frac{\partial y}{\partial \varphi} \Big/ \frac{dm}{d\varphi} \end{aligned}$$

We obtain a non-linear system of four equations and four unknowns (a, b, ν, ν). Note that the above system of equations shows (if we find at least one real solution) that every differentiable projection in the infinitesimally small neighbourhood of an arbitrary point can be conceived of as a local affine transformation, i.e., the existence of a real solution would prove Tissot's theory.

Interestingly, in general, any matrix can be decomposed into a product of a rotation matrix, a diagonal matrix and another rotation matrix; this is called the singular value decomposition of the matrix. The elements of the diagonal matrix (i.e., in our particular example, the minimum and maximum linear scales a and b) are called the singular values of the transformation matrix.

Each of the four equations is squared and added together. The square sum of the left-hand sides:

$$\begin{aligned} &a^2 \cos^2 \nu \cos^2 \nu + b^2 \sin^2 \nu \sin^2 \nu - 2ab \cos \nu \cos \nu \sin \nu \sin \nu \\ &+ a^2 \sin^2 \nu \cos^2 \nu + b^2 \cos^2 \nu \sin^2 \nu + 2ab \sin \nu \cos \nu \cos \nu \sin \nu \\ &+ a^2 \cos^2 \nu \sin^2 \nu + b^2 \sin^2 \nu \cos^2 \nu + 2ab \cos \nu \sin \nu \sin \nu \cos \nu \\ &+ a^2 \sin^2 \nu \sin^2 \nu + b^2 \cos^2 \nu \cos^2 \nu - 2ab \sin \nu \sin \nu \cos \nu \cos \nu \end{aligned}$$

Terms in red cancel each other. Factoring the remaining terms, the expression is simplified as follows:

$$(a^2 + b^2)(\sin^2 \nu + \cos^2 \nu)(\sin^2 \nu + \cos^2 \nu) = a^2 + b^2$$

So the number of unknowns is reduced to two:

$$a^2 + b^2 = \left(\frac{\partial x}{\partial \lambda} \Big/ \frac{dn}{d\lambda} \right)^2 + \left(\frac{\partial x}{\partial \varphi} \Big/ \frac{dm}{d\varphi} \right)^2 + \left(\frac{\partial y}{\partial \lambda} \Big/ \frac{dn}{d\lambda} \right)^2 + \left(\frac{\partial y}{\partial \varphi} \Big/ \frac{dm}{d\varphi} \right)^2$$

E. Alternative derivation of Tissot's theory

Notice that this equation is equivalent to $a^2 + b^2 = h^2 + k^2$ of the geometric derivation, since the blue and green terms are just the formulæ for the distortions along graticule lines.

Now take the original system of four unknown equations and subtract the product of the second and third equations from the product of the first and fourth equations, i.e. calculate the determinant of the transformation matrix. Again, we first deal only with the left-hand sides.

$$\begin{aligned}
 & -a^2 \cos \nu \cos \nu \sin \nu \sin \nu - b^2 \sin \nu \sin \nu \cos \nu \cos \nu + ab \sin^2 \nu \sin^2 \nu \\
 & + ab \cos^2 \nu \cos^2 \nu + a^2 \sin \nu \cos \nu \sin \nu \cos \nu + b^2 \cos \nu \sin \nu \cos \nu \sin \nu \\
 & + ab \sin^2 \nu \cos^2 \nu + ab \cos^2 \nu \sin^2 \nu
 \end{aligned}$$

The red terms are again cancelled, the remaining terms are factored:

$$ab(\sin^2 \nu + \cos^2 \nu)(\sin^2 \nu + \cos^2 \nu) = ab$$

So the determinant of the left-hand matrix is equal to the determinant of the right-hand matrix:

$$ab = \frac{\partial x}{\partial \lambda} \frac{dn}{d\lambda} \times \frac{\partial y}{\partial \varphi} \frac{dm}{d\varphi} - \frac{\partial y}{\partial \lambda} \frac{dn}{d\lambda} \times \frac{\partial x}{\partial \varphi} \frac{dm}{d\varphi}$$

This equation is equivalent to equation $ab = p = hk \sin \vartheta$ of the geometric derivation, because the right-hand side is equivalent to one of the formulæ obtained for p . This means that the areal scale of a mapping is equal to the determinant of the matrix describing it.

We now have two equations and two unknowns left, namely $a^2 + b^2 = h^2 + k^2$ and $ab = 2hk \sin \vartheta$, which we solved earlier in Sec. VIII.3. Thus, the algebraic derivation gave the same result as the geometric one. However, from the algebraic derivation we also found that:

- Every projection can be locally described by a 2×2 matrix.
- The areal scale of the projection is the determinant of the matrix describing the transformation.
- The extremal values of the linear scales in the projection are the singular values of the matrix.

Recent research in map projections often treats distortions in this way, because this approach sometimes gives more useful formulæ for complex reference frames.

Substituting the solutions obtained for a and b back into the original system of equations, ν and ν can be expressed, which have an important geometric meaning: ν , the angle of the first rotation, indicates the angle on the reference frame between parallels and the first principal direction of

E. Alternative derivation of Tissot's theory

the projection. ν , the second rotation indicates the angle between the first principal direction of the projection and the horizontal coordinate axis on the map, i.e. it is used to construct the ellipse of distortion in the correct direction on the map.

Appendix F

Old projection systems in Hungary

The stereographic projection (Sec. X.5) was used in Hungary from 1857 until the 1970s. Since this projection gives a favourable representation of the polar region, it is advisable to use a metagracule (Sec. V.3). However, this is much more difficult to define on an ellipsoid than on a sphere. Therefore, a double mapping (Sec. XI.4) was used: from the datum HD1863 based on the BESSEL ellipsoid, the first projection mapped onto the old Gaussian conformal sphere (Sec. IX.3) where the spherical latitude of the equidistant parallel is $\varphi_s = 46^\circ 30'$, the other values are given in Tab. F.1.

We rotate the graticule. The metapole is taken at the origin (Gellérthegy). Since the area of Hungary was much larger than the area within which the distortions of the stereographic projection can be neglected, a metapole was established in Transylvania on Kesztej Hill near Marosvásárhely (Târgu Mureş) (Tab. F.2).

Finally, the formulæ of the tangent stereographic projection are applied. Since both the auxiliary sphere and the stereographic projection are conformal, the result of the double mapping is also conformal. The coordinate axes are oriented to the South and to the West (Fig. F.1). The Hungarian stereographic projection is the oldest conformal double mapping used in the world.

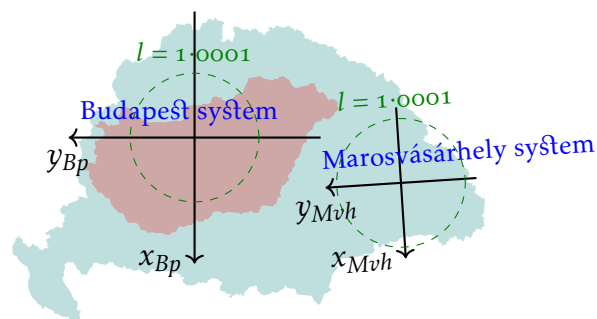


Figure F.1: Hungarian stereographic projections

Table F.1: *Coefficients of the conformal sphere*

	Notation	Old auxiliary sphere	New auxiliary sphere
Reference frame	—	BESSEL ellipsoid	IUGG1967 ellipsoid
Major semi-axis	a	6 377 397·155 m	6 378 160 m
Minor semi-axis	b	6 356 078·963 m	6 356 774·516 m
First numeric eccentricity	e	0·081 696 683 121 57	0·081 820 567 940 7
Radius of the Gaussian sphere	R	6 378 512·966 m	6 379 743·001 m
	χ	1·003 016 135 133	1·003 110 007 693
	n	1·000 751 489 594	1·000 719 704 936
Equidistant parallel	Φ_s	46°32'43·410 41''	47°10'
Equidistant parallel	φ_s	46°30'	47°7'20·057 80''
Prime meridian from Ferro	Λ_o	36°42'53·5733''	—
Prime meridian from Greenwich	Λ_o	19°3'7·5533''	19°2'54·8584''

Table F.2: *Central point of the metagraticule*

	Notation	Budapest	Marosvh.	HÉR	HKR	HDR	EOV
Ellipsoidal latitude	Φ_o / Φ_c	47°29' 9·6380''	46°33' 6·4273''	48°42' 56·3180''	47°8' 46·7267''	45°34' 36·5869''	47°8' 39·8147''
Ellipsoidal longitude (from Ferro, but from Greenwich for the EOv)	Λ_o / Λ_c	36°42' 53·5733''	42°3' 20·9550''	36°42' 53·5733''	36°42' 53·5733''	36°42' 53·5733''	19°2' 54·8584''
Spherical latitude	φ_o / φ_c	47°26' 21·1372''	46°30' 22·9804''	48°40'2''	47°6'	45°31'59''	47°6'
Spherical longitude (from Gellérthey)	λ_o / λ_c	0°	+5°20' 41·8290''	0°	0°	0°	0°

F. Old projection systems in Hungary

From 1936 onwards, the former ‘Civil’ coordinates were translated and the axes of the new ‘Military’ coordinates were oriented to the North and to the East in order to eliminate negative coordinates. The value of the translation was 500 km for Budapest and 600 km for Marosvásárhely (Fig. F.2; Tab. F.3). In the case of the Ivanić system found in the former Croatia-Slavonia, the ‘Civil’ (and hence the ‘Military’) coordinates do not have a specific projection, but can be estimated using the CASSINI–SOLDNER projection (Sec. XIV.2).

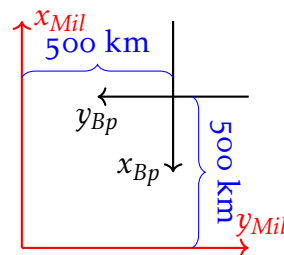


Figure F.2: ‘Civil’ and ‘Military’ coordinates

Because of its advantageous properties, the MERCATOR projection (Sec. XIII.2) is the projection of modern Hungarian civilian topographic maps, but it is used in oblique aspect. Its introduction in 1908 is attributed to FASCHING Antal. He rotated the points of the previous stereographic system by $6.44''$ clockwise around Gellérthegy, so the ellipsoidal coordinates were changed, although the BESSEL ellipsoid remained the reference frame. The new datum is HD1909.

FASCHING’s cylindric system is also a double mapping: first projects onto the old Gaussian sphere, then rotate the graticule so that the metaequator passes through the territory of Hungary. Three origins are designated for the territory of the country on the Gellérthegy meridian (Fig. F.3; Tab. F.2): at spherical latitudes $45^{\circ}31'59''$, $47^{\circ}6'$ and $48^{\circ}40'2''$. Finally, the MERCATOR projection was calculated. The coordinate axes here are also oriented to the South and to the West.

The three cylindric systems are named *HÉR*, *HKR* and *HDR*, i.e. *North*, *Central*, and *South cylindric system*. The boundaries of the three systems followed the boundaries of the villages so that a single system was used within each village. This projection was used exclusively for cadastral purposes, with the civil topography using the stereographic projection simultaneously.

In the 1970s, the need arose to use a single projection for topography and cadastral. As the existing systems were still designed for the old Hungary, it was felt necessary to create a new projection system adapted to the present

F. Old projection systems in Hungary

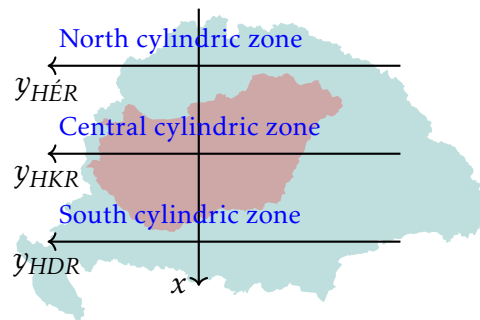


Figure F.3: Zonal cylindrical projections

area of the country. This resulted in the introduction of the *EOV*, which was described in detail in Sec. XIV.6. We must pay attention, because the *EOV* uses a different reference frame, and a new Gaussian sphere (Tab. F.1).

Table F.3: False easting and false northing of ‘Military’ coordinates

Budapest	Marosvásárhely	Ivanić
500 000 m	600 000 m	400 000 m

Table F.4: Constants of the cylindrical projections

Notation	HÉR / HKR / HDR	EOV
c	-1	0.999 93
X_0	0 m	200 000 m
Y_0	0 m	650 000 m

Appendix G

Projection systems in Europe

Tab. G.1 shows how some countries have tackled the issue of mapping. The South European and Scandinavian countries not listed here generally use the UTM projection, while in the successor states of the Soviet Union, we still find the GAUSS–KRÜGER coordinates with reference frame S42. Of particular interest is Germany, where no uniform system has been developed: in the former East Germany, the 1942 system is used, while in the former West Germany, the federal states have developed their own systems, typically with a reference frame of BESSEL ellipsoid and 3° wide zones. The purpose of the table is to illustrate the diversity, what to look out for when using a topographic map of a foreign country, what differences there may be from Hungarian solutions.

Two countries (Switzerland and the Netherlands) are particularly important, because while the Hungarian projections are poorly supported by GIS, the projections of these two countries are very similar to the Hungarian ones. The former is not a coincidence: FASCHING Antal, the developer of the zonal cylindrical systems, worked in Switzerland before coming to Hungary, and returned from there bringing the state-of-the-art mapping of the era. The different standard parallel of the Gaussian sphere was a decision taken for the Austro-Hungarian Empire: the auxiliary sphere was to be determined once for the whole Empire, and its central latitude was chosen to be distortion-free.

Table G.1: *Projection systems of European countries*

Country	Reference	Projection	Notes
Czechia Slovakia	S-JSTK (BESSEL)	KŘOVÁK (Fig. XVI.3)	Double mapping: Gaussian sphere ($\Phi_s = 49^\circ 30'$, $\Lambda_o = 24^\circ 50'$), followed by a reduced LAMBERT conformal conic projection in oblique aspect. Metapole $\varphi_o = 59^\circ 45' 27''$, standard parallel $\varphi'_s = 78^\circ 30'$; reduction $d = 0.9999$. Axis X points to the North, Y to the West.
Romania	S42 (KRASOVSKIY)	Stere070 (ROUSSILHE projection)	This is an oblique, non-perspective, conformal projection similar to the UPS directly from ellipsoid to plane. Contrary to its name, it is not stereographic, just very similar to it. The formulæ used in practice are derived from a complex series. Origin of the projection: $\Phi_o = 46^\circ$, $\Lambda_o = 25^\circ$, reduction: 0.99975, translation: 500 km
Austria	MGI (BESSEL)	GAUSS– KRÜGER	Uses 3° zones and the prime meridian of Ferro, central meridians 28° , 31° , 34° (from Greenwich $10^\circ 20'$, $13^\circ 20'$, $16^\circ 20'$)
Former Yugoslavia	MGI (BESSEL)	Reduced GAUSS– KRÜGER	3° zones, reduction 0.9999, central meridians 15° , 18° , 21° , 24° . In Croatia, only one zone is used with a central meridian of $16^\circ 30'$, here and in Slovenia coordinates are now referenced to WGS84.
Ukraine	S42 (KRASOVSKIY)	GAUSS– KRÜGER	3° zones
Poland (before 2009)	S42 (KRASOVSKIY)	UKŁAD (ROUSSILHE projection)	A projection similar to that of Romania was used, dividing the country into four zones along the borders of the voivodeships with distinct projection origins. For some reason, the GAUSS–KRÜGER was used in Upper Silesia.
Poland (after 2009)	WGS84	GAUSS– KRÜGER	3° zones reduced by a factor of 0.99923.

Table G.1: (contd.)

Country	Reference	Projection	Notes
Bulgaria (after 2010)	BGS2005 (GRS80)	LAMBERT conformal conic and UTM	The former top-secret (still unknown) projection has been replaced for cadastral and topographic purposes by two different systems: the former uses the UTM projection with a Bulgarian reference frame, the latter uses an ellipsoidal conic projection with central meridian $25^{\circ}30'$ divided into two zones. The northern zone has a standard parallel at $43^{\circ}20'$ and the southern zone at 42° .
Switzerland	CH1903 (BESSEL)	Oblique conformal cylindrical	This double mapping inspired the Hungarian cylindrical projections. Its origin is the Bern Observatory ($\Phi = 46^{\circ}57'8.66''$, $\Lambda = 7^{\circ}26'22.5''$), here is the intersection of the metaequator and the prime meridian and its latitude is also the standard latitude of the Gaussian sphere. to avoid swapping signs and coordinates, a translation of $Y_0 = 600$ km, $X_0 = 200$ km was applied. From a Hungarian point of view, this is very significant, because the principle of the EOVS differs only in that the standard latitude of the Gaussian sphere is not at the projection origin (causing a few cm deviation), so if any GIS software does not know the formulæ of the EOVS (which is unfortunately 99% of the software available), it usually recommends a reparametrization of the Swiss projection.

Table G.1: (contd.)

Country	Reference	Projection	Notes
Netherlands	Amersfoort (BESSEL)	Oblique secant stereographic	Also a double mapping, the origin this time is the fortress Amersfoort ($\Phi = 52^{\circ}9'22.18''$, $\Lambda = 5^{\circ}23'15.5''$). The auxiliary sphere is, like the Swiss example, true-scale along the latitude of the projection origin. The reduction compared to the tangent stereographic projection is 0.9999079, the axes are translated by 155 km to the East and 463 km to the North, so $x < 280$ km and $y > 300$ km. The projection is significant from a Hungarian point of view: it is the most similar projection to the Budapest stereographic system, and can be approximated to centimetre accuracy by reparametrization (i.e. the deviation is negligible compared to the error of the datum transformation).
France (before 2001)	NTF (CLARKE)	LAMBERT conformal conic	Everything is French in this projection. Prime meridian at Paris, everything is in gradians. The country is divided into three conic projections along parallels, the standard parallels are 55° , 52° , and 49° ; in Corsica, $46^{\circ}85^c$.
France (after 2001)	RGF93 (WGS84)	LAMBERT conformal conic	Now, in line with the international trend, the French also measure in degrees from Greenwich. The country was divided into 3° zones along parallels and each band is represented by a separate ellipsoidal conformal conic projection. The true-scale parallels are located $45'$ north and south from the mid-latitude of the band, the central meridian is at 3° .

Table G.1: (contd.)

Country	Reference	Projection	Notes
Belgium	WGS84	LAMBERT conformal conic	The Belgians have recently switched from datum BD72 based on the HAYFORD ellipsoid to WGS84, but the projection is unchanged. The prime meridian passes through the Brussels Observatory ($4^{\circ}21'33.18''$), the conformal conic projection is true-scale at latitudes $49^{\circ}50'$ and $51^{\circ}10'$.
United Kingdom	OSGB1936 (AIRY)	Reduced GAUSS– KRÜGER	The whole country is a single zone, the central meridian is 2° W, the reduction is about 0.9996 (not exactly due to the conversion between metres and feet). The vertical axis is translated 400 km east of the central meridian, the horizontal axis is placed 100 km north from the intersection of the central meridian and latitude 49° .
Ireland	IRENET95 (GRS80)	Reduced GAUSS– KRÜGER	The principle of the mapping is very similar to the British one, the central meridian is 8° W, the intersection of this with latitude $53^{\circ}30'$ is at 600 km on the horizontal axis and 750 km on the vertical axis, the reduction factor is 0.99982.

Appendix H

Inverse formulæ of oblique projections

For GIS applications, it is often necessary to calculate inverse projection formulæ. Usually, functions for projections in the normal aspect are easy to invert, but it is difficult to invert projections in oblique aspects. Therefore, I will now demonstrate the necessary concepts on two examples, the inverses of the oblique **stereographic** and **MERCATOR** projections.

The square of the radius function in the *tangent stereographic* projection:

$$\begin{aligned} x^2 + y^2 = \rho^2 &= 4R^2 \tan^2 \frac{\beta'}{2} = 4R^2 \frac{2 \sin^2 \frac{\beta'}{2}}{2 \cos^2 \frac{\beta'}{2}} = 4R^2 \frac{1 - \left(1 - 2 \sin^2 \frac{\beta'}{2}\right)}{1 + \left(2 \cos^2 \frac{\beta'}{2} - 1\right)} \\ &= 4R^2 \frac{1 - \left(\cos^2 \frac{\beta'}{2} - \sin^2 \frac{\beta'}{2}\right)}{1 + \left(\cos^2 \frac{\beta'}{2} - \sin^2 \frac{\beta'}{2}\right)} = 4R^2 \frac{1 - \cos \beta'}{1 + \cos \beta'} = 4R^2 \frac{1 - \sin \varphi'}{1 + \sin \varphi'} \end{aligned}$$

Introduce the auxiliary variable t .

$$t = \frac{x^2 + y^2}{4R^2}$$

Then substitute the corresponding oblique formulæ from Sec. V.3 for $\sin \varphi'$ into the previous equation.

$$\begin{aligned} t &= \frac{1 - \sin \varphi \sin \varphi_o - \cos \varphi \cos \varphi_o \cos(\lambda - \lambda_o)}{1 + \sin \varphi \sin \varphi_o + \cos \varphi \cos \varphi_o \cos(\lambda - \lambda_o)} \\ t + t \sin \varphi \sin \varphi_o + t \cos \varphi \cos \varphi_o \cos(\lambda - \lambda_o) &= 1 - \sin \varphi \sin \varphi_o - \cos \varphi \cos \varphi_o \cos(\lambda - \lambda_o) \\ \cos \varphi \cos(\lambda - \lambda_o)(t \cos \varphi_o + \cos \varphi_o) &= 1 - \sin \varphi \sin \varphi_o - t - t \sin \varphi \sin \varphi_o \\ \cos \varphi \cos(\lambda - \lambda_o) &= \frac{1 - t - (1 + t) \sin \varphi \sin \varphi_o}{(1 + t) \cos \varphi_o} \end{aligned}$$

H. Inverse formulæ of oblique projections

This is written into the formula for y calculated in Sec. X.5 so that λ is fortunately cancelled.

$$\begin{aligned}
 y &= -2R \frac{\sin \varphi \cos \varphi_o - \sin \varphi_o \frac{1-t-(1+t)\sin \varphi \sin \varphi_o}{(1+t)\cos \varphi_o}}{1 + \sin \varphi \sin \varphi_o + \cos \varphi_o \frac{1-t-(1+t)\sin \varphi \sin \varphi_o}{(1+t)\cos \varphi_o}} \\
 &= -2R \frac{\frac{(1+t)\sin \varphi \cos^2 \varphi_o - (1-t)\sin \varphi_o + (1+t)\sin \varphi \sin^2 \varphi_o}{(1+t)\cos \varphi_o}}{\frac{(1+t) + (1+t)\sin \varphi_o \sin \varphi + (1-t) - (1+t)\sin \varphi \sin \varphi_o}{(1+t)}} \\
 &= -2R \frac{(1+t)\sin \varphi - (1-t)\sin \varphi_o}{2\cos \varphi_o}
 \end{aligned}$$

From this, φ can be expressed simply:

$$\begin{aligned}
 y \cos \varphi_o &= -R(1+t)\sin \varphi + R(1-t)\sin \varphi_o \\
 R(1+t)\sin \varphi &= R(1-t)\sin \varphi_o - y \cos \varphi_o \\
 \varphi &= \arcsin \frac{R(1-t)\sin \varphi_o - y \cos \varphi_o}{R(1+t)}
 \end{aligned}$$

The numerator of the projection formula for x is $\sin \Delta\lambda$, so the formula for $\cos \varphi \cos \Delta\lambda$ can only be replaced by applying the transformation $\sin \Delta\lambda = \tan \Delta\lambda \cos \Delta\lambda$. After that, $\tan \Delta\lambda$ remains in the numerator, and we are trying to express it.

$$\begin{aligned}
 x &= -2R \frac{\tan(\lambda - \lambda_o) \frac{1-t-(1+t)\sin \varphi \sin \varphi_o}{(1+t)\cos \varphi_o}}{1 + \sin \varphi \sin \varphi_o + \cos \varphi_o \frac{1-t-(1+t)\sin \varphi \sin \varphi_o}{(1+t)\cos \varphi_o}} \\
 &= -2R \frac{\frac{\tan(\lambda - \lambda_o)[(1-t) - (1+t)\sin \varphi \sin \varphi_o]}{(1+t)\cos \varphi_o}}{\frac{(1+t) + (1+t)\sin \varphi_o \sin \varphi + (1-t) - (1+t)\sin \varphi \sin \varphi_o}{(1+t)}} \\
 &= -2R \frac{\tan(\lambda - \lambda_o)[(1-t) - (1+t)\sin \varphi \sin \varphi_o]}{2\cos \varphi_o}
 \end{aligned}$$

Let us rearrange!

$$\begin{aligned}
 x \cos \varphi_o &= -\tan(\lambda - \lambda_o)[R(1-t) - R(1+t)\sin \varphi \sin \varphi_o] \\
 \tan(\lambda - \lambda_o) &= \frac{-x \cos \varphi_o}{R(1-t) - R(1+t)\sin \varphi \sin \varphi_o}
 \end{aligned}$$

H. Inverse formulæ of oblique projections

We have a formula for the red expression at the top of the column, on the second line! If I substitute this, $\sin \varphi$ is cancelled and λ can finally be expressed unambiguously:

$$\begin{aligned}\tan(\lambda - \lambda_o) &= \frac{-x \cos \varphi_o}{R(1-t) - R(1-t) \sin^2 \varphi_o + y \cos \varphi_o \sin \varphi_o} \\ \lambda - \lambda_o &= \arctan \frac{-x \cos \varphi_o}{R(1-t)(1 - \sin^2 \varphi_o) + y \cos \varphi_o \sin \varphi_o} \\ \lambda &= \arctan \frac{-x}{R(1-t) \cos \varphi_o + y \sin \varphi_o} + \lambda_o\end{aligned}$$

Now it is time to calculate the inverse of the **MERCATOR projection!** The formulæ for the oblique MERCATOR projection given in Sec. XIII.2 are rearranged here.

$$\begin{aligned}\tan \frac{x}{cR} &= \frac{\sin \lambda}{\tan \varphi \sin \varphi_c - \cos \lambda \cos \varphi_c} \\ e^{\frac{2y}{cR}} &= \frac{1 + \sin \varphi \cos \varphi_c - \cos \varphi \sin \varphi_c \cos \lambda}{1 - \sin \varphi \cos \varphi_c + \cos \varphi \sin \varphi_c \cos \lambda}\end{aligned}$$

Let t and z be the following auxiliary variables:

$$\begin{aligned}t &= e^{\frac{2y}{cR}} \\ z &= \tan \frac{x}{cR}\end{aligned}$$

Then the lower equation rearranged:

$$\begin{aligned}t - t \sin \varphi \cos \varphi_c + t \cos \varphi \sin \varphi_c \cos \lambda &= 1 + \sin \varphi \cos \varphi_c - \cos \varphi \sin \varphi_c \cos \lambda \\ \cos \varphi \cos \lambda (t \sin \varphi_c + \sin \varphi_c) &= 1 + \sin \varphi \cos \varphi_c - t + t \sin \varphi \cos \varphi_c \\ \cos \lambda &= \frac{1 - t + (1+t) \sin \varphi \cos \varphi_c}{(1+t) \sin \varphi_c \cos \varphi}\end{aligned}$$

Substitute this back into the other equation.

$$\begin{aligned}\frac{\sin \lambda}{\tan \varphi \sin \varphi_c - \cos \varphi_c \frac{1-t+(1+t) \sin \varphi \cos \varphi_c}{(1+t) \cos \varphi \sin \varphi_c}} &= z \\ \sin \lambda &= z \frac{(1+t) \sin \varphi \sin^2 \varphi_c + (1-t) \cos \varphi_c + (1+t) \sin \varphi \cos^2 \varphi_c}{(1+t) \sin \varphi_c \cos \varphi} \\ &= z \frac{(1+t) \sin \varphi + (1-t) \cos \varphi_c}{(1+t) \sin \varphi_c \cos \varphi}\end{aligned}$$

We know that $\sin^2 \lambda + \cos^2 \lambda = 1$, i.e:

$$\left[z \frac{(1+t) \sin \varphi + (1-t) \cos \varphi_c}{(1+t) \sin \varphi_c \cos \varphi} \right]^2 + \left[\frac{1-t+(1+t) \sin \varphi \cos \varphi_c}{(1+t) \sin \varphi_c \cos \varphi} \right]^2 = 1$$

H. Inverse formulæ of oblique projections

$$\begin{aligned}
 & (1+t)^2 \sin^2 \varphi (z^2 + \cos^2 \varphi_c) + (1-t)^2 (z^2 \cos^2 \varphi_c + 1) \\
 & \quad + 2(1-t)(1+t) \sin \varphi \cos \varphi_c (z^2 + 1) = (1+t)^2 \sin^2 \varphi_c \cos^2 \varphi \\
 & (1+t)^2 \sin^2 \varphi (z^2 + \cos^2 \varphi_c + \sin^2 \varphi_c) + 2(1-t)(1+t) \sin \varphi \cos \varphi_c (z^2 + 1) \\
 & \quad + (1-t)^2 (z^2 \cos^2 \varphi_c + 1) - (1+t)^2 \sin^2 \varphi_c = 0
 \end{aligned}$$

This is a quadratic equation in $\sin \varphi$. We divide by the leading coefficient to prevent getting mile-long formulæ.

$$\sin^2 \varphi + 2 \frac{1-t}{1+t} \cos \varphi_c \sin \varphi + \frac{(1-t)^2 (z^2 \cos^2 \varphi_c + 1) - (1+t)^2 \sin^2 \varphi_c}{(1+t)^2 (1+z^2)} = 0$$

And then the solver formula for the quadratic equation:

$$\begin{aligned}
 \sin \varphi &= -\frac{1-t}{1+t} \cos \varphi_c \\
 & \pm \sqrt{\left(\frac{1-t}{1+t}\right)^2 \cos^2 \varphi_c - \frac{(1-t)^2 (z^2 \cos^2 \varphi_c + 1) - (1+t)^2 \sin^2 \varphi_c}{(1+t)^2 (1+z^2)}} \\
 &= \frac{(t-1) \cos \varphi_c}{1+t} \pm \sqrt{\frac{(1-t)^2 (\cos^2 \varphi_c + z^2 \cos^2 \varphi_c - z^2 \cos^2 \varphi_c - 1) + (1+t)^2 \sin^2 \varphi_c}{(1+t)^2 (1+z^2)}} \\
 &= \frac{(t-1) \cos \varphi_c}{1+t} \pm \sqrt{\frac{[-(1-t)^2 + (1+t)^2] \sin^2 \varphi_c}{(1+t)^2 (1+z^2)}} \\
 &= \frac{(t-1) \cos \varphi_c}{1+t} \pm \frac{\sin \varphi_c}{1+t} \sqrt{\frac{4t}{1+z^2}}
 \end{aligned}$$

Experience has shown that the sign \pm becomes $+$ if $|x/cR| < \pi/2$, i.e., on the hemisphere centred on the origin, $-$ for points further away. So the result is:

$$\varphi = \arcsin \left[\frac{(t-1) \cos \varphi_c}{t+1} \pm \frac{2 \sin \varphi_c}{1+t} \sqrt{\frac{t}{1+z^2}} \right]$$

H. Inverse formulæ of oblique projections

Now that we know the latitude, let us look at the longitude! We know that $\tan \lambda = \sin \lambda / \cos \lambda$:

$$\begin{aligned} \tan \lambda &= \frac{z(1+t)\sin \varphi + z(1-t)\cos \varphi_c}{1-t + (1+t)\sin \varphi \cos \varphi_c} \\ &= \frac{z(t-1)\cos \varphi_c \pm 2z\sin \varphi_c \sqrt{\frac{t}{1+z^2}} + z(1-t)\cos \varphi_c}{1-t + (t-1)\cos^2 \varphi_c \pm 2\sin \varphi_c \sqrt{\frac{t}{1+z^2}} \cos \varphi_c} \\ &= \frac{\pm 2z\sin \varphi_c \sqrt{\frac{t}{1+z^2}}}{(1-t)(1-\cos^2 \varphi_c) \pm 2\sin \varphi_c \cos \varphi_c \sqrt{\frac{t}{1+z^2}}} \end{aligned}$$

That is, the final result:

$$\lambda = \arctan \frac{\pm 2z\sqrt{\frac{t}{1+z^2}}}{(1-t)\sin \varphi_c \pm 2\cos \varphi_c \sqrt{\frac{t}{1+z^2}}}$$

Thus, the inverse projection is obtained. \pm remains $+$ up to a distance of 90° from the origin, and $-$ further away.

Appendix J

Pseudocylindricals with straight meridians

There is a group of pseudocylindrical projections, in which not only the parallels but also the meridians are mapped to straight lines, but the latter do not cross parallels at a right angle. These projections were sometimes used in the past because of their ease of construction, but they have now been superseded. A major drawback is that the mapped meridians are broken at the Equator.

The author of the oldest such mapping, the *trapezoidal projection*, is unknown and may date from the 15th century. It is sometimes referred to as the *DONIS* projection. In it, the central meridian and the Equator are equidistant, straight meridians connect the Equator and the pointed poles. This gives the projection formulæ:

$$\begin{aligned}x &= \frac{2}{\pi} R \widehat{\lambda} \left(\frac{\pi}{2} - |\widehat{\varphi}| \right) \\y &= R \widehat{\varphi}\end{aligned}$$

The projection in Fig. J.1 is aphylactic. The projection has been used primarily for regional maps. In such cases, often the bounding parallels were made equidistant instead of the Equator. The projection formulæ then correspond to the polyhedric projection described in Sec. XXI.3, with the radius of curvature obviously replaced by the radius of the sphere.

Let us form an equal-area projection! To do this, first try to achieve a correct total area by rescaling! The area of the rhombus is $R\pi \times 2R\pi/2 = R^2\pi^2$, which we want to scale by a factor c in both directions to obtain $4R^2\pi$:

$$\begin{aligned}c^2 R^2 \pi^2 &= 4R^2 \pi \\c &= \frac{2}{\sqrt{\pi}}\end{aligned}$$

After the scaling, we apply the method of auxiliary angles, denoting the auxiliary angle by ψ . The spherical zone is mapped to a trapezium,

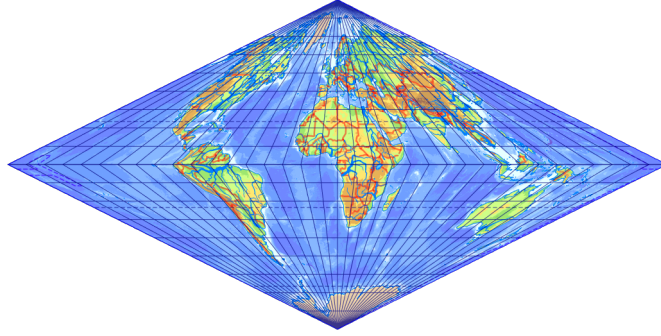


Figure J.1: Trapezoidal projection

its base, the Equator, is $cR2\pi$ long, its height is $cR\widehat{\psi}$, and its upper base is $4cR(\pi/2 - |\widehat{\psi}|)$. The area of the trapezium, i.e. the average of the two bases multiplied by the height, is equal to the surface area $2\pi \sin \varphi$ of the spherical zone:

$$\begin{aligned} \frac{2cR\pi + 4cR\left(\frac{\pi}{2} - |\widehat{\psi}|\right)}{2} cR\widehat{\psi} &= 2R^2 \pi \sin \varphi \\ 2\pi\widehat{\psi} - 2\widehat{\psi}^2 \operatorname{sign} \psi &= \frac{2\pi \sin \varphi}{c^2} \\ 2\widehat{\psi}^2 \operatorname{sign} \psi - 2\pi\widehat{\psi} + \frac{\pi^2}{2} \sin \varphi &= 0 \\ \widehat{\psi} &= \frac{2\pi \pm \sqrt{4\pi^2 - 4\pi^2 \sin \varphi \operatorname{sign} \psi}}{4 \operatorname{sign} \psi} = \frac{\pi(1 \pm \sqrt{1 - \sin|\varphi|})}{2 \operatorname{sign} \varphi} \end{aligned}$$

Since $\widehat{\psi} < \pi/2$, from the two solutions, we can only consider the one with the negative sign, and the signs of φ and ψ are the same. Furthermore:

$$\begin{aligned} 1 - \sin \varphi &= 1 - \cos(90^\circ - \varphi) \\ &= \sin^2 \frac{90^\circ - \varphi}{2} + \cos^2 \frac{90^\circ - \varphi}{2} - \left(\cos^2 \frac{90^\circ - \varphi}{2} - \sin^2 \frac{90^\circ - \varphi}{2} \right) \\ &= 2 \sin^2 \frac{90^\circ - \varphi}{2} \end{aligned}$$

From this:

$$\widehat{\psi} = \frac{\pi}{2} \left(1 - \sqrt{2} \sin \frac{90^\circ - |\varphi|}{2} \right) \operatorname{sign} \varphi$$

J. Pseudocylindricals with straight meridians

Substituting this into the formulæ of the trapezoidal projection, we obtain the equal-area projection of the French COLLIGNON from 1865 (Fig. J.2):

$$x = c \frac{2}{\pi} R \widehat{\lambda} \left(\frac{\pi}{2} - |\widehat{\psi}| \right) = \frac{2\sqrt{2}}{\sqrt{\pi}} R \widehat{\lambda} \sin \frac{90^\circ - |\varphi|}{2}$$

$$y = c R \widehat{\psi} = \sqrt{\pi} R \left(1 - \sqrt{2} \sin \frac{90^\circ - |\varphi|}{2} \right) \text{sign } \varphi$$

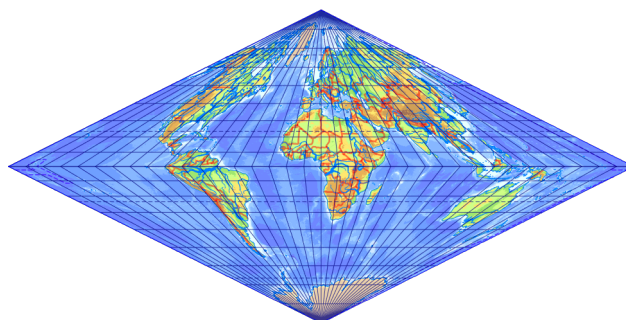


Figure J.2: COLLIGNON projection

Let us construct a blended projection of the **trapezoidal** and the **Plate Carrée** projections.

$$x = c \frac{\frac{2}{\pi} R \widehat{\lambda} \left(\frac{\pi}{2} - |\widehat{\varphi}| \right) + R \widehat{\lambda}}{2} = c R \widehat{\lambda} \left(1 - \frac{|\widehat{\varphi}|}{\pi} \right)$$

$$y = c \frac{R \widehat{\varphi} + R \widehat{\varphi}}{2} = c R \widehat{\varphi}$$

This is the ECKERT I projection (Fig. J.3). ECKERT did not define the relationship between the graticule and the map scale for the mapping given only by construction instructions, so the constant c cannot be defined. However, we can assume that ECKERT may have intended it to have correct total area, just like his other maps. The projection consists of a square with an area of $c^2 R^2 \pi^2$, and two isosceles triangles with an area of $(cR\pi \times cR\pi/2)/2$, while the total area should be $4R^2\pi$:

$$c^2 R^2 \pi^2 + 2 \frac{c^2 R^2 \pi^2}{4} = 4R^2\pi$$

$$\frac{3c^2}{2} \pi = 4$$

$$c = 2 \sqrt{\frac{2}{3\pi}}$$

J. Pseudocylindricals with straight meridians

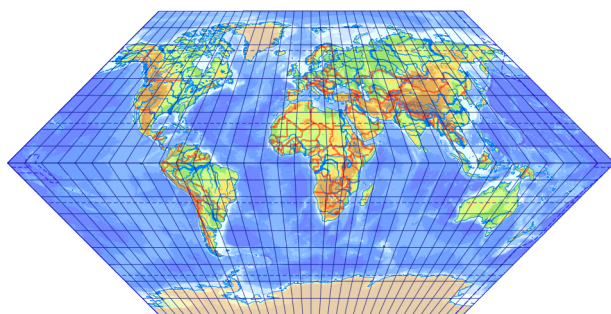


Figure J.3: ECKERT I projection

The ECKERT II projection has a similar appearance (Fig. J.4), but is equal-area. Let us introduce the auxiliary angle ψ again. This time, the mapped spherical zone is almost the same trapezium as in the COLLIGNON projection, but the length of the upper base is now $2cR(\pi - |\widehat{\psi}|)$.

$$\begin{aligned} \frac{2cR\pi + 2cR(\pi - |\widehat{\psi}|)}{2} cR\widehat{\psi} &= 2R^2 \pi \sin \varphi \\ 2\pi\widehat{\psi} - \widehat{\psi}^2 \operatorname{sign} \psi &= \frac{2\pi \sin \varphi}{c^2} \\ \widehat{\psi}^2 \operatorname{sign} \psi - 2\pi\widehat{\psi} + \frac{3\pi^2}{4} \sin \varphi &= 0 \\ \widehat{\psi} &= \frac{2\pi \pm \sqrt{4\pi^2 - 3\pi^2 \sin \varphi \operatorname{sign} \psi}}{2 \operatorname{sign} \psi} = \frac{\pi(2 \pm \sqrt{4 - 3 \sin|\varphi|})}{2 \operatorname{sign} \varphi} \end{aligned}$$

Again, only the root with a negative sign is accepted as the solution, because $\psi < 90^\circ$. Finally:

$$\begin{aligned} x &= cR\lambda \left(1 - \frac{|\widehat{\psi}|}{\pi} \right) = \sqrt{\frac{2}{3\pi}} R\lambda \widehat{\psi} \sqrt{4 - 3 \sin|\varphi|} \\ y &= cR\widehat{\psi} = \sqrt{\frac{2\pi}{3}} R(2 - \sqrt{4 - 3 \sin|\varphi|}) \operatorname{sign} \varphi \end{aligned}$$

This projection, unlike the others, can occur extremely rarely on less old maps. The use of pseudocylindricals with straight meridians in modern GIS occurs only when georeferencing old maps.

J. Pseudocylindricals with straight meridians

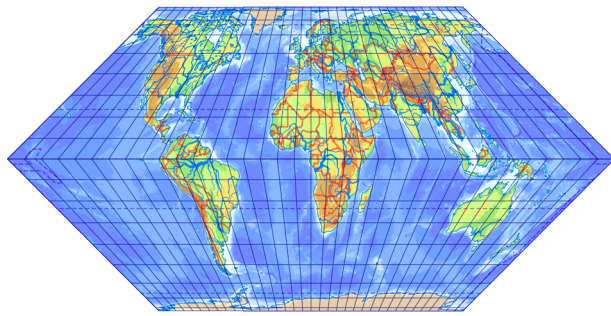


Figure J.4: *ECKERT II projection*

Appendix K

Approximate formulæ of BARANYI's maps

Here you can read the mathematical description of the BARANYI projections given without derivation in Sec. [XXIV.1](#).

In the BARANYI II projection, the Equator is equidistant, i.e. $2R\pi$ long. The length $2y_{max}$ of the central meridian is $7/10$ times the length of the Equator, i.e. $y_{max} = y(90^\circ) = 7R\pi/10$ (Fig. [K.1](#)). Latitude $\varphi_B = 70^\circ$ divides the central meridian in the ratio $13 : 5$, so $y(70^\circ) = 13y_{max}/18 = 91R\pi/180$. The distance between the parallels increases in proportion to the distance from the Equator, i.e. y (in the Northern Hemisphere) is a quadratic function, formulated as $p\widehat{\varphi} + q\widehat{\varphi}^2$. Substituting 90° and then 70° for φ gives two equations:

$$\begin{aligned}\frac{\pi}{2}p + \frac{\pi^2}{4}q &= \frac{7R\pi}{10} \\ \frac{7\pi}{18}p + \frac{49\pi^2}{324}q &= \frac{91R\pi}{180}\end{aligned}$$

Solving the system of equations with e.g. CRAMER's rule, we get $p = 19R/20$ and $q = 9R/(10\pi)$. From this (already taking into account the Southern Hemisphere) we obtain the following projection formula:

$$y = R\left(\frac{19}{20}|\widehat{\varphi}| + \frac{9}{10\pi}\widehat{\varphi}^2\right)\text{sign } \varphi$$

Converting the ordinary fractions to decimal fractions, we obtain the usual form of y .

The centre of the red arc is $R\pi - r_1$ far away from the central meridian. At the same time, the half-length d of the parallel φ_B is longer by $r_1 \cos \delta$:

$$d = R\pi - r_1 + r_1 \cos \delta$$

Next, we define the angle δ , which is the angle between the intersection of the frame arcs and the Equator. On the one hand, from the red arc of

K. Approximate formulæ of BARANYI's maps

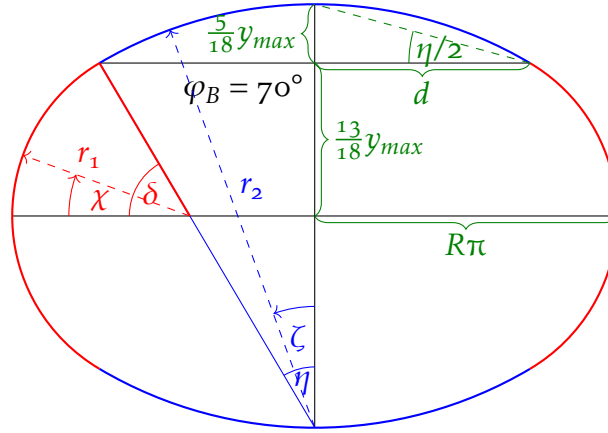


Figure K.1: BARANYI II projection

radius r_1 :

$$\sin \delta = \frac{\frac{13}{18} y_{max}}{r_1} = \frac{\frac{91}{180} R\pi}{r_1}$$

On the other hand, it can be seen from the figure that, because of the smooth connection of the arcs, the complementary angle of δ is η . From the inscribed angle theorem, it follows that the green angle subtended by the same chord is $\eta/2$. However, the tangent of this can be easily read off:

$$\tan \frac{\eta}{2} = \tan \frac{90^\circ - \delta}{2} = \frac{\frac{5}{18} y_{max}}{d} = \frac{\frac{35}{180} R\pi}{R\pi - r_1 + r_1 \cos \delta}$$

From both previous equations, δ can be expressed. The two expressions are necessarily equal:

$$\arcsin \frac{\frac{91}{180} R\pi}{r_1} = 90^\circ - 2 \arctan \frac{\frac{35}{180} R\pi}{R\pi - r_1 + r_1 \cos \delta}$$

In the denominator of the right-hand side, $\cos \delta = \sqrt{1 - \sin^2 \delta}$, the previously obtained formula for $\sin \delta$ can be substituted, leaving only r_1 as unknown. After a sufficient amount of trigonometric transformation, the equation can be solved:

$$r_1 = \frac{R\pi}{1450} \left(1003 - 3\sqrt{\frac{5107}{2}} \right) \approx 1.84466R$$

Substituting back into the previously derived equations, $\delta \approx 59.42867^\circ$ and $d \approx 2.23514R$. Since $\sin \eta = \cos \delta = d/r_2$, $r_2 \approx 4.39461R$ can also be

K. Approximate formulæ of BARANYI's maps

calculated. The latter is slightly smaller than the length of the central meridian.

Let the angle between the radius to the endpoint of the parallel $-70^\circ \leq \varphi \leq 70^\circ$ and the Equator be χ ! Then, from the figure:

$$\sin \chi = \frac{y(\varphi)}{r_1}$$

Furthermore, the centre of the red circle is at a distance $R\pi - r_1$ from axis y and the coordinate x of the endpoint of the parallel is $r_1 \cos \chi$ greater than this. Since parallels are evenly divided by meridians:

$$x = (R\pi - r_1 + r_1 \cos \chi) \frac{\widehat{\lambda}}{\pi}$$

For latitudes $|\varphi| > 70^\circ$, the mapped parallel is $r_2 - y_{max} + y$ far away from the centre of the blue circle. Thus, the angle ζ to the endpoint of the parallel is obtained:

$$\cos \zeta = \frac{r_2 - \frac{7}{10}R\pi + y(\varphi)}{r_2}$$

The coordinate x of the endpoint of the parallel is $r_2 \sin \zeta$, so:

$$x = r_2 \sin \zeta \frac{\widehat{\lambda}}{\pi}$$

This completes the description of projection II. Let us move on to the discussion of projection IV. Here BARANYI did not give the relationship between the units he used and the real distances. If we consider the origin of the projection to be distortion-free, then, knowing that the side length of the 10° degree quadrangles here is 12 units, it follows that one unit is $10R\pi/(180 \times 12) = R\pi/216 \approx 0.0145444R$. In this projection, the radius of the red arc is $r_1 = 100$ units. The length of the Equator is 368 units and the length of the central meridian is 222 units. This implies that the centre of the red circle is 84 units far away from axis y , i.e., $x_0 \approx 1.22172R$ (Fig. K.2).

The centres of the blue and red arcs are $r_2 - r_1$ apart due to the smooth connection. Plotting this distance on axis y from the centre of the blue arc brings us to a distance of $111 - r_1 = 11$ units from the Equator (here we have used the fact that half of the meridian is 111 units). Let us denote the angle between the two equal sections by η !

Then the angle in the upper right corner is $\eta/2$ according to the inscribed angle theorem, and the angle in the upper left corner is also $\eta/2$ due to symmetry. The centres of the blue and red circles and the previously

K. Approximate formulæ of BARANYI's maps

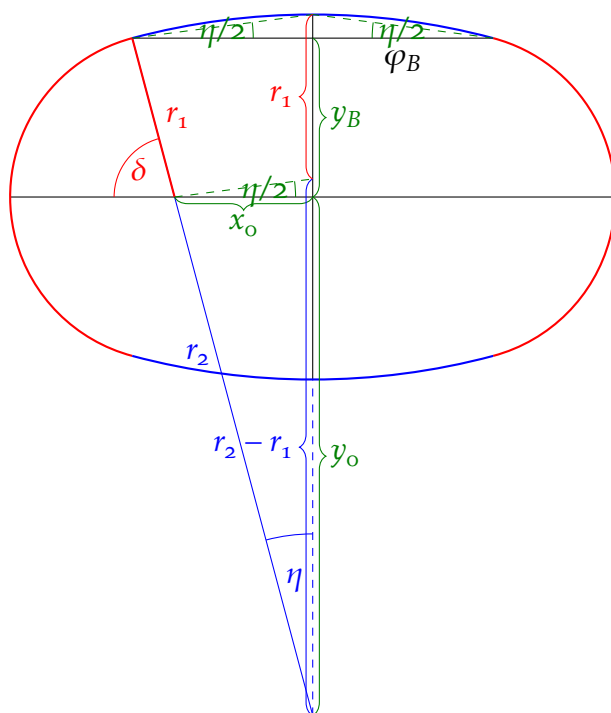


Figure K.2: BARANYI IV projection

marked point on the central meridian define isosceles triangles of leg $r_2 - r_1$, which is similar to one defined by centre of the blue circle, the North Pole and the point where the two circles join. Because of this, the angles in the top left corner and at the centre of the red arc are equal, so the latter is also $\eta/2$. Its tangent (legs measured in units) is:

$$\tan \frac{\eta}{2} = \frac{111 - r_1}{x_0} = \frac{11}{84}$$

That is, $\eta \approx 14.92^\circ$. This gives $\delta = 90^\circ - \eta \approx 75.08^\circ$. Since $y_B = r_1 \sin \delta$, $y_B \approx 96.63$ units. Furthermore:

$$\tan \eta = \frac{84}{r_2 - 111}$$

Thus, $r_2 \approx 426.23$ units, $y_0 = r_2 - 111 \approx 315.23$ units.

The coordinate y is approximated by a 9 degree odd polynomial for symmetry, where the first-degree coefficient is one (the derivative of y at $\varphi = 0$ is R):

$$y = R(\widehat{\varphi} + a\widehat{\varphi}^3 + b\widehat{\varphi}^5 + c\widehat{\varphi}^7 + d\widehat{\varphi}^9)$$

The coefficients are chosen to follow BARANYI's construction instructions given in Sec. XXIV.1. That is, at the Pole, $y = 111$ units, converted to

K. Approximate formulæ of BARANYI's maps

$37R\pi/72$. The distance between parallels near the Pole is at the same as near the Equator, so the derivative of y here is also R . At the Pole and around latitude 45° , the parallels are evenly spaced, i.e. the second derivative of y is zero at these two locations. From this, we obtain four equations:

$$\begin{aligned} R\left(\frac{\pi}{2} + a\frac{\pi^3}{8} + b\frac{\pi^5}{32} + c\frac{\pi^7}{128} + d\frac{\pi^9}{512}\right) &= \frac{37R\pi}{72} \\ R\left(1 + a\frac{3\pi^2}{4} + b\frac{5\pi^4}{16} + c\frac{7\pi^6}{64} + d\frac{9\pi^8}{256}\right) &= R \\ R\left(a\frac{6\pi}{2} + b\frac{20\pi^3}{8} + c\frac{42\pi^5}{32} + d\frac{72\pi^7}{128}\right) &= 0 \\ R\left(a\frac{6\pi}{4} + b\frac{20\pi^3}{64} + c\frac{42\pi^5}{1024} + d\frac{72\pi^7}{16384}\right) &= 0 \end{aligned}$$

The solution of the linear system of equations gives the coefficients a, b, c, d . Substituting these back into the original polynomial, we can find by solving a non-linear equation that $y = y_B$ is reached by the polynomial at latitude $\varphi_B \approx 78.07^\circ$. This is important for determining the projection formulæ for x , because the equations for the red and blue circles are different. They are:

$$\begin{aligned} x_r &= x_o + \sqrt{r_1^2 - y^2} \\ x_b &= \sqrt{r_2^2 - (|y| + y_o)^2} \end{aligned}$$

The slower and slower descending divisions along the parallels are approximated by a logarithm:

$$f(\lambda) = \frac{\ln(1 + A|\widehat{\lambda}|)}{AB} \text{sign } \lambda$$

In the choice of coefficients, we aim for $f(180^\circ) = 1$. For the origin to be distortion-free, we should obtain R by multiplying half-length of the Equator and the derivative of f at 0. From the latter condition, $B = 23\pi/27$, while substituting it back into the former condition, we obtain a non-linear equation from which the approximate value of A can be calculated. Finally, the map coordinate x is obtained as the product of $f(\lambda)$ and x_r or

K. Approximate formulæ of BARANYI's maps

x_b , calculated from the equation of the circle at the given latitude. The final result is:

$$y = R(\widehat{\varphi} + 0.073880\widehat{\varphi}^3 - 0.0538964\widehat{\varphi}^5 + 0.01560242\widehat{\varphi}^7 - 0.001639406\widehat{\varphi}^9)$$

$$x = \frac{\ln(1 + 0.11679|\widehat{\lambda}|)}{0.31255} \operatorname{sign} \lambda \times \begin{cases} \left(\frac{1.22172R + \sqrt{2.115393R^2 - y^2}}{\sqrt{38.4308R^2 - (4.58448R + |y|)^2}} \right) & \text{if } |\varphi| \leq \varphi_B \\ \left(\frac{1.22172R + \sqrt{2.115393R^2 - y^2}}{\sqrt{38.4308R^2 - (4.58448R + |y|)^2}} \right) & \text{if } |\varphi| > \varphi_B \end{cases}$$

Appendix L

Modified polyconic projection

In the modified polyconic projection described in Sec. XXVI.2, the ellipsoidal reference frame is divided into geographical quadrangles, extending 4° in latitude and 6° in longitude up to $\pm 60^\circ$, 12° to $\pm 76^\circ$, and finally 24° to $\pm 84^\circ$. Each quadrangle is mapped onto a separate plane, and each mapped quadrangle is a distinct map sheet with its own planar coordinate system. Adjacent sheets can be aligned along either the bounding parallels or the bounding meridians, but the corners of the sheets are not right angles, so it is impossible to fit four adjacent sheets without a gap.

Let $\Lambda_{1,2}$ be the longitude of the boundaries, $\Phi_{1,2}$ the latitude of the boundaries (also equidistant), in addition, $\Lambda_0 = (\Lambda_1 + \Lambda_2)/2$ is the central meridian and $\Lambda_3 = \Lambda_0 + 2(\Lambda_2 - \Lambda_0)/3$ is one of the equidistant meridians. The mapped meridians are straight, the radii of the circular mapped parallels are given by the formula $\rho = N(\Phi) \cot \Phi$, which is usual for polyconic projections. The intersection point of the parallel and the y axis is at a distance t from the origin, $t_1 = 0$ as shown in Fig. L.1. Find the coordinates x, y of the point P . The coordinates of points $P_{1,2}$ can be obtained from the radius function and the equidistance of the bounding parallels:

$$\begin{aligned}x_{1,2} &= N(\Phi_{1,2}) \cot \Phi_{1,2} \sin\left[(\Lambda_3 - \Lambda_0) \sin \Phi_{1,2}\right] \\y_{1,2} &= t_{1,2} + N(\Phi_{1,2}) \cot \Phi_{1,2} \left(1 - \cos\left[(\Lambda_3 - \Lambda_0) \sin \Phi_{1,2}\right]\right)\end{aligned}$$

From the equations above, t_2 is unknown (since, exceptionally, we have not prescribed the equidistance of the central meridian), so y_2 is unknown. However, the distance P_1 and P_2 is the same as the ellipsoidal distance:

$$\sqrt{(x_2 - x_1)^2 + (y_2 - y_1)^2} = \int_{\Phi_1}^{\Phi_2} M(\Phi) d\Phi$$

Of this, only y_2 is unknown, and by expressing it and then substituting t_2 into the equation above, y_2 can be calculated. Let the point P_3 be the intersection of the parallel through point P with meridian Λ_3 . Then, on

L. Modified polyconic projection

Point P is located on the line through points P_4 and P_5 :

$$\frac{x - x_4}{x_5 - x_4} = \frac{y - y_4}{y_5 - y_4}$$

On the other hand, the PYTHAGOREAN theorem just applied is also true for the black dashed right triangle of hypotenuse ρ :

$$\rho^2 = x^2 + [\rho - (y - t)]^2$$

The last two equations give a quadratic system of equations with two unknowns for the coordinates x, y , which can be solved, for example, by substituting into each other and then utilizing the solver of quadratic equations.

This apylactic projection was applied to the *International Map of the World* (Internationale Weltkarte) at a scale of 1 : 1 000 000. The idea for the map was conceived in 1891 and the choice of projection was decided in 1909. LALLEMAND developed the construction instructions in 1911, but SNYDER published the analytical formulæ only in 1982. Since 1962, the map series has been drawn in the LAMBERT conformal conic projection.

Appendix M

Index

A

- ADAMS, OSCAR SHERMANN (1874–1962), American mathematician, [253](#), [254](#)
- AGNESE, BATTISTA (1500?–1564), Italian cartographer, [176](#)
- AIRY, SIR GEORGE BIDDELL (1801–1892), English astronomer, [261](#), [264](#), [299](#)
- AIRY–KAVRAYSKIY criterion, [263](#), [264](#)
- AITOFF proj., [241](#), [242](#), [245](#), [260](#)
- AITOV, DAVID ALEKSANDROVICH (1854–1933), Russian cartographer, [241](#)
- ALBERS, HEINRICH CHRISTIAN (1773–1833), German cartographer, [135](#)
- ALBERS equal-area conic, [134–138](#), [150](#), [216](#)
- American (ordinary) polyconic, [222](#), [223](#)
- aphylactic proj., [59](#)
- APIAN I proj., [173](#), [176](#), [233](#)
- APIAN II proj., [174–176](#), [183](#), [185](#), [192](#), [195–197](#), [241](#)
- Armadillo proj., [247](#)
- aspect of proj., *see* metacoordinates
- Atlantis proj., [193](#), *see also* MOLLWEIDE proj.

- auxiliary sphere, [78–80](#), [97](#), [98](#), [116](#), [117](#), [122](#), [123](#), [142](#), [169](#), [290](#), [293](#), [295–298](#)
- azimuthal equidistant, [91–93](#), [95](#), [133](#), [150](#), [179](#), [209](#), [233](#), [240](#), [241](#), [245](#), [260](#)
- azimuthal proj., [58](#), [82](#)

B

- BARANYI JÁNOS (1932–1990), Hungarian cartographer, [205](#), [207](#), [209](#), [210](#)
- BARANYI II proj., [205](#), [310–312](#)
- BARANYI IV proj., [206](#), [210](#), [264](#), [312](#), [313](#)
- interrupted, [208](#)
- BARTHOLOMEW, JOHN CHRISTOPHER (1923–2008), Scottish cartographer, [193](#), [242](#), [244](#), [248](#)
- BEHRMANN, WALTER EMMERICH (1882–1955), German geographer, [106](#)
- BEHRMANN proj., [106](#)
- BESSEL, FRIEDRICH WILHELM (1784–1846), German geodesist, [49](#), [54](#), [98](#), [119](#), [142](#), [150](#), [290](#), [293](#), [295–298](#)
- blended proj., [181](#), [183](#), [185](#), [189](#), [196](#), [203](#), [240](#), [242](#), [307](#)
- BLUDAU, ALOIS (1861–1913), German cartographer, [235](#)

- BONNE, RIGOBERT (1727–1794), French cartographer, 216
 BONNE proj., 216, 218, 247, 264
 BORKOWSKI, KAZIMIERZ M., Polish astronomer, 39, 279
 BOWRING, BERNARD RUSSELL (1925–2006), English geodesist, 39
 BRAUN, CARL, SJ (1831–1907), German astronomer, 103, 113
 BRAUN proj., 103, *see also* quasi-perspective proj.
 BRIESEMEISTER proj., 242, *see also* HAMMER proj.
 BURŠA–WOLF transform, *see* HELMERT transform
- C**
- CAHILL, BERNARD JOSEPH STANISLAUS (1866–1944), American architect, 254
 cardioid proj., *see* WERNER proj.
 CASSINI DE THURY, CÉSAR-FRANÇOIS (1714–1784), French geodesist, 109
 CASSINI proj. (CASSINI–SOLDNER proj.), 109, 116, 293
 CAUCHY–RIEMANN differential equation, 249
 central cylindrical proj., 101
 central meridian, 77
 central parallel, 125
 CHAMBERLIN proj., 258
 CHEBYSHEV, PAFNUTIY LVOVICH (1821–1894), Russian mathematician, 74, 89, 112, 250, 263
 CLAIRAUT’S relation, 47
 CLARKE, ALEXANDER ROSS (1828–1914), British geodesist, 54, 223, 298
 colatitude, 82, 83, 125, 218, 219
 COLLIGNON proj., 307, 308
 complex number, 99, 141, 159, 250
 composite proj., 202–204, 208, 247, 254
 cone constant, 125
 conformal proj., 59, 70, 72, 250
 conic proj., 58, 125
 CRAIG proj., 246
 CRASTER proj., 257
 cylindrical proj., 58, 100
 cylindrical stereographic, *see* BRAUN proj.; GALL proj.
- D**
- datum, *see* geodetic datum
 datum transform
 3 parameter, *see* MOLODENSKIY transform
 7 parameter, *see* HELMERT transform
 grid shift, 56, 150, 155
 DE L’ISLE, JOSEPH-NICOLAS (1688–1768), French cartographer, 131
 DEETZ, CHARLES HENRY (1864–1946), American cartographer, 223
 detectproj, 256
 distorted cartogram, 145
 distortion value
 global, 262–264
 local, 261, 262
 DONIS proj., *see* trapezoidal proj.
 double mapping, *see* auxiliary sphere
 DÜRER, ALBRECHT (1471–1528), German painter, 253
 Dymaxion proj., 254

- E**
- ECKERT-GREIFENDORFF, MAX (1868–1938), German geographer, 181, 196
- ECKERT I proj., 307
- ECKERT II proj., 308
- ECKERT III proj., 183, 185, 189
- ECKERT IV proj., 191, 192, 218, 264
- ECKERT V proj., 182, 184, 188
- ECKERT VI proj., 189, 202
- EISENLOHR proj., 263
- EOV, 123, 124, 148, 292, 294, 297
- EPSG number, 148
- Equal Earth proj., 211
- equal-area polyconic, 227
- equal-area (equivalent) proj., 59, 66, 70
- equidistant conic, 131, 150
- equidistant line, 59
- equiarectangular proj., 108, 183, 185, 242, 264
- equivalent proj., *see* equal-area proj.
- ÉRDI-KRAUSZ GYÖRGY (1899–1972), Hungarian cartographer, 203, 256
- ETZLAUB, ERHARD (1460?–1532), German cartographer, 110
- EULER-LAGRANGE differential equation, 264
- F**
- FASCHING ANTAL (1879–1931), Hungarian geodesist, 293, 295
- first eccentricity, 15, 51, 53, 291
- flattening, 15, 54, 55
- Flex Projector, 211
- FULLER, RICHARD BUCKMINSTER (1895–1983), American architect, *see* Dymaxion proj.
- G**
- GALL, JAMES (1808–1895), Scottish cartographer, 103, 106
- GALL proj., 103
- GALL-PETERS proj., 106, 205, 211
- GAUSS, CARL FRIEDRICH (1777–1855), German mathematician, 34, 49, 52, 62, 118, 139
- Gaussian sphere, *see* osculating sphere
- GAUSS-KRÜGER proj., 118–121, 141, 150, 153, 295, 296, 299, *see also* UTM
- GAUSS-SCHREIBER proj., 113, 251, *see also* GAUSS-KRÜGER proj.
- geodesic (geodesic line, orthodrome), 13, 19, 27, 28, 47–50, 77, 80, 85, 116, 122, 124, 142, 179, 246, 254
- geodetic datum
- horizontal, 54–56, 98, 118, 123, 142, 148–150, 153–161, 290, 293
- vertical, 280–284
- geographical quadrangle, 20, 39, 40, 61, 65, 185, 205, 256, 260, 312, 316
- geoid, 53–55, 280–282, 284
- geoid undulation, 39, 55, 282, 284
- GILBERT, EDGAR NELSON (1923–2013), American mathematician, 229
- GINZBURG, GEORGIY ALEKSANDROVICH, Soviet cartographer, 95, 212, 219, 237, 260
- GINZBURG III proj., 219

- GINZBURG VIII proj., 212
 GINZBURG'S azimuthal proj., 96, 219
 GINZBURG'S pseudopolyconic projs., 237, 260, 264
 gnomonic proj., 85, 95, 254, 260
 GOODE, JOHN PAUL (1862–1932), American cartographer, 202
 GOODE proj., 202–204, 247
- H**
 HAMMER, ERNST HERMANN HEINRICH VON (1858–1925), German geodesist, 241, 246
 HAMMER proj., 241, 242, 244, 260, 264
 HASSLER, FERDINAND RUDOLPH (1770–1843), Swiss geodesist, 223
 HELMERT transform, 56, 148, 150, 151, 153, 158, 160
 homolographic proj., *see* MOLLWEIDE proj.
 homolosine proj., *see* GOODE proj.
 HOTINE proj., 124, 149
 hyperboloid proj., 146
- I**
 IMW polyconic, *see* modified polyconic
 interrupted proj., 203, 207, 247
 isocol, 74, 75, 89, 91, 94, 108, 112, 131, 142, 177, 218, 219, 250, 260, 263
- K**
 KARNEY, CHARLES F. F., English geodesist, 49
 KAVRAYSKIY, VLADIMIR VLADIMIROVICH (1884–1954), Soviet cartographer, 198, 202, 261, 262
 KAVRAYSKIY V proj., 257, 264
 KAVRAYSKIY VI proj., 202
 KAVRAYSKIY VII proj., 197, 264
 KRASOVSKIY, FEODOSIY NIKOLAYEVICH (1878–1948), Soviet geodesist, 54, 119, 296
 KŘOVÁK proj., 142, 296
 KRÜGER, JOHANN HEINRICH LOUIS (1857–1923), German geodesist, 118
- L**
 LAGRANGE, JOSEPH-LOUIS (1736–1813), French mathematician, 232, 264
 LAGRANGE proj., 230, 251
 LALLEMAND, CHARLES JEAN-PIERRE (1857–1938), French geodesist, 223, 318
 LAMBERT, JOHANN HEINRICH (1728–1777), Swiss mathematician, 94, 105, 113, 138, 139, 232
 LAMBERT azimuthal equal-area, 75, 94, 95, 138, 150, 241, 244
 LAMBERT conformal conic, 139–142, 150, 226, 296–299, 318
 LAMBERT equal-area conic, 138
 LAMBERT equal-area cylindrical, 105
 LAMBERT–GAUSS proj., *see* LAMBERT conformal conic
 latitude
 astronomical, 281
 geocentric, 16
 geographic, 16, 37–39
 parametric, 16, 39
 spherical, 13

- LEE, LAWRENCE P., New Zealander geodesist, 118, 253, 254
- LEGENDRE, ADRIEN-MARIE (1752–1833), French mathematician, 49
- LICHTENSTERN proj., *see* polyhedric proj.
- LITTROW, JOSEPH JOHANN VON (1781–1840), Austrian astronomer, 232
- LITTROW proj., 168, 232, 246, *see also* LAGRANGE proj.
- longitude, 13, 37–39
- loximutal proj., 179
- loxodrome, *see* rhumb line
- lune, 21, 110, 118
- M**
- MAURER, HANS (1868–1945), German cartographer, 227
- MCCAW, GEORGE TYRRELL (1870–1942), British geodesist, 226
- mean sea level, 280
- MENDELEYEV proj., 131
- MERCATOR, GERARDUS (1512–1594), Dutch cartographer, 110, 114, 177
- MERCATOR proj., 77, 106, 110–114, 116, 117, 122, 165, 172, 229, 293, 302, *see also* Pseudo Mercator
- MERCATOR–SANSON proj., *see* sinusoidal proj.
- meridian convergence, 75, 77, 103, 169, 244
- MESHCHERYAKOV, GERMAN ALEKSEYEVICH (1924–1992), Soviet geodesist, 262, 264
- metacoordinates, 43–46, 60, 91, 97–99, 110, 112, 116, 117, 122–124, 142, 165–167, 219, 246, 254, 260, 290–293, 296, 297
- MGRS, 121
- MILLER, OSBORN MAITLAND (1897–1979), Scottish cartographer, 114, 250
- miscellaneous proj., 163
- modified (IMW) polyconic, 223, 316–318
- MOLLWEIDE, CARL BRANDAN (1774–1825), German mathematician, 193
- MOLLWEIDE proj., 164, 193, 200–204, 242, 260
- MOLODENSKIY transform, 56, 148, 149, 153, 160
- MÜFFLING proj., *see* polyhedric proj.
- N**
- Natural Earth proj., 211
- NICOLOSI proj., 233
- Nordic proj., 242, *see also* HAMMER proj.
- normal aspect, *see* metacoordinates
- O**
- oblique aspect, *see* metacoordinates
- ordinary polyconic, *see* American polyconic
- ORTELIUS proj., 176
- orthoapsidal proj., *see* Armadillo proj.
- orthodrome, *see* geodesic
- orthographic proj., 86, 95, 105, 127, 167, 246
- orthophanic proj., *see* ROBINSON proj.

osculating sphere (Gaussian sphere), 57, 80, 98, 99, 122–124, 142, 290, 291, 293–297

P

PÉCSI ALBERT (1882–1971), Hungarian geographer, 242

PÉCSI proj., 242, *see also* HAMMER proj.

PEIRCE, CHARLES SANDERS (1839–1914), American mathematician, 253

PEIRCE proj., 253, 260

perspective conic proj., 126–129, 221

perspective proj., 58, *see also* vertical perspective proj.; central cylindrical proj.; quasi-perspective proj.; perspective conic proj.

PETERS, ARNO (1916–2002), German historian, *see* GALL–PETERS proj.

Plate Carrée proj., 108, 116, 180, 183, 307

plumb line, 280–283

polyazimuthal proj., 163, 237

polyconic proj., 127, 163, 221, *see also* pseudopolyconic proj.; American polyconic

polyhedral proj., 253, 254

polyhedral proj., 185, 223, 253, 305

POSTEL, GUILLAUME (1510–1581), French astronomer, 91

Prime meridian, 15, 77

PROJ.4, 149

Projection Wizard, 260

Pseudo Mercator (Web Mercator), 116, 148, 150, 169

pseudoazimuthal proj., 163, 218

pseudoconic proj., 163, 214

pseudocylindrical proj., 163, 171

pseudopolyconic proj., 222, 230

PTOLEMY I proj., 133

PTOLEMY II proj., 169, 216, *see also* BONNE proj.

PUTNIŃŠ projs., 257

Q

quasi-perspective proj., 103, 113, 127

R

radius function, 82, 95, 125, 213, 219, 221, 230, 300, 316

radius of curvature

Gaussian, 51–53, 57, 124, *see also* osculating sphere

meridional, 34, 35, 51

prime-vertical, 36, 51, 276

RAISZ ERVIN (1893–1968), Hungarian cartographer, 247, *see also* Armadillo proj.

rectangular polyconic (War Office proj.), 226, 227

rectangular proj., 65, 72, 164

retroazimuthal proj., 246

rhumb line (loxodrome), 28–32, 111, 179, 180

ROBINSON, ARTHUR HOWARD (1915–2004), American cartographer, 209

ROBINSON proj., 209–211, 235, 244

ROSENMUND proj., 122, 124, 150

ROUSSILHE proj., 98, 296

S

ScapeToad, 146

SCHWARZ, KARL HERMANN AMANDUS (1843–1921), German mathematician, 251

- SIEMON, KARL, German cartographer, 179, 195, 199
- SIKLÓSI MIKLÓS, Hungarian cartographer, 147
- simple polyconic, *see* American polyconic
- sinusoidal proj. (MERCATOR–SANSON proj.), 177, 180, 181, 183, 186, 195, 196, 198, 200–203, 216, 242
- SNYDER, JOHN PARR (1926–1997), American cartographer, 260, 318
- SOLDNER, JOHANN GEORG VON (1776–1833), German mathematician, 116
- spherical
 lune, *see* lune
 triangle, 22–27, 44–46, 272–275
 zone, 21, 171, 185, 188, 189, 192, 199, 221, 223, 305, 308
- SPILHAUS proj., 253
- STAB proj., *see* WERNER proj.
- standard line, 60, 106
- stereographic proj., 46, 75, 87–90, 95, 98, 103, 127, 141, 143, 150, 226, 230, 232, 237, 246, 250, 251, 260, 263, 290, 296, 298, 300
- T**
- TISSOT, NICOLAS-AUGUSTE (1824–1907), French geodesist, 67–71, 75, 77, 168, 249, 285
- TISSOT'S indicatrix, 70, 74
- TOBLER, WALDO RUDOLPH (1930–2018), American cartographer, 179, 193
- transverse aspect, *see* metacoordinates
- trapezoidal (DONIS) proj., 305, 307, *see also* polyhedral proj.
- trapezoidal projection, 307
- true-scale line, *see* standard line
- U**
- Umbeziffern, 195, 197–199, 229, 240, 244, *see also* WAGNER transform
- UPS, 97, 121, 153
- URMAYEV, NIKOLAY ANDREYEVICH (1895–1959), Soviet geodesist, 202, 211
- UTM, 97, 121, 122, 148, 153, 295, 297
- V**
- VAN DER GRINTEN, ALPHONS JOHANN (1852–1921), German cartographer, 233
- VAN DER GRINTEN I proj., 235, 236, 244, 260, 264
- VAN DER GRINTEN II proj., 257, *see also* BLUDAU
- VAN DER GRINTEN III proj., 256, *see also* BLUDAU
- VAN DER GRINTEN IV proj., 235
- vertical deflection, 15, 55, 281, 282
- vertical perspective proj., 83
- VESPUCCI, AMERIGO (1451–1512), Italian explorer, 173
- W**
- WAC, 142
- WAGNER, KARLHEINZ (1906–1985), German cartographer, 195, 197, 199–201, 245

- WAGNER I proj., *see* KAVRAYSKIY VI proj.
- WAGNER III proj., 196
- WAGNER IV proj., 201
- WAGNER VI proj., 196
- WAGNER VII proj., 245
- WAGNER IX proj., 245
- WAGNER transform, 199, 201, 203, 244, 264
- War Office proj., *see* rectangular polyconic
- WATERMAN proj., 254
- Web Mercator, *see* Pseudo Mercator
- WERNER (STAB) proj., 216
- WGS84, 54, 55, 57, 97, 121, 142, 148, 149, 161, 296, 298, 299
- WIECHEL proj., 75, 219
- WILLIAM-OLSSON proj., 248
- WINKEL, OSWALD (1874–1953), German cartographer, 244
- WINKEL I proj., 183
- WINKEL II proj., 185
- WINKEL III (Tripel) proj., 242, 246, 263
- WKT, 148